DOE/ID/13378--T20

# DEMONSTRATION OF OXYGEN-ENRICHED AIR STAGING AT OWENS-BROCKWAY GLASS CONTAINERS

Final Technical Report for the period
April 1, 1995 to February 28, 1997

RECEIVED
FEB 23 1998
OSTI

D. Rue
H. Abbasi

October 1997

Work Performed Under Contract No. DE-FC07-95ID13378

For
U.S. Department of Energy
Assistant Secretary for
Energy Efficiency and Renewable Energy
Washington, DC

PROCESSED FROM BEST AVAILABLE COPY

By
Institute of Gas Technology
Des Plaines, IL

MASTER

DISTRIBUTION OF THIS DOCUMENT IS UNLIMITED

**DOE/ID/13378--T20**
**Distribution Category UC-1400**

# DEMONSTRATION OF OXYGEN-ENRICHED AIR STAGING AT OWENS-BROCKWAY GLASS CONTAINERS

Final Technical Report for the Period
April 1, 1995 to February 28, 1997

D. Rue
H. Abbasi

October 1997

Work Performed Under Contract No. DE-FC07-95ID13378

Prepared for the
U.S. Department of Energy
Assistant Secretary for
Energy Efficiency and Renewable Energy
Washington, DC

Prepared by
Institute of Gas Technology
1700 S. Mt. Prospect Road
Des Plaines, IL 60018

## DISCLAIMER

Portions of this document may be illegible electronic image products. Images are produced from the best available original document.

RESEARCH SUMMARY

| | |
|---|---|
| Title: | Demonstration of Oxygen-Enriched Air Staging At Owens-Brockway Glass Containers |
| Contractor: | Institute of Gas Technology (contract no. 5095-230-3364<br>Combustion Tec, Inc. - subcontractor<br>Air Products and Chemicals, Inc. - subcontractor |
| Principal Investigators: | H.A. Abbasi, D.M. Rue |
| Report Period: | April 1, 1995 to February 28, 1997 |
| Objective: | The overall objective of this program was to demonstrate the use of a previously developed combustion modification technology to reduce $NO_x$ emissions from sideport regenerative container glass melters.<br><br>A 19-month development program was established with specific objectives to: 1)acquire baseline operating data on the host sideport furnace in Vernon, California, 2) evaluate secondary oxidant injection strategies based on earlier endport furnace results and through modeling of a single port pair, 3) retrofit and test one port pair (the test furnace has six port pairs) with a flexible OEAS system, and select the optimal system configuration, 4) use the results from tests with one port pair to design, retrofit, and test OEAS on the entire furnace (six port pairs), and 5) analyze test results, prepare report, and finalize the business plan to commercialize OEAS for sideport furnaces. The host furnace for testing was an Owens-Brockway 6-port pair sideport furnace in Vernon, California producing 300-ton/d of amber container glass. |
| Technical Perspective: | The U.S. glass industry is reportedly the fourth largest industrial energy consumer. The majority of glass, representing container, flat, pressed, and blown, is produced in large (100 to 1000 ton/day) regenerative glass tanks, which operate continuously for up to 10 years. The glass container segment, representing flint, soda lime, amber, and green glass, accounts for about two-thirds of the total glass produced, and utilizes over 63 billion cubic feet of natural gas per year. Nearly all container and flat glass is produced in two types of regenerative furnaces – endport and sideport. Endport furnaces are smaller (100-400 ton/day) with two ports located on one end of the glass tank. Sideport furnaces are larger (up to 1000 ton/day) with three to seven ports located on either side of the furnace. Container glass production is roughly split between the two furnace types, while nearly all flat glass is produced in sideport furnaces. |

Regenerative glass melters utilize extremely high combustion air preheat temperatures (1800° to 2500°F) to improve production rate, product quality, and furnace thermal efficiency. Furnace and flame temperatures and consequently, $NO_x$ generation, are quite high. $NO_x$ emissions of over 3000 vppm are not uncommon from natural gas-fired glass melters. Although there are no current U.S. national regulations on $NO_x$ emissions, this could change in light of the 1990 Clean Air Act. $NO_x$ emissions are restricted in certain regions of the country, the most stringent restrictions being in Southern California. The South Coast Air Quality Management District currently restricts $NO_x$ emissions from glass melters to 3.3 lb/ton of glass produced. Even stricter regulations are being considered. The glass industry, in some cases, has met regulations through relatively simple combustion modification techniques, developed by IGT and Combustion Tec, Inc. (CTI) with funding support from GRI and SoCalGas, and by increasing the electric boost as well as the percent of cullet in the feed. Some melters have been switched to fuel oil to control $NO_x$. Fuel oil offers somewhat lower $NO_x$ emissions, but at the expense of additional $SO_x$ and particulate emissions, higher fuel system operating costs, and other operating problems. Further, the presence of vanadium and sulfur, and higher crown temperatures from oil firing reduce furnace service life. The high levels of electric boost currently utilized are not desirable because of increased energy costs and reduced furnace service life.

OEAS utilizes a unique method of combustion air staging to control $NO_x$ formation by reducing the oxygen available in the flame's high temperature zone and improving flame temperature uniformity and combustion efficiency. The amount of primary combustion air is reduced to decrease $NO_x$ formation in the flame, and oxygen-enriched air is injected into the furnace near the exit port(s) to complete combustion in a second stage within the furnace. OEAS has been successfully retrofitted to five endport container glass furnaces producing flint and amber glass with capacities of 135 to 320 ton/day. With endport furnace $NO_x$ reduction levels of 50-70%, OEAS showed an excellent potential for similar performance on sideport furnaces. Sideport furnaces are used for nearly 65% of U.S. glass production. The potential for successful OEAS application to sideport furnaces is high, but considerable design effort and development testing were required. Endport and sideport furnaces are similar in concept, but these furnaces are significantly different in physical design and flame characteristics.

Technical Approach:

The development approach used for demonstration of OEAS on the first sideport furnace is indicative of the strategy for extending the

technology to all furnaces to avoid interfering with production. Furnace baseline data was acquired on operations and emissions followed by an evaluation of secondary oxidant injection strategies based on earlier endport results through modeling of a single port pair. OEAS was then tested on one of the six port pairs evaluating a full range of operating conditions and injection locations including side-of-port (inside the exhaust port), underport with one or two injection holes, and furnace crown with one injection hole. Two hole underport injection was determined to be the preferred position for secondary oxidant injection, and the full furnace was retrofit using this strategy. Full furnace testing then followed including parametric testing, long-tern testing, testing with high and low electric boost, and operation with a PLC system controlling OEAS and interfacing with the furnace control system.

Results: CFD modeling demonstrated effective CO burnout can be achieved with OEAS, furnace crown temperatures are not increased, CO emissions decrease with increased staging oxidant injection velocity, thermal efficiency is either unaffected or slightly increased, and side-of-port injection results in CO burnout in the exhaust port instead of over the glass with secondary oxidant not entering the furnace. The single port pair testing showed the best results with enriched air containing 35% oxygen. Testing demonstrated significant $NO_x$ reductions of up to 35%, effective CO burnout, and no exhaust port temperature increase at preferred OEAS operating conditions. Best results were with side-of-port and two hole underport injection. Two hole underport injection was chosen for the full furnace to provide effective CO burnout and to recover the heat from CO burnout inside the furnace over the glass.

Full furnace testing confirmed a 35% $NO_x$ reduction with secondary oxidant containing 30 to 35% oxygen. Preferred furnace conditions with OEAS operating are a primary stoichiometric ratio of 1.02 and an overall stoichiometric ratio of 1.08 to 1.10. This furnace has very low baseline $NO_x$ emissions (without OEAS operating). Therefore, reducing $NO_x$ to as low as 1.8 lb/ton of glass was considered a clear validation of OEAS for this furnace. Greater $NO_x$ reduction is expected for furnaces with higher initial $NO_x$ emission levels.

The furnace operated somewhat differently when firing from the right and left sides. A PLC control system was installed to interface the $NO_x$ control technology with the furnace control system. The PLC allows OEAS to operate with different overall stoichiometric ratios on the two firing sides, provides a smooth touch-screen control interface which gives ease of operation, and connects OEAS to the furnace control system. PLC operation of OEAS provided even

higher $NO_x$ reductions of 35 to 40% since staging on the right and left sides of the furnace can be optimized. OEAS has been operating smoothly on this furnace with PLC control for more than six months providing $NO_x$ reductions of 35% to the furnace operators.

Project Implications:

Successful completion this project has extended the application of OEAS technology to side-port regenerative glass furnaces. To date the technology has been applied only to container glass furnaces. The next step is to apply the technology to flat glass furnaces, provided there is a need and it is technically and economically feasible relative to the other $NO_x$ control technologies for flat glass furnaces.

# EXECUTIVE SUMMARY

This report presents the work performed by the Institute of Gas Technology, and subcontractors Combustion Tec, Inc. and Air Products and Chemicals, Inc., under contract No. DE-FC07-95ID13378 with the U.S. Department of Energy, Idaho Operations Office. Other sponsors for this project included the Gas Research Institute (GRI), the Southern California Gas Co. (SoCalGas), and the IGT Sustaining Membership Program (SMP).

IGT and its commercial partners have developed a technology, oxygen-enriched air staging (OEAS), which has been shown in tests at three commercial endport furnaces to reduce $NO_x$ levels by 50 to 70%. In this program, the OEAS technology has been demonstrated on the other main type of glass furnace, sideport furnaces.

The OEAS technology utilizes a unique method of combustion air staging to control $NO_x$ formation by reducing the oxygen available in the flame's high temperature zone and improving flame temperature uniformity. The amount of primary combustion air entering through the port(s) is reduced to decrease $NO_x$ formation in the flame, and oxygen-enriched air is injected into the furnace near the exhaust port(s) to complete the combustion in a second stage within the furnace. The OEAS technology has been successfully retrofitted to five endport container glass furnaces, including the first three commercial demonstrations followed by two commercial sales.

Owens-Brockway, the largest container glass producer in the United States, has joined the team to test the potential of the OEAS technology and has chosen to demonstrate it on its 300-ton/day, Furnace C, in Vernon, California. The field evaluation is the subject of this project.

For the successful application of the OEAS technology to sideport furnaces, the key development areas are, 1) to provide good mixing of the secondary oxidant with the primary zone combustion products, and 2) to provide the proper secondary oxidant distribution strategy (equally split between the ports or optimized for each port) to minimize overall $NO_x$ emissions and maximize combustible burnout in the second stage within the furnace, while minimizing oxygen (used to enrich the secondary oxidant) consumption. These key areas can only be addressed through development testing on a representative sideport glass furnace.

The development approach was to 1) acquire baseline operating data on the host sideport furnace in Vernon, California; 2) evaluate secondary oxidant injection strategies based on earlier endport results and through modeling of a single port pair; 3) retrofit and test one port pair (the test furnace contains six port pairs) with a flexible OEAS system; 4) based on the results from testing the one port pair (item 3), design, retrofit, and test OEAS on the entire furnace (six port pairs); and 5) analyze test results, prepare report, and finalize the business plan to commercialize OEAS for sideport furnaces.

The modeling work by Air Products and Chemicals, using a FLUENT CFD approach, provided valuable insights into various staging options. Modeling results concluded that OEAS does not increase crown temperatures. CO emissions were calculated to be effectively reduced with staging with CO emissions decreasing with an increase in jet velocity for the same amount of staging air. Side-of-port staging jets were

determined to be incapable of penetrating into the furnace which means all combustible burnout will occur in the exhaust port(s). OEAS arrangements were estimated to not negatively impact furnace thermal efficiency. Furnace thermal efficiencies were not determined to be decreased until the primary stoichiometric ratio is reduced to 0.86. A $NO_x$ reduction of 34% was calculated for side-of-port and two-hole underport injection. Lower $NO_x$ reductions were found for furnace crown and one-hole underport injection. Furnace crown injection was observed to produce secondary oxidant impingement of the glass surface. One-hole underport injection was calculated to cause secondary oxidant-flame interaction and poor port coverage, resulting in higher $NO_x$ and ineffective CO burnout.

The single port testing has shown the best results with OEAS using enriched air with 35% oxygen. Testing demonstrated significant $NO_x$ reduction of up to 35%, effective CO burnout, and no exhaust port temperature increases at preferred OEAS operating conditions. Both two hole underport and side-of-port injection are acceptable OEAS positions. Two-hole underport injection is preferred because high CO burnout is achieved, burnout occurs inside the furnace, and jet-glass impingement or hot spot formation occurs.

The project team evaluated the modeling and single port pair testing results and determined to proceed with two-hole underport injection as the OEAS strategy for the full furnace retrofit. Full furnace parametric testing with OEAS, long-term OEAS testing with high boost and low boost, and testing after installation of the Programmable Logic Controllers (PLC) system were all conducted in this project.

In the parametric test series, the effects of primary stoichiometric ratio (PSR), overall stoichiometric ratio (OSR), staging oxidant oxygen concentration, staging balance between the ports, and different OEAS operation on the two sides of the furnace were evaluated. All secondary oxidant was introduced by two hole underport injection. A low combustion stoichiometric ratio (primary stoichiometric ratio or PSR) of 1.02 was selected as a base condition for conducting OEAS tests. a secondary oxidant oxygen concentration of 35% was selected, and tests were conducted to determine the needed overall stoichiometric ratio (OSR). An OSR of 1.08 to 1.10 was sufficient to burn out the CO produced in the primary flame. The $NO_x$ emissions were decreased more than 30% to an average furnace value of 1.8 lb/ton. The low initial value (4lb/ton) for $NO_x$ kept the decrease low, but even so, the $NO_x$ level with OEAS operating is extremely low. Testing showed the two sides of the furnace were not identical.

Long-term, full furnace OEAS tests were conducted in which the primary stoichiometric ratio was decreased to 1.02 and staging was employed at an OSR (overall stoichiometric ratio) of 1.10. The OEAS was operated continuously and monitored for 48 hours. The $NO_x$ emission levels dropped approximately 35% to 2.3 lb/ton while CO emissions remained low. A test series was conducted with pull rate held constant while electric boost was reduced by one third and natural gas consumption was increased by 10 percent. Exhaust gas temperature, crown temperature, and $NO_x$ level all increased. The same level of $NO_x$ reduction (30 to 35%) was achieved at low boost as was achieved at high boost. $NO_x$ levels with OEAS operating were higher since initial $NO_x$ levels were higher with low boost.

A PLC system was installed to control the OEAS system. An operations manual was prepared, and furnace operators were trained in OEAS operation. The project team conducted tests to set optimum OEAS operating conditions with the PLC controlling the system . $NO_x$ reductions as high as 40% were achieved. The OEAS system was left operating at conditions which provided the highest possible $NO_x$ reduction while using oxygen at a rate acceptable to the plant and using a level of secondary air in the center of the blower skid's range. The average $NO_x$ emission from the furnace was 2.5 lb/ton at the end of the week, after optimizing the OEAS system.

The final work in this project was to prepare a business plan for OEAS on sideport furnaces. This business plan is an update of the OEAS business plan for endport furnaces.

TABLE OF CONTENTS


| | Page |
|---|---|
| INTRODUCTION | 1 |
| BACKGROUND | 2 |
| $NO_x$ From Glass Tanks | 2 |
| Oxygen-Enriched Air Staging (OEAS) | 3 |
| Sideport and Endport Furnaces | 5 |
| OEAS Field Evaluation | 6 |
| HOST FURNACE DESCRIPTION | 9 |
| SINGLE PORT PAIR MODELING | 10 |
| RETROFIT DESCRIPTION | 14 |
| OEAS Background and Description | 14 |
| Retrofit Design Basis | 15 |
| Retrofit System Components | 16 |
| Test Instrumentation | 18 |
| Gas Sampling | 18 |
| Temperature Measurements | 22 |
| FIELD EVALUATION TESTS AND RESULTS | 24 |
| Furnace Baseline Parameters | 24 |
| OEAS System Parameters | 26 |
| Emissions | 26 |
| Description of Tests | 27 |
| Discussion of Results | 27 |
| Single Port Pair Testing | 27 |
| Full Furnace Parametric Testing | 30 |
| Full Furnace Long-Term Testing | 35 |
| Testing at Reduced Electric Boost | 38 |
| Testing with PLC controlling OEAS system | 40 |
| CONCLUSION AND RECOMMENDATIONS | 42 |
| REFERENCES | 45 |
| APPENDIX A. SINGLE PORT PAIR MODELING | A1 |
| APPENDIX B. OEAS SYSTEM DESCRIPTION AND OPERATION | B1 |
| APPENDIX C. OEAS FIELD EVALUATION TESTS | C1 |
| APPENDIX D. BUSINESS PLAN | D1 |

LIST OF FIGURES


| Figure | | Page |
|---|---|---|
| 1 | EFFECT OF FIRST-STAGE STOICHIOMETRIC RATIO ON $NO_x$ EMISSIONS | 4 |
| 2 | EFFECT OF FIRST STAGE STOICHIOMETRIC RATIO ON HEAT TRANSFER | 5 |
| 3 | OXYGEN-ENRICHED AIR STAGING FOR ENDPORT GLASS MELTING FURNACE | 6 |
| 4 | OXYGEN-ENRICHED AIR STAGING FOR SIDEPORT GLASS MELTING FURNACE | 6 |
| 5 | OWENS-BROCKWAY GLASS CONTAINER PLANT, VERNON, CALIFORNIA | 9 |
| 6 | MATERIAL AND ENERGY STREAMS (SANKEY) DIAGRAM FOR THE SIDE-OF-PORT OEAS ARRANGEMENT | 11 |
| 7 | MODELED REGION: FRONT VIEW. CROWN, UNDERPORT AND SIDE-OF-PORT INJECTIONS | 11 |
| 8 | MODELED REGION: TOP VIEW. SIDE-OF-PORT INJECTIONS ARE ANGLED TOWARD THE EXHAUST FLOW | 12 |
| 9 | STAGING COMBUSTION WITH SIDE-OF-PORT OEAS | 13 |
| 10 | SCHEMATIC DRAWING OF THE GAS SAMPLING PROBE ASSEMBLY | 19 |
| 11 | PROBE USED TO COLLECT GAS SAMPLES FROM THE REGENERATOR | 20 |
| 12 | GAS SAMPLING PROBE INSTALLED IN THE REGENERATOR | 20 |
| 13 | FLOW CONTROL AND DISTRIBUTION PANEL | 22 |
| 14 | CONTINUOUS EMISSIONS MONITORING SYSTEM (CEMS) | 23 |

| | | |
|---|---|---|
| 15 | THE EFFECT OF REDUCED STOICHIOMETRIC RATIO ON $NO_X$ | 28 |
| 16 | THE EFFECT OF REDUCED STOICHIOMETRIC RATIO ON CO | 29 |
| 17 | EFFECT OF ENRICHED AIR (35%) STAGING ON $NO_x$ AT PORT 5 | 29 |
| 18 | EFFECT OF ENRICHED AIR (35%) STAGING ON CO AT PORT 5 | 30 |
| 19 | THE EFFECT OF OVERALL STOICHIOMETRIC RATIO (OSR) ON $NO_X$ AND CO EMISSIONS WITH NO STAGING | 31 |
| 20 | $NO_X$ EMISSIONS AT HIGH BOOST DURING PARAMETRIC TESTING - LEFT SIDE FIRING | 32 |
| 21 | $NO_X$ EMISSIONS AT HIGH BOOST DURING PARAMETRIC TESTING - RIGHT SIDE FIRING | 33 |
| 22 | THE EFFECT OF ENRICHED AIR STAGING ON $NO_X$ AND CO EMISSIONS | 34 |
| 23 | THE EFFECT OF OEAS OXYGEN CONCENTRATION ON $NO_X$ AND CO EMISSIONS | 35 |
| 24 | $NO_X$ EMISSIONS AT HIGH BOOST DURING LONG-TERM TESTING - LEFT SIDE FIRING | 37 |
| 25 | $NO_X$ EMISSIONS AT HIGH BOOST DURING LONG-TERM TESTING - RIGHT SIDE FIRING | 37 |
| 26 | $NO_X$ EMISSIONS AT LOW BOOST - LEFT SIDE FIRING | 39 |
| 27 | $NO_X$ EMISSIONS AT LOW BOOST - RIGHT SIDE FIRING | 40 |
| 28 | $NO_X$ EMISSIONS WITH PLC CONTROLLING THE OEAS | 41 |
| 29 | CO EMISSIONS WITH PLC CONTROLLING THE OEAS | 41 |

LIST OF TABLES


| Table | | Page |
|---|---|---|
| 1 | COMMERCIAL GLASS MANUFACTURING (1992) (GRI-IUPAG, Feb95) | 7 |
| 2 | OEAS SYSTEM HARDWARE DESCRIPTION | 16 |
| 3 | BASELINE FURNACE EMISSIONS DATA | 25 |
| 4 | OEAS SIDEPORT DEMONSTRATION TEST CAMPAIGNS | 27 |
| 5 | ECONOMICS OF LOWERING ELECTRIC BOOST WITH OEAS OPERATION ON A TYPICAL REGENERATIVE SIDEPORT GLASS FURNACE | 38 |

# INTRODUCTION

The objective of the program was to demonstrate the use of a previously developed combustion modification technology to reduce $NO_x$ emissions from sideport regenerative container glass melters. This technology, known as oxygen-enriched air staging (OEAS), has been demonstrated, and is now being commercialized, for endport container glass furnaces. A 19-month development program was conducted with specific objectives to: 1) acquire baseline operating data on the host sideport furnace in Vernon, California, 2) evaluate secondary oxidant injection strategies based on earlier endport furnace results and through modeling of a single port pair, 3) retrofit and test one port pair (the test furnace has six port pairs) with a flexible OEAS system, and select the optimal system configuration, 4) use the results from tests with one port pair to design, retrofit, and test OEAS on the entire furnace (six port pairs), and 5) analyze test results, prepare report, and finalize the business plan to commercialize OEAS for sideport furnaces. The host furnace for testing in this program was an Owens-Brockway 6-port sideport furnace in Vernon, California producing 300-ton/d of amber container glass. The baseline $NO_x$ level of this optimized furnace is about 4.0 lb/ton of glass. Secondary oxidant staging techniques considered included oxygen-enriched ambient air staging (OEAS), ambient air staging, and oxygen staging (OS).

The OEAS technology utilizes a unique method of combustion air staging to control $NO_x$ formation by reducing the oxygen available in the flame's high temperature zone and improving flame temperature uniformity and combustion efficiency. The amount of primary combustion air entering through the ports is reduced to decrease $NO_x$ formation in the flame, and oxygen-enriched air is injected into the furnace near the exit port to complete combustion in a second stage within the furnace. The OEAS technology has been successfully retrofitted to five endport container glass melting furnaces; a 150 ton/d endport glass tank producing flint glass in Huntington Park, California, a 200 ton/d endport glass tank producing amber glass in Houston, Texas, and a 320 ton/day endport glass tank producing flint glass in Huntington Park, California and two 135 ton/day amber glass furnaces in Colorado. With endport furnace $NO_x$ reduction levels of 50-70%, the OEAS technology showed an excellent potential for similar performance on sideport furnaces. Sideport furnaces are used for nearly 65% of U.S. glass production. Although the potential successful application of OEAS to sideport furnaces is high, considerable design effort and development testing were required. Endport and sideport furnaces are similar in concept, but these furnaces are significantly different in physical design and flame characteristics.

The project team consisted of IGT, which originated the concept and was the prime contractor, and the following subcontractors: Combustion Tec. Inc. (CTI), combustion equipment manufacturer and commercialization partner; Air Products and Chemicals, Inc. (APCI), $O_2$ supplier and commercialization partner; and Owens-Brockway Glass Containers, glass producer, and owner of the host site.

## BACKGROUND

The glass industry in the United States is reportedly the fourth largest industrial energy consumer. The majority of glass, representing container, flat, pressed, and blown, is produced in relatively large (100 to 1000 ton/day) regenerative glass tanks, which operate continuously for up to 12 years. The glass container (soda-lime) segment alone, representing flint, amber, and green glass, accounts for about two-thirds of the total glass produced, and utilizes over 63 billion cubic feet of natural gas per year. Nearly all of the container and flat glass is produced in two types of regenerative furnaces -- endport and sideport. Endport furnaces are smaller (100-400 ton/day) with two ports located on one end of the glass tank. Sideport furnaces are larger (up to 1000 ton/day) with three to seven ports located on either side of the furnace. Container glass production is roughly split between the two furnace types, while nearly all of the flat glass is produced in sideport furnaces. A typical container glass furnace uses about $5 \times 10^6$ Btu of energy per ton of glass produced, while a typical flat glass furnace uses about $7 \times 10^6$ Btu. Overall, endport glass tanks consume 25 billion cubic feet of fuel to produce 5 million tons of glass, while sideport glass tanks consume 53 billion cubic feet of fuel to produce 9 million tons of glass. The bulk of the fuel used is natural gas, which is the fuel of choice. However most of the glass furnaces utilize electric boosting and a few use fuel oil. In this application, fuel oil produces somewhat lower $NO_x$ than natural gas. Fuel oil, however, also produces $SO_x$, which may require additional exhaust gas cleaning equipment.

### $NO_x$ From Glasses Tanks

The regenerative glass melters utilize extremely high combustion air preheat temperatures (1800° to 2500°F) to improve production rate, product quality and furnace thermal efficiency. Furnace and flame temperatures and, consequently, $NO_x$ generation, are quite high. $NO_x$ emissions of over 3000 vppm are not uncommon[1,2] from natural gas-fired glass melters. Although, currently, there are no national regulations on $NO_x$ emissions in the U.S., this could change in light of the 1990 Clean Air Act. On a regional basis, these emissions are restricted in certain areas, the most stringent restrictions being in Southern California. The South Coast Air Quality Management District currently restricts the $NO_x$ emissions from glass melters to 4.0 lb/ton of glass produced. Even stricter regulations are now being considered for this region. The glass industry, in some cases, has been able to meet the current regulations through relatively simple combustion modification techniques, developed earlier[3,4] by IGT and Combustion Tec, Inc. (CTI) with funding support from GRI and SoCalGas, and by increasing the electric boost as well as the percent of cullet in the feed. Some melters have been switched to fuel oil to control $NO_x$. Fuel oil does offer somewhat lower $NO_x$ emissions, but at the expense of additional $SO_x$ and particulate emissions, higher fuel system operating costs, and other operating problems. Further, the presence of vanadium and sulfur, and the higher crown temperatures that result from oil firing somewhat reduce the furnace service life.[5] The high levels of electric boost currently utilized are also not desirable because of increased energy costs and reduced furnace service life.

It should be noted that in recent years, there have been some significant activities toward developing pure oxygen/natural gas-fired combustion technologies for glass

melters because of the potential for significant $NO_x$ reduction when compared to current regenerative glass melters. Emission levels below 1 lb/ton $NO_x$ may be obtained if high purity oxygen is employed. This, however, usually results in a significant increase in operating cost and product price. One solution is to use industrial oxygen (95% - 96% purity), which can be produced on site and thus is significantly less expensive than pure oxygen. $NO_x$ emissions, however, are then substantially higher, once again requiring advanced technologies, such as those proposed, to achieve the required $NO_x$ emission levels. There are also questions about the effect of oxygen use on furnace service life, cost benefits (even with industrial oxygen), and timing. It is not clear that existing regenerative glass tanks, which normally operate continuously for about 8 years between repair and modifications, would, before the end of this century, be economically converted to pure oxygen/natural gas firing. This approach, however, has significant potential to capture a larger share of the market in the long term.

The only currently available retrofit technologies for $NO_x$ reduction for glass tanks are selective non-catalytic reduction (SNCR), selective catalytic reduction (SCR) and wet scrubbers, in increasing levels of $NO_x$ reduction (50%, 90%, and >95%, respectively) and cost. The lowest cost technology, SNCR, can reduce $NO_x$ by 50% at a cost of $2000/ton of $NO_x$ removed, for a typical 250 ton/day glass tank. This represents $365,000 annually, or an increase in glass production fuel costs by 20%. Furthermore, SNCR suffers from a number of drawbacks including $NH_3$ slip, hazards of storing $NH_3$, and the potential for higher CO, $N_2O$, and particulate emissions. There is, therefore, a need to develop advanced lower cost low-$NO_x$ technologies for retrofit to natural gas-fired regenerative glass melters.

Oxygen-Enriched Air Staging (OEAS)

Combustion air staging is accomplished by reducing the combustion air flow (primary air) to the port and injecting secondary oxidant (air, oxygen-enriched air, or oxygen) downstream. The bulk of the combustion is relatively oxygen deficient (or even fuel-rich) to inhibit $NO_x$ formation.

Splitting the combustion air in a regenerative glass tank is difficult because 1) it can require major modifications and 2) properly mixing the secondary air with the primary combustion gases requires higher secondary air pressures that are not desirable. A more attractive method is to operate the furnace with near-stoichiometric air and inject a small amount of high-velocity preheated (or ambient) secondary oxidant near the exit port to burn out any residual CO and total hydrocarbons (THC). This method of air staging was tested by IGT on its glass tank simulator using ambient secondary air and on two endport furnaces in Huntington Park, California and an endport furnace in Houston, Texas,[6,7] using somewhat different approaches. In all cases, air staging was found to be very effective in reducing $NO_x$ emissions.

Figure 1, representing data obtained on the IGT Glass Tank simulator and commercial furnaces (endport and sideport), shows that, in a furnace operating with a typical stoichiometric ratio of 1.15 (15% overall excess air), a $NO_x$ reduction of 32% (from the current 4 lb/ton to 2.7 lb/ton) could be achieved by operating the port at a

stoichiometric ratio of 1.04 to 1.06 which should not be very difficult. In the tests at IGT, there was a significant increase in heat transfer (Figure 2) at this level of primary air even though the secondary air was ambient and was injected downstream of the exhaust port. The data also show that even greater $NO_x$ reduction can be achieved by further decreasing the primary stoichiometric ratio. The heat transfer would, however, decrease somewhat compared to the optimum at a stoichiometric ratio of 1.04 to 1.06 and would be comparable to levels achieved at 15% excess air.

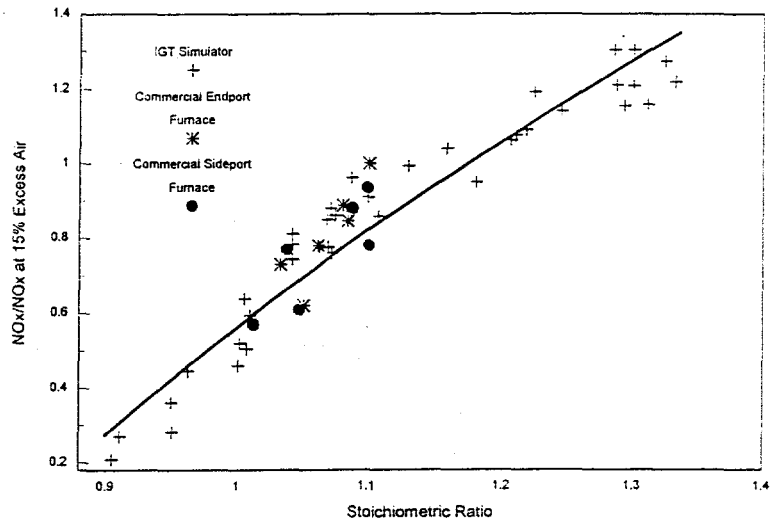


Figure 1. EFFECT OF FIRST-STAGE STOICHIOMETRIC RATIO ON $NO_x$ EMISSIONS

(IGT Glass Tank Simulator)

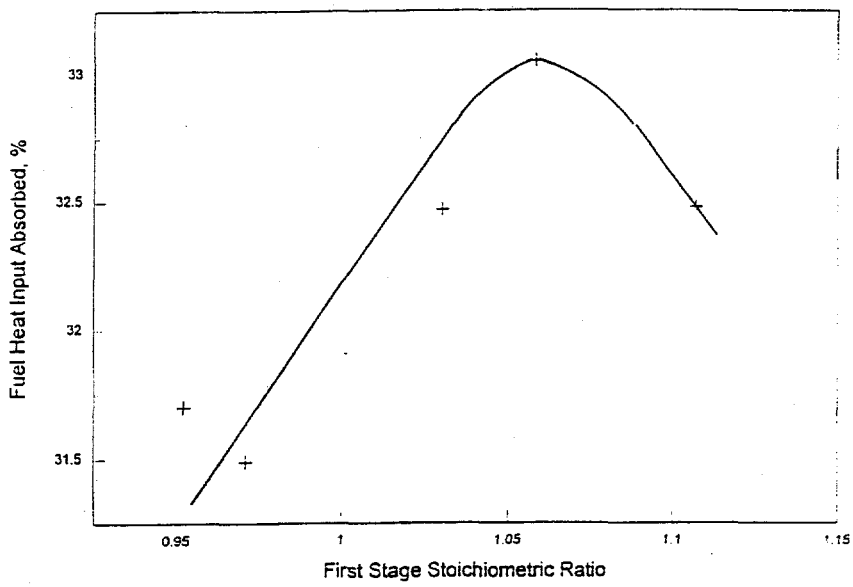


Figure 2. EFFECT OF FIRST STAGE STOICHIOMETRIC RATIO ON HEAT TRANSFER

Sideport and Endport Furnaces

The numbers of endport and sideport furnaces, their operating characteristics and capacities, and their combustion properties are discussed elsewhere in this report. Figures 3 and 4 depict implementation of oxygen-enriched air staging on these two types of furnaces. Both drawings provide top-down views of melters showing the glass tank, the regenerators, the flames, and the OEAS systems. The application of OEAS is similar on both types of furnaces with added complexity on sideport furnaces. Engineering efforts must be applied on sideport furnaces to balance the staging to all ports and to allow CO burnout above the glass inside the furnace and away from the primary flame.

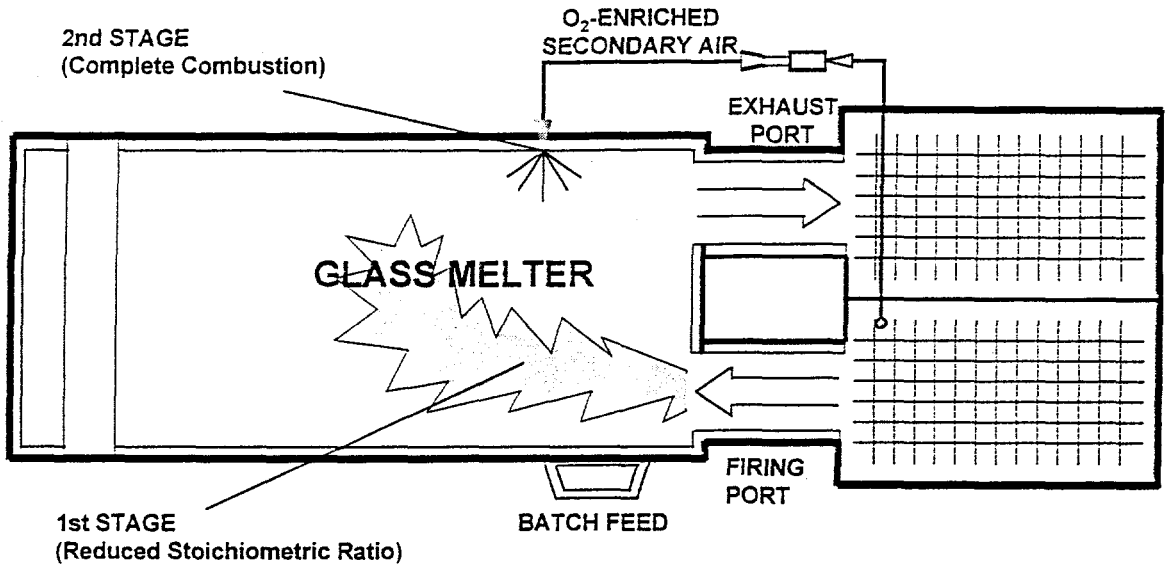


Figure 3. OXYGEN-ENRICHED AIR STAGING FOR ENDPORT GLASS MELTING FURNACE

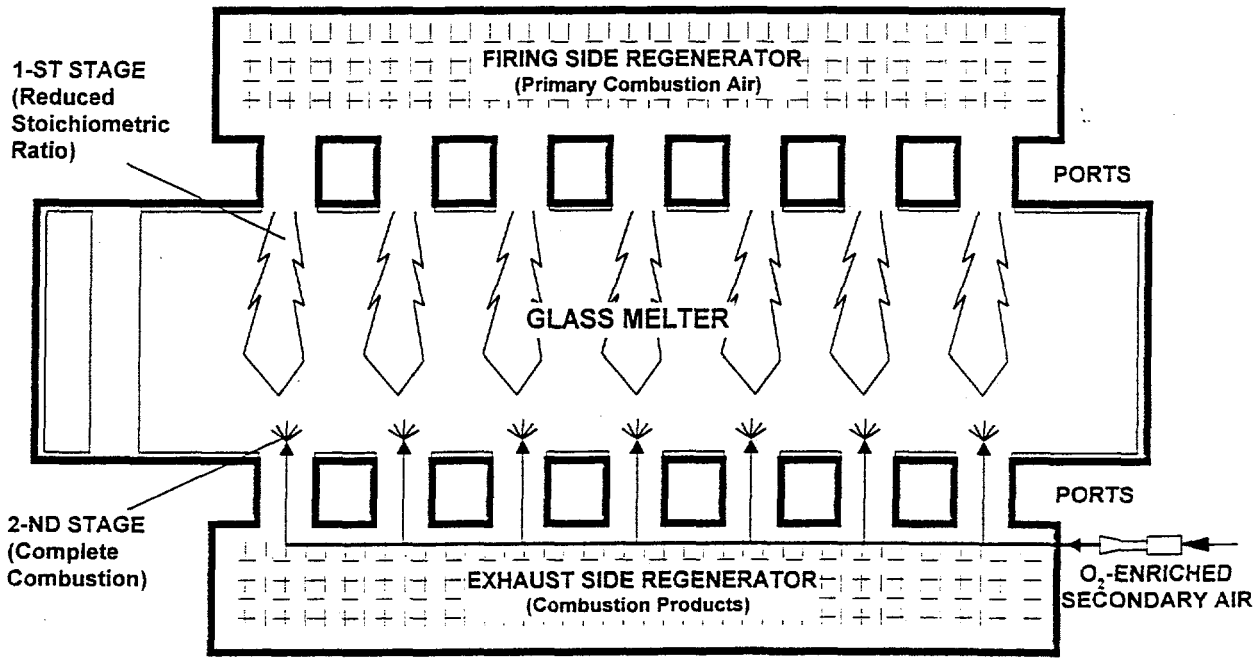


Figure 4. OXYGEN-ENRICHED AIR STAGING FOR SIDEPORT GLASS MELTING FURNACE

OEAS Field Evaluation

Although OEAS had been applied only to endport furnaces before this project, it showed very good potential for similar performance on sideport furnaces. Table 1 shows sideport furnaces represent one-half of regenerative container glass and all of regenerative flat glass production in the U.S. Because of unique challenges posed by sideport furnaces, additional development effort carried out through field evaluation testing on a

sideport furnace was required before the OEAS technology can be commercialized for these furnaces. Several key technical areas must be addressed.

Sideport furnaces have relatively longer flames (as a proportion of the available combustion products flow path) resulting in elevated CO levels in the exhaust ports as compared to endport furnaces. This means that when OEAS is applied to a sideport furnace, and the amount of primary air is decreased, the level of CO entering the second stage may be higher, and the residence time available in the second stage for burnout of this CO is lower, as compared to endport furnaces. In both the endport and IGT simulator tests , CO was rapidly burned out. However, it was determined that, because of the very high temperatures (2800°F+) near the exhaust port, the main parameter that controls CO burnout in OEAS is the mixing of secondary oxidant with the primary zone combustion products. This was a focus area in designing the secondary oxidant injection system for this project. When the secondary oxidant is properly mixed with the primary zone combustion products, upstream of the exhaust port, the CO can be effectively burned out within the furnace. The secondary oxidant injection location, injection angle, and injection velocity were modeled using Air Products' existing glass furnace combustion/aerodynamics model. Selected OEAS strategies were tested through parametric tests on one port pair in the host furnace prior to retrofitting the entire furnace.

Table 1. COMMERCIAL GLASS MANUFACTURING (1992)
(GRI-IUPAG, Feb95)

| | No. of Plants | Tons per Day | Furnaces | Regenerative Sideport | Regenerative Endport. | Unit Furnaces | OxyFuel | All Elec. |
|---|---|---|---|---|---|---|---|---|
| Container | 68 | 48,000 | 154 | 68 | 66 | -- | 13 | 7 |
| Flat | 29 | 19,000 | 38 | 36 | -- | -- | 1 | 1 |
| Wool Fiber | 24 | 1,400 | 58 | -- | -- | 16 | 5 | 37 |
| Textile Fiber | 12 | 2,100 | 60 | -- | -- | 47 | 6 | 7 |
| Lighting/TV | 19 | 3,000 | 60 | 19 | -- | 30 | 9 | 2 |
| Press & Blown | 31 | 3,400 | 95 | 32 | 10 | 33 | 11 | 9 |
| Sodium Silicate | 24 | 4,500 | 25 | 20 | -- | 5 | -- | -- |
| Total | 207 | 81,400 | 490 | 175 | 76 | 131 | 45 | 63 |

The air/fuel stoichiometric ratios vary among the different sideport furnace ports, and the extent of this variation may change at different furnace pull rates. This is actually of much less concern for an OEAS application than for other technologies, such as reburning (in which reducing conditions must be created in each exhaust port), or cascade firing (in which fuel staging must be fine-tuned on each port).

As illustrated in Figure 1, $NO_x$ formation decreases with decreasing stoichiometric ratio over a wide range from 1.4 (40% excess air) to 0.85 (15% deficient air). Therefore, regardless of the level of the baseline stoichiometric ratio, $NO_x$ will always decrease as the stoichiometric ratio is decreased. For example, if one port operates at a baseline stoichiometric ratio of 1.2 and another at 1.0 and if secondary oxidant is used to reduce the primary air by 0.15 stoichiometric ratio, then the $NO_x$ level on the two ports will decrease by 35% and 70% (Figure 1) respectively, or an average of over 50%.

With OEAS, therefore, it is not necessary to fine-tune the level of secondary oxidant for each port. In all cases, the $NO_x$ level at each exit port will decrease upon reduction of the primary stoichiometric ratio. The overall $NO_x$ reduction can be expected to be consistent with the overall reduction in the primary stoichiometric ratio. The fully controllable level of secondary oxidant flow to each port can provide an even greater $NO_x$ reduction (deeper staging on high $NO_x$ producing ports and less staging in already lower $NO_x$ ports) and better heat release profile to improve the overall glass melting furnace performance. This can reduce $NO_x$ while improving energy efficiency and increasing furnace productivity.

In sideport furnaces, there is an unknown amount of cross flow of combustion gases within the furnace and in the top of the regenerator. This is not expected to cause problems with OEAS. Depending on the level of cross flow, which in general is not substantial, some ports might operate slightly richer (greater $NO_x$ reduction) and some ports slightly leaner (smaller $NO_x$ reduction) than indicated by port or regenerator top $O_2$ measurements. The average $NO_x$ reduction, however, should be consistent with the overall reduction in the primary combustion air flow ratio.

Based on the above discussion, it appears that the OEAS technology has very good potential to reduce $NO_x$ levels in sideport furnaces, while also improving furnace efficiency and production rate.

The key development areas are to:

1) Provide good mixing of the secondary oxidant with the primary zone combustion products,

2) Provide the proper secondary oxidant distribution strategy to minimize overall $NO_x$ emissions and maximize combustible burnout within the furnace, with a minimum consumption of added oxygen.

These key areas could only be addressed through development testing on a representative sideport glass furnace, which was conducted in this program. Considerable design effort and development testing were required to address the above issues and commercialize OEAS for $NO_x$ reduction from sideport furnaces.

With successful demonstration on a sideport furnaces, the OEAS technology is now applicable to all regenerative furnaces used for glass production. Table 1 lists these furnaces which represent 76% of container and flat, one-third of lighting/TV, nearly one-half (mostly larger ) of press and blown, and 80% (mostly larger) of sodium silicate glass furnaces, and account for nearly 90% of all glass produced in the U.S.

## HOST FURNACE DESCRIPTION

This program was the first demonstration of the OEAS technology for $NO_x$ reduction on a sideport container glass furnace. Owens-Brockway Glass Containers allowed Furnace C at their plant in Vernon, California (shown in Figure 5) to serve as host site for this demonstration. Plant and corporate support from Owens-Brockway was invaluable in the successful completion of this field demonstration. The host furnace has six port pairs and produces 300 ton/day of amber container glass. Single pass regenerators located on both sides of the furnace yield preheated air for combustion with natural gas. Burner and port designs are proprietary to Owens-Brockway. Electrodes immersed in the molten glass are used to control melt mixing patterns and to provide additional heat to the furnace.

The plant currently has two operating furnaces and operating $NO_x$ analyzers. Data from project stack measurements could not be compared with plant data because the plant emissions monitoring system measures the exhaust gases from two furnaces after they have been sent to a common manifold.

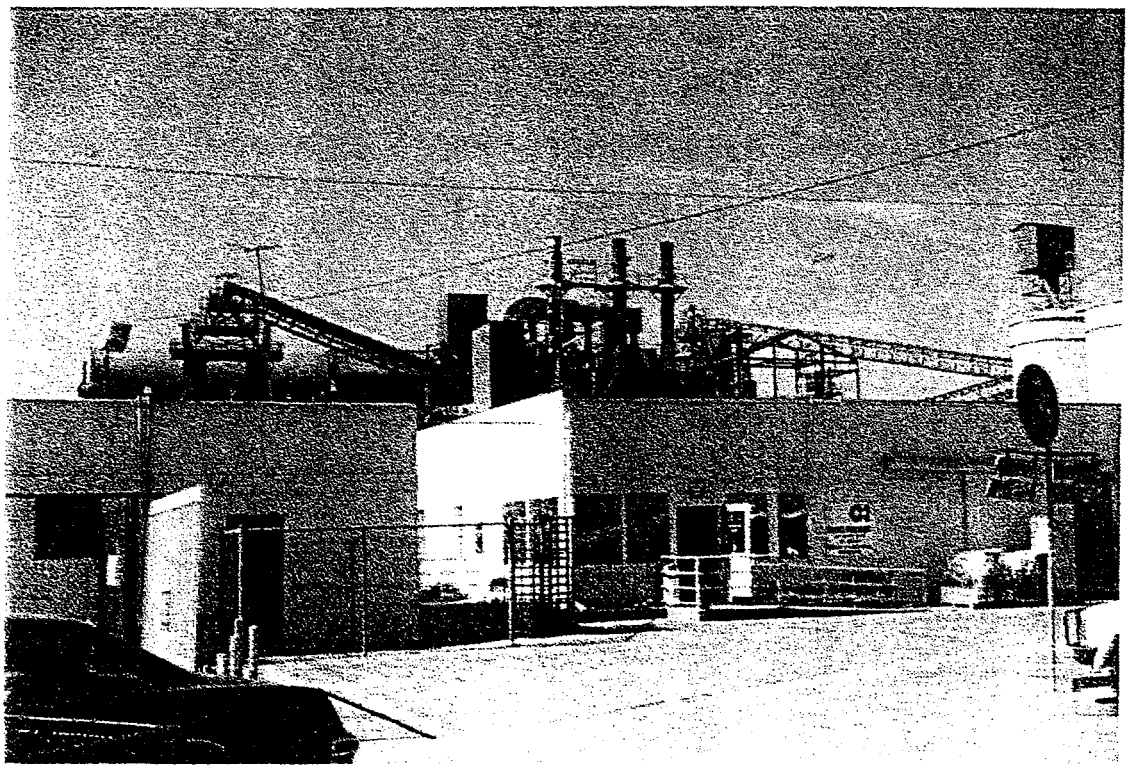

Figure 5. OWENS-BROCKWAY GLASS CONTAINER PLANT, VERNON, CALIFORNIA

## SINGLE PORT PAIR MODELING

Prior to the implementation of OEAS on a single port pair of the sideport furnace, several staging options were examined. Detailed results of the modeling work are presented in Appendix A, Single Port Pair Modeling. Modeling work was conducted by Air Products and Chemicals, Inc. using a FLUENT computational fluid dynamics package. The draft report of the modeling work was provided to IGT, CTI, and Owens-Brockway for review. The final modeling report, presented in the Appendix, includes responses to questions raised by the draft report. This process expanded the scope of the modeling effort but allowed the project team, including the host site owner, to obtain a much detail as possible concerning critical aspects of the OEAS application to the Owens-Brockway furnace.

Variables that had to be considered in the modeling effort were the amount of $O_2$ in the staging oxidant, the velocity of the oxidant, and the location and number of staging jets. Logistically, it was convenient to introduce the staging oxidant through backup oil burner ports from the two sides of the port neck ("side-of-port") because no modification to the melter was required. However, this injection strategy might not achieve effective CO burnout, and the secondary combustion might not take place inside the melter. To gain insight into these issues and, in general, to eliminate a number of the variables prior to field testing, Air Products and Chemicals, Inc. conducted extensive computational modeling.

Material and energy balances were performed at a system level to assess the gross effects of OEAS and particularly, the impact of lowering the primary stoichiometric ratio (PSR) from 1.1 to 0.95 on overall furnace efficiency. The two regenerators were included in the analysis, as illustrated in Figure 6. Under the new PSR conditions, it was determined that the amount of preheat air through the regenerator decreases while the preheat air temperature increases by approximately 70°F. The analysis further showed that the thermal efficiency of the melter remains the same or improves slightly; however, if the PSR is reduced below 0.86, there will be a penalty to thermal efficiency. At the PSR selected for $NO_x$ reduction, the furnace efficiency is not expected to be negatively affected.

Information from the thermodynamic analysis was used in a detailed computational fluid dynamics (CFD) model of the number 5 port area of the melter. The model incorporates the two-equation $k-\varepsilon$ turbulence model of Launder and Spalding.[8] Radiation heat transfer is computed with the discrete transfer radiation model (DTRM) by Shah.[9] This model solves the radiative transfer equation directly along discrete rays emanating from all surfaces and is highly desirable for natural gas-air flames due to their relative transparency. A two-step chemical reaction mechanism describes the combustion kinetics and the Magnussen-Hjertager[10] model takes into account the turbulence-chemistry interactions. All physical properties of the mixture are computed from individual species properties which are functions of temperature as described in the JANAF tables.

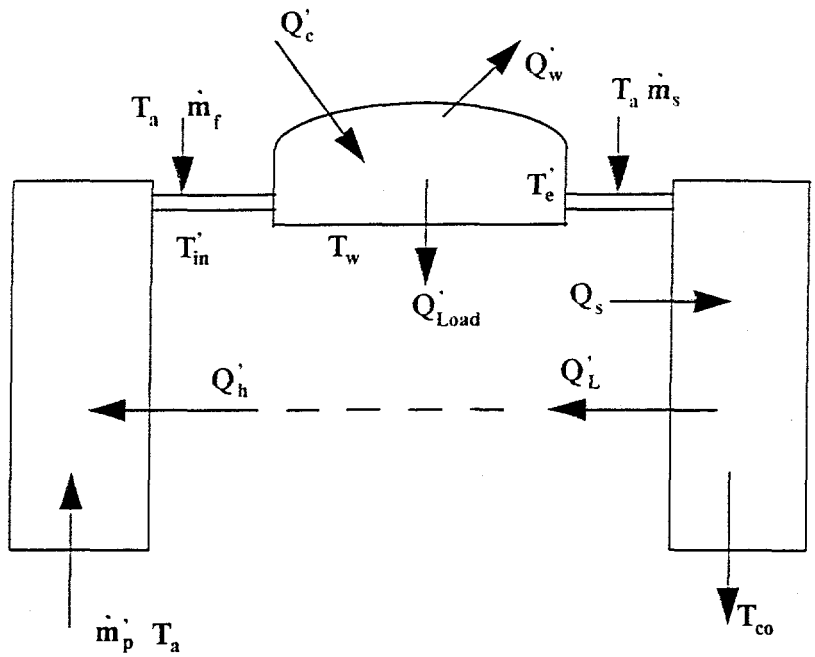


Figure 6. MATERIAL AND ENERGY STREAMS (SANKEY) DIAGRAM FOR THE SIDE-OF-PORT OEAS ARRANGEMENT

The governing equations for the conservation of mass, momentum, energy and chemical species are solved with the FLUENT software package.[11] It uses a control volume based finite difference scheme where nonlinear variations of dependent variables are included inside each control volume to ensure physically realistic results even on relatively coarse grids. The current CFD model (region of the #5 port pair as shown in Figures 7 and 8) has approximately 62,000 grid control volumes. A nonuniform grid was employed so that regions of high gradients would have denser mesh. It was important, for example, that the staging nozzle regions have enough grid density to ensure accurate predictions of jet penetration and mixing.

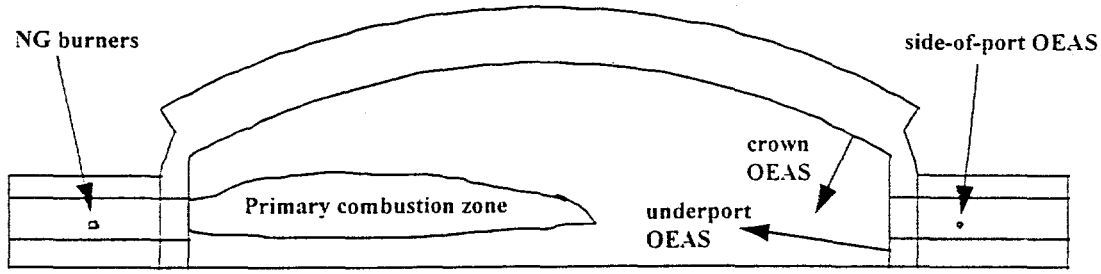


Figure 7. MODELED REGION: FRONT VIEW. CROWN, UNDERPORT AND SIDE-OF-PORT INJECTIONS

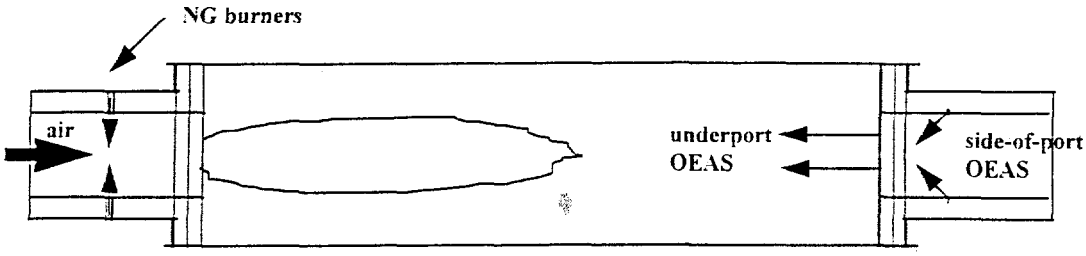


Figure 8. MODELED REGION: TOP VIEW. SIDE-OF-PORT INJECTIONS ARE ANGLED TOWARD THE EXHAUST FLOW

The current operating conditions were modeled starting with the baseline case, which established the datum for comparison. Next, OEAS with side-of-port staging injection at three jet velocities was evaluated. The PSR was changed from 1.10 to 0.95 while the overall stoichiometric ratio (OSR) remained at 1.10; oxygen enrichment for the staging injection was set at 35%. The model output revealed that peak temperatures on the melter crown and breastwalls should remain essentially the same while temperature distributions within the port neck through the target wall region would remain within the normal temperature band defined by the reversals of the regenerators. It was also determined that complete CO destruction could be achieved at high jet velocities (approximately 300 ft/s). Relative to the assumed baseline level of 3.7 lb per ton, $NO_x$ formation was predicted to decrease by at least 34%. However, secondary combustion is shown to occur completely within the exhaust port, as shown in Figure 9. This prediction is consistent with the experimental data of Platten and Keffer[12] who studied the extent of penetration of jets into a uniform stream at various angles in a low speed wind tunnel under isothermal conditions. For maintained thermal efficiency, it is highly desirable that secondary combustion take place inside the melter. This created a need to explore alternate injection strategies.

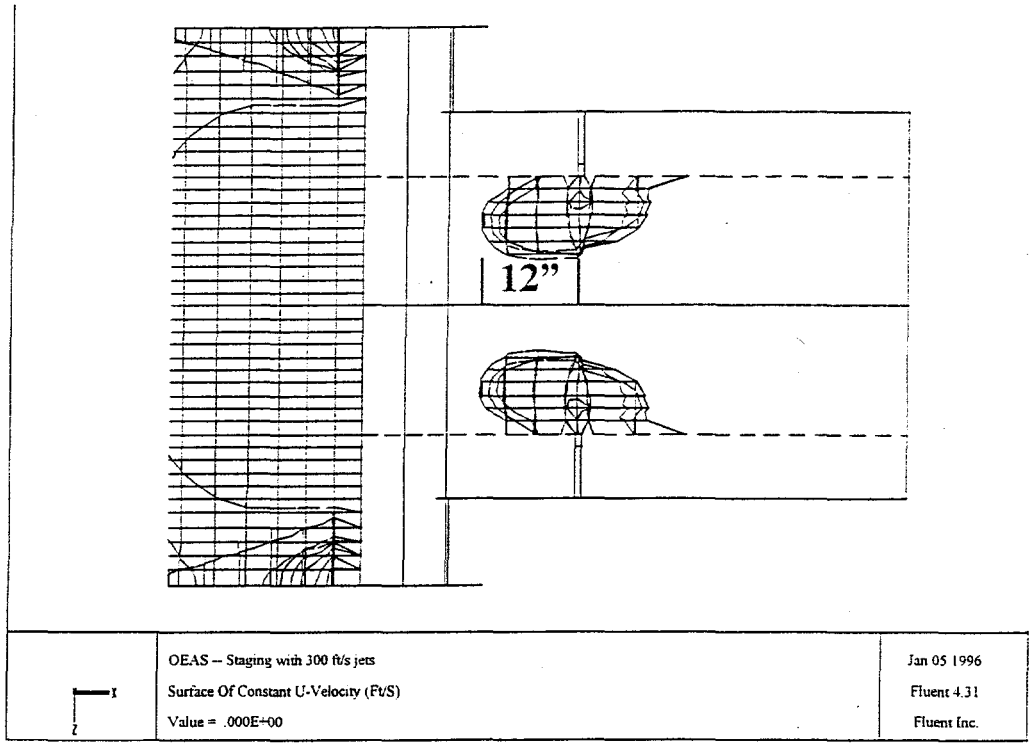


Figure 9. STAGING COMBUSTION WITH SIDE-OF-PORT OEAS

Possible alternate injection locations considered were from the crown and under the port. Crown access is unacceptable to many operators due to safety and refractory life concerns. The location was explored, however as it appeared reasonable that superior staging oxidant coverage of the pre-exhaust port combustion space would be provided. Under-port injection has fewer safety risks but is an intuitively questionable choice since direct opposition to the exhaust flow might again cause jet penetration to be limited. To quantitatively evaluate these options, three models were examined: crown injection with one nozzle, underport injection with one nozzle, and underport injection with two nozzles. The results revealed that while crown injection recovers more than 90% of the energy due to secondary combustion, only about 21% $NO_x$ reduction (as compared to more than 34%) is achieved due possibly to interaction between the staging oxidant and the primary combustion zone. In addition, crown injection intersects the exhaust flow almost perpendicularly, penetrates the combustion gases, and causes flow impingement on the glass bath. Although the single-nozzle underport option does not cause impinging flow to the glass bath, $NO_x$ reduction is similar to that of the crown option. Overall, underport injection with two nozzles was found to be the best staging option considered. Heat recovery is substantial. $NO_x$ reduction is similar to the side-of-port option. Furthermore, there is no physical influence on the glass bath or impact on the main combustion zone. These findings were corroborated by the testing results.

## RETROFIT DESCRIPTION

The OEAS concept essentially involves reducing the amount of primary combustion air at the firing port, and injecting a secondary oxidant (ambient or hot air, oxygen-enriched hot or ambient air or industrial oxygen) downstream of the primary flame (near the exhaust port) to complete the combustion. This section describes retrofit design basis, the retrofit components, and the test instrumentation.

### OEAS Background and Description

Oxygen-enriched air staging is accomplished by reducing the combustion air flow (primary air) to the primary flame zone and injecting secondary oxidant into the furnace near the exhaust port. The staging positioning is selected to mix the secondary oxidant with the products of combustion downstream of the primary flame zone. The bulk of the combustion is relatively oxygen-deficient (or even fuel rich) which inhibits $NO_x$ formation, and the secondary oxidant burns out the remaining CO and hydrocarbon combustibles. In the earliest work at IGT, combustion air staging, with ambient secondary air injected near the exhaust, was found to be very effective in reducing $NO_x$ emissions. The technology was not developed commercially at that time because other, simpler, combustion modification techniques were found sufficient to meet the most stringent $NO_x$ regulations (in southern California) of 5.5 lb/ton of glass. Furthermore, when air is used as the secondary oxidant, the secondary air should be preheated so the furnace productivity and efficiency are not adversely affected.

In earlier demonstrations the OEAS technique was evaluated on three endport container glass furnaces. The drawbacks of ambient secondary air injection were overcome by aspirating hot secondary air from the regenerator top using a small amount of industrial oxygen which is normally supplied at elevated pressures. This advanced staging technique provides a way of "oxygen enrichment" to also potentially increase the furnace production rate. The use of oxygen-enriched secondary air would also enhance second stage combustible burnout to increase the secondary stage temperatures to increase the heat transfer to the load. This increase in temperature, however, is not expected to be high enough to impact the overall $NO_x$ formation. Four variations of OEAS were considered and investigated: 1) $O_2$-enriched hot air staging , 2) hot ambient air staging, 3) ambient air staging, and 4) "pure" $O_2$ staging.

In the earlier tests at IGT, which were carried out on a glass tank simulator using ambient secondary air, combustion air staging was demonstrated to be very effective in reducing NOx emissions without increasing the CO emissions. As stated earlier, a furnace operating with a typical stoichiometric ratio of 1.15 (15% overall excess air), an $NO_x$ reduction of 32% (from the current 4 lb/ton to 2.7 lb/ton) could be achieved by operating the port at stoichiometric ratio of 1.04 to 1.06 which should not be very difficult. In the tests at IGT, there was a significant increase in heat transfer at this level of primary stoichiometric ratio even though the secondary air was ambient and was injected downstream of the exhaust port. The data also show that even greater $NO_x$ reductions could be achieved by further decreasing the primary stoichiometric ratio. The heat transfer would, however, somewhat decrease compared to the maximum at

stoichiometric ratios of 1.04 to 1.06, but even at slightly fuel-rich conditions, it would still be comparable to the levels achieved at 15% excess air.

Data from operating OEAS on three endport furnaces found that over wide ranges of baseline $NO_x$ values and furnace pull rates, OEAS reduced furnace $NO_x$ by 50 to 70%. This was achieved without raising CO emission levels and with maintaining furnace production rate and glass quality. OEAS technology has been accepted by the glass industry as an economical and reliable NOx control technology for endport furnaces. The third demonstration, on an Anchor Glass Container furnace in Houston, was a commercial sale. Since the completion of endport furnace demonstration testing, OEAS systems have been sold for two more furnaces, making a total of five endport furnace installations. Additional OEAS sales are expected soon.

With completion of endport furnace demonstrations, the project team has moved OEAS to larger, more complex sideport container glass furnaces. The OEAS approach can, therefore, not only reduce the NOx emissions, but it may also allow an increase in pull rate or a reduction in electric boosting. The test in this program were designed to demonstrate the effectiveness of OEAS on reducing NOx on a 300 ton/day Owens-Brockway six port pair sideport furnace.

Retrofit Design Basis

The OEAS retrofit system was designed to allow variation of key operating parameters. Since this was the first OEAS sideport furnace demonstration, more flexibility was built into this system than would be built into a commercial system. The design was based on the following criteria:

- Inject up to 25% of the total furnace stoichiometric oxidant requirement as secondary oxidant downstream of the flame.
- Secondary oxidant varied between ambient air and relatively (90-93%) pure oxygen generated by a vacuum pressure swing adsorption system (VPSA). No secondary oxidant preheating was used.
- Secondary oxidant injection locations including side-of-port, underport with two holes per port, underport with one hole per port, and crown injection with one injection hole per port.
- Adjustment of overall and secondary stoichiometric ratios, secondary oxidant enrichment level, staging location, and secondary oxidant flow to various ports.
- Tie into existing operation with minimal increase in operator efforts or changes in existing furnace operation strategy. A PLC control system with touch screen monitor serves as OEAS controller and interface with the furnace control system.
- Interface OEAS system with furnace operating system and alarms using a reliable control system.
- Minimize moving components and include provisions to prevent overheating of the few moving components.

- System design which allows for long term operation, well past the demonstration period.

Retrofit System Components

The oxygen-enriched air staging system was installed as a retrofit on the Owens-Brockway furnace. Glass production was not interrupted during OEAS installation or start-up. A blower air skid and an oxygen skid provide the staging oxidant. The skids were placed on a new platform built above the furnace control room. Lighting and electrical power were provided to the new platform, and oxygen was supplied by piping from elsewhere in the plant. The major components of the final OEAS system are described in Table 2 below. A complete description of the system, along with photographs, is presented in Appendix B. Other system configurations were utilized during demonstration testing in order to accommodate single port pair testing and different staging oxidant injection locations.

Table 2. OEAS SYSTEM HARDWARE DESCRIPTION

| Component | Description | Location |
|---|---|---|
| Oxygen Skid | • 6 in. train with safety and automatic flow control and metering<br>• 2 in. low flow metering leg (single port pair testing)<br>• left and right reversal valves<br>• 6-7 psig supply pressure (VPSA oxygen)<br>• 20,000 SCFH maximum flow | new platform above control room |
| Blower Air Skid | • 10 in. train with automatic ratio flow control and metering<br>• 4 in. low flow metering leg (single post pair testing)<br>• two 15 hp. blowers in series<br>• psig supply pressure<br>• 45,000 SCFH maximum flow | new platform above control room |
| Oxygen Field Piping | • 6 in. stainless steel piping from skid to furnace left and right side oxygen headers<br>• two 4 in. stainless steel oxygen headers with six 2 in. flanged outlets (one per port) | 8 feet above ports |
| Air Field Piping | • 10 in. steel piping from skid to furnace left and right side air headers<br>• two 10 in. steel air headers with six 4 in. flanged outlets (one per port) | 8 feet above ports |
| Oxygen Downcomer | • twelve 2 in. stainless steel downcomers with manual flow control and metering | above each port with access from upper |

| | | |
|---|---|---|
| | | catwalk |
| Air Downcomer | • twelve 3 in. stainless steel downcomers with manual flow control and metering.<br>• Oxygen is introduced to the air downcomer after flow metering and before entering the 3 in. flex hose connecting the downcomer to the injector manifold. | above each port with access from upper catwalk |
| Injector Manifold | • twelve 3 in. manifolds with shut-off valves and mounting brackets.<br>• Two injector ports per manifold | under each port |
| Injectors | • two injectors per port.<br>• Each injector has a 2 in. body reducing to 1 in. at the injector site. | under each port |
| Control System | • Allen Bradley SLC 5/03 processor<br>• Allen Bradley Panelview 900 monochrome touch screen monitor<br>• Local and remote staging control modes<br>• Elaborate control system | Control room |

An Allen Bradley SLC Control system with a monochrome touch screen monitor was selected to interface between the furnace control system and the OEAS system. Staging parameters can be set from the monitor in the control room, and the controller can be operated in local and remote staging control modes.

In local mode, the operator can enter furnace data and staging parameters with the touch screen monitor. Staging setpoint flows are calculated and controlled accordingly. The staging parameters can be set differently for the two sides of the furnace. In remote mode, the control system processor uses the furnace gas and combustion air flow signals and inputted staging parameters to continuously calculate staging flows so that an overall furnace air to fuel ratio is maintained. Again, staging parameters can be set differently for the two sides of the furnace.

The control system has an elaborate set of alarms. The processor monitors oxygen and air skid pressures and flows. The operator is notified when staging flows are too low and when the staging system should be shut down or the overall furnace air fuel ratio should be raised. Staging system countdown timers are used for non-critical alarms. These timers allow the operator to correct problems in a sufficient amount of time before the staging system automatically shuts down. The staging system immediately shuts down if one of two emergency stop buttons is pressed or if the furnace gas safety valve closes. Emergency stop buttons are located on the control cabinet in the control room and on the oxygen skid.

A water-cooled Combustion Tec. Inc. camera was mounted in the furnace at the charging end. A monitor placed in the control room allows viewing of the flames and the batch line (during reversals). The camera system proved valuable during single port pair testing. During OEAS testing at different injection locations and with different oxygen concentrations, the secondary flame was visible. This provided port coverage and jet

penetration information to the project team. Secondary flames were not visible when operating OEAS on the full furnace. The amount of secondary oxidant supplied to each port was much lower for full furnace OEAS operation compared with the oxidant used for the single port pair test.

The CTI camera system is a commercial product including an air and water cooled color camera with a video recording system that includes a 9-inch monitor. The camera uses a cobalt filter to absorb sodium wavelength radiation. This reduces the effects of the visual intensity in the furnace interior and improves flame and batch pattern definition. Numerous features including a reflective exterior surface, cooling water, and cooling air vents, are incorporated into the furnace design to allow long-term operation while exposed to the furnace environment. The video cassette recorder is a time-lapse unit. Time compression can be varied from real time to as little as 6 minutes of viewing time for a 24 hour period. A standard 2 hour tape can hold up to 20 days of furnace camera data.

The complete OEAS system was left operating at Owens-Brockway at the completion of the project. The camera and monitor were operating normally when testing was completed, and they were also left in place and operating at the plant.

## Test Instrumentation

Test instrumentation was used to measure temperature in the port neck of port 5 (between the port and the regenerator) and the gas compositions ($NO_x$, $O_2$, CO, and $CO_2$) in the regenerators, flue tunnels, and stack.

### Gas Sampling

Gas samples were collected from the stack, the flue tunnels, and the regenerators. Stack and flue tunnel samples were collected with non-cooled stainless steel tubes. Regenerator samples were collected using high temperature, water-cooled stainless steel probes. A schematic drawing of the water-cooled probes is shown in Figure 10, and Figures 11 and 12 show photos of a probe ready for insertion in the regenerator and a probe in the sampling position in the regenerator. Gas samples were drawn through the probes using oilless vacuum pumps and conditioned by passing through sample conditioning trains, which consist of:

- a water trap to remove liquid condensate
- indirect electric heaters to heat the sample above the dew point
- a membrane dryer to remove vapor phase water and produce a dry gas sample

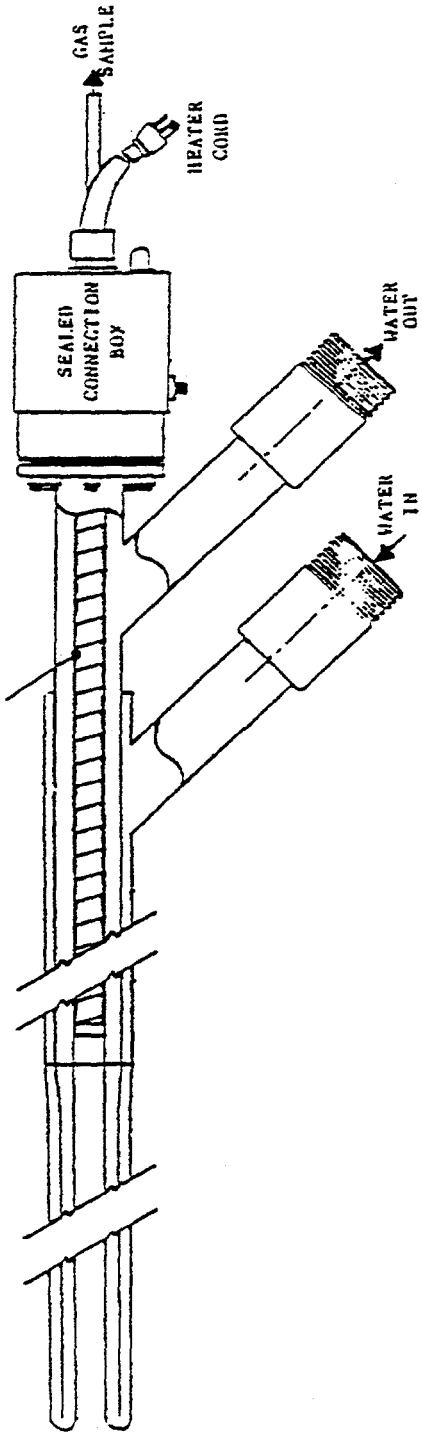


Figure 10. SCHEMATIC DRAWING OF THE GAS SAMPLING PROBE ASSEMBLY

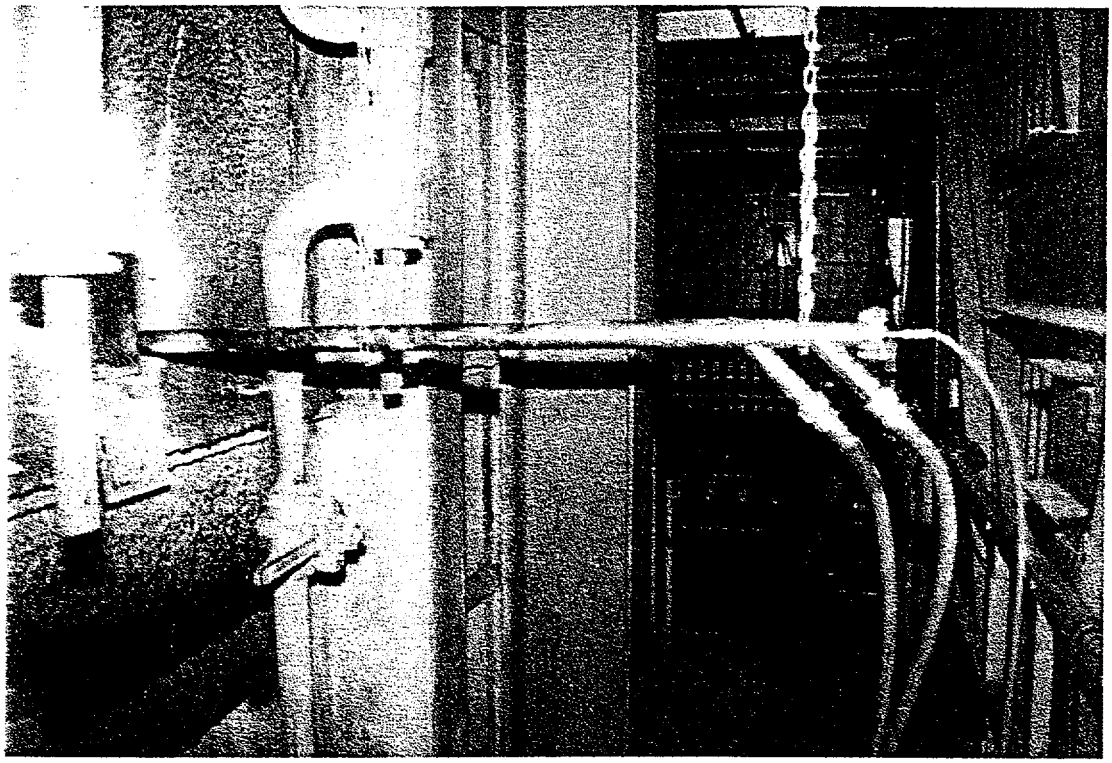

Figure 11. PROBE USED TO COLLECT GAS SAMPLES FROM THE REGENERATOR

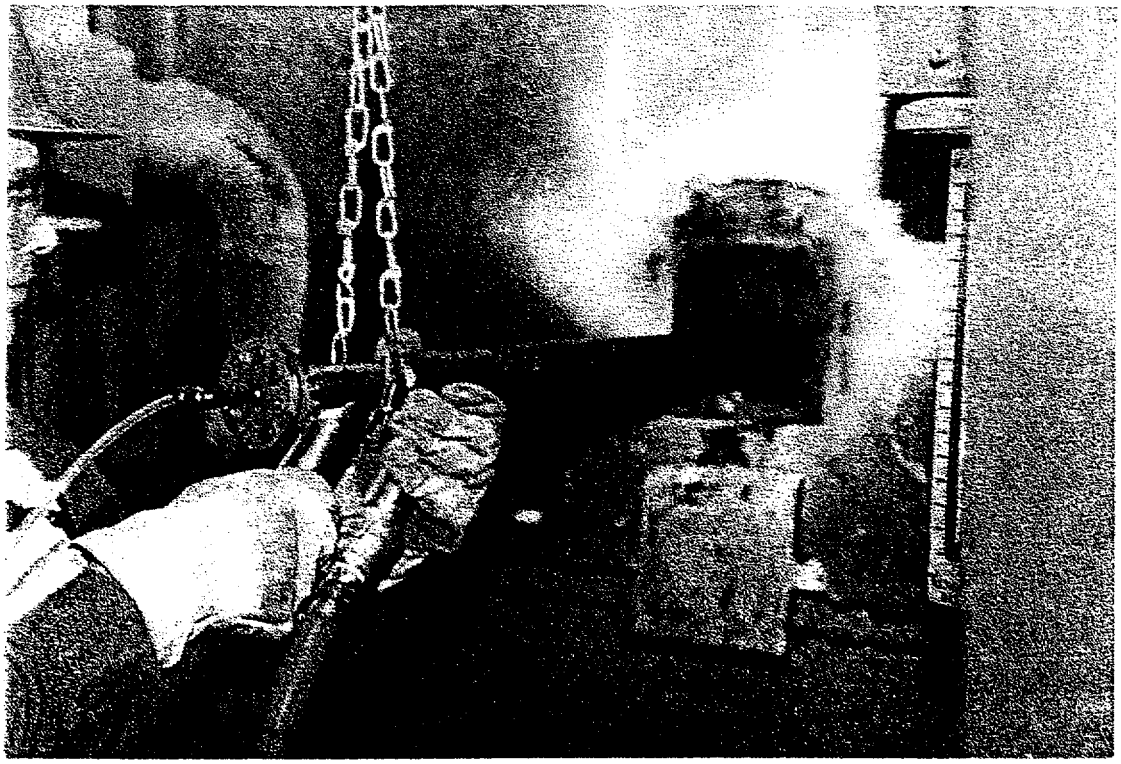

Figure 12. GAS SAMPLING PROBE INSTALLED IN THE REGENERATOR

Regenerator samples were collected with probes inserted in ports located on the back wall of the regenerators directly in line with the ports. Regenerators on the host furnace are 12 feet across with an 18 inch refractory wall. On the left side of the furnace, the wall of the building limited the maximum probe length to 4.5 feet. The gas samples were collected 3 feet inside the regenerator, well away from the back wall, but only 25% of the way across the regenerator to the ports. Longer probes could be used on the right side of the furnace, and samples were taken using 4.5, 6, and 10 foot probes. The longest probes reached two-thirds of the way across the regenerator. Review of the data from different probe lengths found the gas sample compositions varied in the same proportions for all probe lengths used. Therefore, the decision was made to use the same probe length, 4.5 feet, on both sides of the furnace (probe had to go through 18 in. of refractory). Most of the regenerator gas sampling data in this program was collected with 4.5 foot water-cooled probes.

Sample conditioning trains were located near the sampling locations and were followed by stainless steel and Teflon tubing lines used to deliver the gas samples to the continuous emissions monitoring system (CEMS). Gas samples were delivered through a flow control and distribution panel located in the furnace control room (see Figure 13). This panel allowed easy switching between the various gas sample locations while also regulating gas sample flow rates and pressures to the analytical instruments. Instrument calibration samples were also handled by this panel. The gas analyzers used in this program are shown in Figure 14, and they included:

- A ThermoElectron Model 42H chemiluminescence $NO_x$ analyzer
- A Rosemount Model 755R paramagnetic $O_2$ analyzer
- A Rosemount Model 880A infrared CO analyzer
- A Rosemount Model 880A infrared $CO_2$ analyzer

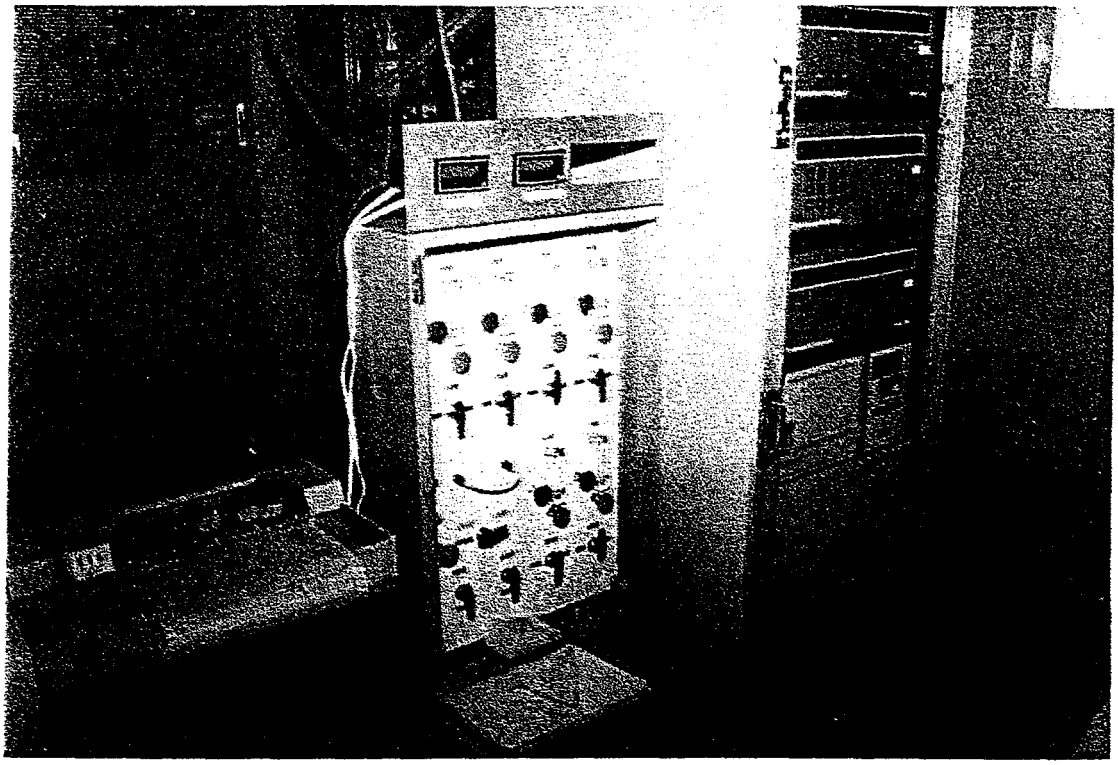

Figure 13. FLOW CONTROL AND DISTRIBUTION PANEL

All of the gas analyzers were calibrated using pure nitrogen as the zero gas and appropriate span gases to set the gains. The nitrogen zero gas and span gas bottles were located outside the furnace control room. Signal outputs from the analyzers ($O_2$, CO, $CO_2$, and $NO_x$) were sent to three-pen strip chart recorders for continuous recording. The strip chart recorders were located next to the flow control and distribution panel in the furnace control room.

Temperature Measurements

Temperatures were measured at the top of port 5 on both sides of the furnace at the rear of the ports where they enter the regenerator. Alumina shielded type R thermocouples were connected to two strip chart channels in the control room. Measurements were made continuously on both sides of the furnace.

Breast wall temperatures were made during reversals using a hand held optical pyrometer. Wall temperature was found to change significantly based on the firing rate in the primary flame zone.

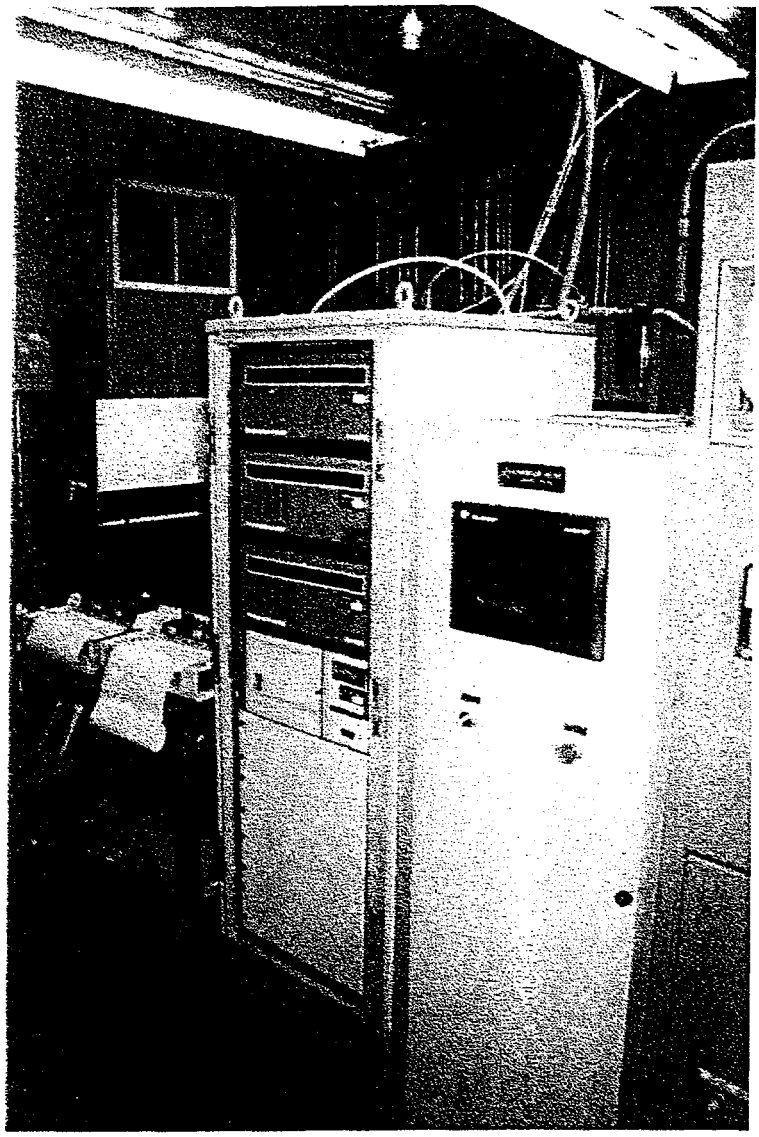

Figure 14. CONTINUOUS EMISSIONS MONITORING SYSTEM (CEMS)

## FIELD EVALUATION TESTS AND RESULTS

Parametric and long-term tests were conducted with the OEAS system on the host furnace to investigate the impacts of the following independent parameters on furnace operation and emissions levels.

- secondary oxidant type - over the full range from air, to oxygen-enriched air (25 to 60% $O_2$), to oxygen (93% $O_2$)
- secondary oxidant injection location - 42° side-of-port, one hole underport, two holes underport, and one hole furnace crown
- primary stoichiometric ratio (PSR)
- overall stoichiometric ratio (OSR)
- secondary oxidant biasing between ports

The operation of the staging system was straightforward during testing. Baseline measurements of $NO_x$, CO, $CO_2$, and $O_2$ were made in the regenerator tops and stack under typical operating conditions with no OEAS operating. Staging was turned on and set at a desired condition, and the furnace operator was then asked to lower the furnace primary air which lowered the primary stoichiometric ratio. The furnace was given sufficient time to come to the new steady state operating condition while emissions were continuously measured in the regenerator tops and the stack. Emissions measurements were made at the most stable and representative furnace operating conditions available. It must be noted that true steady state operation can not be achieved in a regenerative glass furnace because of the reversals and the regular changes in furnace operating parameters needed to maintain desired glass conditions.

### Furnace Baseline Parameters

Field testing was conducted on an Owens-Brockway sideport furnace located in Vernon, California. This six port pair furnace produces amber container glass. Two Owens Illinois burners are fired in each port. Firing rates vary with the highest natural gas firing rates in ports 3, 4, and 5 and the lowest firing rates in ports 1 and 6. Overall furnace oxygen to natural gas primary stoichiometric ratio (PSR) could not be directly measured during single port pair testing but was measured during full furnace OEAS demonstration. Metered flows and exit regenerator measurements showed ports 1 and 2 have the highest PSRs and ports 3, 4, and 5 have the lowest PSR values. All ports are operated with a PSR of more than 1.0.

Before conducting staging tests, baseline data were collected for the furnace. Temperatures were measured with type R thermocouples positioned at the port neck of port 5 at the entrance to the regenerator where they were shielded from furnace radiation. Gas samples were obtained with water cooled probes inserted in the back of the regenerators directly in line with the ports. On the left side of the furnace the building wall required the use of 4.5 foot probes which extended 3 feet into the 12 foot wide regenerator. On the right side of the furnace, 6 foot probes extending 4.5 feet into the regenerator were used. Stack samples were obtained through a stainless steel tube. Table 3 shows baseline port and stack measurements made during single port pair testing.

Baseline furnace conditions were different during full furnace testing, and $NO_x$ stack emission values varied between 2.3 and 3 lb/ton of glass during the week of OEAS testing. Ports are numbered from the charging end.

The baseline emissions monitoring confirmed a wide variation in port stoichiometries with the highest excess air used in ports 1, 2, and 6. Because the ports are not isolated, port emission levels are affected by mixing in the furnace and by regenerator top crossflow. $NO_x$ decreased with decreasing excess air while showing a trend toward higher levels away from the charging end of the furnace. When the exhaust port $O_2$ concentration was below 1.5%, incomplete combustion produced a significant amount of CO. Review of the baseline data led to selection of port 5 for air staging evaluation. Port 5 is not at either end of the furnace and has a high firing rate while producing high $NO_x$ with a moderate level of excess $O_2$.

Initial baseline measurements were made to learn furnace performance characteristics and differences between ports. A number of furnace and ambient factors influence furnace $NO_x$ production. Therefore, baseline data (without OEAS operating) was collected during each day of OEAS testing to serve as reliable as possible baseline for measuring OEAS impact on $NO_x$ and furnace operation.

Table 3. BASELINE FURNACE EMISSIONS DATA

| Sample Location | $O_2$, % | CO, vppm (at 0% $O_2$) | $NO_x$, vppm (at 0% $O_2$) | $NO_x$, lb/ton |
|---|---|---|---|---|
| Right Side Port 1 | 5.0 | 12 | 980 | -- |
| Right Side Port 2 | 4.5 | 14 | 930 | -- |
| Right Side Port 3 | 1.5 | 90 | 910 | -- |
| Right Side Port 4 | 2.1 | 50 | 980 | -- |
| Right Side Port 5 | 1.9 | 190 | 1150 | -- |
| Right Side Port 6 | 3.1 | 250 | 1070 | |
| | | | | |
| Left Side Port 1 | 4.8 | 11 | 940 | -- |
| Left Side Port 2 | 4.3 | 16 | 930 | -- |
| Left Side Port 3 | 1.5 | 130 | 840 | -- |
| Left Side Port 4 | 1.0 | 1500 | 880 | -- |
| Left Side Port 5 | 2.3 | 60 | 1480 | -- |
| Left Side Port 6 | 3.5 | 40 | 1380 | -- |
| | | | | |
| Stack - Right Side Fire | 7.7 | 10 | 1220 | 4.8 |
| Stack - Left Side Fire | 7.7 | 12.8 | 1340 | 5.7 |

In preparation for OEAS testing, CTI installed an oxygen skid with a capacity of 20,000 SCFH and a blower air skid with a capacity of 70,000 SCFH on a platform above the furnace control room. The oxygen skid was connected to the available plant oxygen supply. The skids are sized for full furnace OEAS operation with the capability of feeding air, any level of enriched air, or oxygen as secondary oxidant.

OEAS System Parameters

Data for a number of furnace parameters was collected by host site measurement devices during this project. Some of this information is considered proprietary to Owens-Brockway and is not included in this report. The host furnace data collected included:

- Pull rate, ton/day
- Electric boost, kW
- Natural gas and air rates to the full furnace measured with orifice meters, SCFH
- Natural gas rates to the ports measured with rotometers, SCFH
- Furnace draft measured with a pressure transducer, in. of water
- Bridgewall temperature measured with an optical pyrometer, °F
- Flame monitoring using a CTI-built and -installed CCTV system described in Appendix B

Staging oxidant was supplied with two skids, an ambient air blower skid and an oxygen skid. The oxygen was obtained from the plant oxygen supply which was a combination of VPSA oxygen with liquid oxygen backup. Oxygen concentration in the staging oxidant was controlled by setting and mixing flows of the two skids. The flow of staging oxidant to each port was separately controlled. This allowed the OEAS system to be balanced and to achieve the maximum $NO_x$ reduction while using the lowest amount of secondary oxidant. A detailed description of the staging air and oxygen systems is presented in Appendix B.

Emissions

Exhaust gas composition was measured in three locations:

- Regenerators directly in line with the ports
- Flue gas tunnels
- Stack

Regenerator measurements were made with water-cooled probes inserted 3 ft into the 12 foot wide regenerators. The left side of the furnace is located next to a wall which prevented the use of longer probes. Right side regenerator measurements were made with the probes inserted 3, 4.5, and 8.5 feet into the regenerator. Data from different insertion positions was similar, and for the sake of consistency, only the 3 feet data is included in the discussion. All data collected, from all sampling positions, is included in Appendix C.

Exhaust gas measurements included CO, $CO_2$, $O_2$, and $NO_x$. Gas samples were conditioned by being passed through a heated perma-pure dryer to remove moisture and then through millipore filters to remove particulates. Emissions concentrations were

recorded constantly during each test using a three pen chart recorder. The combustion air and exhaust gas temperatures at port 5 were also recorded on a chart recorder.

Description of Tests

Demonstration testing was conducted in a series of six test campaigns between April, 1996 and February, 1997. The actual dates of testing and the testing performed in each campaign is described in Table 4.

Table 4. OEAS SIDEPORT DEMONSTRATION TEST CAMPAIGNS

| Dates | Testing |
|---|---|
| April 24-29, 1996 | Single port pair parametric testing |
| Sept. 23-28, 1996 | Full furnace parametric testing |
| Oct. 22-25, 1996 | Full furnace long term testing |
| Nov. 12-15, 1996 | Full furnace long term testing |
| Dec. 10-14, 1996 | Full furnace testing at low electric boost |
| Feb. 18-21, 1997 | Full furnace testing with PLC controlling the OEAS system |

The OEAS system was shut down after the test campaigns in April, September, and November, 1996. OEAS was left in operation after the other test series. At the end of the project, the OEAS system was left in operation. The system has been in continuous operation continuously for more than three months when this report was written.

Discussion of Results

After furnace baseline testing was completed, OEAS testing was conducted in a series of test campaigns. The chosen testing protocol allowed the project team to collect all desired furnace and OEAS data and the host furnace operators to become familiar and comfortable with the OEAS system. The testing protocol order consisted of single port pair testing on port 5, full furnace parametric testing, full furnace long term testing at normal (high) boost, full furnace testing at low boost, and full furnace testing with the PLC controller controlling the OEAS system. A full description of all tests and results is presented below.

Single Port Pair Testing

Single port pair testing was conducted at port 5. Side-of-port injection through available burner blocks was tested on both sides of the furnace. Furnace crown and

underport (with one or two injectors) OEAS injection locations were also evaluated. All injectors were connected to both the oxygen and the air skids.

Primary stoichiometric ratios were lowered without air staging to determine optimum PSR values and potential $NO_x$ reduction levels. A preferred PSR was then selected for OEAS testing. OEAS tests evaluated all staging positions and a number of secondary oxidants.

Figures 15 and 16 show the effects of changing port 5 PSR on $NO_x$ and CO. For both right and left side firing, $NO_x$ levels decreased with reduced PSR. $NO_x$ reductions as high as 35% were reached. CO concentrations increased dramatically with decreasing PSR. At low PSRs, the CO concentration in the regenerator was over 3000 vppm.

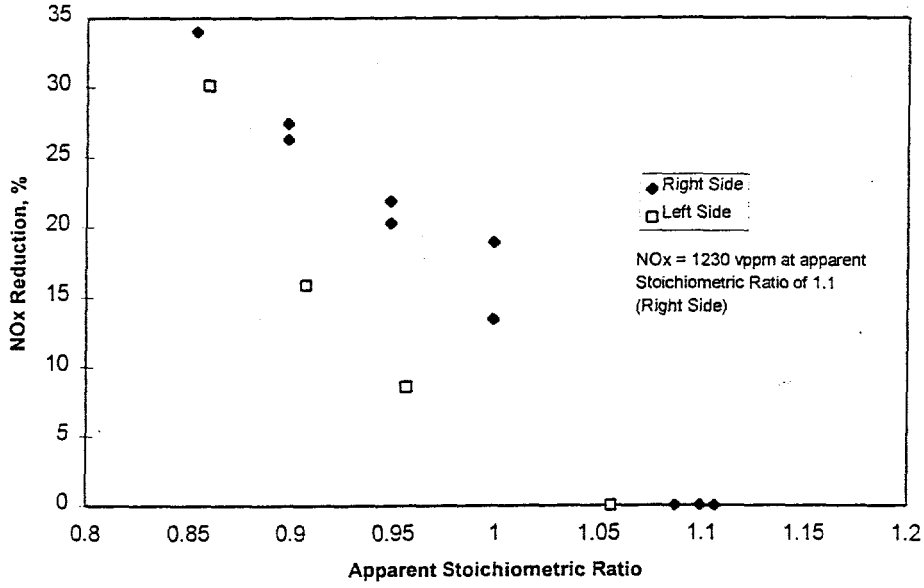


Figure 15. THE EFFECT OF REDUCED STOICHIOMETRIC RATIO ON $NO_X$

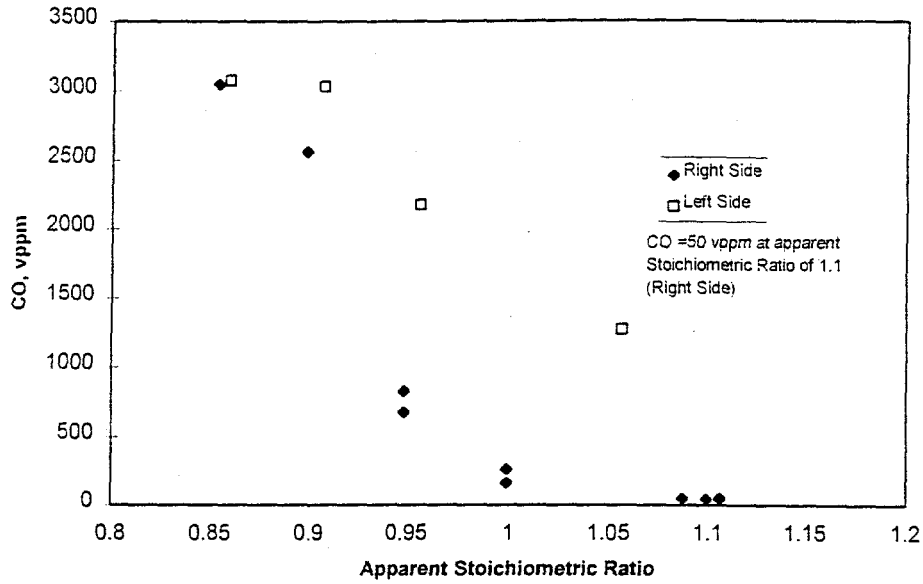


Figure 16. THE EFFECT OF REDUCED STOICHIOMETRIC RATIO ON CO

After baseline testing, a PSR was selected for port 5 which gave a $NO_x$ reduction of 30 to 35%. All single port OEAS testing was conducted at the same port 5 PSR value.

Figures 17 and 18 show the effects of enriched air (35% $O_2$) staging on $NO_x$ reduction and CO burnout. Figure 17 shows that side-of-port and two-hole underport injection have only a small effect on the $NO_x$ reduction achieved by lowering the primary stoichiometric ratio. At the same time, Figure 18 shows that CO is effectively burned out with both side-of-port and two-hole underport injection.

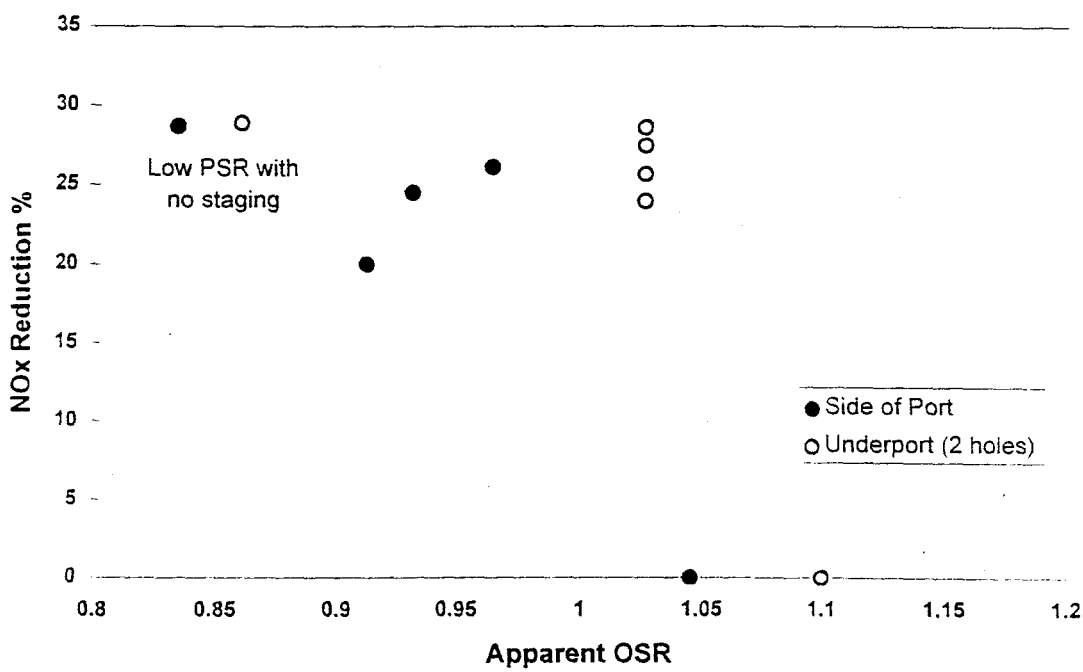


Figure 17. EFFECT OF ENRICHED AIR (35%) STAGING ON $NO_x$ AT PORT 5

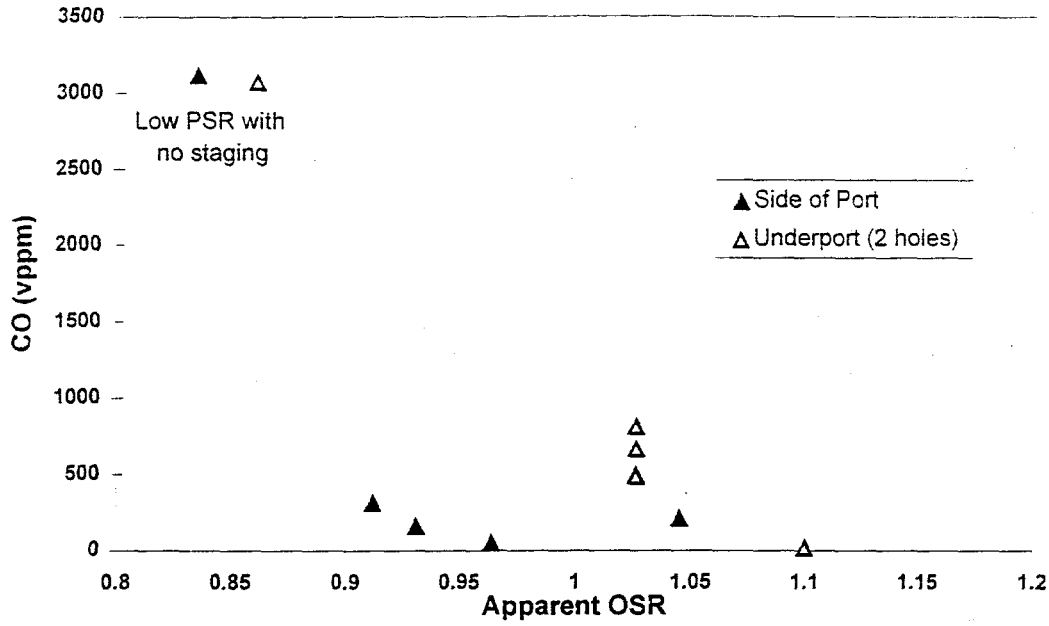


Figure 18. EFFECT OF ENRICHED AIR (35%) STAGING ON CO AT PORT 5

The $NO_x$ reduction achieved by lowering PSR was reduced by approximately 50% with both one-hole underport injection and furnace crown injection. These two staging options may generate $NO_x$ when oxidant interacts with the primary flame. The furnace crown position appears to significantly reduce CO from 3000 vppm to under 1000 vppm, but the one-hole underport injection approach produced exhaust gas with 2000 vppm CO which will produce high stack CO levels. This underport position may not provide good port mouth coverage which would allow high CO-content product gases to enter the port.

$NO_x$ levels increased when oxygen was used as the secondary oxidant and high temperature combustion zones were formed. This effect was seen at all staging locations with side-of-port injection producing the smallest increase in $NO_x$. Staging with highly enriched air (50% $O_2$ or more) and oxygen caused the exhaust port temperature to increase by 20° to 80°F. This temperature was lower or unchanged when staging with 35% enriched air and air. For the full furnace retrofit, overall PSR will be decreased by lowering total furnace air flow. With OEAS operating along with a lower full furnace PSR, exhaust port temperatures are expected to be equal to or lower than under baseline furnace operating conditions.

Full Furnace Parametric Testing

During the first two weeks of September, the full furnace OEAS installation was completed. This work consisted of drilling two holes under each port, installation of injectors in each hole, running piping to all the ports, connecting the piping and injectors

with downcomers, and attaching flow adjustment valves to each port. The holes were drilled by Ed Blin and the retrofit work was conducted by Combustion Tec, Inc. with assistance from Lilja personnel.

IGT personnel set up measurement instrumentation on Sept. 18 - 20, and full furnace OEAS parametric testing was conducted during the period Sept. 23 - 28. During this test period, the furnace was operated with high electric boost and a very low $NO_x$ emission level below 3 lb/ton. Baseline data was taken during which the combustion stoichiometric ratio was found to be 1.12. Tests were then conducted in which the stoichiometric ratio was decreased to 1.01 and no staging was employed. The $NO_x$ emission levels dropped approximately 35% to 1.7 lb/ton while CO emissions rose almost exponentially.

Figure 19 illustrates the effects of lowering the combustion air to fuel ratio (the overall stoichiometric ratio) on emissions. This baseline data with no oxygen-enriched air staging operating on the furnace clearly shows that $NO_x$ decreases essentially linearly with decreasing combustion air to fuel ratio while CO levels rise exponentially at overall stoichiometric ratios below 1.12.

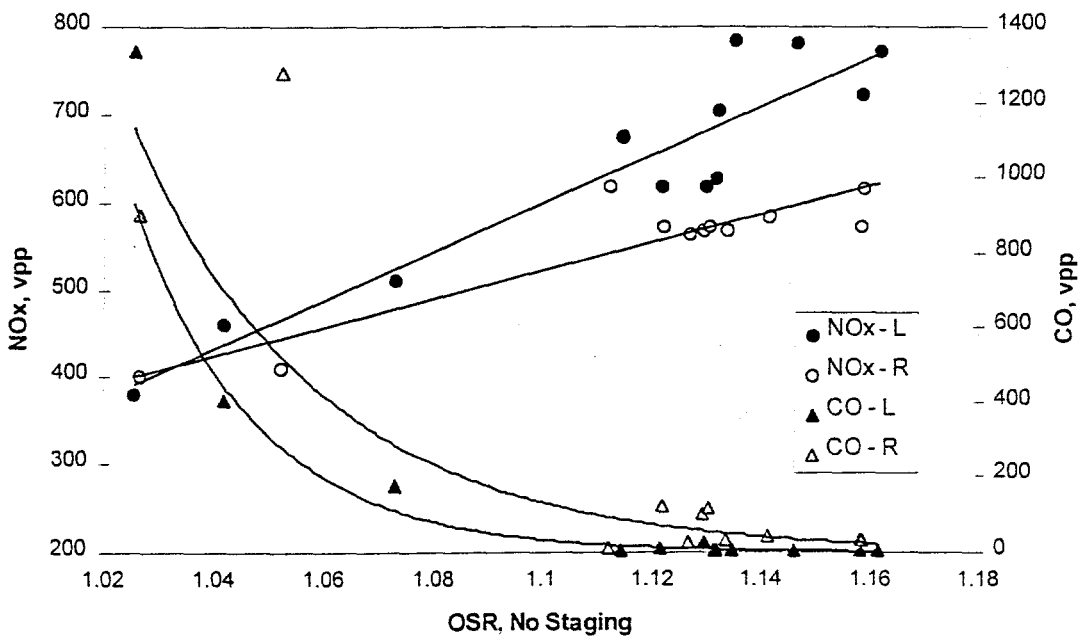


Figure 19. THE EFFECT OF OVERALL STOICHIOMETRIC RATIO (OSR) ON $NO_x$ AND CO EMISSIONS WITH NO STAGING

Data on $NO_x$ emissions collected from the stack during parametric testing is shown for left and right side firing in Figures 20 and 21. The behavior of the furnace is similar from the two firing sides, but not identical. The left side of the furnace tended to have somewhat higher $NO_x$ and lower CO at baseline conditions and when OEAS was operating. The furnace air to fuel ratio was set to be the same when firing from both sides, but a number of factors could influence the air to fuel ratio on the overall furnace

and at individual ports. Therefore, the project team was not surprised to find differences in emissions between the two sides of the furnace. Placing an automatic controller on the combustion system so the air to fuel ratio could be set differently for left and right side firing would allow the average $NO_x$ emissions from the furnace to be lowered.

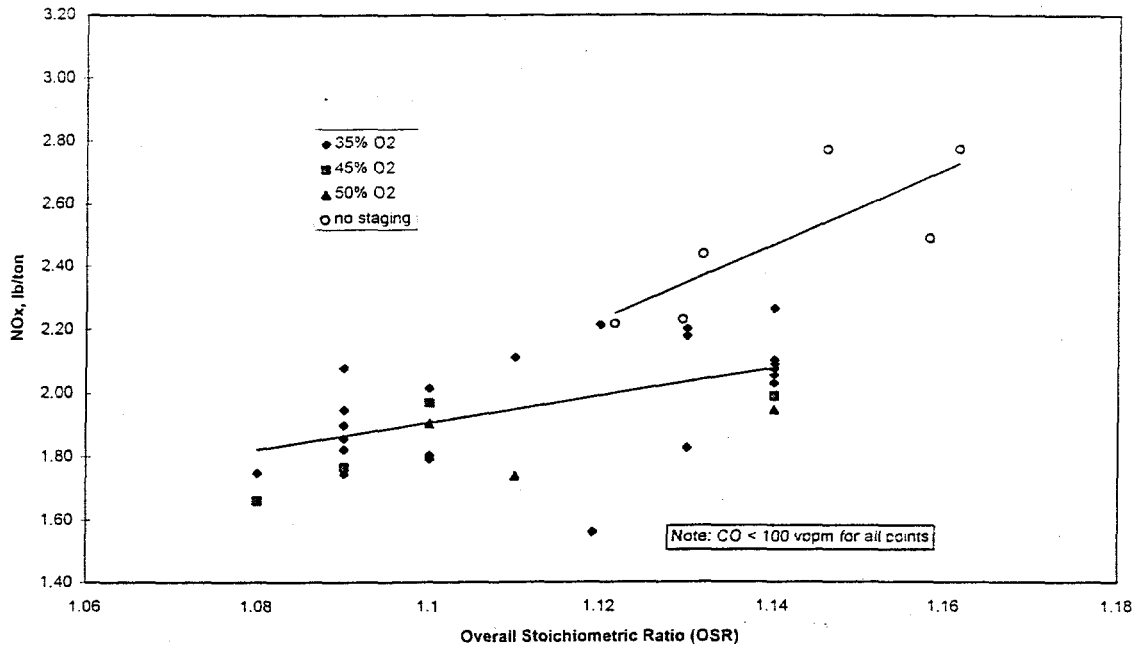


Figure 20. $NO_X$ EMISSIONS AT HIGH BOOST DURING PARAMETRIC TESTING - LEFT SIDE FIRING

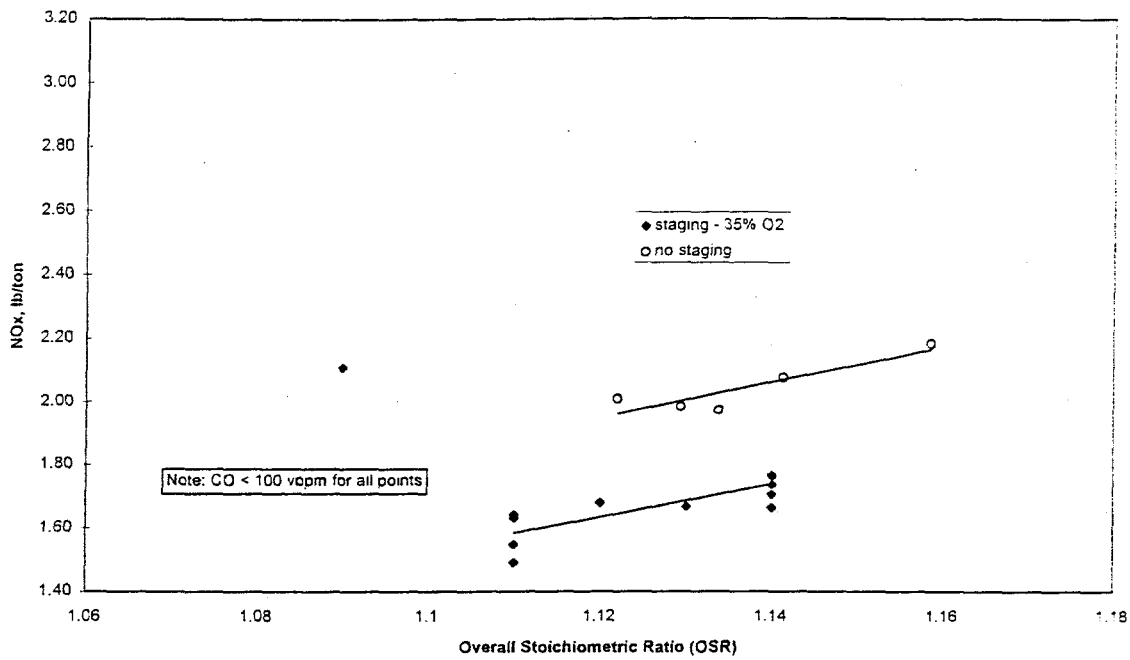


Figure 21. $NO_X$ EMISSIONS AT HIGH BOOST DURING PARAMETRIC TESTING - RIGHT SIDE FIRING

Analysis of the data in Figure 19 in conjunction with a desire to keep an overall oxidizing primary flame stoichiometry led to the selection of a PSR value of 1.02 for OEAS demonstration. Staging was then applied to all ports using enriched air containing 35% $O_2$ to raise the overall stoichiometric ratio to various levels. The results of this testing are presented in Figure 22. Firing the furnace from the left and right side produces different $NO_x$ values at the same stoichiometric ratio, but the trend is the same for both. With the PSR kept at 1.02, OEAS effectively reduced the $NO_x$ emissions at the stack by more than 30% to an average value of 450 to 500 vppm. This corresponds to a $NO_x$ production level of 1.8 lb/ton of glass. OSR values of 1.08 to 1.10 were effective at burning out CO produced in the primary flames. Stack CO values were similar to the baseline case with high PSR and no staging. Data is only reported for OSR values down to 1.08. Further decreases in OSR produced lower $NO_x$ but CO levels could not be controlled and rose exponentially.

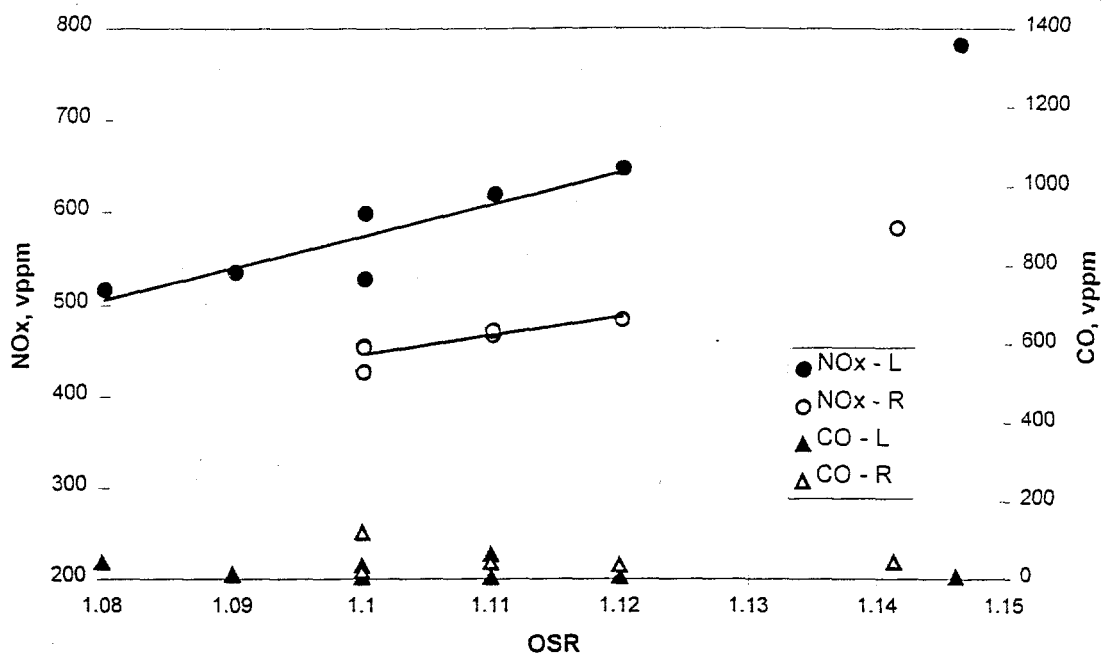


Figure 22. THE EFFECT OF ENRICHED AIR STAGING ON $NO_X$ AND CO EMISSIONS

Testing was also conducted to determine the effect of increasing the concentration of oxygen in the staging oxidant. At a PSR of 1.02 and an OSR of 1.10, the oxygen concentration was varied between 35 and 50%. Results are shown in Figure 23. A small decrease in $NO_x$ of approximately 6% was realized by increasing the oxygen concentration from 35 to 50%. While the result is desirable, there are concerns about possible temperature increases using more highly enriched oxidant and about the higher cost of more enriched oxidant.

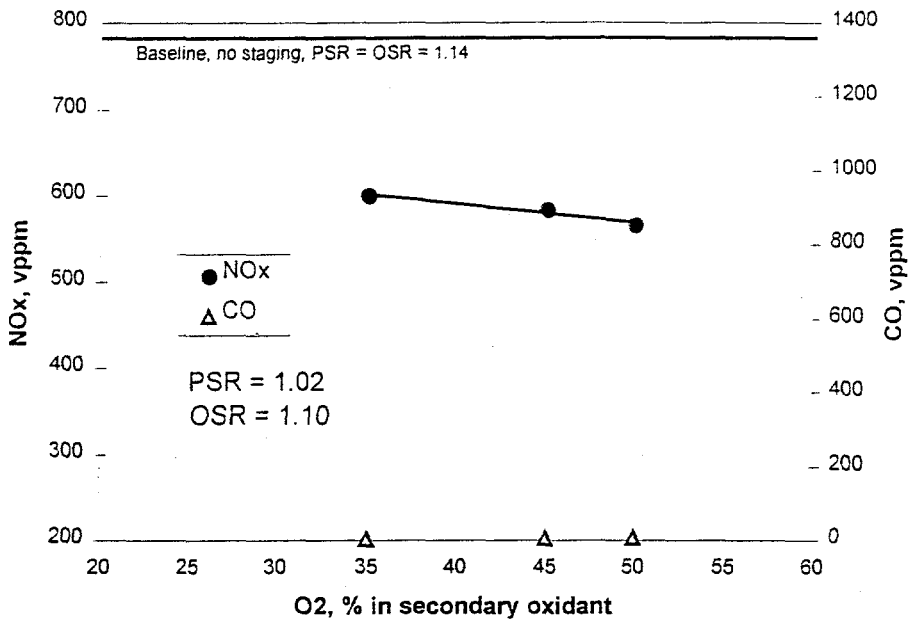


Figure 23. THE EFFECT OF OEAS OXYGEN CONCENTRATION ON $NO_X$ AND CO EMISSIONS

A long series of tests was conducted to balance the staging oxidant to the various ports. Proper balancing allows use of the lowest possible amount of staging oxidant because the OSR is the lowest possible value. Also, $NO_x$ emissions decrease with secondary oxidant levels because a small amount of $NO_x$ is generated by the secondary oxidant. The port balancing indicated the OEAS system is robust and not sensitive to small changes in the amount of secondary oxidant sent to each port. This suggests that long term furnace operation will not require frequent adjustment of the OEAS system.

Full Furnace Long-Term Testing

Analysis of the single port pair testing showed that two OEAS staging positions: side-of-port and two holes underport, effectively burn out CO while not increasing the overall $NO_x$ level. Staging with enriched air containing 35% $O_2$ did not increase exhaust port temperatures at either of these positions. Higher oxygen enrichment did result in temperature increases. Evaluation of these two positions revealed significant advantages to the two hole underport position. Therefore, the two hole underport OEAS staging strategy was recommended for the full furnace.

A decision was made to proceed with the full furnace retrofit using the two hole underport injection location. This decision was reached after review of the single port pair testing and examination of the injector locations. Immediately after this decision was agreed to by Owens-Brockway, CTI, and IGT, fabrication of injectors and other equipment was begun at CTI. Efforts were focused on conducting the full furnace parametric testing during September.

Data for left side firing and right side firing collected during parametric testing in September is presented in Figures 20 and 21. Very low levels of $NO_x$ emissions were observed during operation without staging and with OEAS on the furnace operation. The average furnace $NO_x$ level was decreased approximately 30% using OEAS from an average value of 2.5 lb/ton to 1.8 lb/ton. The effect of changing oxygen concentration in the staging oxidant is illustrated in Figure 23. Increasing the oxygen concentration from 35 to 50 percent decreased the $NO_x$ emission level by 5 to 10 percent on average. This improvement in emissions level is small and comes at the expense of higher oxygen flows. After testing was complete, a decision was reached with the plant personnel to operate OEAS with 30 to 35 percent oxygen. OEAS is effective at this oxygen concentration and the plant personnel felt comfortable with the OEAS oxygen requirements while also feeling assured that OEAS was not causing any overheating of the refractory.

Long-term testing of OEAS on the full furnace was conducted in October, 1996. During November, 1996, the project team returned to the host site to conduct additional long-term testing measurements. The second set of measurements were made to confirm reliable OEAS operation and $NO_x$ reduction. Owens-Brockway hired a third-party contractor to measure stack emissions during the November testing period. Stack measurements of $O_2$, CO, and $NO_x$ were essentially identical between the contractor and the project team. Discrepancies were less than one percent in values. The outside contractor followed EPA protocols in making measurements. The IGT measurement protocol varies somewhat from the EPA procedure, but regular calibrations are similar in both protocols, and similar instrumentation is used.

Only minor changes in furnace firing conditions and OEAS operating parameters were made during the testing in November. The measured $NO_x$ levels for left and right side firing are presented in Figures 24 and 25. The furnace $NO_x$ levels were higher both with, and without, OEAS operating than was observed during the parametric testing in September. The average $NO_x$ emission level was still decreased by better than 25 percent, from 3.1 lb/ton to 2.3 lb/ton. The actual level of $NO_x$ reduction was difficult to determine because baseline values measured in November all had CO emissions with more than 100 vppm. The baseline CO level can be reduced by increasing the primary stoichiometric ratio which will also increase the level of $NO_x$ in the stack, but this was not done during the long-term testing in November. The baseline values cited are from the September parametric testing, and these values are likely low based on the furnace operating conditions in November.

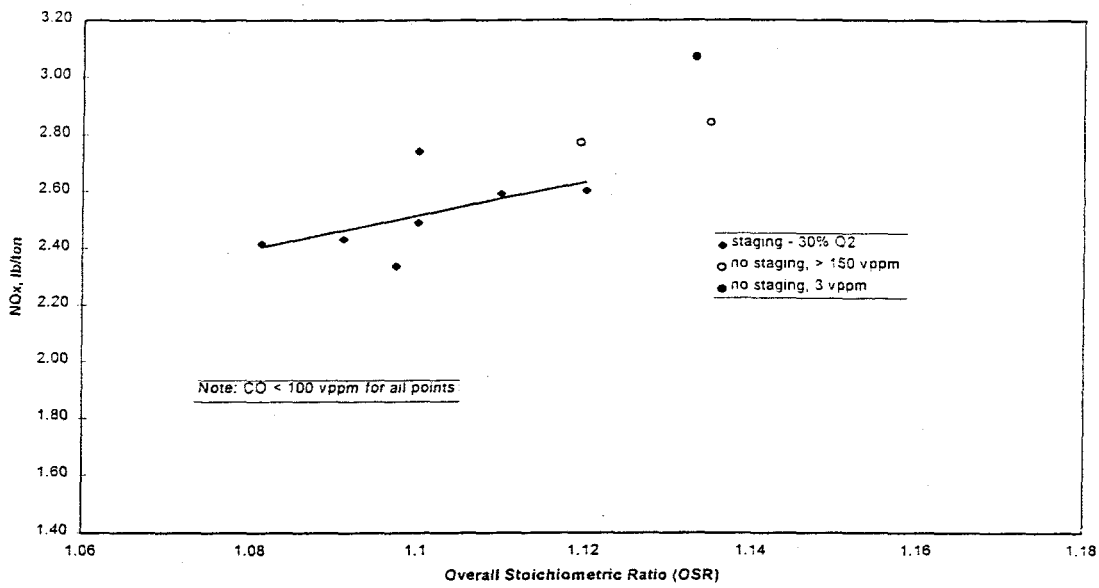


Figure 24. $NO_X$ EMISSIONS AT HIGH BOOST DURING LONG-TERM TESTING - LEFT SIDE FIRING

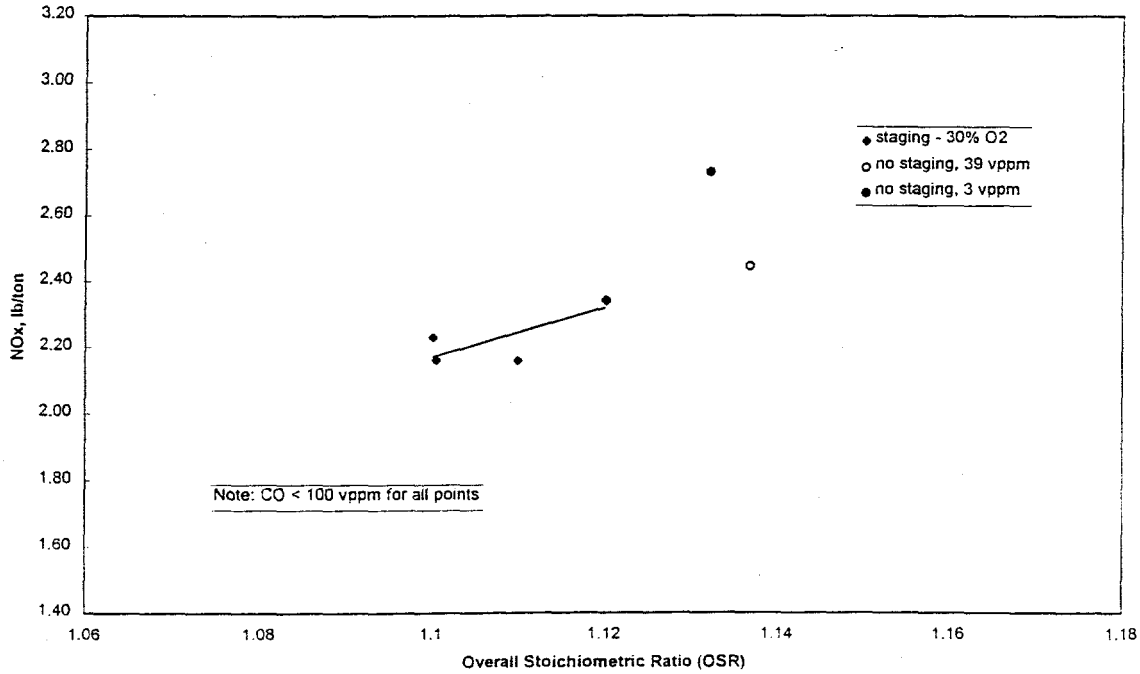


Figure 25. $NO_X$ EMISSIONS AT HIGH BOOST DURING LONG-TERM TESTING - RIGHT SIDE FIRING

Testing at Reduced Electric Boost

The project team was interested in determining the capability of the OEAS system for reducing $NO_x$ at different levels of electric boost on a furnace. Electric boost is important to the glass making process as a means of supplying heat below the melt line, maintaining glass flow patterns, and controlling the glass quality. Electric boost can also be used to reduce $NO_x$ emissions. Electricity typically costs $12 to $20/MM Btu compared with less than $3/MM Btu for natural gas. For economic reasons, a furnace operator would like to operate with the lowest acceptable level of electric boost where the exhaust is in compliance with environmental regulations. The reduction in $NO_x$ emissions provided by operating OEAS on a furnace provides the operator this opportunity to reduce the level of electric boost.

The savings from lowering the electric boost depend strongly on the costs of natural gas, oxygen, and electricity to the plant. Generally, electricity is much more expensive on a unit of energy basis than natural gas. Typically, the cost of oxygen and increased natural gas incurred when OEAS is employed and boost is reduced are generally offset by the savings in electricity cost. Table 5 shows the cost advantage for a representative 300 ton/day glass melter using typical 1996 costs for fuel, oxygen, and electricity.

Table 5. ECONOMICS OF LOWERING ELECTRIC BOOST WITH OEAS OPERATION ON A TYPICAL REGENERATIVE SIDEPORT GLASS FURNACE

| | |
|---|---|
| Glass Pull Rate, ton/day | 300 |
| Gas Cost, $/MM Btu | 2.50 |
| Oxygen Cost, $/MM Btu | 2.00 |
| Electricity Cost, $/kWh | 0.07 |
| Changes With OEAS Operating | |
| Natural Gas, $/ton | 1.00 |
| Oxygen, $/ton | 0.80 |
| Electricity, $/ton | - 2.80 |
| Savings With OEAS Operating, $/ton | 1.00 |

The calculation in Table 5 estimates OEAS will not only reduce furnace $NO_x$ but will reduce the operating cost of production by $1/ton. The savings would vary widely depending on the cost of fuel, oxygen, and electricity and on the amount of boost that could be reduced while still being in compliance with $NO_x$ regulations.

Owens Brockway performed forehearth work on the C furnace in late November and early December. During this time, the pull rate was cut in half (to 150 ton/day) and the natural gas rate and electric boost were reduced. A test campaign was conducted in December, 1996 in which the furnace was brought back to full pull rate with electric boost reduced by approximately one third. Under these conditions, the gas firing rate was

increased by approximately ten percent to provide the necessary heat for the furnace. Variables evaluated at low boost included primary stoichiometric ratio (PSR), overall stoichiometric ratio (OSR), natural gas level, and staging oxygen concentration (21 to 50%).

Results are presented in Figures 26 and 27 for left side firing and right side firing. An average $NO_x$ reduction of 30 percent was achieved. With no staging, the average level of $NO_x$ was 3.4 lb/ton, and this emission level decreased to 2.4 lb/ton when OEAS was employed. The level of $NO_x$ reduction was essentially the same for low boost operation as was achieved with high boost operation. The level of $NO_x$ production was higher under low boost conditions because more fuel was burned and the temperature above the glass was higher.

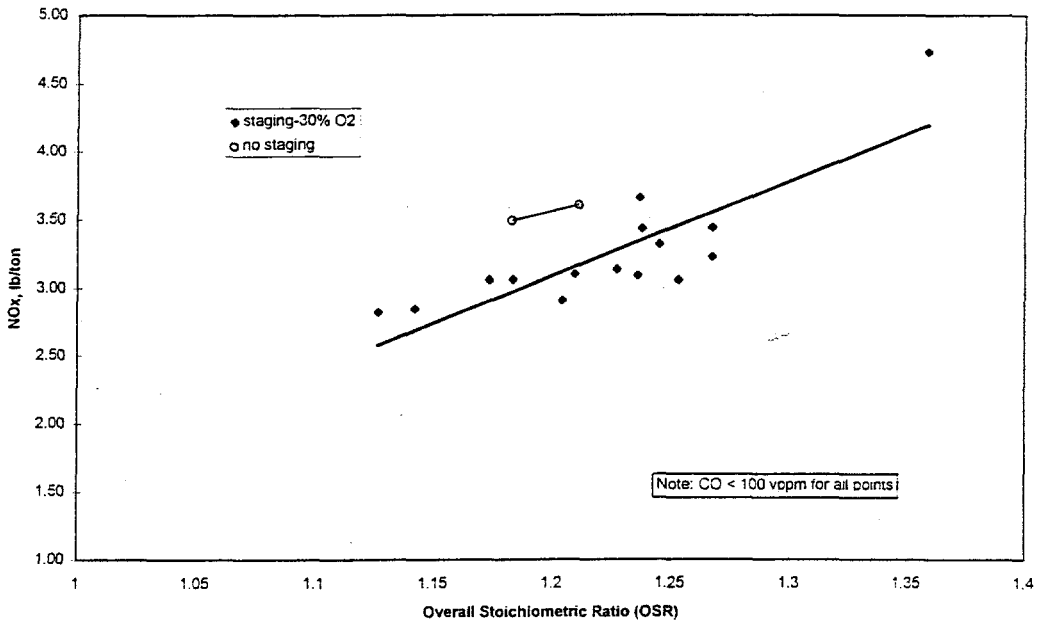


Figure 26. $NO_X$ EMISSIONS AT LOW BOOST - LEFT SIDE FIRING

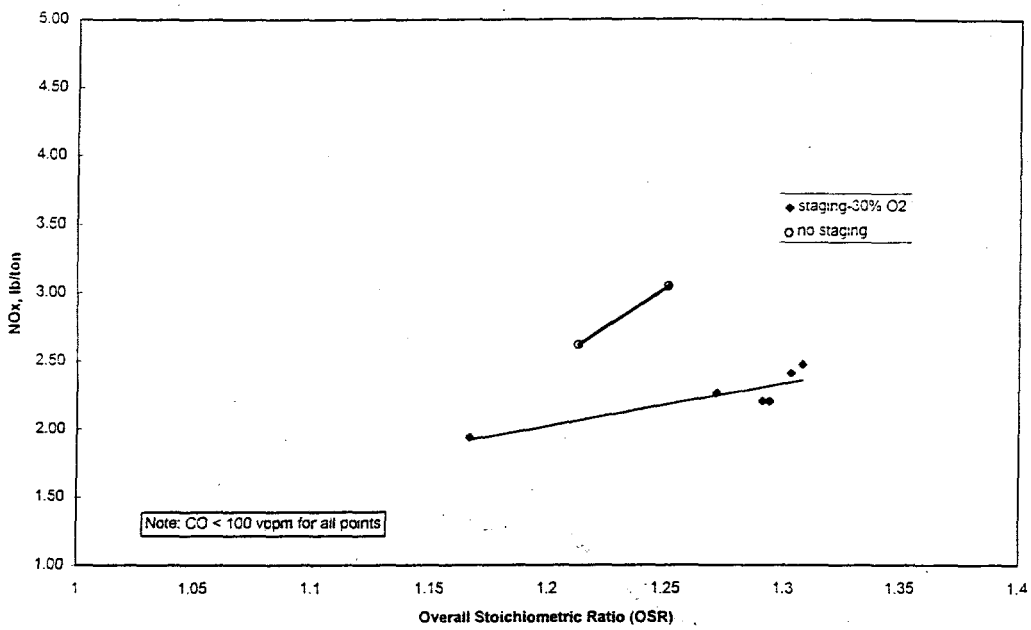


Figure 27. $NO_X$ EMISSIONS AT LOW BOOST - RIGHT SIDE FIRING

Testing with PLC controlling OEAS system

After completing the full furnace parametric testing, the long-term testing and the low electric boost testing, the project team decided to install the PLC in the furnace. The furnace was left with the operating OEAS system with the oxygen and blower air skids and with the PLC control system. Data on $NO_x$ and CO emissions collected during the testing is shown for the left and right side in Figures 28 and 29.

During the testing period, $NO_x$ reductions of up to 40% were observed. This level was higher than the 30 to 35% $NO_x$ reduction achieved in parametric and long-term testing. The PLC system allowed OEAS oxidant flows and air to fuel ratios to be set separately on the right and left side of the furnace which resulted in better control of $NO_x$ emissions while CO levels were kept very low.

Conditions were set for long term testing with the PLC system controlling the OEAS system. The air to fuel ratio on the left and right sides of the furnace were set separately. The PLC was set to handle the slight changes in furnace operating conditions so that CO stayed at a low value (<20 vppm).

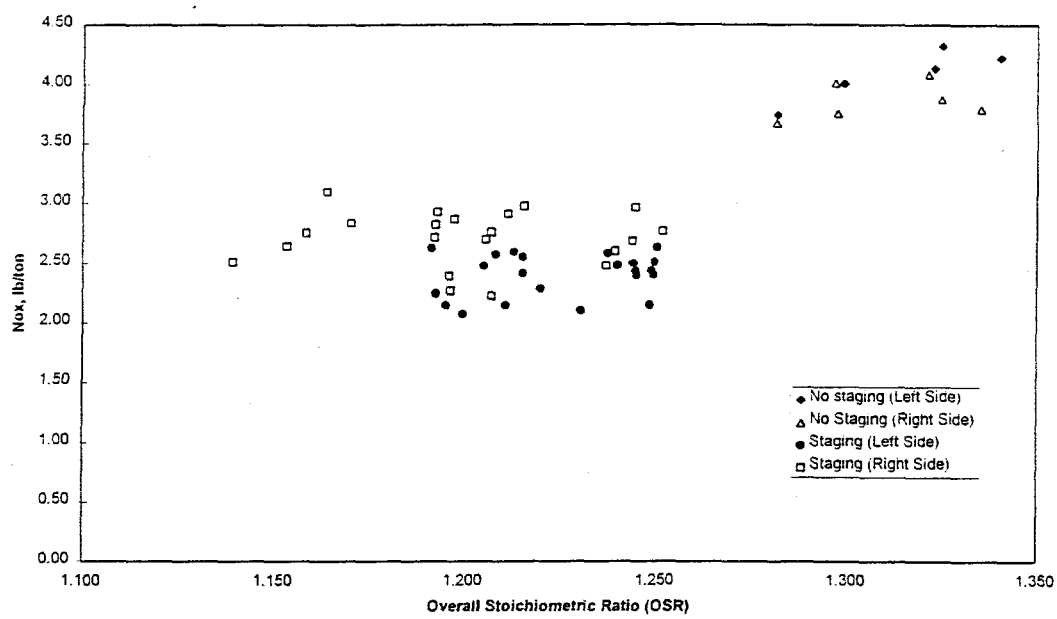


Figure 28. $NO_x$ EMISSION WITH PLC CONTROLLING THE OEAS SYSTEM

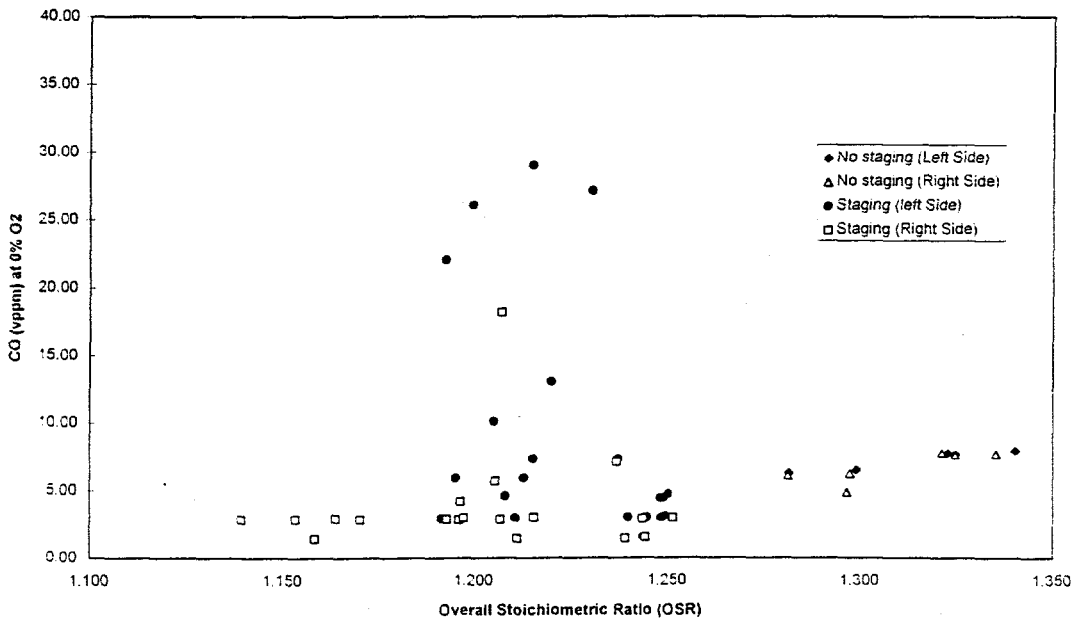


Figure 29. CO EMISSION WITH PLC CONTROLLING THE OEAS SYSTEM

## CONCLUSIONS AND RECOMMENDATIONS

Regenerative glass melters use extremely high air-preheat temperatures, resulting in very high levels of $NO_x$ (uncontrolled $NO_x$ levels above 10 lbs/ton of glass pulled are common). Consequently these furnaces are being placed under stringent regional regulations. For example, the Southern California area now limits $NO_x$ from all container glass tanks to 4 lbs $NO_x$/ton, and is considering even more stringent future regulations.

To help the glass industry meet these regulations, the Institute of Gas Technology (IGT), and their industrial partners -- Combustion Tec, Inc. (CTI) and Air Products and Chemicals, Inc. (APCI) have completed field tests of Oxygen-Enriched Air Staging (OEAS) technology on a natural gas-fired regenerative sideport furnace in Vernon, California. Funding for the project was provided by the Gas Research Institute (GRI) and the US Department of Energy (DOE).

Field tests were conducted at the Owens-Brockway (OB) C furnace in Vernon, California. This furnace is a 300 ton per day six port crossfired furnace producing amber container bottles. Data collected during 6 months of continuous operation indicate a 35% $NO_x$ reduction or maintained $NO_x$ levels near 2lb $NO_x/ton_{glass}$.

The overall market strategy will be to bring this technology to the attention of the glass industry for regenerative furnaces in the USA. The primary market will be the U.S. glass container industry which has approximately 150 furnaces and are about equally divided between sideports and endports. A back-up to direct customer contact will be some literature mailouts, some limited advertising, technical trade show displays, technical articles for trade magazines describing new products and technical papers at seminars and conferences. The Business Plan is explained in Appendix D. Foreign markets will be pursued following the U.S. market, with emphasis on those locations where environmental forces are a driving factor and patent protection is viable and/or patent infringement is not a problem.

Combustion Tec, Inc. has developed spreadsheets to do detailed economic analysis of the staging technology for any given furnace. CTI recognizes that the technology cost can vary widely among different furnaces largely due to furnace size, baseline $NO_x$ levels, type of OEAS system chosen, oxygen costs, and utility rates. Included in the analysis are OEAS capital costs, operating costs, installation costs, and other miscellaneous costs the customer may wish to include. The spreadsheet can also be used to compare other $NO_x$ control technologies' costs to the OEAS technology.

Typically, the productivity cost increase associated with an OEAS system is less than $2.50 per ton of glass produced. This cost increase can range from around $.70/ton for a smaller furnace with either a BAS or CAS system to over $3.00 for a larger furnace using a liquid oxygen supply OEAS system and has moderate baseline $NO_x$ levels. The abatement cost, in dollars per ton of $NO_x$ reduced, ranges from $400-$1000/ton $NO_x$ reduced. Again, this variance is due to furnace size, OEAS system chosen, oxygen costs, and baseline $NO_x$ levels.

Conclusions

Reduction of the stoichiometric ratio on the primary flame of port 5 produced $NO_x$ reductions as high as 35%. The true $NO_x$ decrease is believed to have been greater with measurements influenced by mixing and crossflow. Staging using side-of-port and the two hole underport injection strategies successfully burned out CO generated by the reduced PSR without generating $NO_x$ or increasing exhaust port temperature. The one hole underport injection strategy produced poor port coverage and an increase in $NO_x$. Furnace crown injection was not studied extensively but will require careful selection of position, oxygen enrichment, and velocity parameters to burn out CO without increasing $NO_x$ or impinging on the glass surface. Enriched air proved to be a highly effective secondary oxidant in this furnace. However, an oxygen enrichment level of more that 50% was found to increase both port temperatures and $NO_x$.

The preferred air staging option was determined to be two hole underport injection. Side-of-port injection also provided effective CO burnout without generating $NO_x$, but direct oxidant injection into the furnace provides several benefits. Burnout of the CO above the glass provides heat recovery inside the furnace where the energy is needed while preventing the burnout from overheating the refractory.

Full furnace OEAS demonstration with two hole underport injection confirmed the single port pair testing results. A reduction of PSR with 35% oxygen staging decreased the $NO_x$ by more than 30% to approximately 1.8 lb/ton. The amount of $NO_x$ reduction reflects the very low furnace baseline NOx levels. The best $NO_x$ reduction was achieved with the lowest possible OSR corresponding to the smallest amount of staging oxidant. A lower amount of staging oxidant is also desirable from an economic standpoint. OSR values of 1.08 to 1.10 in combination with a PSR of 1.02 produced optimum $NO_x$ reduction and effective CO burnout in the furnace.

Increasing the oxygen content of the staging oxidant from 35 to 50% produced a decrease in $NO_x$ emissions of approximately 6%. Choice of the oxygen concentration in the secondary oxidant over this range is expected to be an economic decision for the furnace operator.

A PLC system proved to be effective in long-term OEAS operations while providing means to operate the right and left sides of the furnace at different overall stoichiometric ratios to maximize $NO_x$ reduction and stable operation. $NO_x$ reductions as high as 40% were achieved with the PLC controlling OEAS. This was somewhat higher that the reduction achieved by manual operation and was considered a reliable full-time OEAS control process. The OEAS system was left operating, under PLC control, at conditions which provided the highest possible $NO_x$ reduction while using oxygen at a rate acceptable to the plant and while using a level of secondary air in the center of the blower skid's range. The average $NO_x$ emission from the furnace was 2.5 lb/ton at the end of the first week of PLC control, after optimizing the OEAS system. This $NO_x$ level was maintained during operation after completion of this project. The OEAS system has now been operating successfully for eight months.

Operation of the air staging system on this furnace has involved hardware, modeling, and practical expertise. The OEAS system is stable and operation is not adversely affected by minor changes in furnace operation. The system is flexible but must be adapted to each furnace on an individual basis. Installation requires an understanding of the air staging impact on $NO_x$, CO, furnace temperatures, gas flows, and mixing.

Recommendations

With the successful completion of this demonstration program, the OEAS development team has brought the technology to commercial status for all natural-gas fired endport and sideport container glass furnaces. The team recommends further application and development be followed along two paths: commercial application on furnaces where OEAS has been successfully demonstrated and extension of the technology to furnaces making other types of glass as well as other furnaces operating at high temperatures and suffering from high $NO_x$ emissions. The development team offers the following recommendations for future OEAS application and development:

- continue aggressively selling the OEAS technology to owners of natural gas-fired endport regenerative glass melters for container glass production,
- begin aggressively selling the OEAS technology to owners of natural gas-fired sideport regenerative glass melters for container glass production,
- find a flat glass furnace for demonstration of the OEAS $NO_x$ control technology on this type of glass furnace,
- pursue application of the OEAS $NO_x$ reduction technology in the non-ferrous and ferrous metal industries through field demonstration on high-temperature commercial furnaces.

## REFERENCES


1. Barklage-Hilgefort, H., "Reduction of $NO_x$ Emission of Glass Melting Furnaces by Primary Measures."
2. Abbasi, H. A. and Fleming, D. K., "Development of $NO_x$ Control Methods for Glass Melting Furnaces," Final Report GRI-87/0202, Chicago, August 1987.
3. Moilanen, G. L., Van Kalsbeek, B. and McQueen, A., "Glass Furnace Applications of SNCR $NO_x$ Control Technology: Comparison of Predicted and Actual Performance," in Wilcox, D. L. and Bergernon, C. G., Eds., Proceedings of the 52nd Conference on Glass Problems. Westerville, Ohio: The American Ceramic Society, Inc., November 12-13 1991.
4. Abbasi, H. A., Khinkis, M. J., and Fleming, D. K., "Development of $NO_x$ Control Methods for Glass Melting Furnaces," Annual Report GRI-84/0053, Chicago, September 1983.
5. Carvahlo, M. and Lockwood, F. C., "Thermal Comparison of Glass Furnace Operation With Oil and Natural Gas," Glastech. Ber. 63 Nr. 9 (1990).
6. Grosman, R. E., and Abbasi, H. A., "Technical Support for Air Staging Field Test on an Endport Glass Tank in Houston."
7. Joshi, M. J., Wishnick, D. B., Abbasi, H. A., Grosman R. E., et al, "Cost Effective NOx Production Using Oxygen-Enriched Air Staging (OEAS) on Regenerative Glass Burners". Paper presented at 55th Conference on Glass Problems, Nov. 8-9, 1994, Ohio State University, Columbus, Ohio.
8. Launder, B. E. and Spalding, D. B., "The Numerical Computation of Turbulant Flows," Imperial College of Science and Tecnology, London, England, NTIS N74-12066, January 1973.
9. Shah, N. G. *A New Method of Computation of Radiant Heat Transfer in Combustion Chambers*, Ph.D. Dissertation, Imperial College of Science and Technology, London, England, 1979.
10. Magnussen, B. F. and Hjertager, B. H., "On Mathematical Models of Turbulent Combustion with Special Emphasis on Soot Formation and Combustion," *Proc. 16th Symposium (Int'l.) on Combustion*, Cambridge, MA, August 15-20 1976.
11. *FLUENT User's Guide*, Version 4.3, Fluent Inc, Lebanon, NH, March 1995.
12. Platten, J. L. and Keffer, J. F. "Entrainment in deflected axisymmetric jets at various angles to the stream, " Technical Publication Series, UTMETP-6808, Department of Mechanical Engineering, University of Toronto, June 1968.

# APPENDIX A
# SINGLE PORT PAIR MODELING

# Effect of Oxygen Enriched Air Staging on CO Emission for an Owens-Brockway Side-Port Regenerative Container Glass Furnace

Final Report for
The Institute of Gas Technology, Des Plaines, IL
with regard to
IGT Proposal No. U62G3/95A

Xianming Li, Air Products and Chemicals
January 31, 1996

## Summary

Implementing side of port OEAS with cold secondary oxidant containing 35% oxygen in this side-port furnace is expected to reduce NOx emissions substantially without affecting the furnace thermal efficiency or production rate. If a simple reduction in the primary stoichiometric ratio is employed without secondary oxidant injection, CO emissions will be two orders of magnitude higher than the current level. Staging appears to be an effective method of reducing CO emissions. In particular, staging with a higher nozzle velocity is preferred. With the best staging arrangement, CO emissions are reduced to within four times the current level. An important feature of OEAS is CO burnout in the furnace to recover heat and to prevent overheating. The CFD analyses show that OEAS can realize these benefits without the adverse effect of overheating the furnace superstructure.

The three alternate OEAS strategies: crown injection with a single nozzle, under-port lancing with two nozzles and under-port lancing with one nozzle, do not overheat the furnace superstructure, have no negative impact on the furnace thermal efficiency, and they result in complete CO destruction at the port neck exit. With crown injection, 90% of the CO gets destroyed in the melter, whereas 50% of the CO burnout takes place in the melter for the under-port lancing options. Under-port lancing with two nozzles at 300 ft/s and angled 30° from horizontal seems the best choice in terms of CO destruction, impact on flow above the glass and furnace thermal efficiency. Crown injection with one nozzle must have a slower jet so that it does not impinge on the glass surface.

The proposed OEAS arrangement is effective in CO and NOx reductions, and does not incur fuel penalty. In fact, the increased air preheat temperature and a more luminous flame may even increase the thermal efficiency (production rate). Additional gain in thermal efficiency can result from capturing the heat of CO combustion inside the furnace which is achievable with preheated staging oxidant or pure oxygen injection. With 35% oxygen content, the cold staging jets in the current plan require more energy to heat up than the available CO combustion heat release. Pure oxygen jets require much less energy to heat up due to the reduction in gas volume. Alternative injection strategies are evaluated to ensure CO burning above the load. To further increase NOx reduction, the primary stoichiometric ratio may have to be decreased below 0.95.

## 1. Introduction

Oxygen Enriched Air Staging (OEAS) will be applied to an Owens-Brockway side-port, regenerative, container glass furnace in Vernon, CA to demonstrate its $NO_X$ reduction benefits. It is known that NOx production decreases in oxygen-deficient conditions. However, oxygen deficiency causes an increase in CO emission. Therefore, the key to OEAS technology is to determine the best means of CO destruction inside the furnace for emission compliance and checker protection. OEAS technology has been proven to achieve significant NOx reduction with CO compliance in an end-port regenerative furnace (Joshi et. al, 1994). This study examines CO production and destruction in the primary and staging combustion zones. The furnace is fired with natural gas-air burners. Under the current operating conditions, the stoichiometric ratio is 1.10. During the proposed OEAS demonstration, the stoichiometric ratio in the primary combustion zone is lowered to 0.95 (slightly fuel rich). However, oxygen introduced through the proposed staging arrangement will bring the overall stoichiometric ratio back to 1.10, or about 2% excess oxygen. The staging air will result in secondary combustion that could affect the operation of the furnace. A number of concerns must be addressed before this technology can be implemented:

- How does staging affect the carbon monoxide (CO) emission?
- Where does the secondary combustion take place?
- Will the secondary combustion affect the crown or the exhaust port temperatures?
- How does staging affect furnace efficiency (production rate)?

These issues are examined through thermodynamic and computational fluid dynamics (CFD) analyses. This report summarizes the results.

In addition to side of port injection, it is advisable to examine three alternate OEAS strategies: crown injection with a single nozzle, under-port lancing with two nozzles, and under-port lancing with one nozzle, all at an injection velocity of 300 ft/s. The injection arrangements are shown in Figure A-1. The oxygen content of the enriched air is 35 mole percent. The major parameters for these alternate cases are shown in bold face in Table A-1 along with the in-port options. All strategies have been examined via CFD modeling, and the results are reported in this report.

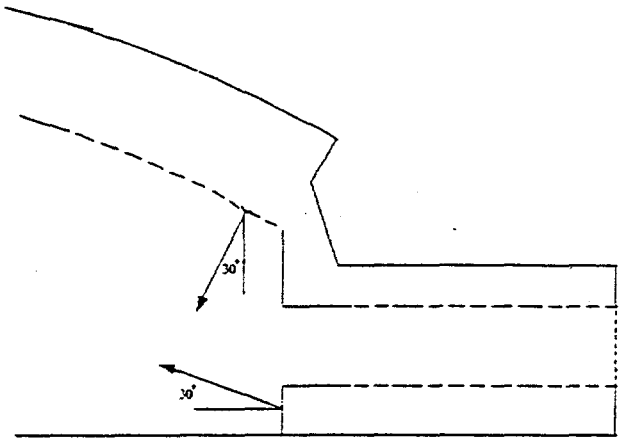


Figure A-1. Crown injection and under-port lancing arrangements.

## 2. Modeling Approach, Assumptions and Plan

### 2.1. Furnace Geometry and Boundary Conditions

The Owens-Brockway, regenerative 6-port side-port, container glass furnace has a permitted throughput of 320 tons per day with 1.5 MW electric boost available. In this study, one section of the furnace containing only a single port pair (port 5) is examined. This choice simplifies the geometry enough to permit detailed analysis for CO emission predictions. Port 5 has similar operating conditions to its neighbors, thus symmetry conditions can be applied to the section boundaries. The refractory walls are modeled in this study using manufacturer's information on thermal properties. The glass bath is represented by a smooth surface whose temperature is assumed to be equal to that of the tuckstone and was measured with an optical pyrometer by the furnace operator (2770°F). The modeled geometry is shown in Figure A-2.

The port geometry is simplified to facilitate the analysis. These simplifications will affect the flow pattern and the flame shape near the port opening to the furnace. However, as discussed in a later section, their impact to the primary objectives of this study is minor.

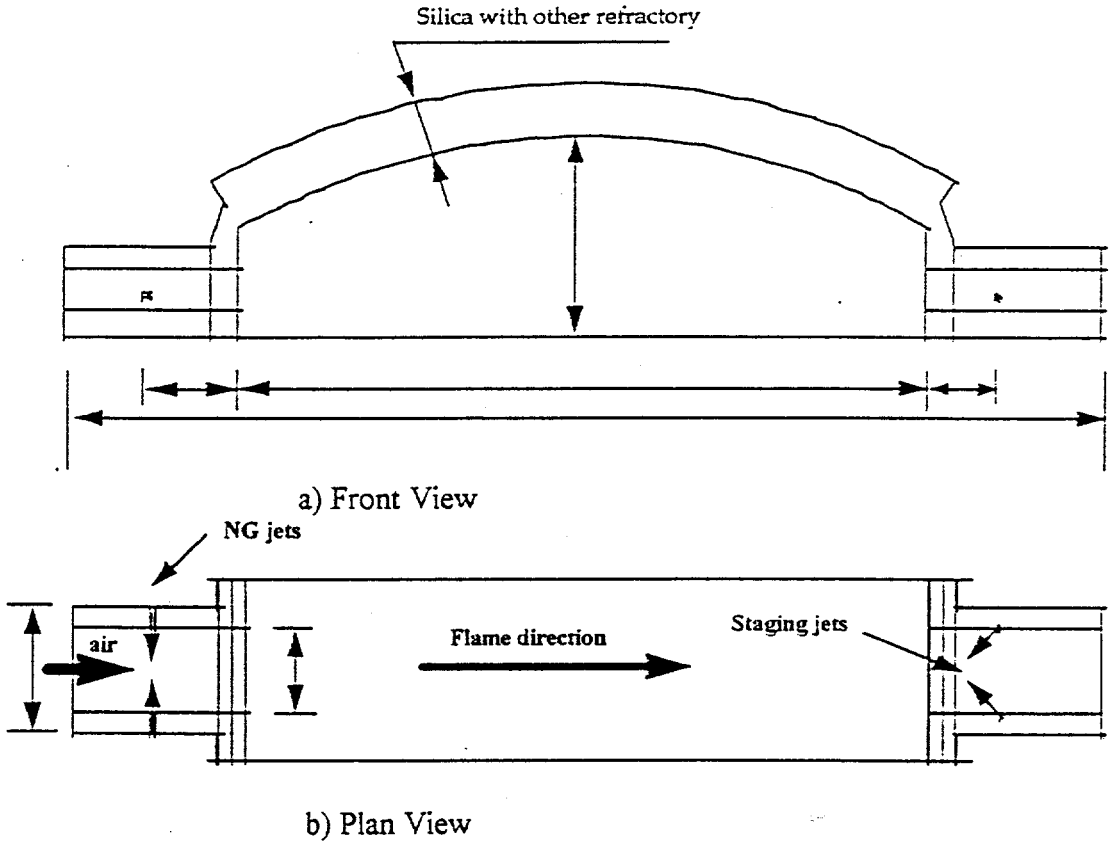


Figure A-2. Geometry for the port-to-port CFD model.

Port 5 as modeled in this study has a total natural gas flow rate of 9450 SCFH, or 385.8 pounds per hour (lbm/hr). This amount of fuel is split evenly between two gas injectors and comes in perpendicular to the primary air flow at 80°F. Thus, each burner is rated at 4.158 MMBtu/hr, and the resulting natural gas velocity is 26.8 ft/s.

Primary air is preheated in the regenerator to approximately 2300°F when the primary stoichiometric ratio (PSR) is 1.10 under the current operating condition. With a PSR of 0.95, the air flow rate decreases from 7300 lbm/hr to 6304 lbm/hr. The preheat temperature will rise because of the reduction in mass flow through the checker, its value will be found with the thermodynamic analysis to follow (2370°F). Thus, the average air velocity under the current operating condition is 32.1 ft/s, and it becomes 27.7 ft/s under OEAS conditions. The turbulence intensity at the air and the gas inlets are set to 10%, i.e. $u'/U = 0.1$. Normally this level of turbulence intensity is quite high, but it is needed here to account for flow conditions prior to the inlets in the checker and in piping system.

The exterior walls of the crown and the breastwalls lose heat via natural convection and radiation to the environment. However, the pattern of the natural convection flow field is quite different due to the difference in wall orientations. From correlations of natural convection heat transfer (Bejan, 1984), the crown cold face has an external heat transfer

coefficient of 0.195 Btu/hr/ft$^2$/°F, and the breastwalls 0.346 Btu/hr/ft$^2$/°F. All inside walls have an emissivity of 0.8 except the glass surface. The glass surface emissivity is 0.92.

The enriched staging air has an oxygen content of 35 mole percent. The total flow rate is 619.8 lbm/hr, and it comes in at 80°F. This amount of enriched air is fixed in all of the OEAS cases and is distributed evenly between one or two nozzles. The nozzles inject the oxidant inside the port, opposing the exhaust flow. The angle between the nozzle centerline and the port centerline is fixed at 42 degrees (see Figure A-2) for in-port injection. Since the total amount of staging air is fixed, the jet velocity is varied to investigate the effect of jet momentum on overall performance. The jet diameter is calculated based on the jet velocities.

## 2.2. Key Physical Models

Flow in the furnace is highly turbulent. Although more advanced models of turbulence such as the RNG $k-\varepsilon$ model (Yakhot and Orszag, 1986) and the full Reynolds stress model (Launder, Reece and Rodi, 1975) are available, the standard two-equation $k-\varepsilon$ turbulence model (Lauder and Spalding, 1973) is used in this study. This model is robust and computationally efficient with a proven track record of reliable results.

Radiation heat transfer is computed with the discrete transfer radiation model (DTRM) by Shah (1979). This model solves the radiative transfer equation directly along discrete rays emanating from all surfaces. It is applicable for participating media ranging from optically thin to optically thick. For natural gas-air flames, the optical thickness is in the middle of the range, therefore, the DTRM model is desirable.

With CO emission prediction as a key objective, the following species list is the required minimum: $CH_4$, $O_2$, $CO_2$, $H_2O$, CO, $N_2$. This mixture is assumed to obey the ideal gas law. The viscosity, thermal conductivity and specific heat of the mixture are computed from individual species properties which are functions of temperature as described in the JANAF tables. Experience shows that accurate physical properties are a prerequisite of CO emission predictions. The reaction mechanism considered in this study is the following:

$$CH_4 + 1.5\,O_2 \Longrightarrow CO + 2\,H_2O$$
$$CO + 0.5\,O_2 \Longrightarrow CO_2$$

Although the flow in the furnace is highly turbulent, chemical reactions still take place much more rapidly than the rate of mixing. Therefore, the reaction rate will be mixing limited. In the context of the Magnussen-Hjertager model (Magnussen and Hjertager, 1976), the kinetic rates for these two reactions are thus deliberately set very high so that turbulent mixing is guaranteed to be the controlling rate. Mathematically, these statements translate into the following equation:

$$\dot{R}_{i,k} = \min\left\{ A\frac{Y_F}{\nu_{Fk}M_F}, A\frac{Y_O}{\nu_{Ok}M_O}, AB\frac{\sum Y_P}{\sum \nu_{Pk}M_P} \right\} \nu_{ik} M_i \rho \frac{\varepsilon}{k}$$

where $\dot{R}_{i,k}$ is the mass production rate for species $i$ due to reaction $k$. $Y$ is mass fraction, $\nu$ is molar stoichiometric coefficients, $A$ and $B$ are empirical constants, $M$ is molecular weight, $\rho$ is mixture density. Subscripts $O$, $F$ and $P$ denote oxygen, fuel, and product, respectively. The key observation here is that the reaction rates are proportional to the ratio $\frac{\varepsilon}{k}$ with various proportionality constants.

## 2.3. Numerical Method

The governing equations for the conservation of mass, momentum, energy and chemical species are solved with the FLUENT software package (FLUENT User's Guide, 1995). It uses a control volume based finite difference scheme where nonlinear variations are included inside each control volume, similar to the concept of a shape function in a finite element scheme. This method is a variation of the original approach by Patankar (1980). This formulation ensures the balances of mass, momentum, energy and species locally (within each control volume) to achieve physically realistic results even on coarse grids.

The current CFD model has approximately 62,000 grid points. A nonuniform grid is designed so that areas of large variable gradients have denser mesh. In particular, the nozzles are represented with 4 control volumes, as shown in Figure A-3. With 12 equations and the radiation model, each iteration takes approximately 2 minutes on an IBM RS6000/580 unix workstation. On average, 1500 iterations are needed to ensure convergence of the solution as measured independently with overall mass and energy balances. Thus, each case requires approximately 50 hours of CPU time.

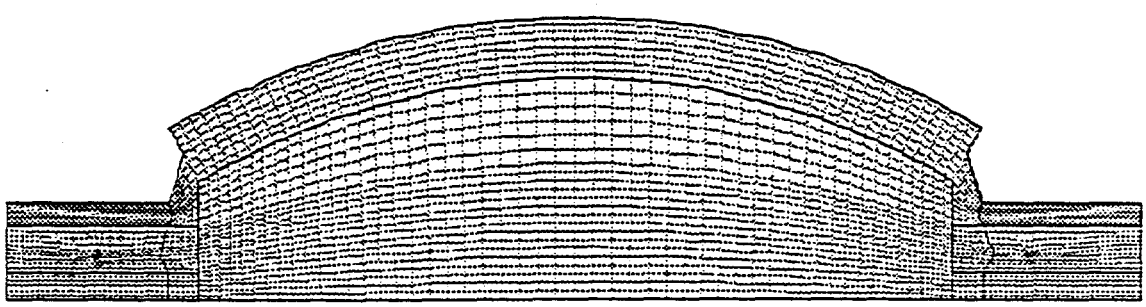

Figure A-3. A nonuniform grid allows adequate resolution in regions of particular importance such as the injection nozzles.

## 2.4. Study Plan

The overall study plan is the following. The current operating condition is studied first as the baseline. Then four variations of the OEAS arrangement will be examined. The fuel-

rich primary combustion without secondary oxidant injection will be referred to as the "OEAS zero" case because the injection velocity is zero. The remaining three cases are for staging with three different velocities: 100 ft/s, 200 ft/s and 300 ft/s. They are to be called "OEAS 100", "OEAS 200" and "OEAS 300" in this report. The corresponding nozzle diameters for delivering the same mass flow rate are 1.761", 1.245" and 1.017", respectively. These parameters are summarized in Table A-1 for ease of reference. The final three cases: crown (crown injection with one injector), underport 1 (underport with one injector), and underport 2 (underport with two injectors) were based on a velocity of 300 ft/s.

Table A-1. Summary of Case Definitions (alternate strategies in **boldface**)

| Case | Name | PSR | OSR | Staging velocity (ft/s) | Nozzle diameter (inch) | Notes |
|---|---|---|---|---|---|---|
| 1 | baseline | 1.10 | 1.10 | NA | NA | current condition |
| 2 | OEAS zero | 0.95 | 0.95 | 0 | NA | in-port injection |
| 3 | OEAS 100 | 0.95 | 1.10 | 100 | 1.761 | in-port injection |
| 4 | OEAS 200 | 0.95 | 1.10 | 200 | 1.245 | in-port injection |
| 5 | OEAS 300 | 0.95 | 1.10 | 300 | 1.017 | in-port injection |
| **6** | **crown 1** | **0.95** | **1.10** | **300** | | **crown, one nozzle** |
| **7** | **underport 1** | **0.95** | **1.10** | **300** | | **underport, one nozzle** |
| **8** | **underport 2** | **0.95** | **1.10** | **300** | | **underport, two nozzle** |

## 3. Thermodynamic Analysis

Global effects of OEAS on the furnace operation can be assessed through an overall energy and material balance, or a thermodynamic analysis. The Sankey diagram for the current furnace operating condition is shown in Figure A-4. Denote the overall stoichiometric ratio (OSR) as $f_o$, the oxygen mole fraction of the primary air as $x$, the molecular weights of oxygen, nitrogen and fuel as $M_o$, $M_N$ and $M_F$, respectively, and the molar oxidizer/fuel ratio as $v_o$. Then the stoichiometric oxidizer/fuel mass ratio for the primary air $r_p$ is computed as

$$r_p = \frac{v_o\left(M_o + \frac{1-x}{x} M_N\right)}{M_F}$$

While $r_p$, the primary air mass flow rate can be expressed in terms of that of fuel:

$$\dot{m}_p = f_o r_p \dot{m}_f$$

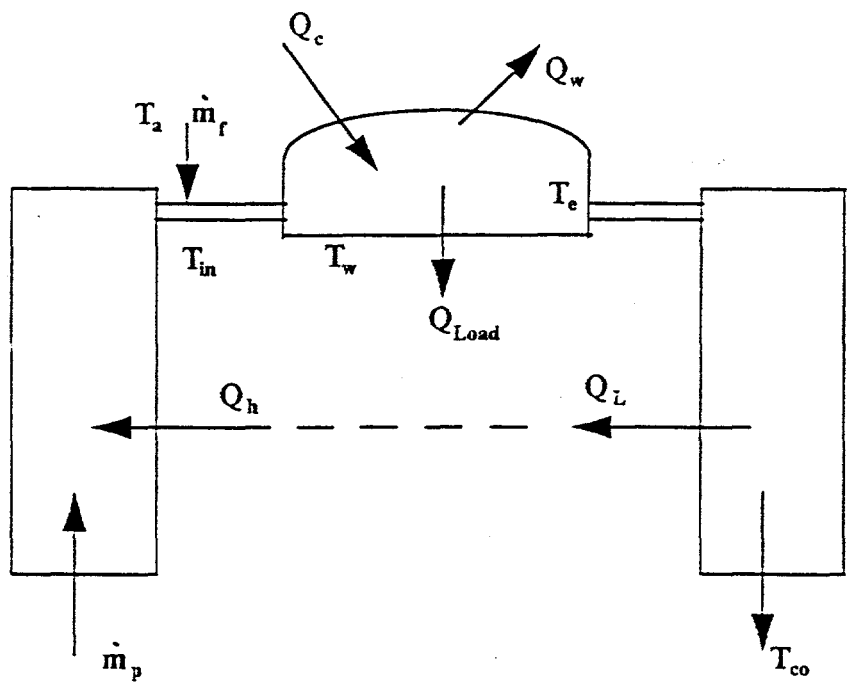


Figure A-4. Sankey diagram for the current furnace operating condition.

Assume the specific heat of the gases at ambient temperature $T_a$ is $c_{pa}$, and at elevated temperatures is $c_p$. Since the preheat air temperature $T_{in}$ at the current operating condition is a measurable quantity, we can find out the amount of heat the primary air stream draws from the checker:

$$Q_h = \dot{m}_f f_o r_p \left(c_p T_{in} - c_{pa} T_a\right)$$

Now consider the energy balance around the furnace. Suppose the furnace gas temperature is uniform and that it can be represented by the temperature immediately before the exhaust entrance, $T_e$. Then the total chemical energy released by the fuel $Q_c$ must be balanced by the wall losses $Q_w$, heat transfer to the load $Q_{load}$ and the flue losses:

$$\dot{m}_f f_o r_p c_p T_{in} + \dot{m}_f c_{pa} T_a + Q_c - Q_{load} - Q_w = \dot{m}_f \left(1 + f_o r_p\right) c_p T_e$$

Recall that the total chemical energy is the product of fuel mass flow rate and the lower heating value of the fuel:

$$Q_c = \dot{m}_f q_{lhv}$$

Let the wall losses and the heat transfer to the load be represented as fractions of the total chemical energy:

$$\alpha = \frac{Q_{load}}{Q_c} \qquad \beta = \frac{Q_w}{Q_c}$$

Note that $\alpha$ as defined above is the combustion efficiency of the furnace. Substituting these relations into the furnace energy balance, we obtain the following equation for $T_e$:

$$f_o r_p c_p T_{in} + c_{pa} T_a + q_{lhv}\left(1 - \alpha - \beta\right) = \left(1 + f_o r_p\right) c_p T_e$$

In the actual operation of a regenerative furnace, the flow direction through the furnace alternates. Thus, the checker on either side of the furnace alternately stores and discharges energy. On the average, the amount of energy discharged must be equal to the amount of energy stored to sustain a periodic steady state operation. This observation is illustrated as a dotted line in the Sankey diagram. Mathematically, this relationship is

$$Q_L = Q_h$$

With this relationship, we can calculate the exhaust side checker efficiency:

$$\eta = \frac{Q_h}{\dot{m}_f \left(1 + f_o r_p\right)\left(c_p T_e - c_{pa} T_{co}\right)}$$

where $T_{co}$ is the gas temperature at the checker outlet. Since the concept of efficiency relates the actual amount of energy extracted with the available energy, $T_{co}$ should be set to the ambient temperature, $T_a$.

When a secondary oxidant is introduced under the proposed OEAS strategy, the energy flows change, as illustrated in Figure A-5. The changing quantities are denoted with a prime (′). The primary air flow rate is related to the primary stoichiometric ratio (PSR) rather than the OSR:

$$\dot{m}'_p = f_p r_p \dot{m}_f$$

Under the current plan, the PSR is less than 1.0, thus some fuel in various intermediate forms will remain in the exhaust. The worst case scenario occurs when all remaining combustible material burns inside the checker. Suppose that scenario is analyzed, then the total chemical energy released in the furnace is

$$Q_c = \dot{m}_f f_p q_{lhv}$$

The remaining portion burns in the checker:

$$Q_s = \dot{m}_f \left(1 - f_p\right) q_{inv}$$

Furnace wall losses are controlled by heat conduction through the insulation. Conduction heat transfer is linearly proportional to the temperature difference across the medium. In other words, when the furnace temperature changes, wall losses will change approximately as follows:

$$Q'_w = Q_w \frac{T'_e - T_a}{T_e - T_a}$$

Heat transfer to the load, on the other hand, is radiation dominated. Thus,

$$Q'_{load} = Q_{load} \frac{T'^4_e - T^4_w}{T^4_e - T^4_w}$$

where $T'_e$ is the new furnace gas temperature under OEAS, and $T_w$ is glass surface temperature. The reduced PSR at sub-stoichiometric level is expected to increase the flame luminosity which may enhance radiant heat transfer to the load. That effect is not included in the above relation, thus, the thermal efficiency estimate may be conservative.

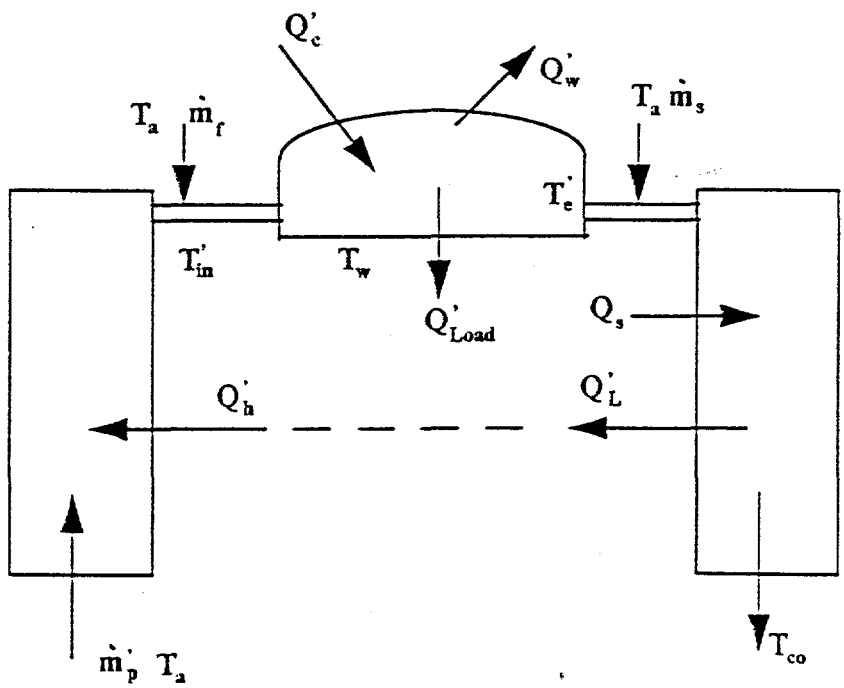


Figure A-5. Sankey diagram for the proposed staging arrangement.

The heat transfer mode through the checkers depends on whether the checker is in the storage phase or discharging phase. According to Delrieux (1980), the discharging phase at the intake side is completely convection controlled, while the storage phase at the exhaust side has an 80/20 split between radiation and convection. Because turbulent convection heat transfer is proportional to $Re^{0.8}$ (Kays and Crawford, 1980), the energy drawn by the primary air will be

$$Q_h' = Q_h\left(\frac{f_p}{f_o}\right)^{0.8}$$

Under the current OEAS proposal, $f_p = 0.95$, and $f_o = 1.1$, thus $Q_h'/Q_h = 88.9\%$.

On the exhaust side, assume that the checker efficiency is controlled by radiation alone:

$$\eta' = \eta\frac{T_e'^4 - T_a^4}{T_e^4 - T_a^4}$$

It is expected that $T_e'$ will be larger than $T_e$. Therefore, more energy can be stored in the checker. However, because heat storage and discharge must be equal on the average as discussed earlier, the checker efficiency will be limited by the convection heat transfer rate at the discharge phase, i.e.

$$Q_h' = Q_L' = Q_h\left(\frac{f_p}{f_o}\right)^{0.8}$$

With this relationship, we can obtain the new preheat air temperature $T_{in}'$ immediately:

$$Q_h' = \dot{m}_f f_p r_p\left(c_p T_{in}' - c_{pa}T_a\right)$$

To find out the new furnace gas temperature $T_e'$, consider the energy balance around the furnace:

$$\dot{m}_f f_p r_p c_p T_{in}' + \dot{m}_f c_{pa}T_a + Q_c' - Q_{load}' - Q_w' = \dot{m}_f\left(1 + f_p r_p\right)c_p T_e'$$

Substitute the expressions for $Q_c'$, $Q_w'$ and $Q_{load}'$ to obtain an equation for the new furnace temperature:

$$f_p r_p c_p T_{in}' + c_{pa}T_a + q_{lhv}\left(f_p - \alpha\frac{T_e'^4 - T_w^4}{T_e^4 - T_w^4} - \beta\frac{T_e' - T_a}{T_e - T_a}\right) = \left(1 + f_p r_p\right)c_p T_e'$$

The new checker efficiency at the exhaust side is found with the following energy balance for the checker:

$$Q_L' = \eta'\left[\left(1 + f_p r_p\right)c_p T_e' + \left(f_o - f_p\right)r_s c_{pa}T_a + \left(1 - f_p\right)q_{lhv} - \left(1 + f_p r_p + f_o - f_p\right)c_p T_{co}\right]$$

where the oxidizer/fuel mass stoichiometric ratio $r_s$ based on the oxygen mole fraction of the staging oxidant $x_s$ is:

$$r_s = \frac{v_o\left(M_o + \frac{1 - x_s}{x_s}M_N\right)}{M_F}$$

Values of various parameters as listed in Table A-2 can be substituted into the preceding equations to obtain numerical results. The wall losses and heat transfer to the load as fractions of total firing power for the current conditions are based on the CFD results. The objective here is to find what changes take place as a result of the OEAS arrangement. Thus, these values should not be held as absolute, rather, they should be treated as typical

and reasonable estimates. Trial calculations with a range of specific heat from 0.239 Btu/lb./°F to 0.477 Btu/lb./°F show that the furnace temperature $T_e$ is relatively insensitive to $c_p$. Since the furnace thermal efficiency $\alpha$ is related to $T_e$, it is expected that $\alpha$ is also relatively insensitive to $c_p$. For the results here, $c_p = 0.382$ Btu/lb./°F, and $c_{pa} = 0.239$ Btu/lb./°F.

The thermodynamic analysis is summarized in Table A-3. The key observation is that the thermal efficiency of the furnace under the OEAS plan will be similar to, or even better than, the current operating condition, mainly because of a higher air preheat temperature.

Table A-2. Values of Physical Parameters Used in the Thermodynamic Analysis

| Variable | Symbol | Units | Value |
|---|---|---|---|
| Primary stoichiometric ratio (PSR) | $f_p$ | | 0.95 |
| Overall stoichiometric ratio (OSR) | $f_o$ | | 1.10 |
| O2 mole fraction in primary oxidant | $x$ | | 0.21 |
| O2 mole fraction in secondary oxidant | $x_s$ | | 0.35 |
| Stoi. air/fuel mass ratio for primary oxidant | $r_p$ | | ***17.17*** |
| Stoi. air/fuel mass ratio for secondary oxidant | $r_s$ | | ***10.50*** |
| Specific heat - Hot combustion products | $c_p$ | Btu/lb./°F | 0.382 |
| Specific heat - cold air | $c_{pa}$ | Btu/lb./°F | 0.239 |
| Lower heating value (LHV) of fuel | $q_{lhv}$ | Btu/lb. | 21,580 |
| Ambient temperature | $T_a$ | °F | 80 |
| Fuel Mass flow rate per burner | $\dot{m}_f$ | lb./hr | 192.9 |
| Heat transfer to load as fraction of firing rate | $\alpha$ | | 0.35 |
| Wall losses as fraction of firing rate | $\beta$ | | 0.09 |
| Temperature at checker exit to stack | $T_{zo}$ | °F | 80 |
| Glass surface temperature | $T_w$ | °F | 2770 |
| CH4 molecular weight | $M_C$ | | 16 |
| O2 molecular weight | $M_O$ | | 32 |
| N2 molecular weight | $M_N$ | | 28 |

Table A-3. Summary of Thermodynamic Analysis

| Quantity | Symbol | Units | Current | Staging |
|---|---|---|---|---|
| Preheated air temperature | $T_{in}$ | °F | 2300 | *2370* |
| Furnace gas temperature | $T_e$ | °F | *3766* | *3811* |
| Furnace thermal efficiency (÷) | $\alpha$ | | *35% (÷)* | *37%* |
| Checker efficiency | $\eta$ | | *59%* | *60%* |
| Total mass flow at exhaust side checker | | lb./hr | *3,830* | *3,640* |

(÷) The furnace thermal efficiency for the current condition is based on the CFD result for port 5 alone. It is meant to be a reasonable estimate so that the change of efficiency can be analyzed for OEAS

The IGT proposal outlines five methods of introducing the secondary oxidant: 1) enriched air with 35% oxygen at ambient temperature, 2) enriched air with 35% oxygen at preheat temperature, 3) pure oxygen at ambient temperature, 4) air at ambient temperature, and 5) air at preheat temperature. The preceding results correspond to the first arrangement. How does the furnace thermal efficiency change with these different methods of secondary oxidant introduction, assuming the PSR is fixed at 0.95 and the injection location remains inside the port? Interestingly, the answer is none based on the thermodynamic analysis, because the checker efficiency is limited by the convection heat transfer rate at the intake side and the secondary oxidant enthalpy does not even enter the furnace efficiency equation. Of course, factors such as NOx and/or CO levels, the extent of furnace modification and operational issues are not considered in this analysis which can be important.

What if the PSR is lowered further for NOx reduction reasons? If the injection location remains inside the port, the furnace thermal efficiency will suffer a penalty if PSR is less than 0.86.

## 4. Results

### 4.1. Staging does not increase crown temperature.

The peak value of crown temperature remains at 2830°F in all cases. However, the size of the crown surface area with the peak temperature is about three times larger with OEAS than the current operating condition as shown in Figure A-11 (color pages at the end). Note that due to some idiosyncrasy of the CFD package the temperature in this figure can only be in Rankine rather than Fahrenheit without software modification. Temperature in other figures are in Fahrenheit, however.

Under the alternate strategies (crown and underport injection) the peak crown temperature remains the same as the baseline condition (2830 °F). The size of the peak temperature is comparable to that of the baseline case when crown injection with one nozzle is used. For under-port lancing options, the size is about three times larger, similar to the hot spot size for the in-port options shown in Figure A-11. No discernible difference in the breastwall temperature can be observed among all operating conditions.

## 4.2. Staging reduces CO emission effectively. CO emissions decrease with an increase in jet velocity for the same amount of staging air.

The reduction in CO comes as a result of correcting the fuel-rich condition in the primary mixture so that oxygen is now available to react with CO. The faster jets mainly improve mixing of the staging oxygen as discussed later in this report. The CO emission levels at the exit of the exhaust port are summarized in Table A-4 (includes alternate strategies). For the crown and underport injection strategies, the CO level at the exit of the port neck is comparable to the baseline, which means complete CO destruction and better than in-port injection strategies. With in-port injection strategies, all CO destruction takes place inside the port. With the one-nozzle crown injection strategy, 90% of the CO burnout takes place inside the melter. At least half of CO burnout takes place inside the melter for the under-port lancing options. The difference has to do with the mixing pattern.

Underport lancing with one nozzle creates a strong jet in the low velocity region in the middle of the two primary flames, which it penetrates with relative ease. It then meets the recirculating flue gases just outside the primary flames. The lower temperature flue gases tend to dive toward the glass surface. The combined motions result in a spiraling flow around the primary flames that carries the secondary oxygen farther upstream in the vicinity of the primary combustion regions. The substoichiometric condition in the primary zones may be disturbed. Furthermore, in the post-flame region relatively less secondary oxygen is available to react with CO, thus CO burnout in the melter is incomplete (50%).

Crown injection with one nozzle also creates a strong jet that penetrates the low velocity region in between the primary flames easily. In fact, at 300 ft/s this jet easily impinges on the glass surface. After this point, the mixing pattern is very different from that of underport lancing with one nozzle. The impingement flow scatters in all directions and mixes almost immediately with the surrounding fluid. In this particular arrangement, the point of impingement is substantially inside the post-flame zone. The good mixing of secondary oxygen in this region implies more complete CO burnout inside the melter (90%).

Underport lancing with two nozzles has two thinner jets at 300 ft/s. They have more difficulty penetrating the high velocity regions aligned with the flames. Yet a significant portion of the secondary oxidant does make it upstream to create a condition, to a lesser degree, similar to that of underport lancing with one nozzle. The outcome is incomplete CO burnout inside the melter (50%).

Regardless of the extent of CO burnout inside the melter, the remaining CO will be completely destroyed in the port because now all remaining oxygen must pass through this passage. Flow acceleration from the melter to the port creates high levels of turbulence which promotes mixing and CO destruction inside the port.

The oxygen mass fraction at the level of the primary burners (17.5" from the glass surface) is shown in Figure A-15 for all three arrangements above. For comparison purpose, the OEAS 300 case is also shown. For reasons of resolving the fine details, oxygen mass fraction above 5% is cut off and appears as white blotches in the plot.

Table A-4. CO Emissions for all OEAS Strategies (alternate strategies in **boldface**)

| | | *Baseline* | in-port OEAS 0 | in-port OEAS 100 | in-port OEAS 200 | in-port OEAS 300 | **crown one hole** | **underport 2 holes** | **underport one hole** |
|---|---|---|---|---|---|---|---|---|---|
| CO at exit of port | lb/hr (raw) | 0.0168 | 1.9670 | 0.7322 | 0.2240 | 0.0700 | **0.0033** | **0.0078** | **0.0195** |
| | ppm | 4 | 584 | 177 | 55 | 17 | **1** | **2** | **5** |
| | lb/MM Btu | 0.0040 | 0.4731 | 0.1761 | 0.0539 | 0.0168 | **0.0008** | **0.0019** | **0.0047** |
| | lb/ton (glass) | 0.0120 | 1.4050 | 0.5230 | 0.1600 | 0.0500 | **0.0024** | **0.0056** | **0.0139** |
| CO at inlet to exhaust port | lb/hr (raw) | 0.4455 | 2.2651 | 2.3141 | 2.8808 | 3.0481 | **0.2693** | **1.2373** | **1.3930** |
| | ppm | 111 | 680 | 695 | 869 | 919 | **68** | **334** | **376** |
| | lb/MM Btu | 0.1071 | 0.5448 | 0.5565 | 0.6928 | 0.7331 | **0.0648** | **0.2976** | **0.3350** |
| | lb/ton (glass) | 0.3182 | 1.6179 | 1.6529 | 2.0577 | 2.1772 | **0.1924** | **0.8838** | **0.9950** |

Note that the nominal throughput used to present the CO emission data in Table A-4 is 320 tons per day. The effect of the electric boost is neglected. Recall also that port 5 has 21% of total fuel input. With these values, the unit energy consumption is 2.97 MMBtu per ton, which provides the connection between emissions and glass production rate. Compared to the current operating condition, the decrease in primary stoichiometric ratio from 1.10 to 0.95 causes the CO emission to increase by 117 times. Staging combustion reduces this vast amount of CO by 96.4% to a level within 4.2 times the current operating condition.

4.3. Staging jets in the current configuration do not penetrate into the furnace. CO reduction and consumption of the remaining fuel all take place inside the exhaust port. Higher jet velocities merely promote mixing of staging air with the exhaust flow.

Flow pattern inside the furnace remains unchanged with in-port OEAS, as illustrated by velocity vectors in Figure A-12. Of course, flow pattern inside the port is very different.

Nevertheless, the staging jets do not penetrate inside the furnace. This fact may seem counter-intuitive. For that reason, a detailed analysis is provided below.

### 4.3.1. Theoretical Analysis

#### 4.3.1.1. Two-Dimensional Potential Flow Estimate

Since the total staging air is only 9.3% of the primary mixture mass flow, penetration of the staging air into the furnace is rather limited. In fact, the penetration distance can be estimated with the potential flow theory (Sabersky et. al, 1971). The flow inside the port can be modeled as the superposition of a uniform flow and a source, as illustrated in Figure A-6. The uniform flow represents the main stream inside the port at about $U_0 = 36$ ft/s. The source flow consists of 14 slot jets whose velocity ($U_j$) is that of the staging flow ($U_s$) at $\theta = 42$ degrees off center ($U_j = U_s \cos\theta$), and whose width is the staging nozzle diameter ($D$). These slot jets are arranged around a 360-degree circumference, because the cone angle of a slot turbulent jet is approximately 26 degrees (Beer and Chigier, 1972). The penetration distance as normalized by the jet diameter is then $\frac{L}{D} = \frac{7}{\pi}\frac{U_j}{U_0}$. At $U_s = 300$ ft/s, the penetration distance is thus estimated at 14". With 100 ft/s, the penetration distance is about 8".

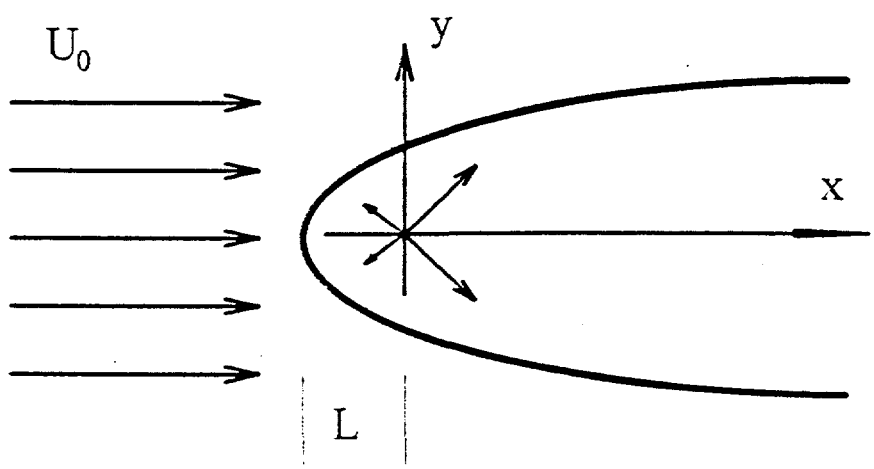


Figure A-6. Jet penetration distance can be estimated by superposing a uniform flow with a source.

#### 4.3.1.2. Three-Dimensional Potential Flow Estimate

In the preceding analysis, the potential source is made of 2D slot jets arranged in a circle. Since the jet stream is small compared to the main flow, the flow field is truly 3D. The jets should be arranged in a sphere to form the potential source. To pack a sphere of radius R with cones of angle α, *n* cones are needed which is determined as follows:

$$n = \frac{4\pi R^2}{\pi\left(R\sin\left(\frac{\alpha}{2}\right)\right)^2} = \frac{4}{\sin^2\left(\frac{\alpha}{2}\right)}$$

With 26-degree cones (α = 26 degrees), $n = 79$. The potential source therefore has a strength $q = n\pi\frac{D^2}{4}U_j$. The jet penetration distance is where the uniform flow velocity becomes equal to the velocity from the spherical source:

$$U_0 = \frac{q}{4\pi L^2} = \frac{n}{16}\left(\frac{D}{L}\right)^2 U_j$$

$$\frac{L}{D} = \sqrt{\left(\frac{n}{16}\frac{U_j}{U_0}\right)}$$

At 300 ft/s, the jet penetration distance is thus 5.6", or $L/D = 5.5$. At 100 ft/s, it is 5.6", or $L/D = 3.2$. Note that these estimates are considerably shorter than the 2D results.

### 4.3.2. Experimental Results

Experimental data are available for round jets into a uniform stream at various angles under isothermal conditions (Platten and Keffer, 1968). The experiment was carried out in an 8' by 4' cross section low speed wind tunnel. The nominal tunnel velocity was 5.2 ft/s, while the jet velocity was varied to create a nominal jet-to-stream velocity ratios of 4, 6, and 8. The initial jet angle with respect to the incoming stream varied from 45 degrees (in the general direction opposing the stream) to 135 degrees (in the general direction of the stream). The configuration is shown in Figure A-7. With the notation in this figure, the jet-to-stream angle varies from -45 degrees to 45 degrees.

For the staging jet configurations, the jet-to-stream velocity ratio is 8.3 at 300 ft/s, and 2.7 at 100 ft/s, which is close to the experimental velocity ratio range. The staging jet is 42 degrees opposing the oncoming stream, which is close to the experimental data point of -45 degrees. Figure A-8 shows the experimental data for the jet-to-stream velocity ration of 8 which is applicable to the staging configuration at 300 ft/s. It can been seen that the penetration distance into the on-coming stream is about $L/D = 6$, or 6.1". For the staging configuration at 100 ft/s, Figure A-9 shows that the penetration distance is approximately $L/D = 2$, or 3.5".

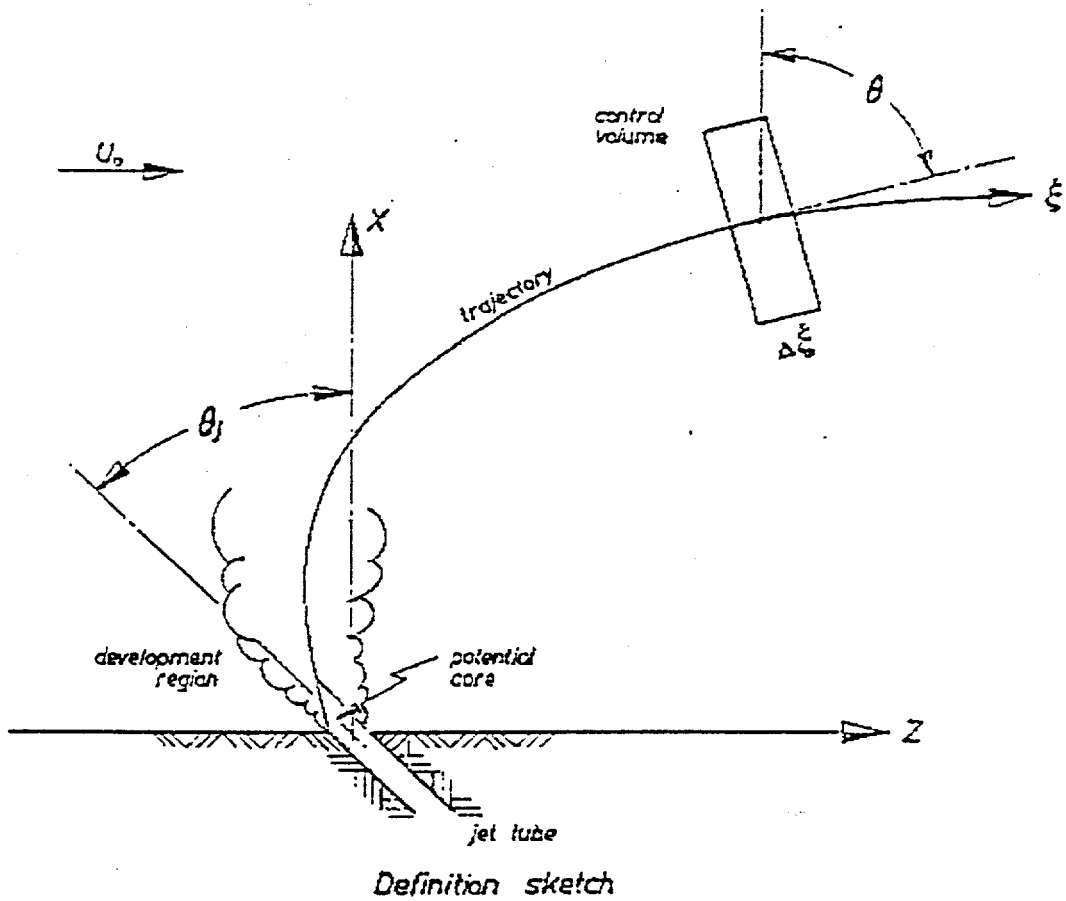


Figure A-7. The experimental configuration of a round jet into a uniform stream.

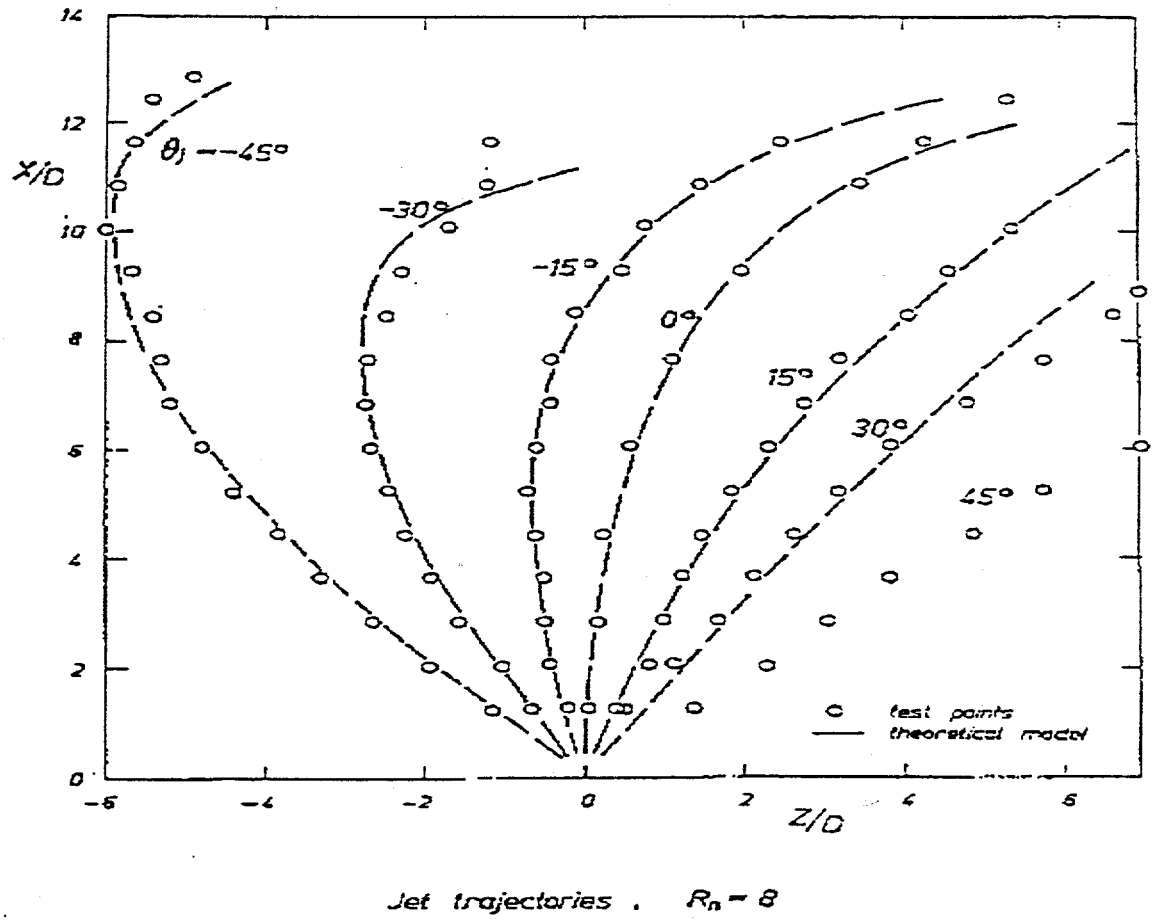


Figure A-8. Experimental data for a round jet into a uniform stream with nominal jet-to-stream velocity ratio 8. The curve with $\theta = -45°$ applies to the staging configuration with 300 ft/s jets.

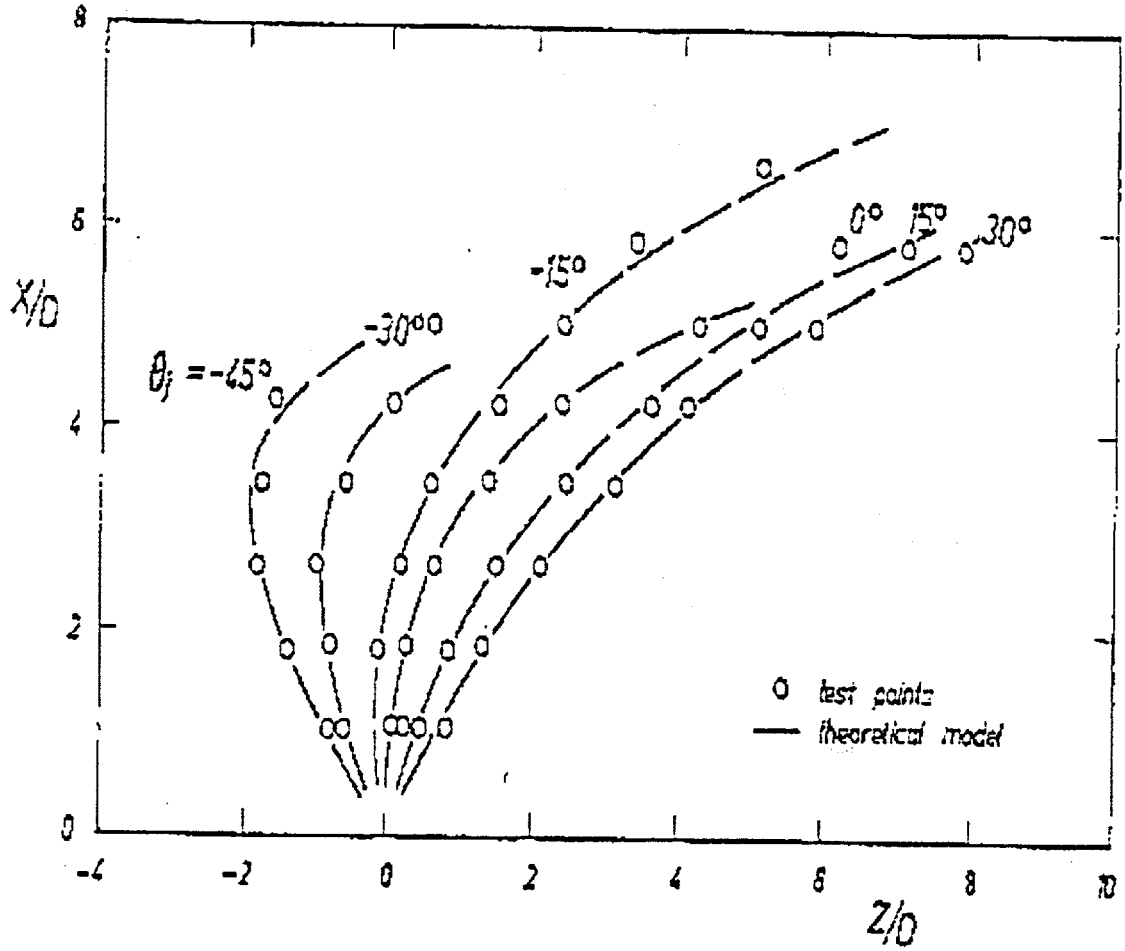


Jet trajectories, $R_n = 4$

Figure A-9. Experimental data for a round jet into a uniform stream with nominal jet-to-stream velocity ratio 4. The curve with $\theta = -45°$ applies to the staging configuration with 100 ft/s jets.

### 4.3.3. Computational Fluid Dynamics Results

The CFD results show that the jet penetration distance is approximately 12" and 8", respectively, for staging jets at 300 ft/s and 100 ft/s, as seen in Figure A-10.

The results presented so far can be summarized concisely, as shown in Table A-5.

Table A-5. Jet Penetration Distance.

| | Potential Flow-2D | | Potential Flow-3D | | Exp. Data | | CFD | |
|---|---|---|---|---|---|---|---|---|
| | *L/D* | in. | *L/D* | in. | *L/D* | in. | *L/D* | in. |
| Staging -- 100 ft/s Jet dia. *D=1.761"* | 4.6 | **8.1** | 3.2 | **5.6** | 2 | **3.5** | 4.5 | **8** |
| Staging -- 300 ft/s Jet dia. *D=1.017"* | 13.8 | **14** | 5.5 | **5.6** | 6 | **6.1** | 11.8 | **12** |

### 4.3.4. Effect of Density Difference and Other Issues

One major assumption in the potential flow estimates and the experimental data is that the main stream and the jet are at the same temperature. In the staging arrangement, the staging jets are at 80 °F, while the exhaust stream is about 2840 °F, therefore the jet stream density is approximately 6 times higher. According to Beer and Chigier (1972), the effect of different density can be corrected with an equivalent jet diameter, $D_e = D\sqrt{\frac{\rho_j}{\rho_m}}$, where $\rho_m$ is the main stream density. That is, the equivalent jet diameter is $\sqrt{6} = 2.45$ times larger than the real jet diameter, thus the penetration distance of a non-isothermal free jet is that much larger than the isothermal estimate. When a jet enters a cross flow as in the staging configuration, however, a second entrainment mechanism exists due to the presence of the "counter-rotating vortex pair" (Platten and Keffer, 1968) in addition to the shear flow entrainment mechanism of the free jet. Therefore, the entrainment rate will be larger and the density difference between the jet and the stream will disappear faster. Thus the penetration distance of a cross flow jet will be smaller than the free jet. In the current situation, the density correction factor will be smaller than 2.45.

From Table A-5, the CFD result, which takes into account the density difference, is approximately twice the experimental data and the 3D potential flow estimate. Based on the preceding argument concerning the effect of density, the CFD result is credible. This fact also points out that *the numerical accuracy of the CFD solution is within bounds of experimental data and no further grid refinement is necessary*. Furthermore, suppose that the exhaust stream temperature has an error of 10%, the penetration distance would only change by 12% based on the equivalent diameter concept. In other words, further grid refinement in the CFD model would not change the order of magnitude of the penetration distance. Since the 2D potential flow estimate ignores the fact that fluid can get around the jet on the sides, its apparent agreement with the CFD result is fortuitous.

The phase 1 report for the OEAS project (Slavejkov and Gershtein, 1994) showed much longer penetration because the configuration was quite different. In that study, an end-port furnace was examined, and the staging oxidant was injected on the side wall into the furnace rather than inside the exhaust port. The gas velocity inside the furnace is much smaller than that inside the port because the volume of the furnace space is much larger than the exhaust port. Furthermore, the staging jets were perpendicular to the main flow rather than opposing the main flow so that the jet momentum was not partially canceled. Because of the partial cancellation, penetration in the opposing direction of the main flow is much more difficult than that in the transverse direction. Figures A-8 and A-9 show that the -45 degree jets penetrate twice as far in the transverse direction as in the main flow direction.

The momentum ratio between the staging jets and the main stream ranges from about 0.2 to 0.6. Because of the large disparity in momentum, the flow pattern created by the staging jets into the primary mixture resembles that of jet impingement on a solid surface at an angle. The jet stream splashes and gets carried away by the main flow. The higher the jet velocity, the harder the two streams collide, therefore the farther the jet stream splashes. The result is improved mixing of the staging air with the main stream.

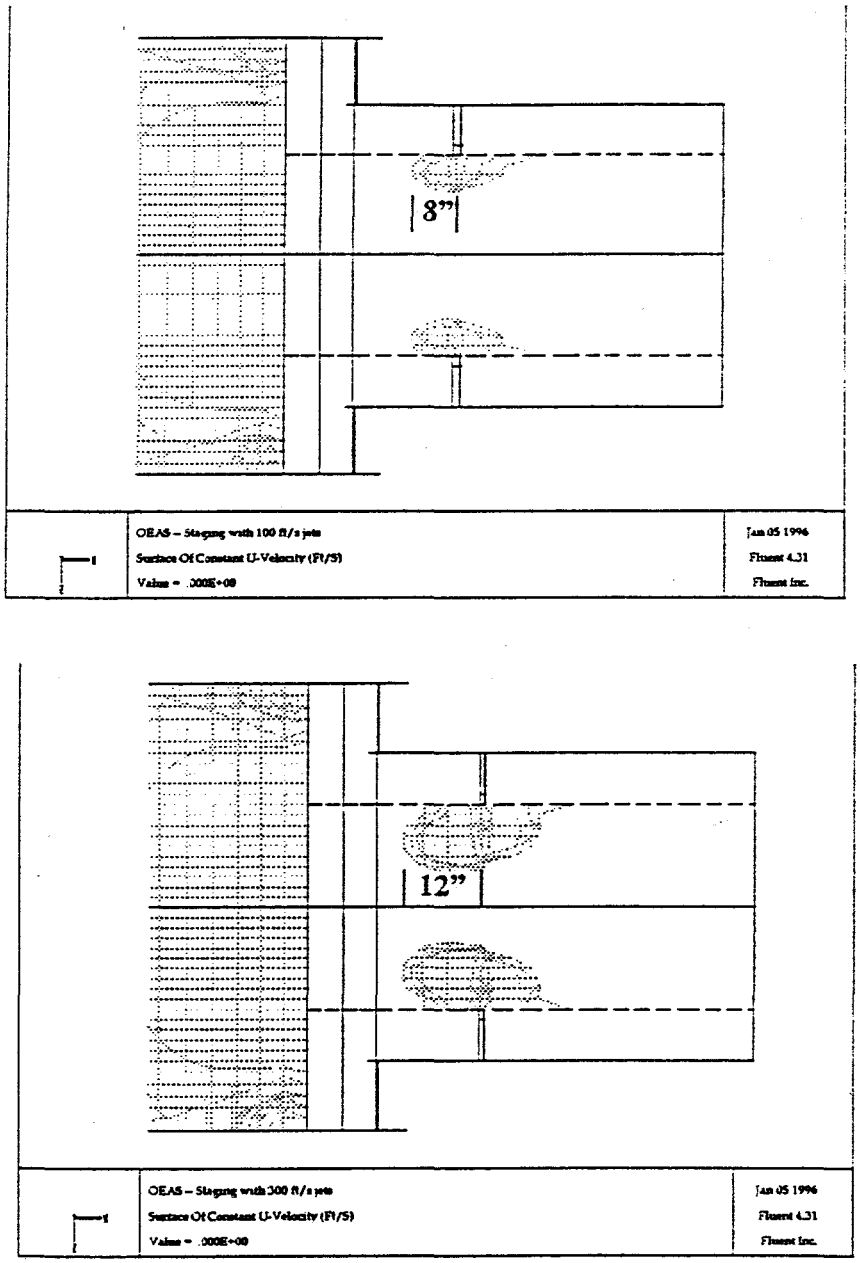


Figure A-10. Staging jets do not penetrate inside the furnace.

Although the jets can not penetrate far into the main stream, the effect of flow blockage is felt all the way up to the inlet port. This "air curtain" has the strongest influence when only one port pair is converted into OEAS, and may redistribute the exhaust flow and affect CO and NOx measurements for the converted port. In the single-port model, the blockage effect produces differences in flow and turbulence structures large enough to result in discernible changes in CO reaction rates, as shown in Figures A-13 and A-14. When all ports are converted with OEAS, however, the aggregate effect will simply be a change in

the damper position to maintain the normal furnace operating pressure. Thus, the "air curtain" influence will be less pronounced.

4.4. Although reactions due to staging take place inside the port, temperature at the port exit is actually lower than that without staging. Therefore, there is no danger of overheating the port walls due to staging combustion.

In fact, the mixture entering the exhaust port is hotter than that exiting the port, because the staging air comes in cold, the energy due to combustion is not even sufficient to raise its temperature to the same level as the exhaust. This point seems counter-intuitive at first, but can be verified readily with thermodynamic analysis. For example, the gas temperature at the inlet to the exhaust port remains constant at 2840°F for all OEAS cases. Without oxidant injection, the temperature drop due to heat loss to the port walls is approximately 77°F. With oxidant injection, even though reactions unleash 416,600 Btu/hr additional chemical energy from unburnt fuel and CO, the energy requirement for sensible heating of the cold staging air to 2840°F is 444,900 Btu/hr ($\overline{c_p} \approx 0.26$ Btu/lb./°F). The final outcome is an additional temperature drop of about 55°F. For the current operating condition, the port exit temperature is 70 °F lower than that at the port inlet.

4.5. The amount of heat transfer to the glass bath is unchanged in the OEAS cases as compared to the current operating condition. That is, OEAS arrangements will not negatively impact the furnace thermal efficiency.

Although the thermodynamic analysis shows a 2% improvement in thermal efficiency under OEAS, the CFD model predicted the efficiency to be the same. Furthermore, there is no difference in thermal efficiency among various jet velocities. As the thermodynamic analysis suggests, the efficiency change is intimately related to the preheat air temperature. With a reduction in the PSR, the preheat air temperature under OEAS increases by 70°F. Since a portion of the fuel is consumed outside the furnace, the overall furnace efficiency will be the result of the higher preheat temperature and the lower combustion heat release. The CFD model incorporates much more realistic physical properties and more sophisticated heat transfer models than the thermodynamic analysis. Therefore, its accuracy is expected to be higher.

One uncertainty in the above results relates to the change in radiation properties of the furnace gas. When the PSR is reduced to 0.95, the amount of soot is expected to increase which might enhance heat transfer to the load. Although the CFD package has the ability to differentiate such changes, the computation is fairly time-consuming and may be done in the future. At this point, one can say that reduced stoichiometry under OEAS can positively impact the thermal efficiency of the furnace.

## 4.6. The OEAS arrangements are expected to result in significant NOx reductions as compared to the current operating condition.

NOx emission is computed with the extended Zeldovich model (Fluent NOx Module User's Guide, 1995). The predicted NOx emission for the current operating condition is 2.0 lb. NO/ton. Compared to the furnace data of 3.7 lb. NO/ton, this prediction is quite reasonable considering the simplifications employed in the single-port model. With a reduction in PSR but without secondary oxidant injection (OEAS Zero case), the NOx emission becomes 1.3 lb. NO/ton, about 34% lower than the baseline. There is no significant difference in NOx reduction among OEAS arrangements with different jet velocities. Because of the simplifications in geometry, uncertainties in boundary conditions, and idealizations in flow parameters, the predicted NOx reduction level can only be indicative of the magnitude of actual reduction. The value of the predictive model lies in confirming the trend and the "significant" nature of the reduction. It is thus reasonable to conclude that the goal of 50% NOx reduction via OEAS is realistic and achievable.

## 4.7. Residence time of secondary oxidant for alternate strategies

The in-port OEAS options have residence times of about 120 milliseconds for the injected oxidant. The oxidant simply turns around from the injection direction and follows the flue gas to the port neck exit (see Figure A-16). With the crown and under-port injections, the oxidant particles get into the large recirculation pattern in the furnace and stay in the furnace for a much longer time. In general, the residence time is at least an order of magnitude larger, ranging from 26 to 65 times.

## 4.8. Impact on flow pattern in the alternate strategies

All options produce significant changes in the general flow pattern. The region in the immediate vicinity of the molten glass is of the greatest interest. For that region, the underport lancing options do not create significant changes. However, crown injection results in a discernible change in velocity magnitude above the glass, which may be undesirable (see Figure A-17). The jet velocity will have to be reduced from the current value of 300 ft/s when crown injection is implemented in the trial. When pure oxygen is used, the jet penetration would be much smaller due to reduced mass flow rate, therefore impingement on the glass surface will be of less concern.

However, when the crown injection velocity is reduced, the mechanism for rapid mixing is disturbed. Since that mechanism is responsible for complete CO burnout inside the melter, it is expected that more CO will be burnt in the port.

## 5. Discussion

Implementing OEAS in this side-port furnace is expected to reduce NOx emissions significantly without affecting the furnace thermal efficiency. In fact, the increased air preheat temperature and a more luminous flame are expected to increase the thermal efficiency. If a simple reduction in the primary stoichiometric ratio is employed without the secondary oxidant injection, the CO emission will be 117 times higher the current level. Staging appears to be an effective method of reducing CO emission. In particular, staging with a higher nozzle velocity is preferred. With the best staging arrangement, the CO emission is reduced to within 4.2 times of the current level. The CFD analyses show that OEAS can realize these benefits without the adverse effect of overheating. These results are based on the assumptions described earlier in this report. While every effort is made to ensure the accuracy of this study, a few issues should be discussed at this point.

The strength of the CFD analysis lies in predicting the trend of variation, rather than pinpointing the exact numerical values. Uncertainties in determining physical dimensions of the furnace, the exact fuel and air flow rates, the boundary conditions such as the temperature of the glass melt and the preheated air all contribute to errors in the final prediction. Therefore, the CO and NOx levels as shown in this report should be interpreted as representative. In fact, according to the IGT report, the current NOx emission is 3.7 lb. NO/ton as opposed to 2.0 lb. NO/ton, even though such an agreement is excellent considering the uncertainties to be discussed next. Nevertheless, only the trend of CO and NOx reductions should be regarded as reliable.

The single most important boundary condition in this model is the glass surface because it controls the majority of the heat loss from the combustion gases (about 80% of all wall heat transfer in this study). Heat loss directly affects the gas temperature which in turn influences the reaction rates and CO levels. In this study, the glass temperature is assumed to be the same as the tuckstone temperature which is measured by the furnace operator. Whether indeed the glass temperature equals the tuckstone temperature remains unknown, although they are believed to be close. In addition, the variation of glass temperature across the furnace is not considered.

The port geometry is also simplified to expedite the analysis. In the furnace, the port narrows down towards the furnace space. That is, the flow accelerates at the inlet port while it decelerates at the exit port. An accelerating flow for the primary mixture tends to elongate the flame. By the time the combustion gases reach the exit port, however, any difference would have been minimal because of the large furnace width. The decelerating flow at the exit port could make the staging jets penetrate somewhat further into the main stream. But based on the fact that the penetration distance changes from 8" to 12" when the staging jet velocity increases from 100 ft/s to 300 ft/s, the effect of deceleration due to the port geometry on jet penetration will be minimal, thus the current conclusions remain valid.

Observations by the furnace operator indicate that the flame from the primary port forms a single rolling shape into the furnace. In the current study, the two side gas injectors in the inlet port produce two distinct flames. The difference in flame appearance is partly due to the decelerating flow effect discussed above. In addition, the baffles inside the port which are not modeled can also create turbulence and promote earlier ignition and flame anchoring. The resulting mixture will be more uniform, and the flames from the two gas injectors might combine. Of course, the "rolling" appearance is solely a result of turbulence which is inherently unsteady. The CFD model only shows a steady, time-averaged appearance. Again, such flame details would be irrelevant by the time staging reactions occur. Thus, the present results should still be valid.

The chemical reaction scheme used in this study is a global two-step mechanism. It is well known that the true reaction pathway of methane involves many more steps and many more intermediate species. Furthermore, natural gas contains other hydrocarbons as well which in turn involve additional pathways. It is impractical for a CFD model to consider all these steps and species. The global reaction mechanism represents a balance between accuracy and practicality and has been used widely. Nevertheless, it should be pointed out that details such as the exact location of ignition and the decomposition of methane can not be predicted with the global mechanism. For instance, the CFD model shows that the methane mole fraction at the exhaust port exit is 0.47% in the baseline case which represents 18.3 lbm/hr of unburnt methane (out of 385.8 lbm/hr total for port 5). In reality, methane would have decomposed into intermediate species before reaching the port exit.

Temperature distribution in the refractory walls shows that heat transfer in those walls is one-dimensional except in small regions near the corners of the furnace. This observation implies that the heat transfer boundary condition for refractory walls can be simplified with an overall heat transfer coefficient. That is, the inclusion of the refractory walls in the CFD model is not necessary. In the current study, that simplification could have reduced the model size by 40% and saved the computing time by approximately 5%.

The CO variation inside the exhaust port is very steep, thus the position of a measurement probe greatly affects its reading. Extra caution should be exercised with water-cooled gas sampling probes in the tight quarters between the furnace and the checkers.

Finally, the "air curtain" effect with staging as a result of flow blockage needs to be kept in mind. If only one port is converted to OEAS, the elevated pressure will divert flow to the neighboring ports. The overall stoichiometric ratio inside the staging port will be higher than 1.10, less CO will emit from the staging port, while some CO will escape to the checkers through neighboring ports along with the diverted flow. When all ports are equipped with OEAS, this effect shows up as a change in the damper position to maintain normal furnace operating pressure, and becomes less of an issue.

## 6. Conclusions

Implementing OEAS in this side-port furnace is expected to reduce NOx emissions significantly without affecting the furnace thermal efficiency as production rate. In fact, the increased air preheat temperature and a more luminous flame may even increase the thermal efficiency. If a simple reduction in the primary stoichiometric ratio is employed without the secondary oxidant injection, the CO emission will be 117 times higher the current level. Staging appears to be an effective method of reducing CO emission. In particular, staging with a higher nozzle velocity is preferred. With the best staging arrangement, the CO emission is reduced to within 4.2 times of the current level. The CFD analyses show that OEAS can realize these benefits without the adverse effect of overheating the furnace superstructure.

Also, the alternate OEAS strategies do not overheat the furnace superstructure, have no negative impact on furnace thermal efficiency, and result in complete CO destruction at the port neck exit. With crown injection, 90% of the CO gets destroyed in the melter, whereas at least 50% of CO burnout takes place in the melter for the under-port lancing options.

It is evident that the mixing pattern in the furnace completely determines the effectiveness of CO burnout and other characteristics of various OEAS strategies. The mixing pattern in turn is governed by the velocity, angle, flow rate and location of the injections. Changes in any of these parameters can produce a result that is different from those studied in this report. Yet it is expected that some discrepancies in these parameters will occur while implementing OEAS strategies under the hostile conditions of a live glass furnace. Therefore, the results here should be interpreted with caution when compared with those measured during the trial.

## 7. Suggestions

The proposed OEAS arrangement is effective in CO and NOx reductions, and the increased air preheat temperature and a more luminous flame may even increase the thermal efficiency. Additional gain in thermal efficiency can result from capturing the heat of CO combustion inside the furnace which is achievable with preheated staging oxidant or pure oxygen injection. In this regard, the injection locations and the type of oxidant will be examined.

1. Change the angle of injection through the oil burner block from 42° in the current plan to 15° using a ceramic sleeve, and increase the injection velocity to 450 ft/s. A calculation using the 3D potential flow theory shows that the jet penetration distance is essentially the same as the 42°-300 ft/s combination because the nozzle diameter becomes smaller ($D = 0.83"$). As a result, CO combustion may still take place inside the port. Furthermore, the ceramic sleeve may not survive the port conditions.

2. Furnace crown injection. A preliminary examination of the furnace shows it is possible to place the nozzle on the crown about 13" from the hot face and at 48° from vertical position. Examination of the CFD flow field reveals that the average velocity of the furnace gas along the jet path is approximately 10 ft/s, and the average angle between the jet flow and the furnace gas flow is 56°. If one nozzle is used to inject oxidant at 300 ft/s ($D = 1.438$"), then the jet penetration distance is about three to four feet, barely enough to reach the majority of the exhaust flow. Two nozzles will result in $\sqrt{2}$ times smaller penetration. If the angle is changed to 30° from vertical, the penetration distance will be about 10% larger. Thus, it is recommended to have two nozzles at 30° from vertical for coverage and penetration.

3. Side wall injection above the ports. Two nozzles can be placed at 66° from vertical and 23° from the port centerline to inject oxidant at 300 ft/s ($D = 1.017$"). The calculated jet penetration distance is about two feet, sufficient for mixing with the exhaust flow in this configuration.

4. Under-port lancing. Two nozzles can be placed between 25° and 45° from vertical to inject oxidant at 300 ft/s ($D = 1.017$"). The calculated jet penetration distance ranges from 24" to 21", all sufficient for mixing with the exhaust flow in this configuration. Note than a smaller angle such as 25° can increase the residence time of the oxidant, thus might lead to better CO reduction.

5. Pure oxygen lancing. The injection locations can be crown, above or below the port. With 35% oxygen content and PSR at 0.95, the current cold staging jets require more energy to heat up than the available CO combustion heat release. Thus, simply ensuring CO burning above the load will improve thermal efficiency only if the jets are preheated. Pure oxygen jets require about 60% less energy to heat up than the current arrangement due to the reduction in gas volume. Potentially, up to 3% increase in furnace thermal efficiency can be achieved.

6. Crown injection with one nozzle and under-port lancing with two nozzles, all at 300 ft/s, seem equally suitable in terms of overall CO destruction, CO burnout inside the melter and furnace thermal efficiency. Crown injection with one nozzle must have a slower jet so that it does not impinge on the glass surface. According to the previous point, the furnace thermal efficiency can increase by 3% if pure oxygen is used and all CO combustion occurs in the melter.

The above calculations address only the issue of jet penetration. The issue of jet coverage mixing is not explored, which must be done with a 3D CFD model. To further increase NOx reduction, the PSR may have to be decreased below 0.95. One should keep in mind that PSR below 0.86 might incur an efficiency penalty according to the thermodynamic analysis.

## 8. Acknowledgment

This report was the result of a team effort among many of my colleagues. Steve Hope, the APCI contact for this IGT-coordinated joint OEAS project, provided constant help and advice. The refractory thermal property data by Leon Chang was valuable. Kevin Lievre helped me to get glass surface temperature measurements. Drs. Yangping Zhang and Bryan Hoke both carefully reviewed my drafts and provided valuable feedback and suggestions. My discussions with Dr. George Harriot lead to the 3D potential flow model. With his enormous experience in the glass industry, Buddy Eleazer gave me insight and helped me put things in perspective. Their help is hereby greatly appreciated.

## 9. References

Beer, J.M. and Chigier, N.A. *Combustion Aerodynamics*, John Wiley and Sons, New York, 1972.

Bejan, A. *Convection Heat Transfer*, John Wiley and Sons, New York, 1984.

Delrieux, J. "The influence of the thermal properties of refractories and their mode of utilization on the heat balance in regenerators," *Glass Technology*, Vol. 21, No. 4, August, 1980.

*FLUENT NOx Module User's Guide*, Version 2, Fluent Inc, Lebanon, NH, March, 1995.

*FLUENT User's Guide*, Version 4.3, Fluent Inc, Lebanon, NH, March, 1995.

Joshi, M. et. al, "Cost-effective NOx reduction using oxygen-enriched air staging (OEAS) on regenerative glass furnaces," *Proc. 55th Conference on Glass Problems*, Columbus, Ohio, November 8-9, 1994.

Kays, W.M. and Crawford, M.E. *Convective Heat and Mass Transfer*, Second Edition, McGraw Hill, New York, 1980.

Launder, B.E. and Spalding, D.B. "The numerical computation of turbulent flows," Imperial College of Science and Technology, London, England, NTIS N74-12066, January, 1973.

Launder, B.E., Reece, G.J. and Rodi, W. "Progress in the development of a Reynolds-stress turbulence closure," Journal of Fluid Mechanics, Vol. 68, Part 3, pp. 537-566, April, 1975.

Magnussen, B.F. and Hjertager, B.H., "On mathematical models of turbulent combustion with special emphasis on soot formation and combustion," *Proc. 16th Symposium (Int'l.) on Combustion*, Cambridge, MA, August 15-20, 1976.

Patankar, S.V. *Numerical Heat Transfer and Fluid Flow*, Hemisphere Publication Corp., Washington, DC, 1980.

Platten, J.L. and Keffer, J.F. "Entrainment in deflected axisymmetric jets at various angles to the stream," Technical Publication Series, UTMETP-6808, Department of Mechanical Engineering, University of Toronto, June, 1968.

Sabersky, R.H., Acosta, A.J. and Hauptmann, E.G. *Fluid Flow: A First Course in Fluid Mechanics*, Second Edition, Macmillan Publishing Co., Inc., New York, 1971.

Shah, N.G. *A New Method of Computation of Radiant Heat Transfer in Combustion Chambers*, Ph.D. Dissertation, Imperial College of Science and Technology, London, England, 1979.

Slavejkov, A. G. and Gershtein, V. Y. "NOx reduction in natural gas high performance burners," Phase 1 Final Report for The Institute of Gas Technology, January, 1994.

Yakhot, V. and Orszag, S. "Renormalization group analysis of turbulence. I. Basic theory," *Journal of Scientific Computing*, Vol. 1, No. 1, pp. 1-51, 1986.

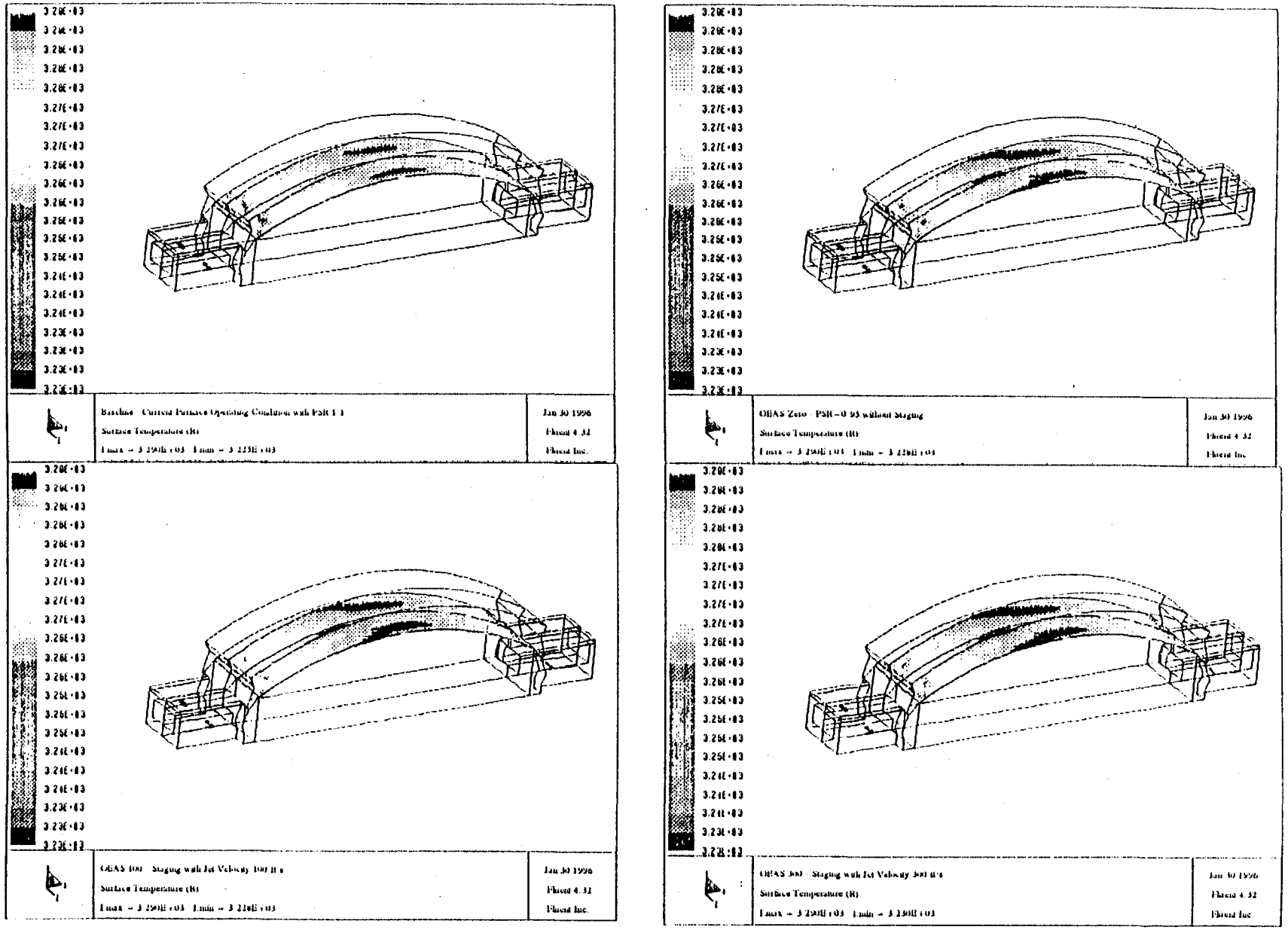


Figure A-11. Peak crown temperature remains unchanged with OEAS although the size of the crown surface area with the peak temperature is about three times as large as the current operating condition.

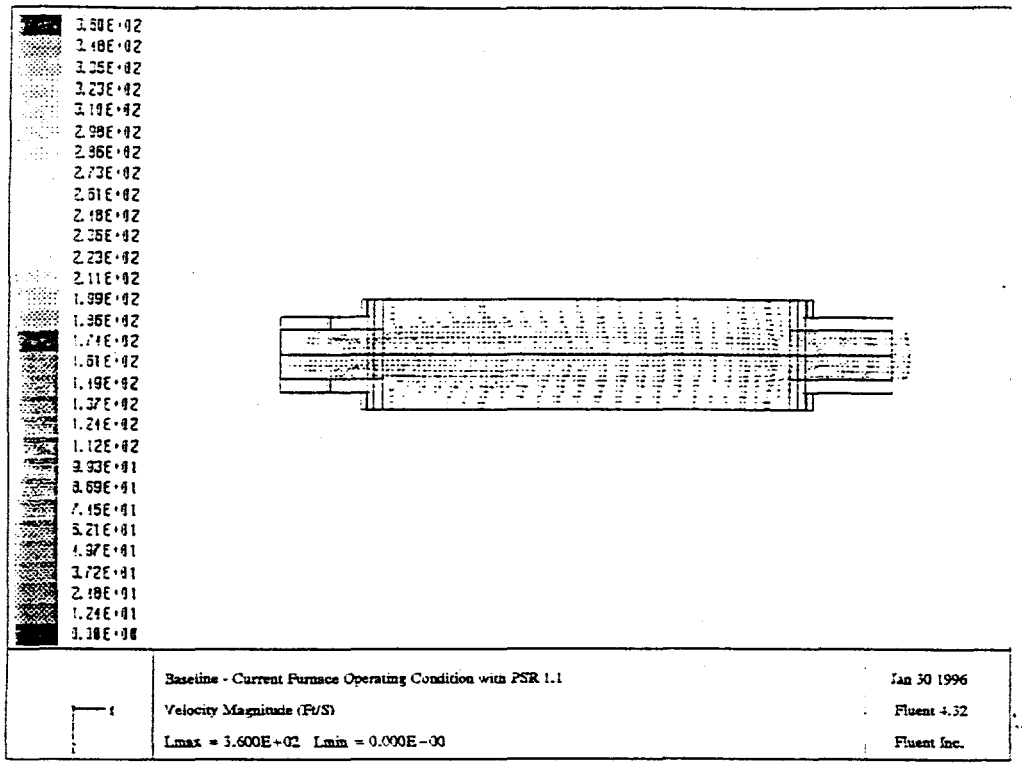


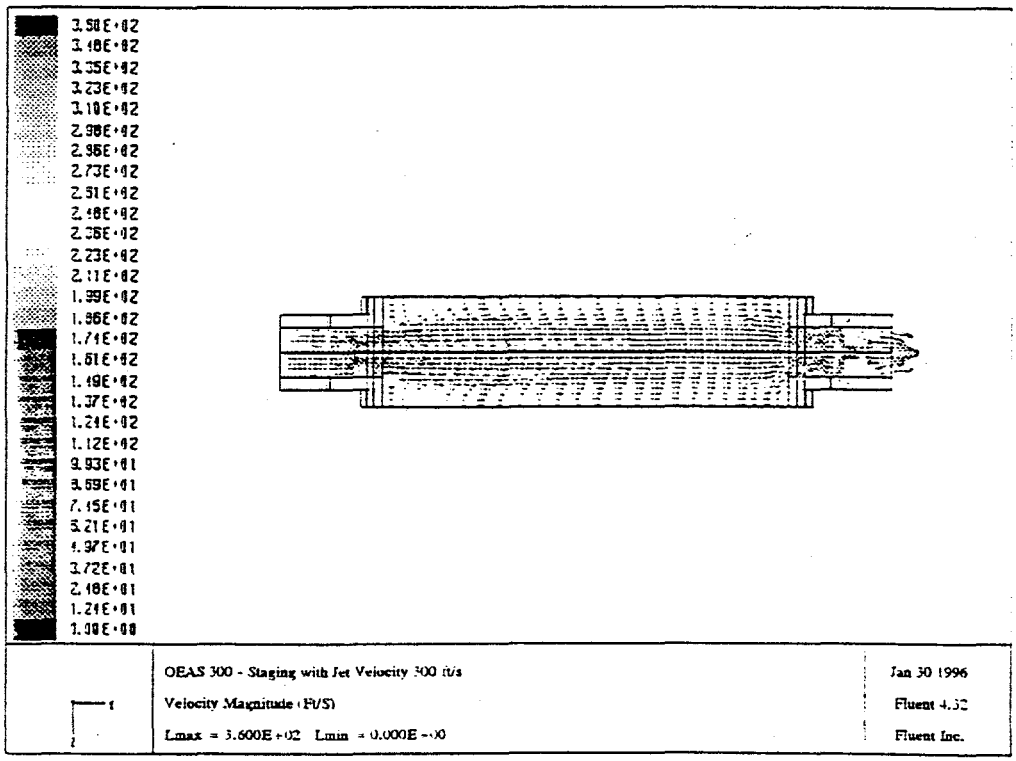


Figure A-12. Flow pattern inside the furnace remains unchanged with OEAS. Staging jets do not penetrate into the furnace.

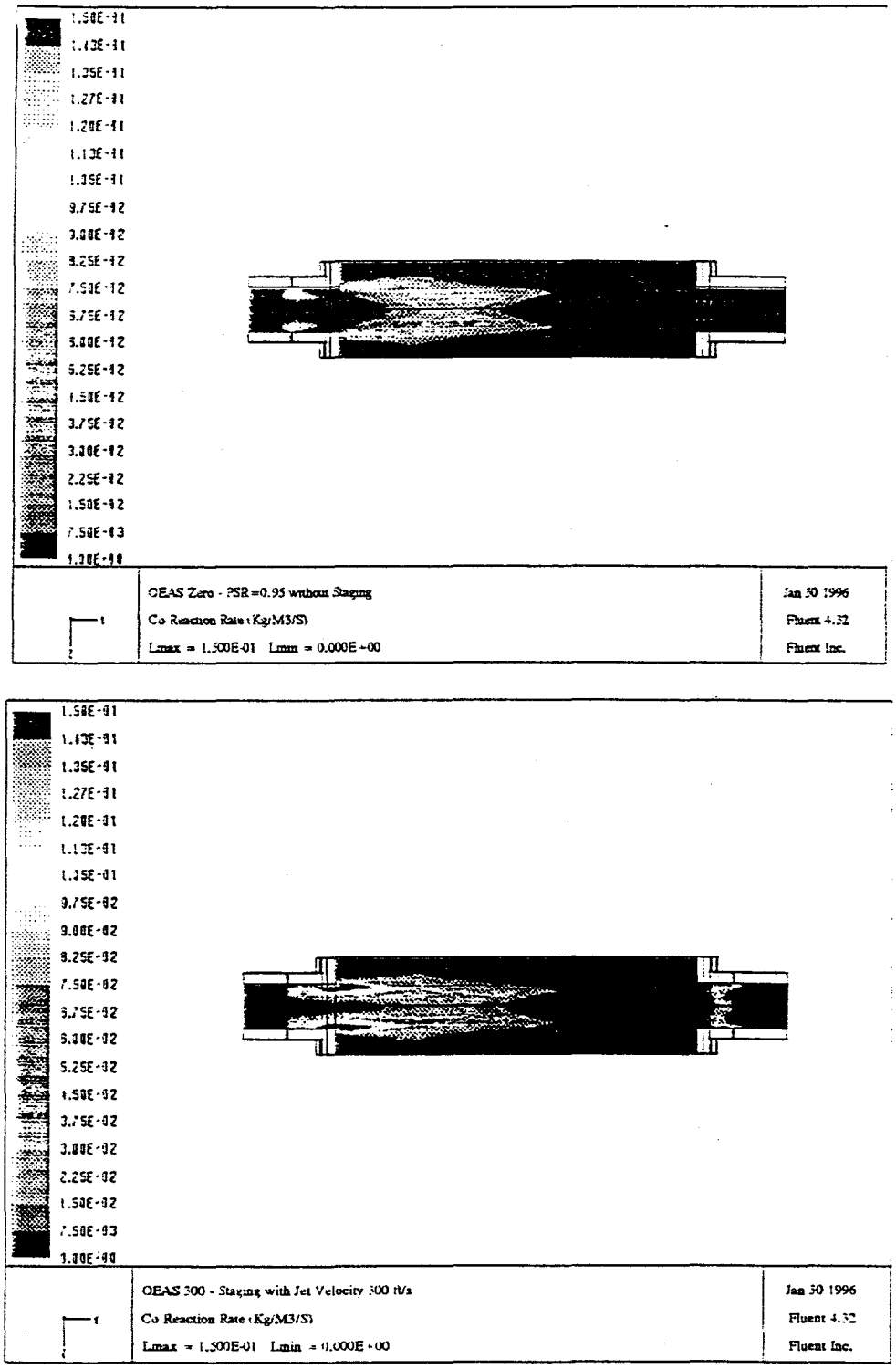


Figure A-13. CO generation rate at the level of the burners. Note that among OEAS cases reaction occurs earlier and is more vigorous in the furnace as a result of the "air curtain" effect due to staging.

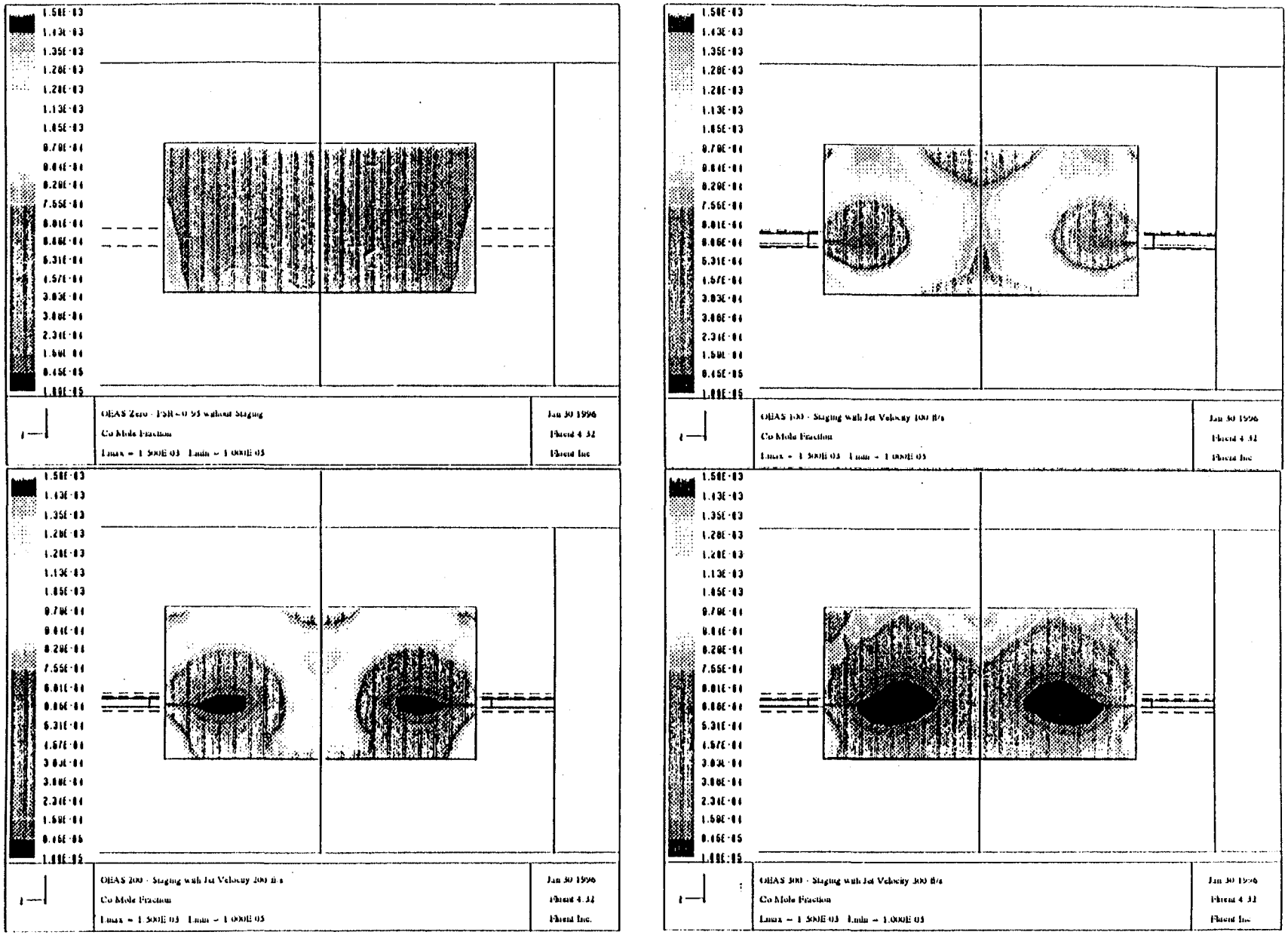


Figure A-14. CO mole fraction at the location of the staging nozzles for all OEAS cases. Higher jet velocity promotes mixing and reduces CO to a lower level eventually, but CO level is initially higher with oxidant injection at the nozzle location due to the "air curtain" effect.

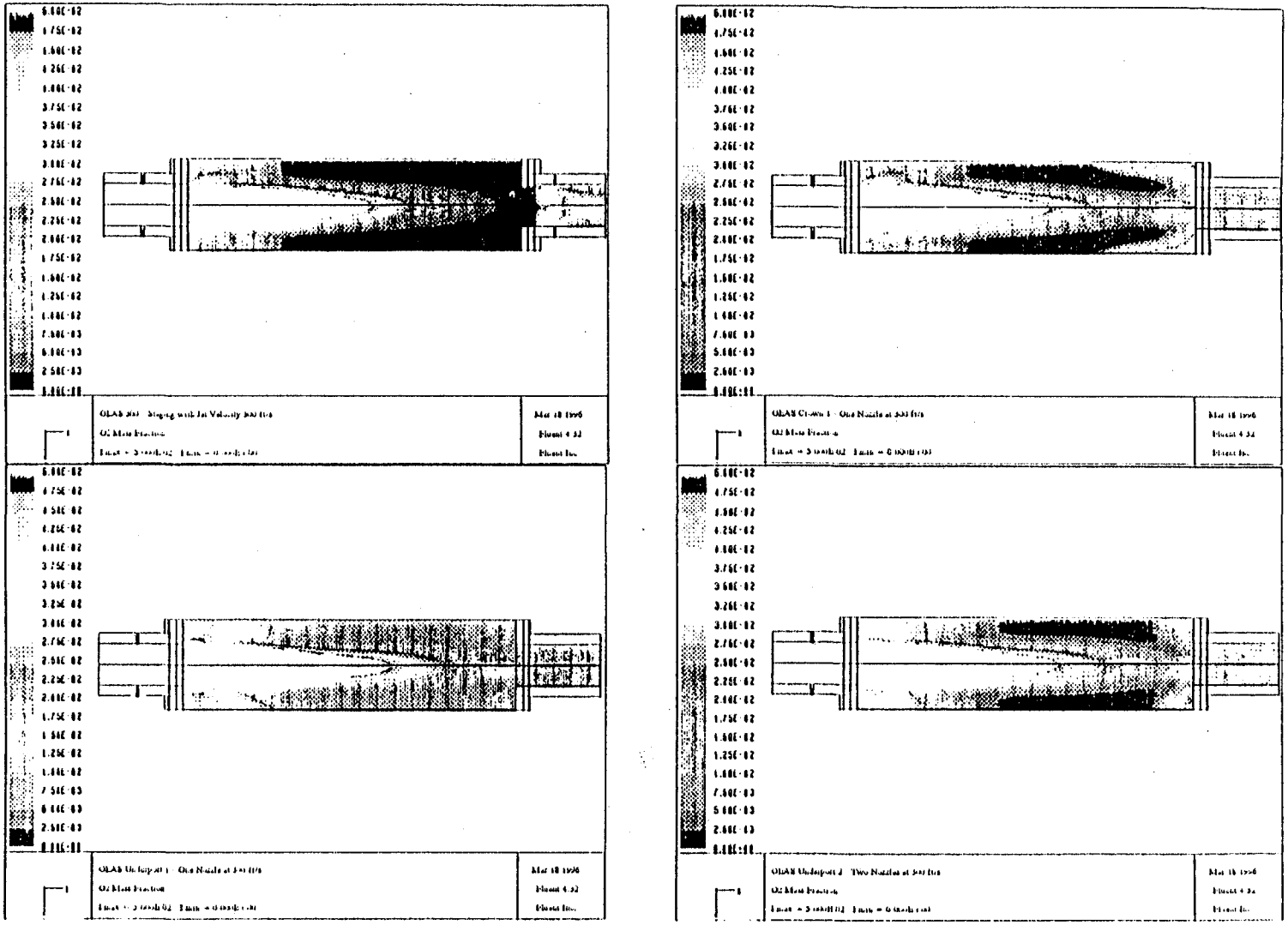

Figure A-15. Oxygen mass fraction in the immediate vicinity of the primary flames has to do with CO burnout in the melter.

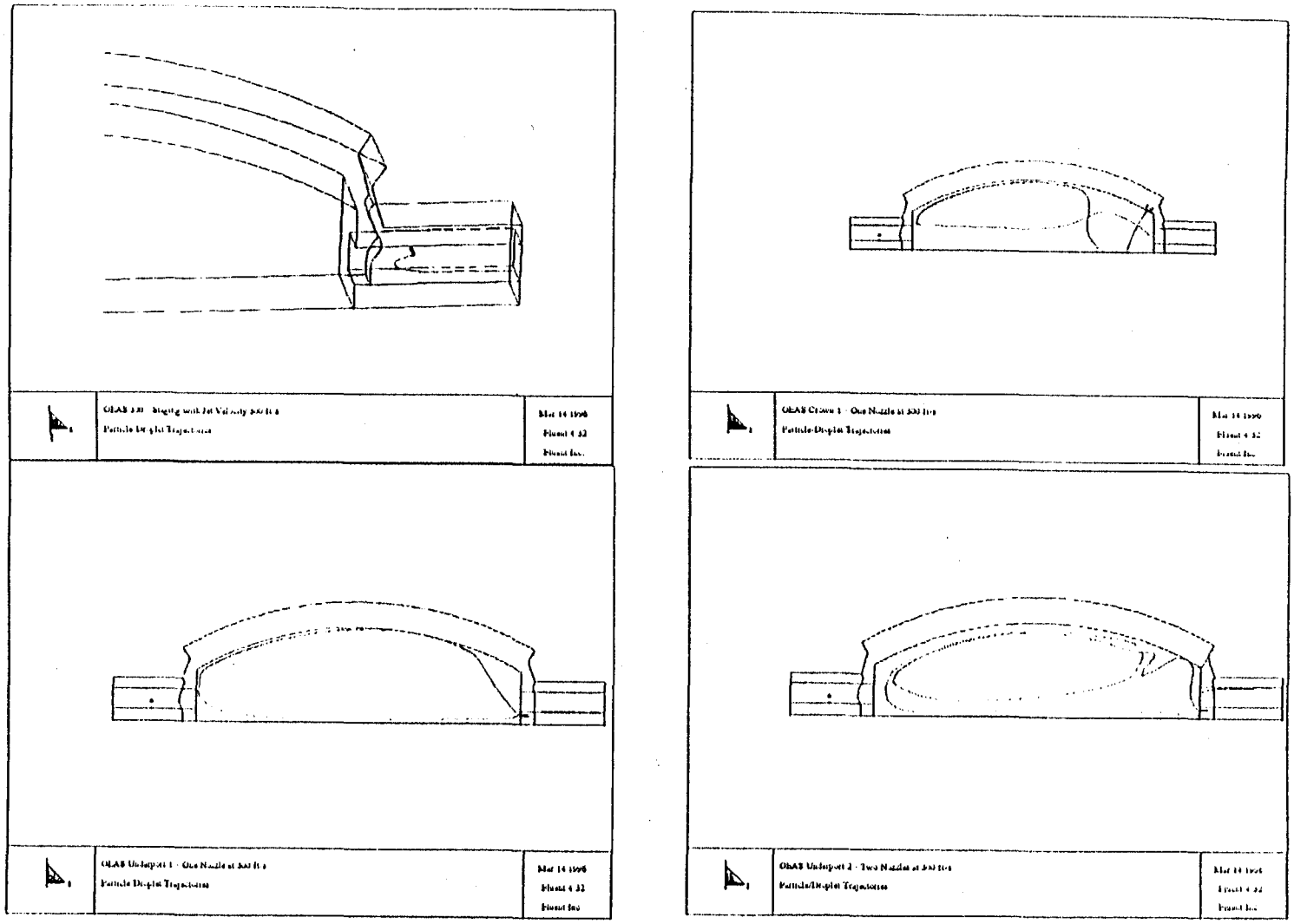

Figure A-16. Secondary oxidant can get into the recirculating flow in the furnace and have very larger residence times.

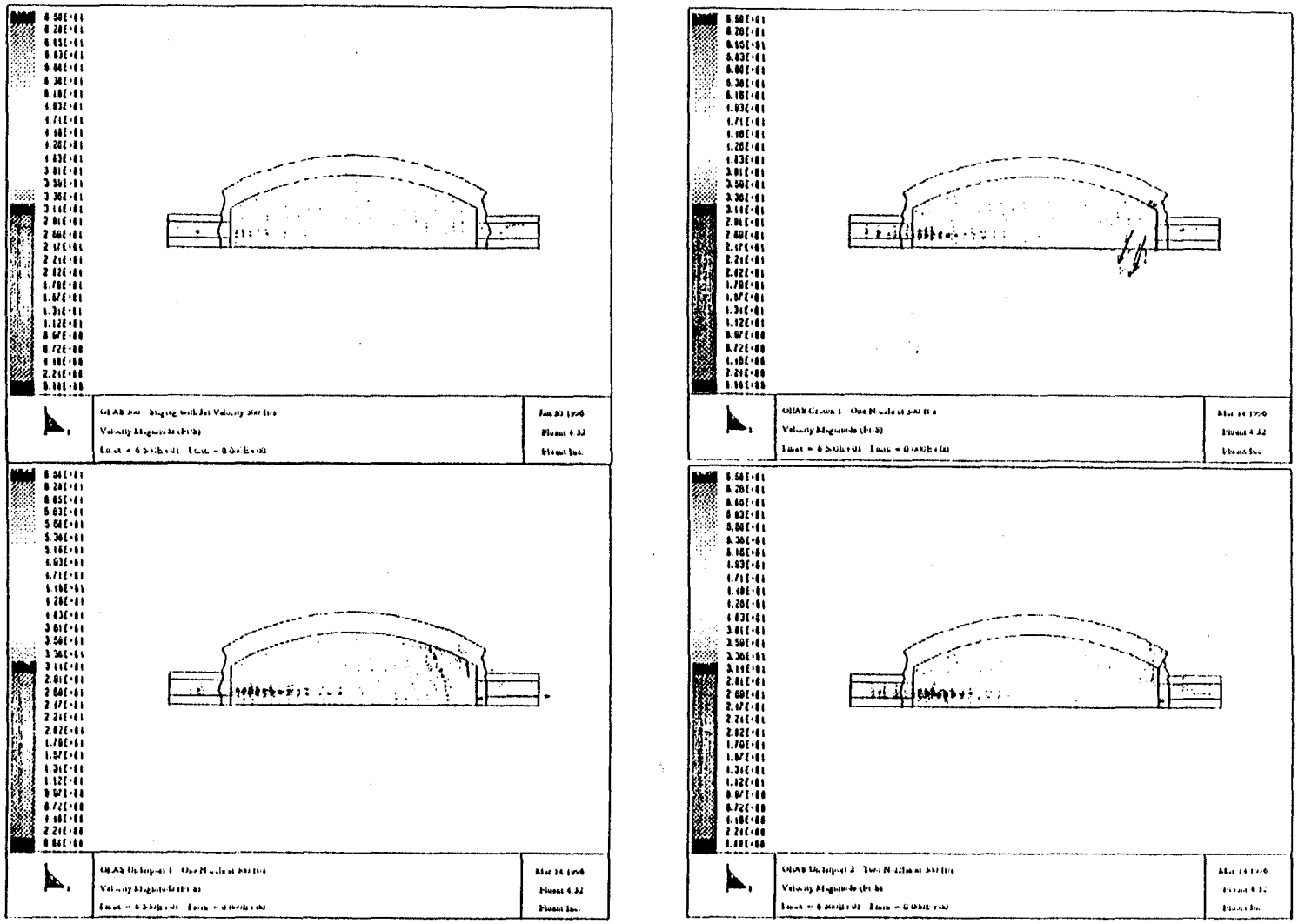

Figure A-17. Secondary oxidant from crown injection at 300 ft/s may impinge on the molten glass surface.

# APPENDIX B
# OEAS SYSTEM DESCRIPTION AND OPERATION

# OPERATION MANUAL SUMMARY

COMBUSTION TEC, INC.

VERSION 02/25/97

OXYGEN ENRICHED AIR STAGING (OEAS)

for

OWENSBROCKWAY
VERNON, CA
FURNACE "C"

JOB #8759

PREPARED BY

COMBUSTION TEC, INC.
2501 CLARK STREET
APOPKA, FLORIDA 32703
U.S.A.
(407)299-7317 FAX: (407)291-7104

TABLE OF CONTENTS

INTRODUCTION.....1

I. Commissioning Procedures.....2
A. Cooling Air.....2
B. Instrument Air.....2
C. Oxygen and Blower Air Valves.....2

II. OEAS Startup Procedures.....4
A. Pre-Startup Checks.....4
B. Power-Up and Exercise Reversal Valves Without Flow.....4

III. Panelview 900 Monitor Screens.....5
A. Overview Screen.....5
B. Manual Staging Control Screen.....6
C. Local Staging Control Screen.....6
D. Remote Staging Control Screen.....7
E. Train Control Screen.....7
F. Flow Limit Screen.....8
G. PID Control Screen.....8
H. Alarm History Screen.....8

IV. Alarms.....9

V. Normal Operation.....12

VI. System Shut Down Procedures.....13

VII. Maintenance.....14

APPENDIX A-1: Panelview 900 Screens.....28

# INTRODUCTION

Staging can be performed in two modes. The modes of staging are:

1. Oxygen Enriched Air Staging (OEAS)
2. Air Staging (AS)

OEAS is the preferred mode and this manual is tailored towards OEAS operation.

The staging system consists of the following components:

1. Oxygen safety and flow metering skid (Figure 1)
2. Blower air safety and flow metering skid (Figure 2)
3. Process control compressed air
4. Oxygen headers
5. Air headers
6. Individual port oxygen flow control and metering downcomers (Figure 3)
7. Individual port air flow control and metering downcomers (Figure 3)
8. Staging injectors (Figure 4)

An Allen Bradley 5/03 processor with Panelview 900 touch screen monitor is used for the control system and is mounted in a cabinet in the control room.

The Project Team led by CTI provided OEAS system operation instructions to the Furnace Operators and provided them with the full Operating Manual describing the system startup, system operation, alarm troubleshooting, system shutdown and use of the Panelview 900 touch screen monitor. Owens Brockway has copies along with CTI and IGT.

## I. Commissioning Procedures

*Typically the procedures in Section I are performed only once during the initial commissioning of the staging system. If you are restarting the system after a brief downtime period, proceed to* Section II - OEAS Startup Procedures. *Operating Manuals were given to the furnace operators describing the full commissioning procedures.*

### A. Cooling Air

The compressed air piping for cooling air is located on the oxygen skid. The compressed air supply system is shown in Figure 5: A1. The valves for the compressed air filter are shown in Figure 5: A2 and A3 or A4 and A5. The valves for the Injector Cooling Air are shown in Figure 6: A26, A27. The valves for the air downcomers are shown in Figure 3: D1. The Staging Manifold valve is shown in Figure 4: E1. The Cooling Air Regulator is shown in Figure 7: A6.

### B. Instrument Air

The compressed air piping for instrument air is located on the oxygen skid. The Reversal/Shutoff Valve Air Regulator is shown in Figure 8: A7. The Compressed Air to Oxygen Safety Valves are shown in Figure 7: A8 and A9. The Shut Off Reversal Signal Manual is shown in Figure 9: A10, A11, A12, A13. The Open Reversal Signal for Automatic Operation is shown in Figure 9: A14, A15, A16, A17. The Compressed Air to Oxygen Reversal Valve Actuators are shown in Figure 10: A18, A19, A20, A21. The Compressed Air to Air Reversal Valve Actuators are shown in Figure 11: A22, A23, A24, A25. The Oxygen Safety Valves are shown in Figure 7: A28, A29. The Oxygen Reversal Valves are shown in Figure 12: A30, A31. The Air Reversal Valves are shown in Figure 13: B1, B2. The Reversal/Shutoff Valve is shown in Figure 8: A7.

### C. Oxygen and Blower Air Valves

The Oxygen Safety Valves are shown in Figure 7: A28, A29. Inactive Oxygen Orifice Plate Lines for low flow (2 inch) are shown in Figure 12: A34, A35. The Active Oxygen Orifice Plate Lines for high flow (6 inch) are shown in Figure 12: A32, A33. The Oxygen Mass Flow Meter is shown in Figure 14: A36, A37, A38. The Inactive Air Orifice Plate Lines are shown in Figure 15: B5, B6. The Active Air Orifice Plate Lines for low flow (4 inch) are shown in Figure 15: B5 and B6.

The Active Air Orifice Plate Lines for high flow (10 inch) are shown in Figure 15: B3 and B4. The valves to open the Air Mass Flow Meter are shown in Figure 16: B7 and B8. The valve to close the Air Mass Flow Meter is shown in Figure 16: B9. The Oxygen Inlet Valve is shown in Figure 17: A39. The Oxygen Skid Valves are shown in Figure 18: A40, A41, A42. The Oxygen Supply Pressure is shown in Figure 17: A43. The Oxygen Skid Flow Control Valves are shown in Figure 19: A44, A45, A46. The Oxygen Metering Downcomers valves are shown in Figure 3: C1.

## II. OEAS Startup Procedures

*The startup procedures are described in the Operating Manual given to the furnace operators.*

### A. Pre-Startup Checks

The Reversal/Shutoff Air Regulator pressure valve is shown in Figure 8: A7. The Cooling Air Regulator Pressure valve is shown in Figure 7: A6. The Compressed Air Valves for Oxygen Reversal Valve Actuators are shown in Figure 10: A18, A19, A20, A21. The Compressed Air Valves for Air Reversal Valve Actuators are shown in Figure 11: A22, A23, A24, A25. Oxygen Safety Valves are shown in Figure 7: A28, A29.

### B. Power-Up and Exercise Reversal Valves Without Flow

To complete the checks power to oxygen skid must be turned on. Figure 20 shows the staging control cabinet located in the control room.

## III. Panelview 900 Monitor Screens

The Panelview screens have been designed for ease for use to display information to the furnace operator to assess the staging operation. Each active button which allows the operator to go to other screens or enter input is filled in or illuminated and the inner text is black. At the bottom of each screen is a screen menu bar or a return button. Pressing a button from the screen menu bar will display the selected screen. Pressing a return button will return the operator to the previous screen. Printouts of the Panelview screens are in Appendix A-1.

### A. Overview Screen

The overview screen is for display purposes only and is divided into three main display areas. The display areas are Main Flame, Furnace, and Staging.

Main Flame: In this display area, the flame's air and gas flows are displayed as bar graphs with actual numerical values displayed below the graphs. At the top of the display are is the indicator which displays whether the flame is on the left or right side or if the furnace is going through a reversal. Also displayed is the flame's air fuel ratio which is calculated from the actual air and gas flows to the flame. Finally, the Primary Stoichiometric Ratio (PSR) is displayed. This is the flame's air/fuel ratio divided byhte stoichiometric air fuel ratio (typically around 9.7 for natural gas).

Staging: In this display area, the staging air and oxygen flows are displayed as bar graphs with actual and set point flow values displayed below the graphs. At the top left of the staging area is an indicator which displays staging left, right, reversal, or off. Another indicator displays the staging control mode, either manual, local, or remote. Another indicator displays the staging option, either OEAS, AS or manual. Below these indicators is the staging mixture oxygen content indicator. It displays the oxygen content in the staging mixture and is calculated from the staging air and oxygen flows.

Furnace: In this display area, stack $NO_x$ and CO are displayed as bar graphs with numerical values below the graphs. Set point and actual overall furnace air/fuel ratios are displayed. Actual furnace air/fuel ratio is calculated from

the flame's combustion air flow plus staging air and oxygen flows all divided by the gas flow. The furnace's Overall Stoichiometric Ratio (OSR) is displayed and is calculated from the furnace's air/fuel ratio divided by the stoichiometric air fuel ratio (around 9.7 for natural gas).

B. Manual Staging Control Screen

Under normal staging operation this screen will nit be used. It is provided primarily for pre-startup in order to verify proper flow control valve operation.

From the manual staging control screen the operator is able to open and close the air and oxygen flow control valves after pressing the manual button on the screen. The flow control valves can be increased or decreased by 0.1% by pressing the arrow up buttons or the arrow down buttons. The desired valve position can also be entered by pressing the valve's percent open display button which opens the scratch pad and the value can be entered. The staging display area is also displayed on this screen and if the valve position are changed from this screen during staging the actual flows will change along with the staging mixture's $O_2$ content.

C. Local Staging Control Screen

Local staging control is used on initial staging system startup to allow initial set points before the flame's air/fuel ratio is reduced. It may also be used if the flame's air and gas signals become corrupted and cannot be used to determined staging flow set points.

On this screen the furnace's gas flow is entered, along with the staging mixture's oxygen content, the supply oxygen's purity, the stoichiometric ratio (9.7 typically for natural gas), the flame's air/fuel ratio for the left and right side firing, and the furnace's overall air/fuel ratio for left and right side firing. The staging display information is also presented on the screen. After the required data is entered the local button is pressed to place the controller in local control mode and staging set points are calculated and displayed below the bar graphs.

If the local control mode is used for normal staging operation, the furnace gas flow and flame's air/fuel ratio must be updated on the screen every time the operator makes a change on the furnace control.

## D. Remote Staging Control Screen

Remote staging control is the preferred mode for normal staging operation. In this mode, the controller uses the flame's actual air flow and gas flow to continually calculate the staging air and oxygen flows. If the operator makes a change to the flame's gas or air flows the staging flows with be automatically updated accordingly.

On this screen the staging mixture's oxygen content, the supply oxygen's purity, the stoichiometric ratio (9.7 typically for natural gas), and the furnace's overall air/fuel ratio for left and right side firing are entered. The staging display information is also presented on the screen. After the required data is entered the remote button is pressed to place the controller in remote control mode and staging set points are continually calculated and displayed below the bar graphs.

## E. Train Control Screen

This screen is used for startup and normal shutdown of the staging system. If an Emergency Stop condition takes place a RESET ESTOP button flashes on the screen and must be pressed before proceeding with startup.

There are four (4) selector switch buttons on this screen from left to right. Startup involves pressing these buttons in the order they appear (left to right). Normal shutdown involves pressing these buttons in the reverse order (right to left).

<u>Staging Mode Selector Switch</u>: The first selector switch is the staging mode. Either manual, OEAS, or AS may be selected. OEAS is the preferred staging mode. If manual is selected no other selector switches are operable. Manual staging mode allows the operator to go to the oxygen skid's electrical panel and open and close the reversal valves with the left-off-right selector switch and visually verify that they are functioning properly. This may be necessary

if staging has not been operating for some time and the valves need to be worked prior to starting staging.

Blower On/Off Selector Switch: After OEAS or AS has been selected the blowers may be turned on with this selector switch.

Oxygen Safety Valves Open/Close Selector Switch: After the blowers have been turned on the oxygen safety valves may be opened with this selector switch.

Staging Start/Stop Selector Switch: If OEAS is selected and the blowers are on and the oxygen safety valves are open, "OR" if AS is selected and the blowers are on then staging may be started using this selector switch. Choosing staging start opens the appropriate reversal valves to send air or air and oxygen to the off-firing side of the furnace.

Under normal shutdown procedures select staging stop, then close the oxygen safety valves, then turn off the blowers. Software logic does not allow any other order for normal shutdown.

## F. Flow Limit Screen

On this screen high and low flow limits are entered for staging air and oxygen. If flows drop below the low flow limit an alarm will be triggered. If flows exceed the high flow limit an alarm will be triggered.

## G. PID Control Screen

This screen contains parameters used for the air and oxygen flow control valves' PID control loops. Each control valve's PID loop has a gain, fast loop update time and slow loop update time associated with it. These values were determined at installation and should not be changed for any reason.

## H. Alarm History Screen

Each time an alarm is triggered which is associated with the staging system the time , date, and brief description of the alarm is recorded on this screen.

## IV. Alarms

There are several alarms that can occur during staging operation. Most alarms, if prolonged, will result in an automatic emergency stop of the system. If an emergency stop occurs, staging will stop (reversal valves close), the oxygen safety valves will close, and the blowers will turn off. Below is a description of each alarm, probable causes, and the staging controller's response.

1. FURNACE GAS SAFETY VALVE CLOSED - If the furnace's gas safety valve closes the staging system will go to an immediate emergency stop. The furnace alarm system will sound, an alarm banner will appear on the Panelview screens, and the alarm will be recorded in the alarm history.

2. STAGING SET POINT TOO LOW - If either the staging air requirements dip below 10,000 scfh or the staging oxygen requirements dip below 500 scfh for more than five seconds an alarm will be triggered. This will result in an alarm banner being displayed on the Panelview screens, the furnace alarm system will sound, and a 300 second countdown clock will be started. If the set point flows are not raised within the 300 second period the staging system will go to an automatic emergency stop. This alarm prevents unnecessary operation of the staging system.

3. LOW OXYGEN PRESSURE - Oxygen supply pressure below 2 psig for more than 5 seconds will trigger an alarm. This will result in an alarm banner being displayed on the Panelview screens, the furnace alarm system will sound, the alarm will be recorded, and a 300 second countdown clock will be started. If the supply pressure is not raised within the 300 second period the staging system will go to an automatic emergency stop. This alarm prevents prolonged operation of the staging system with inadequate supply pressures.

4. HIGH OXYGEN PRESSURE - Oxygen supply pressure above 15 psig for more than 5 seconds will trigger an alarm. This will result in an

alarm banner being displayed on the Panelview screens, the furnace alarm system will sound, the alarm be recorded, and a 300 second countdown clock will be started. If the supply pressure is not lowered within the 300 second period the staging system will go to an automatic emergency stop. This alarm prevents prolonged operation of the staging system with excessive supply pressures.

5. LOW AIR PRESSURE - Blower air pressure less than 15 IWC for more than 5 seconds will trigger an alarm. This will result in an alarm banner being displayed on the Panelview screens, the furnace alarm system will sound, the alarm will be recorded, and a 300 second countdown clock will be started. If the supply pressure is not raised within the 30 second period the staging system will go to an automatic emergency stop. This alarm prevents prolonged operation of the staging system with inadequate supply pressures. The most probable causes are a failed motor or clogged air filter.

6. LOW OXYGEN FLOW - Oxygen flow below the value set in the flow limit screen for more than 5 seconds will trigger an alarm. This will result in an alarm banner being displayed on the Panelview screens, the furnace alarm system will sound, the alarm will be recorded, and a 300 second countdown clock will be started. If the flow is not raised within the 300 second period the staging system will go to an automatic emergency stop. This alarm prevents prolonged operation of the staging system with low flow conditions.

7. HIGH OXYGEN FLOW - Oxygen flow above the value set in the flow limit screen for more than 5 seconds will trigger an alarm. This will result in an alarm banner being displayed on the Panelview screens, the furnace alarm system will sound, the alarm will be recorded, and a 300 second countdown clock will be started. If the flow is not lowered within the 300 second period the staging system will go to an automatic emergency stop. This alarm prevents prolonged operation of the staging system with high flow conditions.

8. LOW AIR FLOW - Air flow below the value set in the flow limit screen for more than 5 seconds will trigger an alarm. This will result

in an alarm banner being displayed on the Panelview screens, the furnace alarm system will sound, the alarm will be recorded, and a 300 second countdown clock will be started. If the flow is not raised within the 300 second period the staging system will go to an automatic emergency stop. This alarm prevents prolonged operation of the staging system with low flow conditions.

9. HIGH AIR FLOW - Air flow above the value set in the flow limit screen for more than 5 seconds will trigger an alarm. This will result in an alarm banner being displayed on the Panelview screens, the furnace alarm system will sound, the alarm will be recorded, and a 300 second countdown clock will be started. If the flow is not lowered within the 300 second period the staging system will go to an automatic emergency stop. This alarm prevents prolonged operation of the staging system with high flow conditions.

10. OVERALL AIR FUEL RATIO < (less than) FLAME AIR FUEL RATIO - In local staging control mode if the operator enters an overall furnace air fuel ratio less than the primary flame's air fuel ratio an alarm will be triggered. An alarm banner will appear on the Panelview screens and the alarm will be recorded, however the furnace alarms will not sound since the operator will be present. The controller will continue to use the previous set point until the error is corrected. This alarm prevents faulting the processor do to a math error.

    Likewise, in remote staging control mode, if the operator enters an overall furnace air fuel ratio less than the flame's actual air fuel ratio (based on combustion air and gas flow) an alarm will be triggered.

## V. Normal Operation

There are several parameters which should be monitored during normal operation.

1. Regularly check compressed air pressure at pressure gauge (Figure 5: A1). At least 60 psi is required for proper functioning of the oxygen and air reversal valve actuators.

2. Regularly check static pressures and differential pressures at each of the air and oxygen down comer orifice plates to verify flow to the injectors (Figures 3 C2, C3, D2, D3).

3. Regularly check cooling air flow meter in the compressed air line on the oxygen skid to verify cooling air flow to the injectors.

4. Regularly replace blower's air filter with a clean filter. If the pressure gage on the air skid is below 75 IWC replace the filter.

## VI. System Shut Down Procedure

At any time either the emergency stop button on the control cabinet in the control room or on the electrical box at the oxygen skid can be pushed to stop staging. Doing so will cause the reversal valves to shut, the oxygen safety valves to close, and the blowers to stop. On re-startup after an emergency stop, the ESTOP buttons must be pulled out and the flashing RESET ESTOP on the train control screen must be pressed. An Operating Manual was given to the furnace operators decribing the operation of the full shut down procedures.

The Oxygen Reversal Valve actuators are shown in Figure 12: A30 and A31. The air Reversal Valve actuators are shown in Figure 7: A27, A28. The Oxygen inlet butterfly valve is shown in Figure 17: A39.

## VII. Maintenance

The Blower's air filter should be cleaned at least once a week. The blower should be maintain per instructions in the blower instruction manual. Both flow control trains should be dusted once a week. For routine maintenance under the ports or on the primary burners, the ball valve on the staging manifolds under the port should be closed to stop the flow of air and oxygen to the staging lances. Once repairs are finished open the ball valve to resume flows through lances.

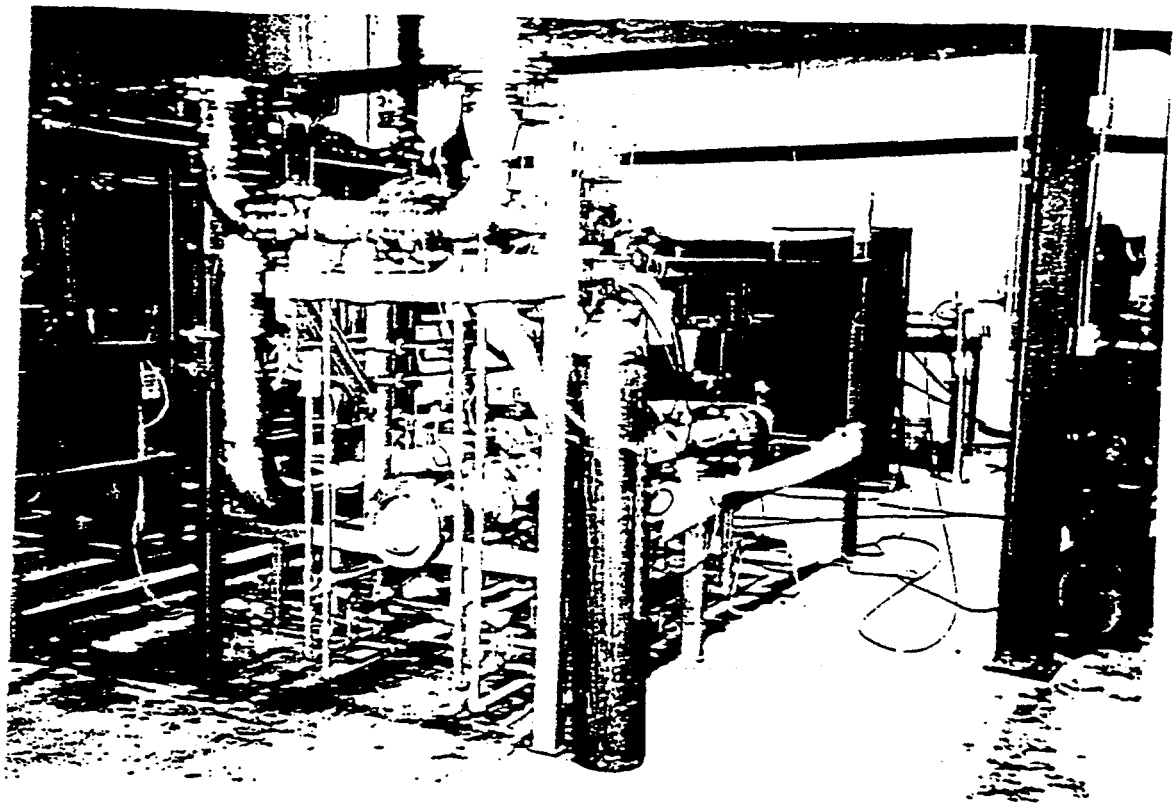

Figure 1. Oxygen Safety and Flow Metering Skid

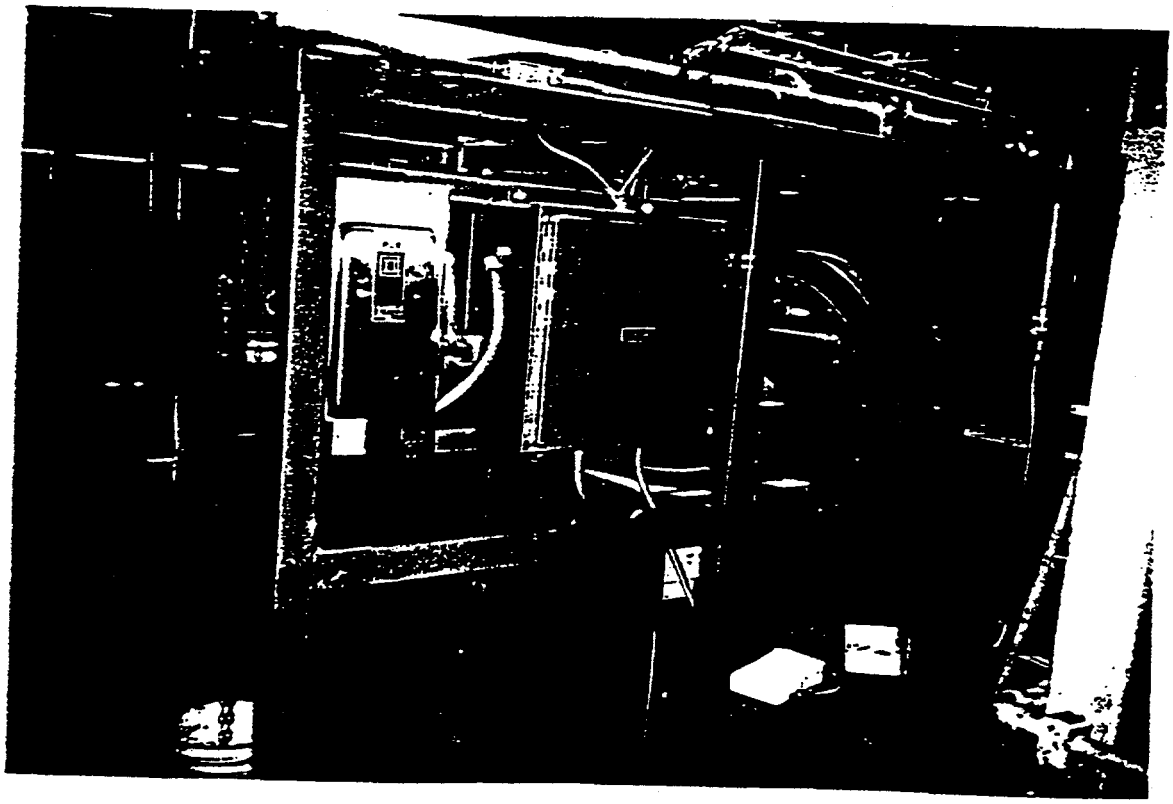

Figure 2. Blower Flow Metering Skid

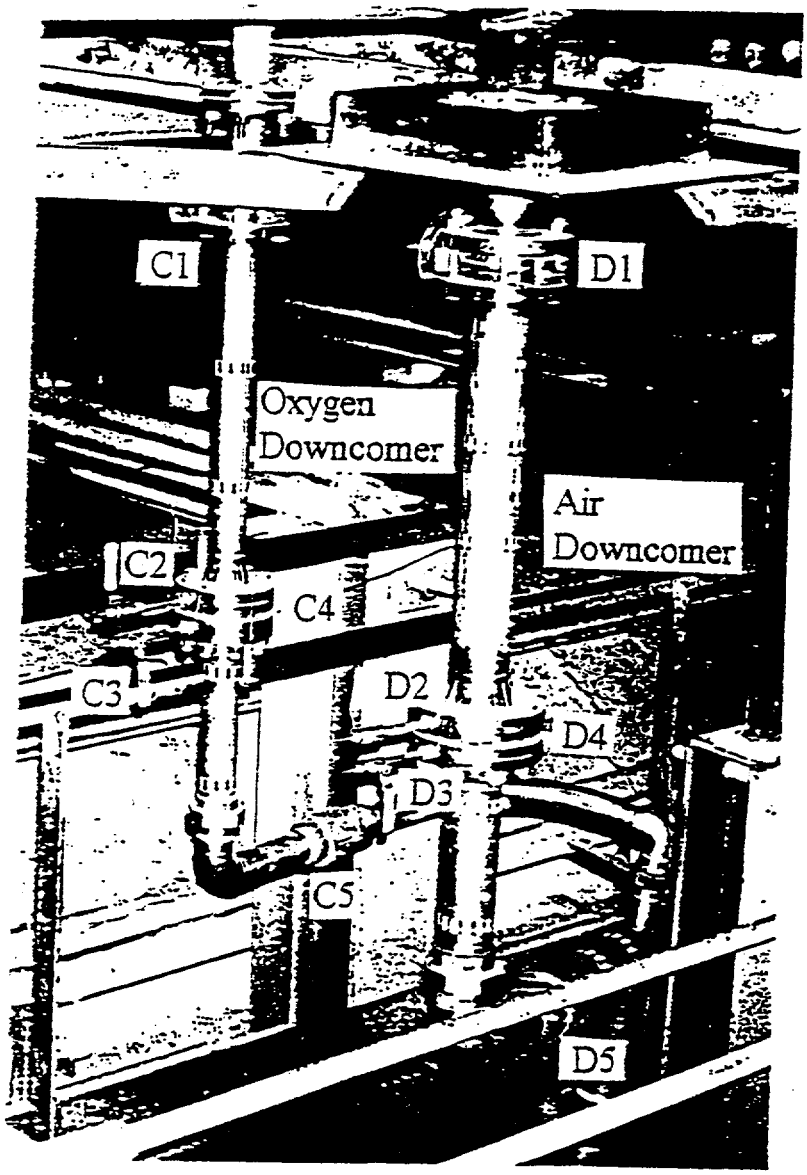


Figure 3. Oxygen and Air Downcomers

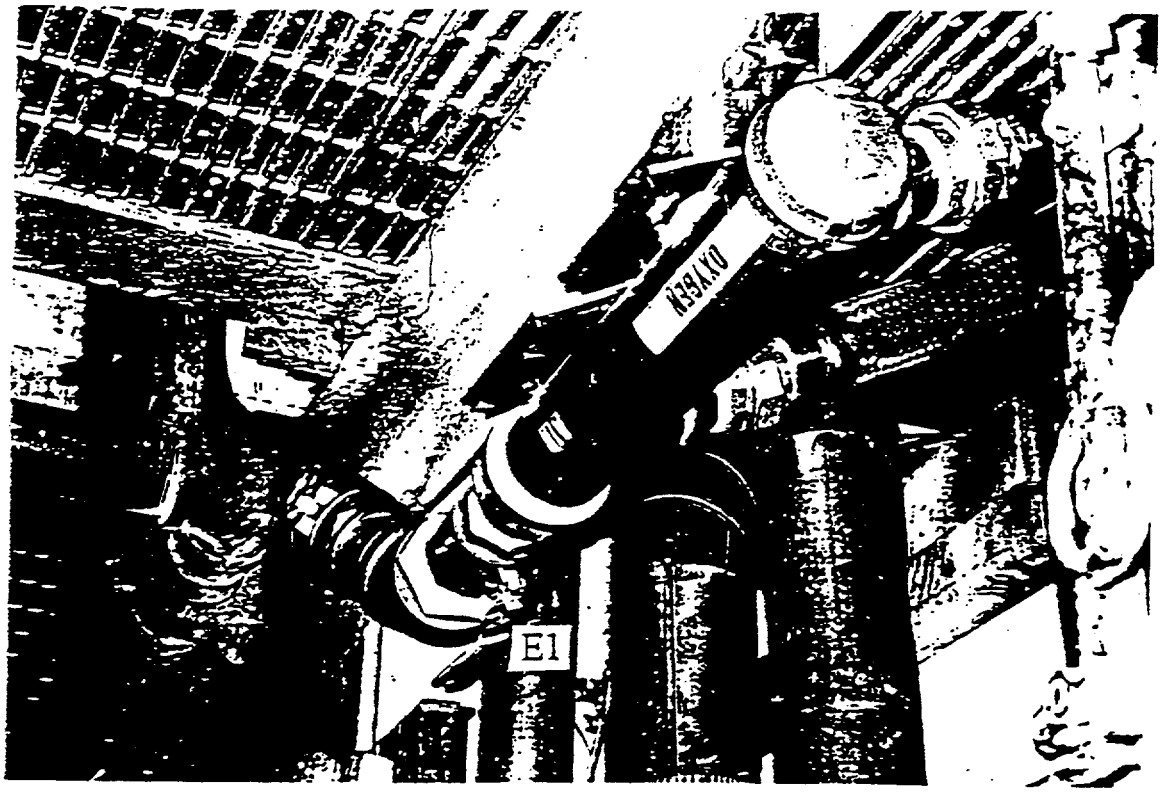


Figure 4. Injector Manifold

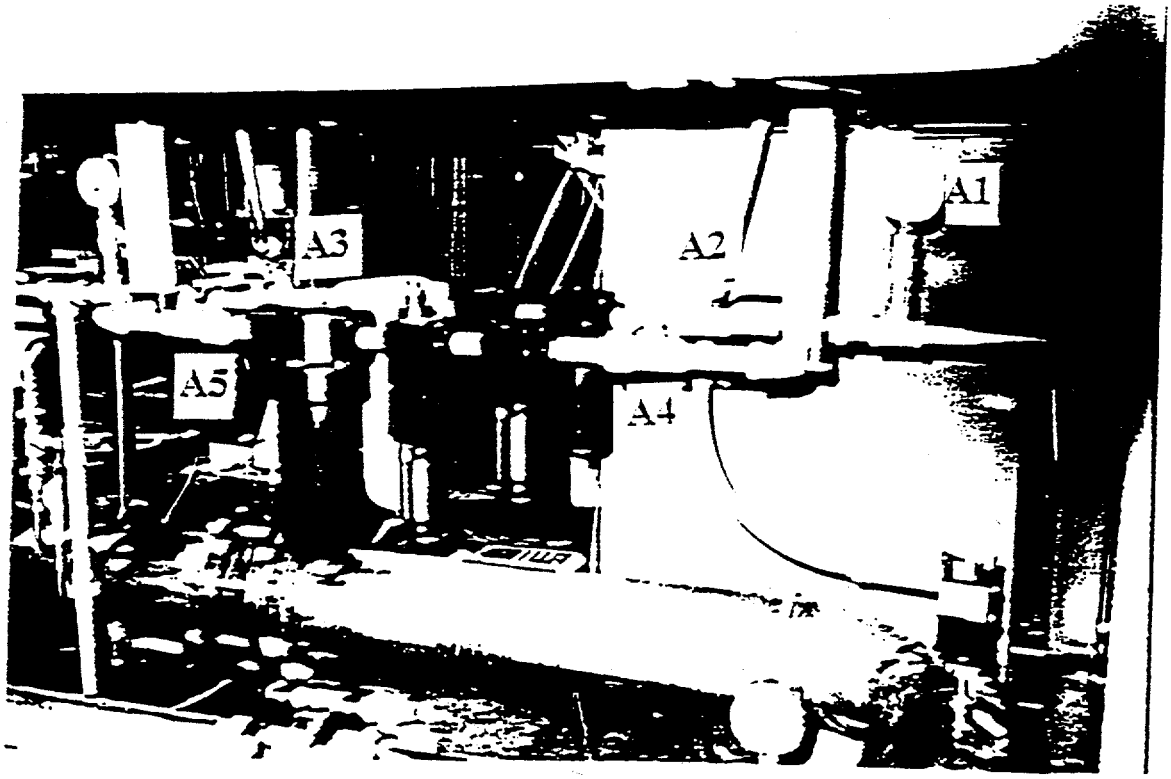


Figure 5. Oxygen Skid-Compressed Air Inlet Pressure Gauge and Filter Sets

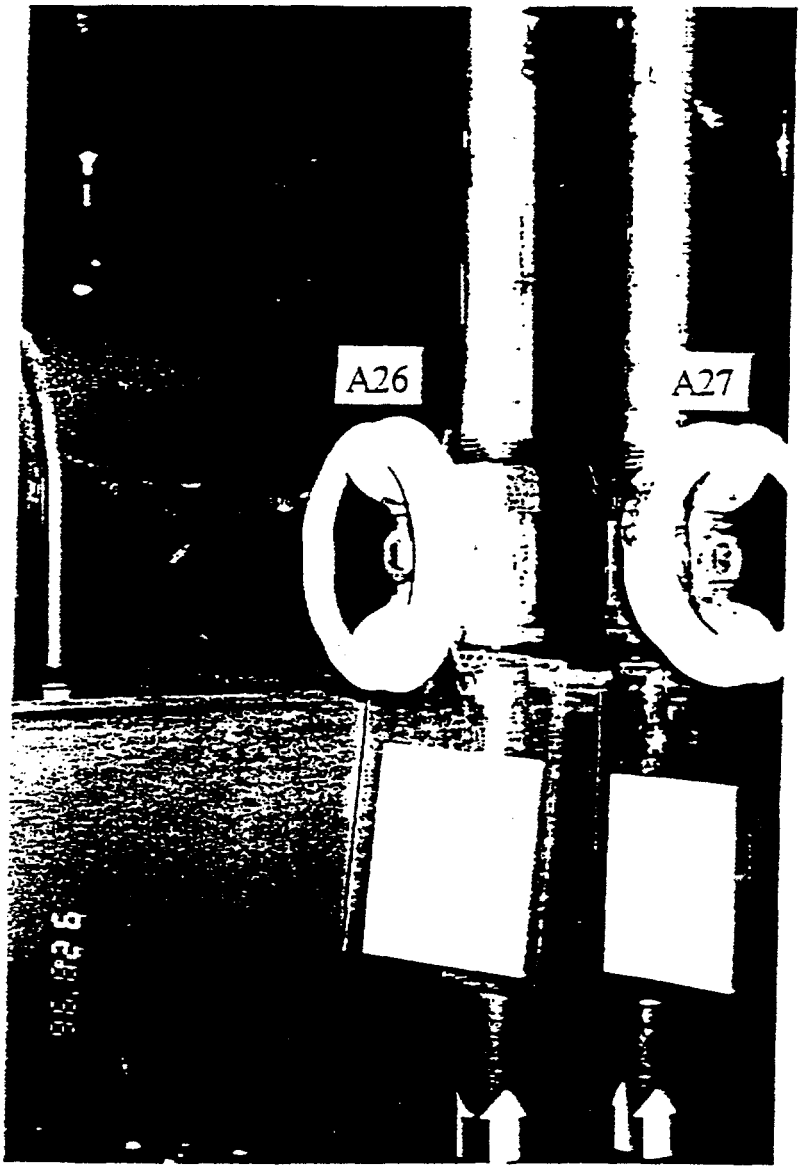


Figure 6. Oxygen Skid-Cooling Air Shut-Off Ball Valves

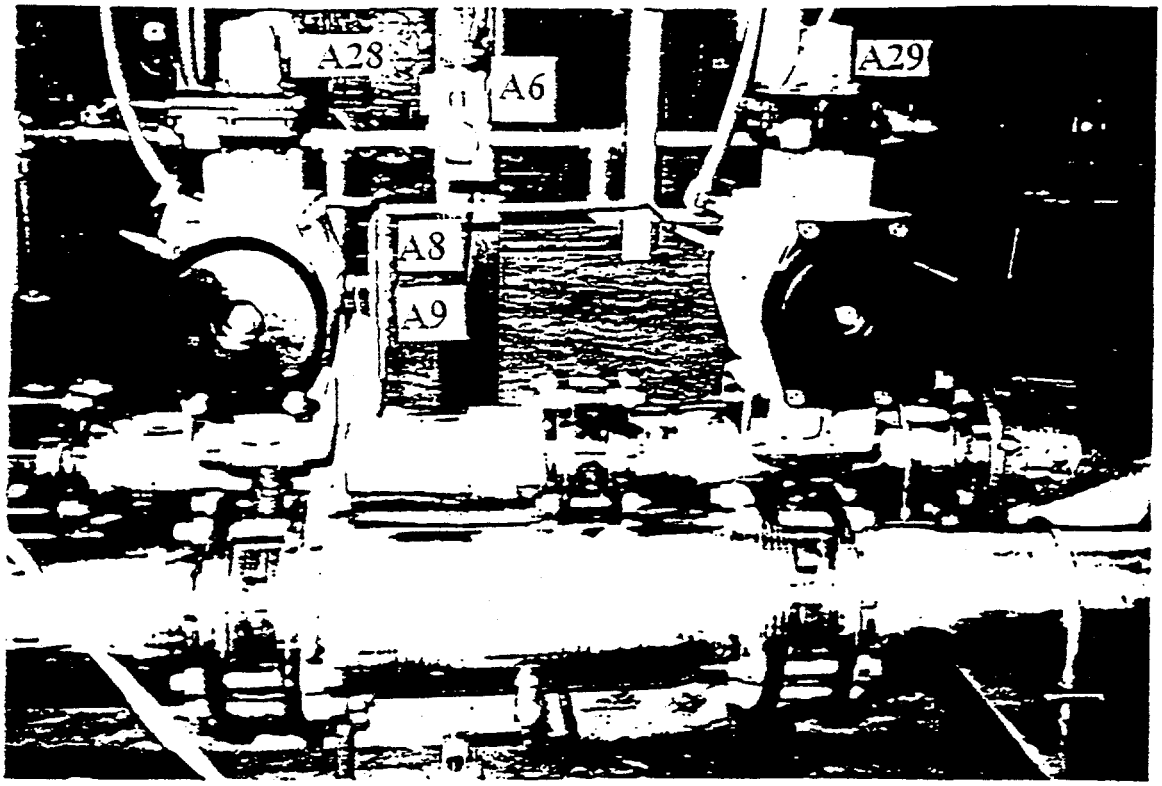


Figure 7. Oxygen Skid-Compressed Air Cooling Air Regulator. Oxygen Safety Valve Actuators

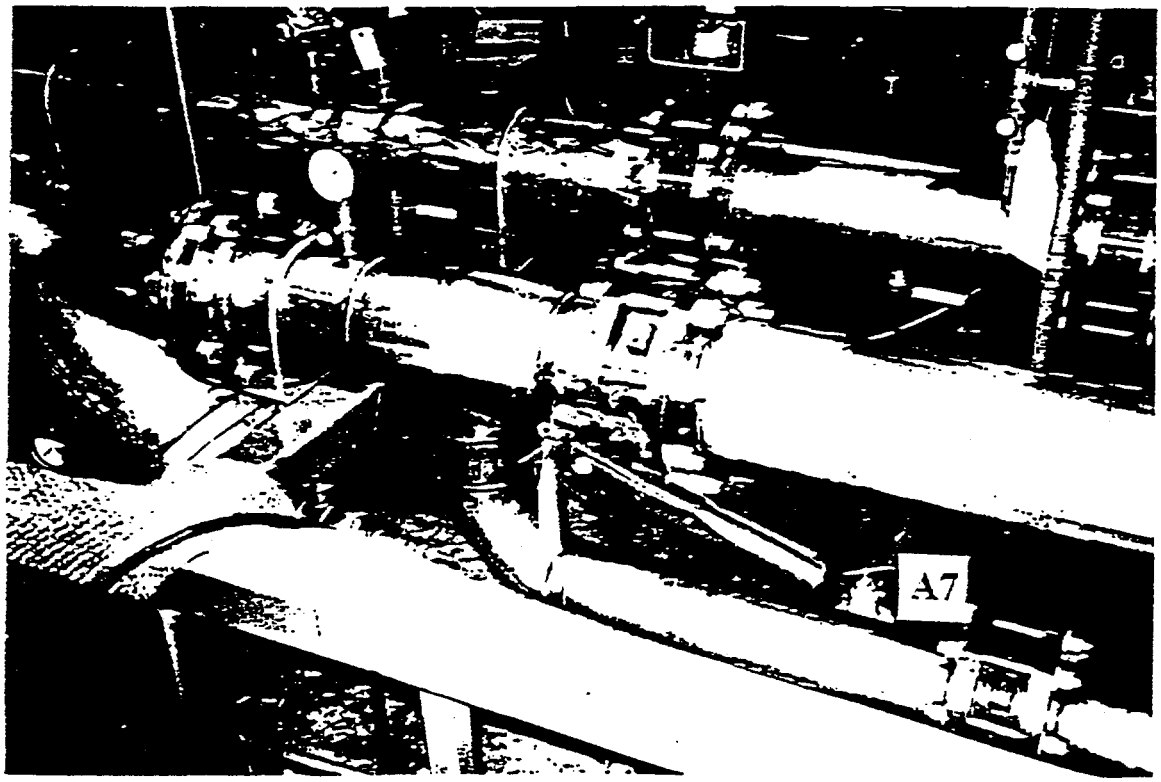


Figure 8. Oxygen Skid-Compressed Air Reversal Air Regulator

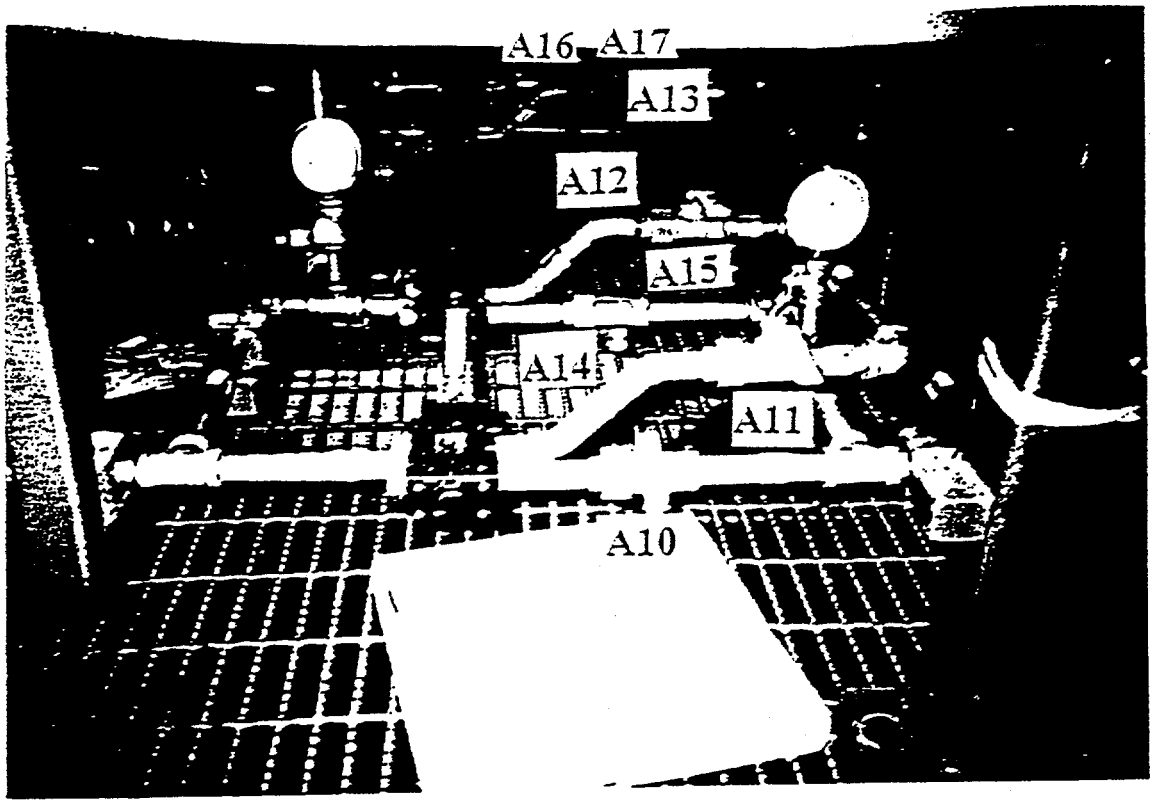


Figure 9. Oxygen Skid-Manual/Automatic Instrument Air Ball Valves

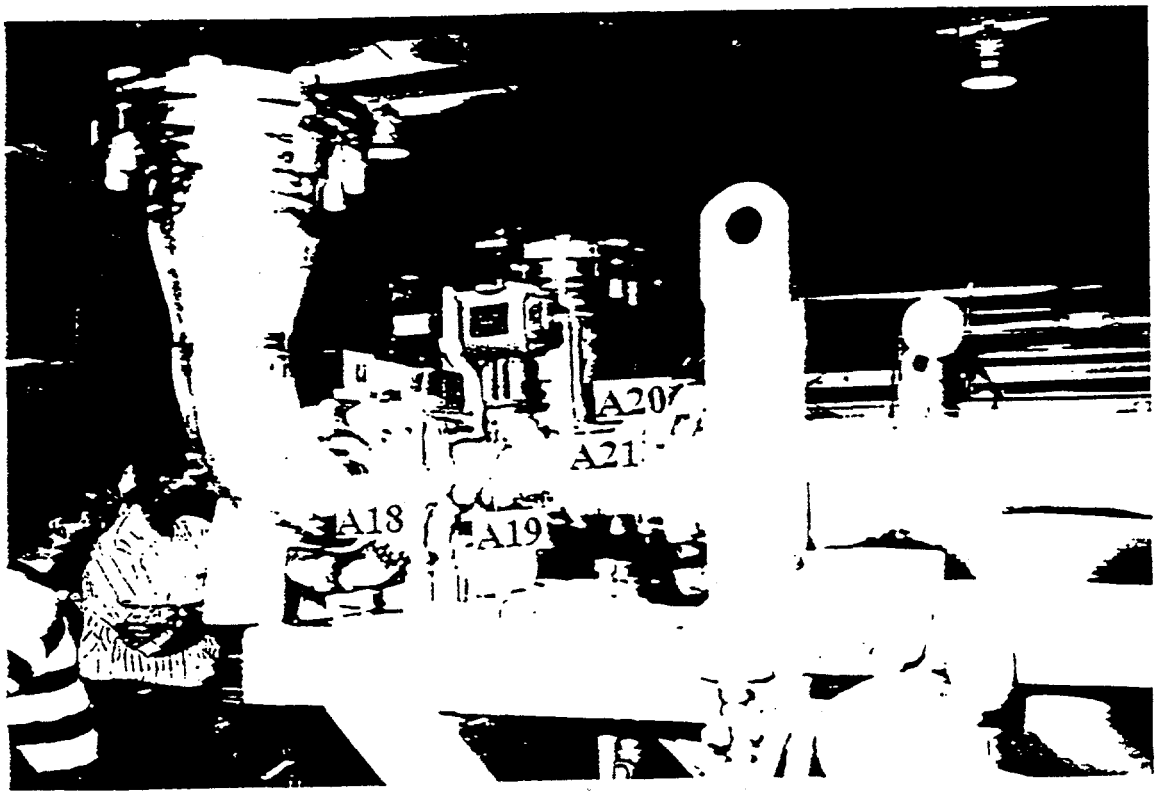


Figure 10. Oxygen Skid-Oxygen Reversal Valve Actuators

Figure 11. Oxygen Skid-Air Reversal Valve
Actuator Ball Valves

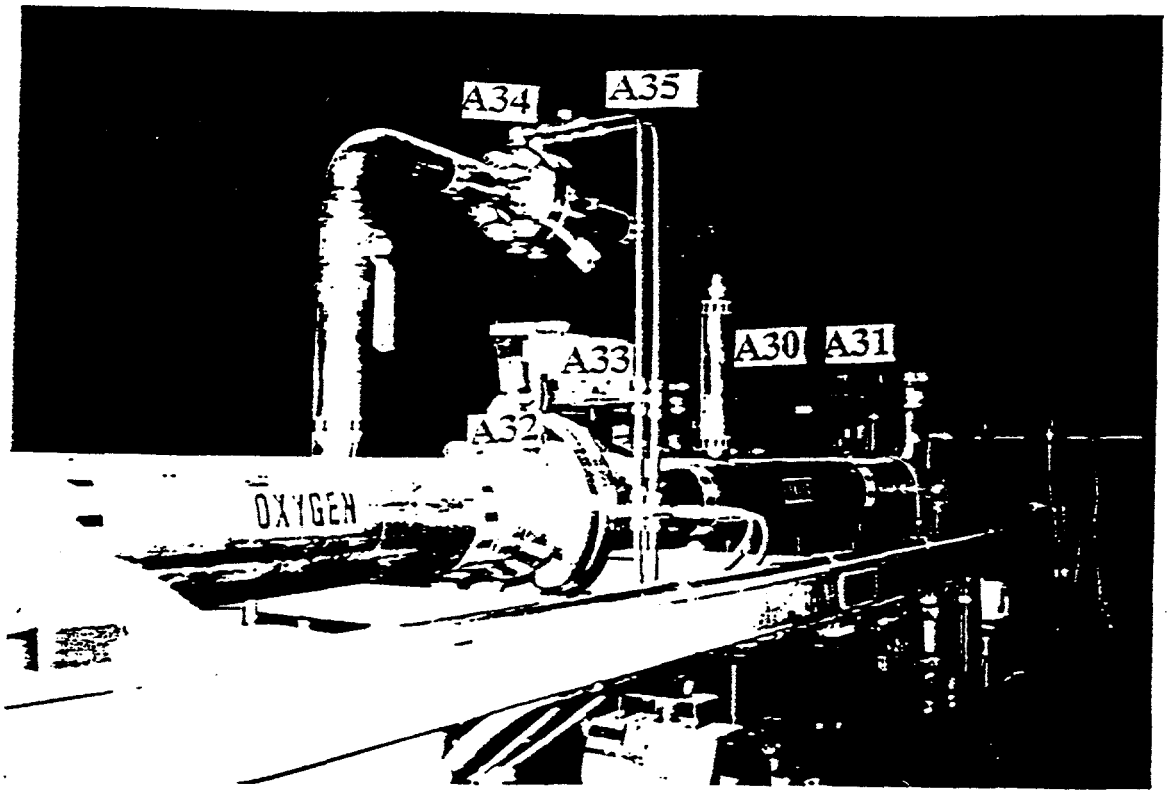


Figure 12. Oxygen Skid-Oxygen Reversal Valve Actuators. Orifice Plate Ball Valves

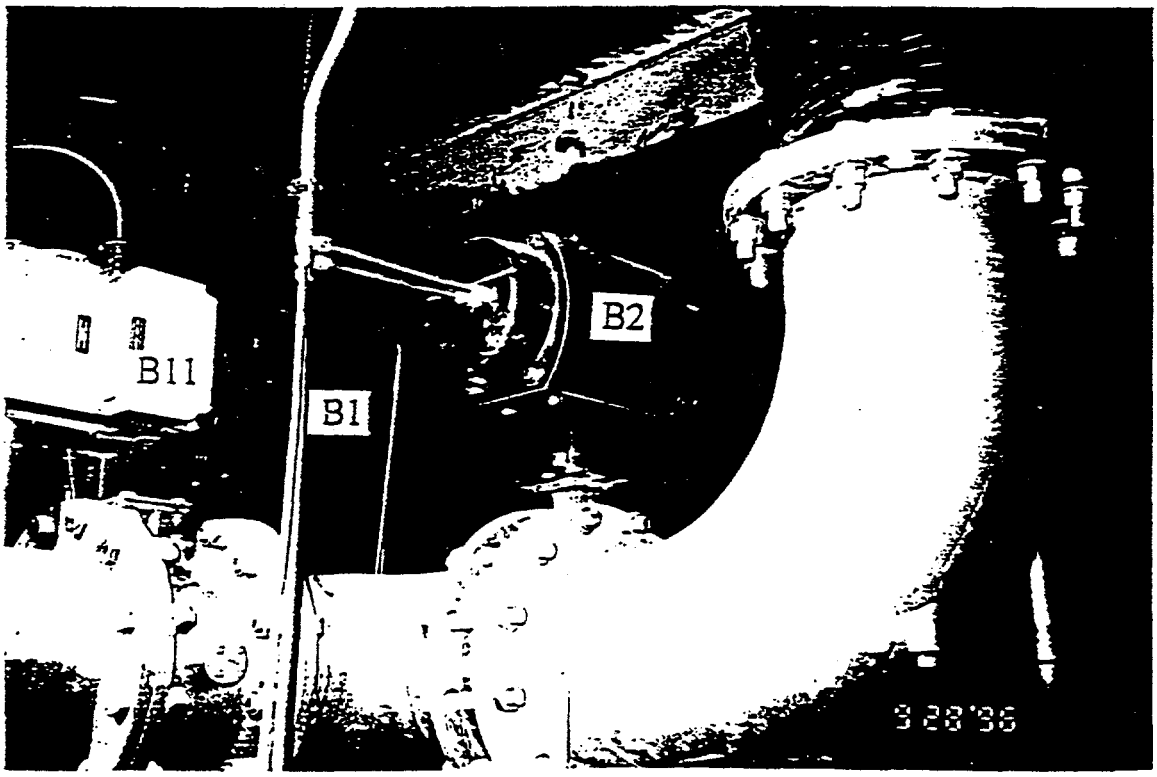


Figure 13. Blower Skid-Air Reversal Valve Actuators. Flow Control Valve

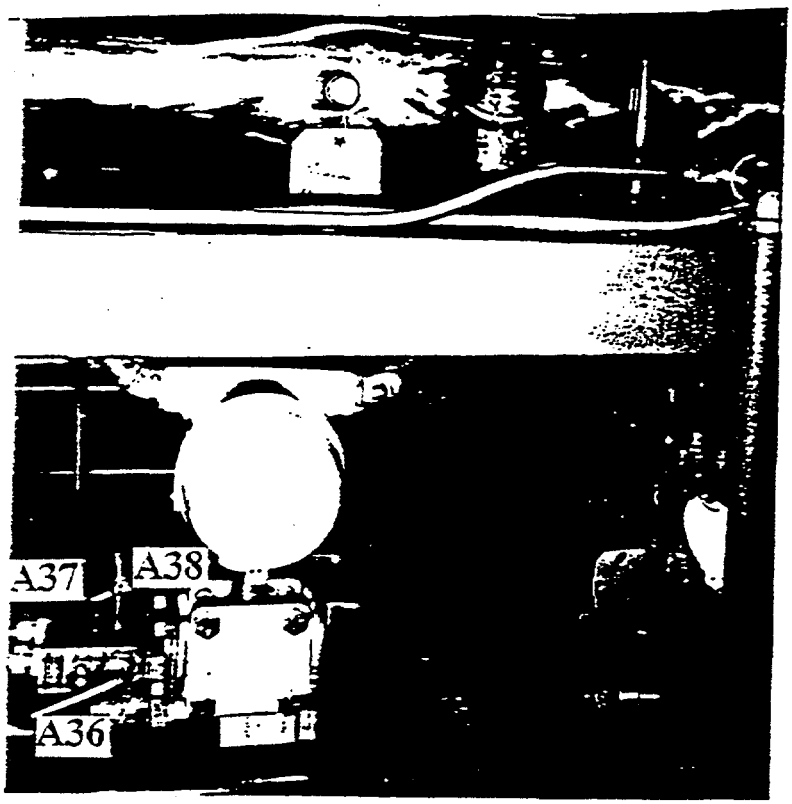


Figure 14. Oxygen Skid-Oxygen Mass Flow Meter

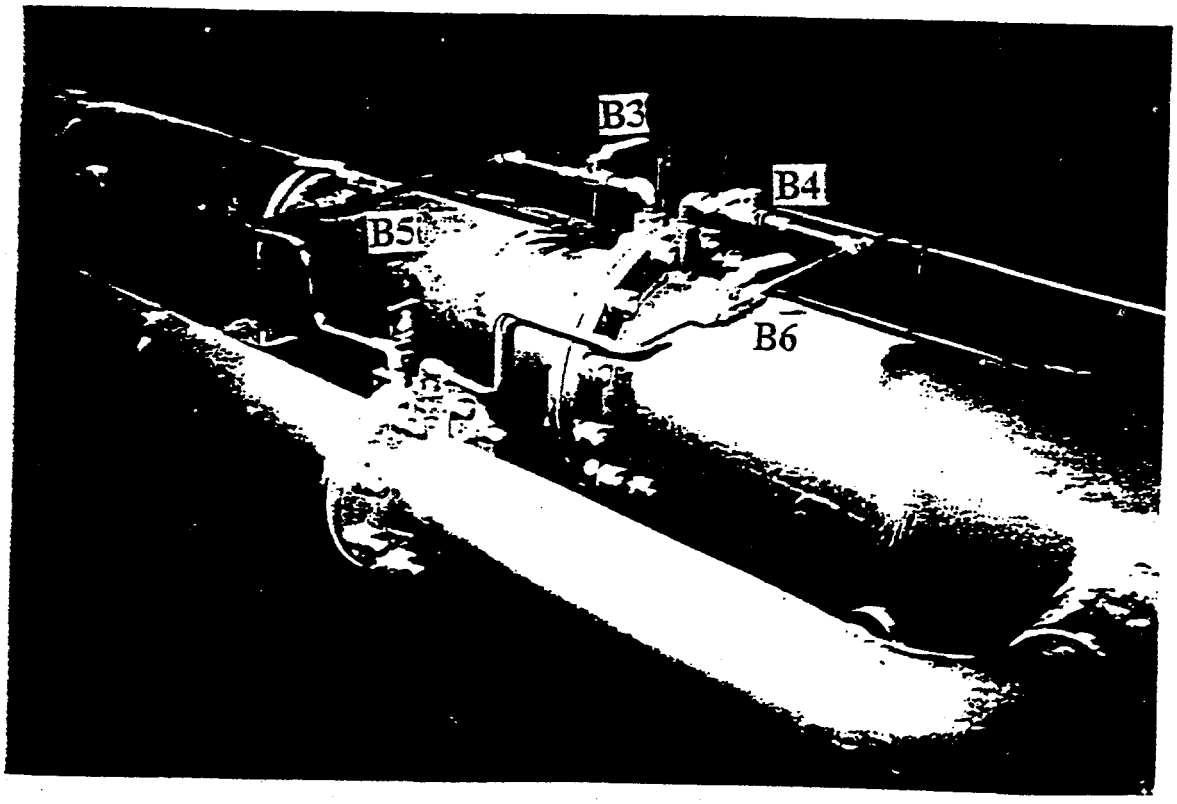


Figure 15. Blower Skid-Orifice Plate Ball Valves

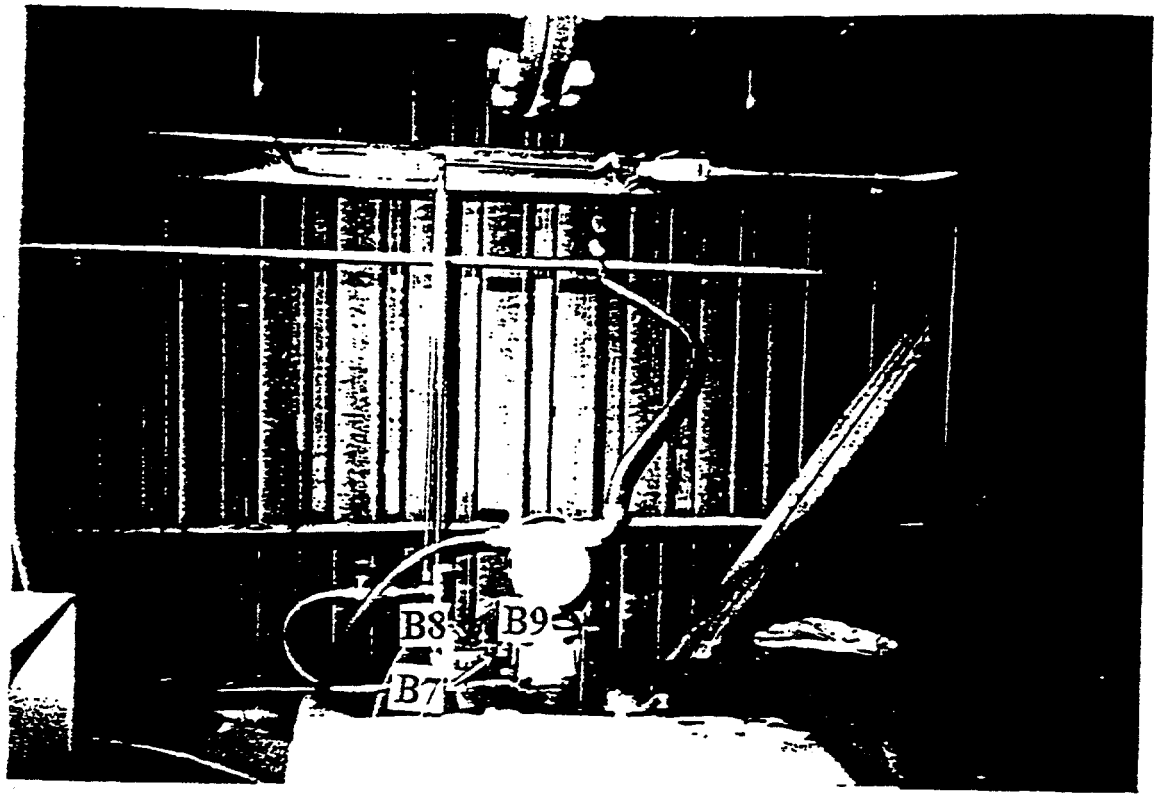


Figure 16. Blower Skid-Air Mass Flow Meter

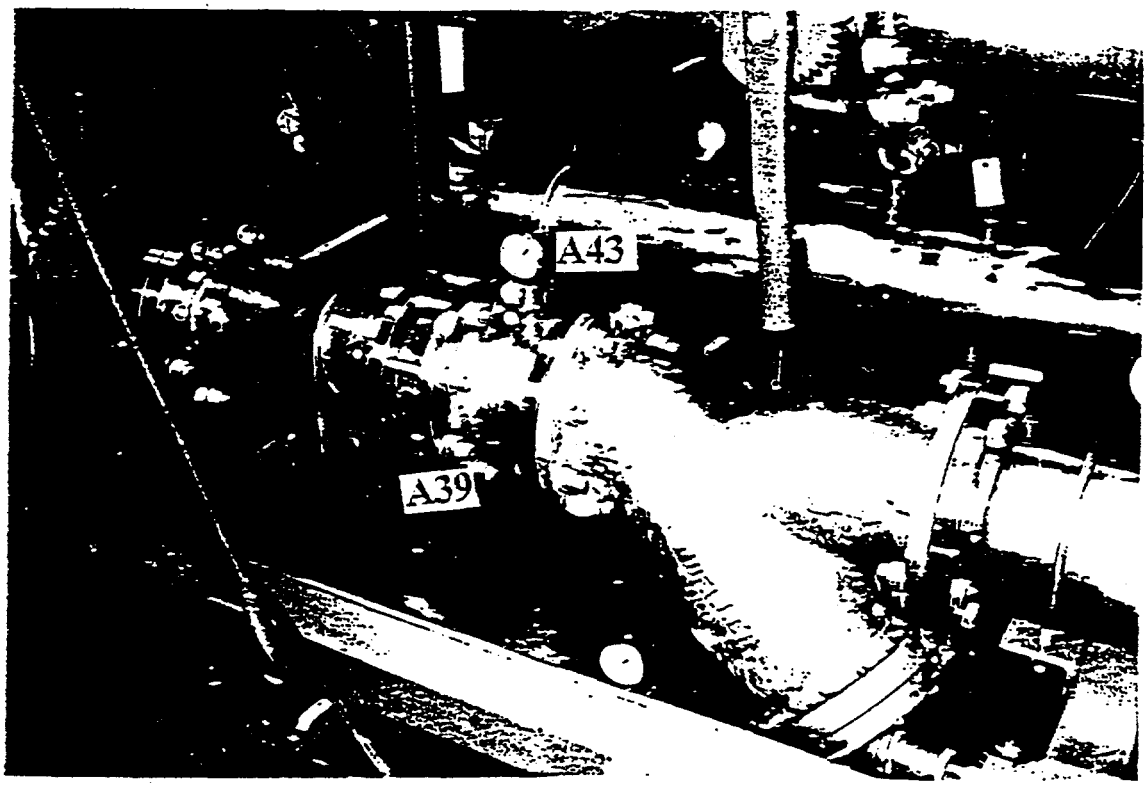


Figure 17. Oxygen Skid-Oxygen Inlet

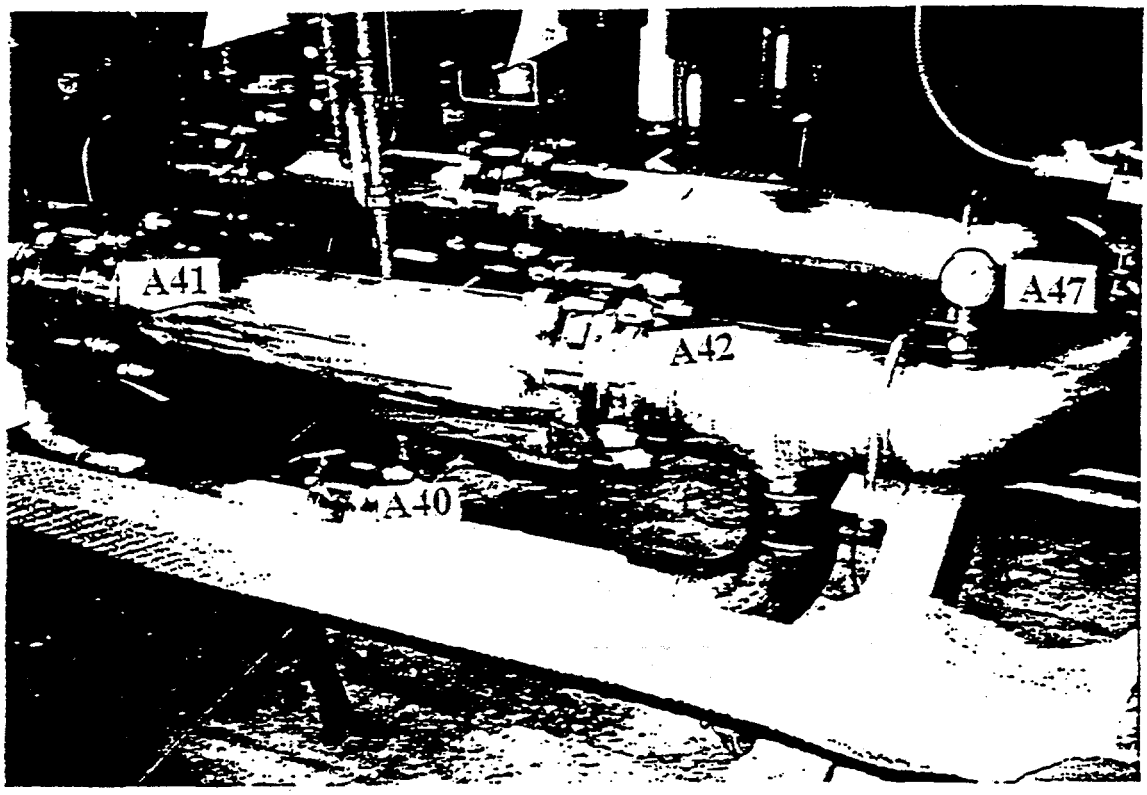


Figure 18. Oxygen Skid-Bypass Leg and Pressure Gauge at Low Pressure Switch

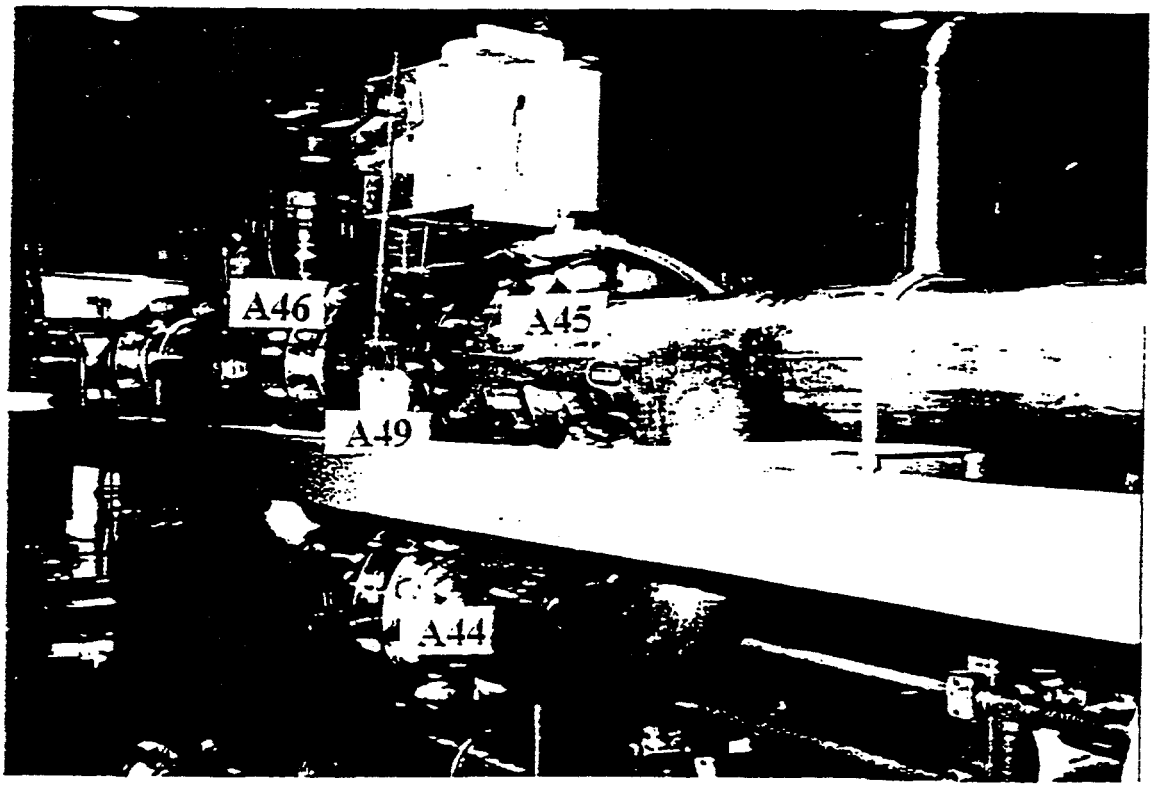


Figure 19. Oxygen Skid-Flow Control Valve

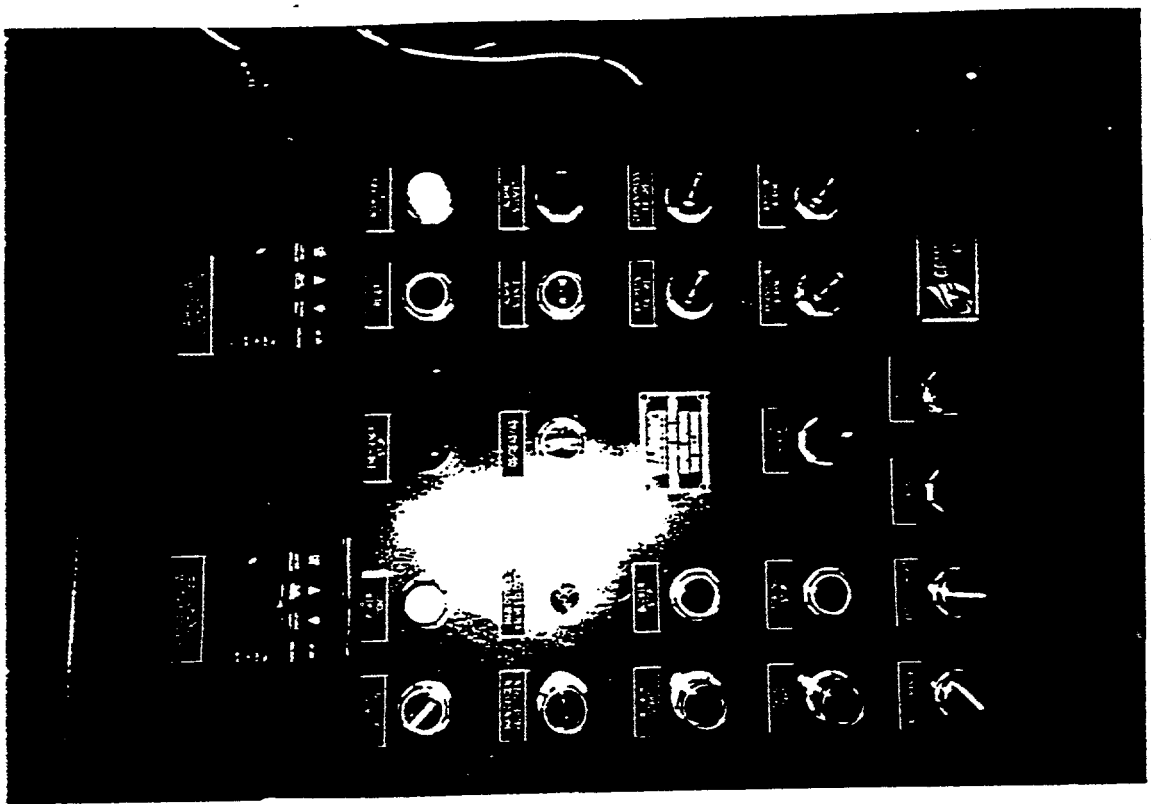

Figure 20. Oxygen Skid-Staging System Control Panel

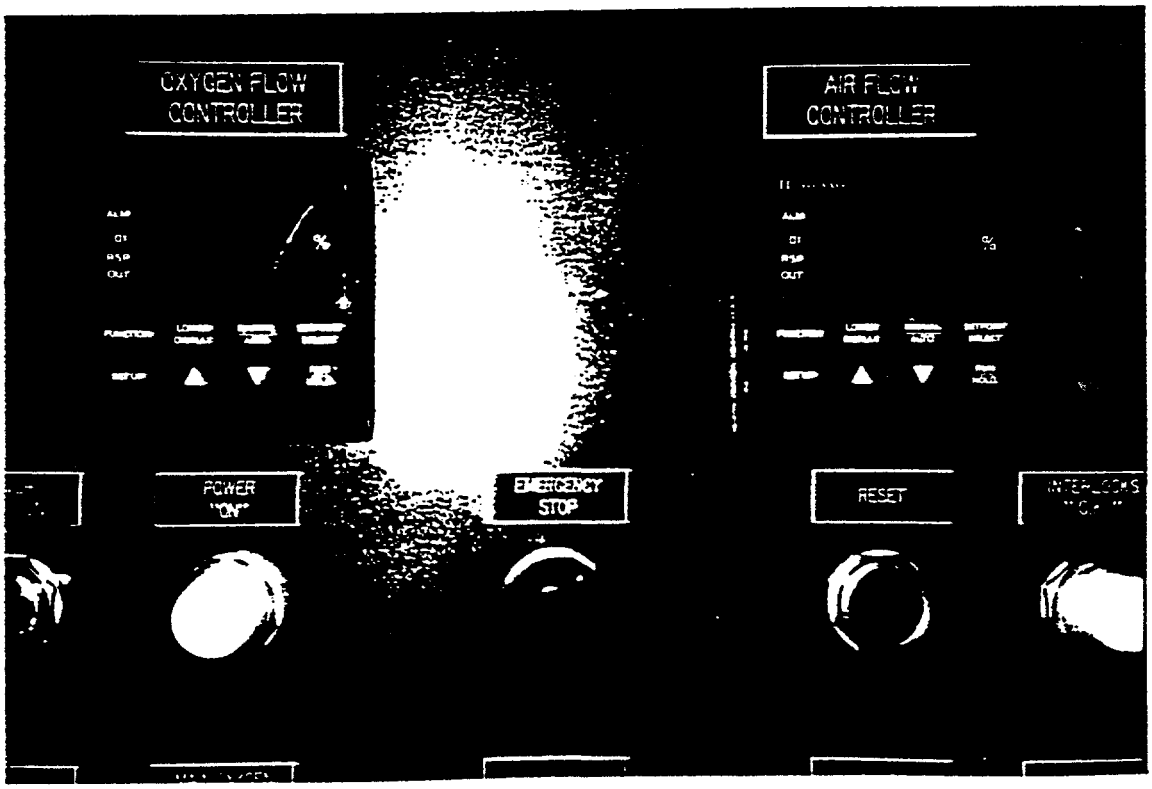


Figure 21. Oxygen Skid-Oxygen and Air Flow Controllers on Control Panel

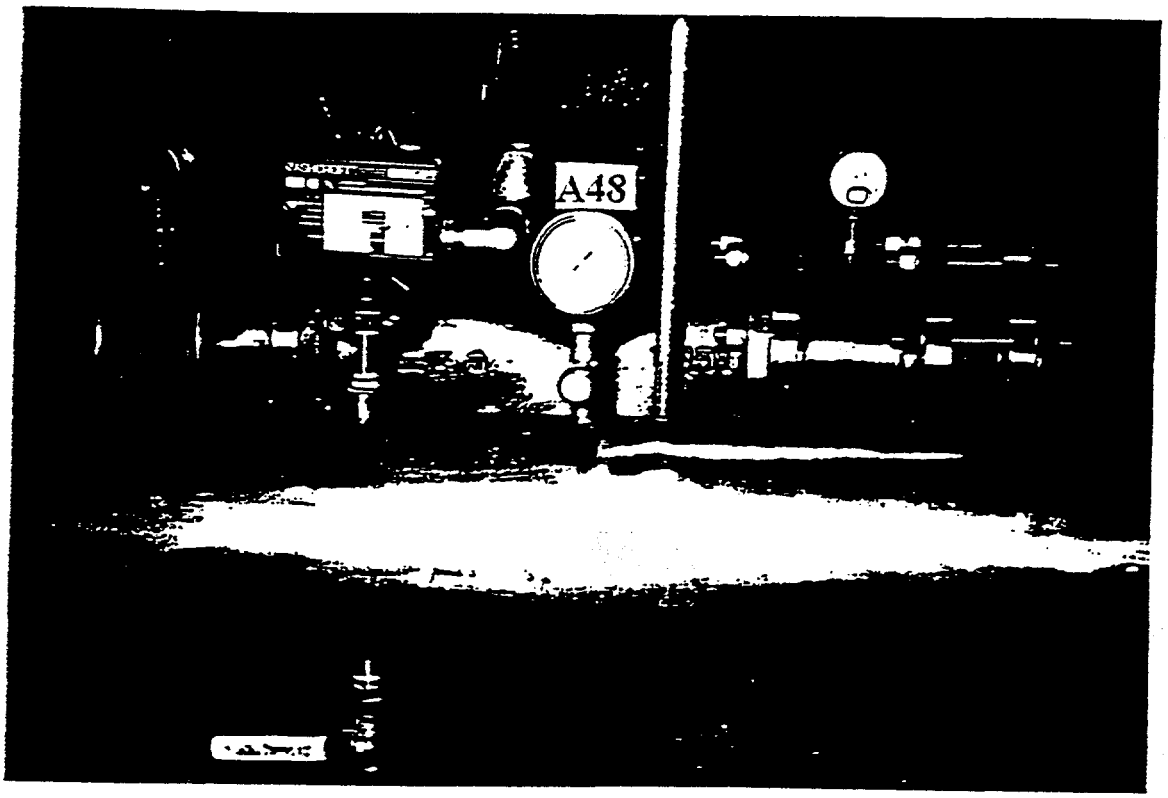


Figure 22. Oxygen Skid-Pressure Gauge at High Pressure Switch

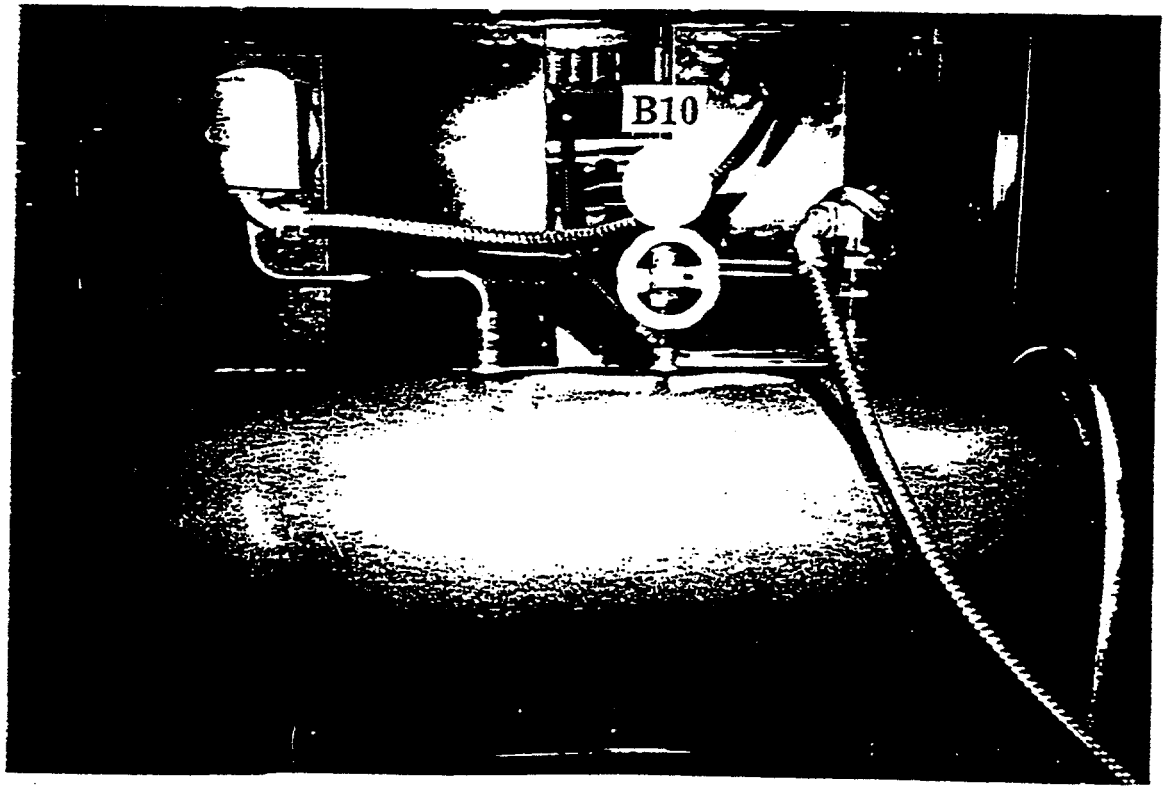


Figure 23. Blower Skid-Pressure Gauge at Low Pressure Switch

# APPENDIX A-1: Panelview 900 Screens

# OVERVIEW

## MAIN FLAME

RIGHT PSR #.##

A/F RATIO ##.##

AIR (kscfh) 750 500 250 0 ###.#

GAS (kscfh) 60 40 20 0 ##.#

## FURNACE

OSR #.##

A/F RATIO

SP ##.# ACT ##.##

STACK NOx (ppm) 0 350 700 ###

## STAGING

LEFT LOCAL OEAS

O2 CONTENT ##.# %

AIR (kscfh) 60 40 20 0 ##.##

OXY (kscfh) 15 10 5 0 ##.##

ACT

SP

OVER VIEW | MAN CNTRL | LOCAL CNTRL | REMOT CNTRL | TRAIN CNTRL | ALARM HIST

# MANUAL STAGING CONTROL

PERCENT OPEN

OXYGEN FLOW CONTROL VALVE ###.# %

AIR FLOW CONTROL VALVE ###.# %

PRESS THE MANUAL BUTTON TO CHANGE VALVE OPENINGS AND TO PLACE IN ==> MANUAL CONTROL

MAN

| OVER VIEW | MAN CNTRL | LOCAL CNTRL | REMOT CNTRL | TRAIN CNTRL | ALARM HIST | FLOW LIMIT |
|---|---|---|---|---|---|---|

STAGING

LEFT | LOCAL | OEAS

O2 CONTENT ##.# %

| | AIR (kscfh) | OXY (kscfh) |
|---|---|---|
| | 60 | 15 |
| | 40 | 10 |
| | 20 | 5 |
| | 0 | 0 |
| ACT | ##.## | ##.## |
| SP | ##.## | ##.## |

# LOCAL STAGING CONTROL

Furnace Gas Flow (kscfh) ##.#

Stoichiometric A/F Ratio ##.#

Staging Mixture Oxygen Content ##.# %

Supply Oxygen Purity ##.# %

| FIRING SIDE | AIR FUEL RATIOS Flame | AIR FUEL RATIOS Overall |
|---|---|---|
| LEFT | ##.# | ##.# |
| RIGHT | ##.# | ##.# |

PRESS LOCAL BUTTON TO PLACE IN LOCAL CONTROL MODE ==> LOCAL

STAGING

LEFT | LOCAL | OEAS

O2 CONTENT ##.# %

| AIR (kscfh) | OXY (kscfh) |
|---|---|
| 60 | 15 |
| 40 | 10 |
| 20 | 5 |
| 0 | 0 |

| | | |
|---|---|---|
| ##.## | ACT | ##.## |
| ##.## | SP | ##.## |

OVER VIEW | MAN CNTRL | LOCAL CNTRL | REMOT CNTRL | TRAIN CNTRL | ALARM HIST | FLOW LIMIT | PID PARAM

# REMOTE STAGING CONTROL

Stoichiometric A/F Ratio ##.#

Staging Mixture Oxygen Content ##.# %

Supply Oxygen Purity ##.# %

| FIRING SIDE | OVERALL AIR FUEL RATIOS |
|---|---|
| LEFT | ##.# |
| RIGHT | ##.# |

PRESS REMOTE BUTTON TO PLACE IN REMOTE CONTROL MODE ==> REM

STAGING

LEFT | LOCAL | OEAS

O2 CONTENT ##.# %

| AIR (kscfh) | OXY (kscfh) |
|---|---|
| 60 | 15 |
| 40 | 10 |
| 20 | 5 |
| 0 | 0 |

| | | |
|---|---|---|
| ##.## | ACT | ##.## |
| ##.## | SP | ##.## |

OVER VIEW | MAN CNTRL | LOCAL CNTRL | REMOT CNTRL | TRAIN CNTRL | ALARM HIST | FLOW LIMIT | PID PARAM

# TRAIN CONTROL

| STAGING MODE | BLOWERS | OXY VALVES | STAGING |
|---|---|---|---|
| AS | ON | OPEN | START |
| OEAS | OFF | CLOSE | STOP |
| MAN | | | |

RESET
ESTOP

| OVER VIEW | MAN CNTRL | LOCAL CNTRL | REMOT CNTRL | TRAIN CNTRL | ALARM HIST |
|---|---|---|---|---|---|

# PID CONTROL LOOP PARAMETERS

| FLOW CONTROL PARAMATERS | AIR FLOW (kscfh) SETPOINT ##.## | ACTUAL ##.## | PERCENT OPEN ###.# | OXY FLOW (kscfh) SETPOINT ##.## | ACTUAL ##.## | PERCENT OPEN ###.# |
|---|---|---|---|---|---|---|
| GAIN | | #####.# | | | #####.# | |
| Fast Loop Update (sec) | | ##.## | | | ##.## | |
| Long Loop Update (sec) | | ##.## | | | ##.## | |
| Deadband | | ### | | | ### | |

ACCEPT VALUES

Goto Config Screen

RETURN

# FLOW ALARM LIMITS

| ALARM | AIR FLOW (kscfh) | OXYGEN (kscfh) |
|---|---|---|
| LO | ##.## | ##.## |
| HI | ##.## | ##.## |

RETURN

# ALARM HISTORY

MM/DD/YY 1H:MM:SSPM Processor Faulted. Call Combustion Tec at (407*

Clear History

| OVER VIEW | MAN CNTRL | LOCAL CNTRL | REMOT CNTRL | TRAIN CNTRL | ALARM HIST |
|---|---|---|---|---|---|

Processor Faulted. Call Combustion Tec at (407) 299-7317.

ACK

CLEAR

# APPENDIX C
# OEAS FIELD EVALUATION TESTS

| | 25-Apr | 25-Apr | 25-Apr | 25-Apr | 25-Apr | 25-Apr | 25-Apr | 25-Apr | 25-Apr | 25-Apr | 25-Apr | 25-Apr |
|---|---|---|---|---|---|---|---|---|---|---|---|---|
| Time | 11:28 | 11:53 | 12:20 | 12:30 | 15:57 | 16:27 | 16:41 | 16:57 | 17:13 | 17:32 | 17:41 | 17:59 |
| Firing Side | L | R | L | L | R | L | L | R | R | L | L | R |
| Injection Location | Side | Side | Side | Side | Side | Side | Side | Side | Side | Side | Side | Side |
| Sample Location | Port 5 | Port 5 | Port 5 | Port 5 | Port 5 | Port 5 | Port 5 | Port 5 | Port 5 | Port 5 | Port 5 | Port 5 |
| O2, % | 0.26 | 1.02 | 0.8 | 0.16 | 1.38 | 0.42 | 0.39 | 0.53 | 0.62 | 1.09 | 1.3 | 2.95 |
| CO, ppm | 1600 | 0.56 | 3072 | 2440 | 0.39 | 600 | 600 | 300 | 200 | 58 | 45 | 28 |
| CO2, % | 12 | 11.3 | 12.4 | 13.2 | 13.7 | 13.7 | 13.7 | 13.6 | 13.4 | 13.3 | 13.9 | 13.6 |
| NOx, ppm | 700 | 870 | 794 | 684 | 749 | 678 | 692 | 820 | 920 | 745 | 670 | 850 |
| Staging | yes | yes | yes | yes | yes | yes | yes | yes | yes | yes | yes | yes |
| Staging O2 | 1462 | 1462 | 1462 | 1462 | 1462 | 1462 | 1462 | 1100 | 875 | 1800 | 2200 | 2800 |
| Staging Air | 6782 | 6782 | 6782 | 6782 | 6782 | 6782 | 6782 | 5100 | 4060 | 6800 | 6800 | 0 |
| PSR | 0.0 | 0.0 | 0.0 | 0.0 | 0.0 | 0.0 | 0.0 | 0.0 | 0.0 | 0.0 | 0.0 | 0.0 |
| OSR | 0.0 | 0.0 | 0.0 | 0.0 | 0.0 | 0.0 | 0.0 | 0.0 | 0.0 | 0.0 | 0.0 | 0.0 |
| NOx, 0% O2 | 708.8 | 914.4 | 825.4 | 689.3 | 801.7 | 691.8 | 705.1 | 841.2 | 948.0 | 785.8 | 714.2 | 988.9 |
| NOx, lb/ton | 1.5 | 2.0 | 1.8 | 1.5 | 1.7 | 1.5 | 1.5 | 1.8 | 2.0 | 1.5 | 1.3 | 0.5 |
| CO, 0% O2 | 1620.1 | 0.6 | 3193.7 | 2458.7 | 0.4 | 612.2 | 611.4 | 307.8 | 206.1 | 61.2 | 48.0 | 32.6 |

| | 25-Apr | 25-Apr | 25-Apr | 25-Apr | 25-Apr | 25-Apr | 25-Apr | 26-Apr | 26-Apr | 26-Apr | 26-Apr | 26-Apr |
|---|---|---|---|---|---|---|---|---|---|---|---|---|
| Time | 19:31 | 19:44 | 20:01 | 20:12 | 20:19 | 20:33 | 20:42 | 9:21 | 9:34 | 9:52 | 10:12 | 11:33 |
| Firing Side | L | L | R | R | R | L | L | R | R | L | L | R |
| Injection Location | Side | Side | Side | Side | Side | Side | Side | Side | Side | Side | Side | Side |
| Sample Location | Port 5 | Port 5 | Port 5 | Port 5 | Port 5 | Port 5 | Port 5 | Port 5 | Port 5 | Port 5 | Port 5 | Port 5 |
| O2, % | 0.75 | 1.53 | 0.6 | 1.43 | 1.3 | 1.8 | 2.7 | 1.32 | 0.02 | 0.06 | 0.67 | 1.55 |
| CO, ppm | 2100 | 210 | 600 | 54 | 90 | 48 | 32 | 65 | 3080 | 3116 | 1005 | 80 |
| CO2, % | 14.4 | 14.5 | 14.3 | 14.6 | 14 | 14.5 | 14 | 12.8 | 12.7 | 11.1 | 12.1 | 13.3 |
| NOx, ppm | 745 | 743 | 840 | 840 | 850 | 719 | 805 | 1080 | 840 | 580 | 922 | 1024 |
| Staging | yes | yes | yes | yes | yes | yes | yes | no | no | no | no | no |
| Staging O2 | 2400 | 3500 | 2400 | 3500 | 3000 | 4000 | 4300 | 0 | 0 | 0 | 0 | 0 |
| Staging Air | 0 | 0 | 0 | 0 | 0 | 0 | 0 | 0 | 0 | 0 | 0 | 0 |
| PSR | 0.0 | 0.0 | 0.0 | 0.0 | 0.0 | 0.0 | 0.0 | 0 | 0 | 0 | 0 | 0 |
| OSR | 0.0 | 0.0 | 0.0 | 0.0 | 0.0 | 0.0 | 0.0 | 0 | 0 | 0 | 0 | 0 |
| NOx, 0% O2 | 772.6 | 801.4 | 864.7 | 901.4 | 906.1 | 786.4 | 923.8 | 1152.4 | 840.8 | 381.7 | 952.4 | 1105.6 |
| NOx, lb/ton | 0.4 | 0.4 | 0.4 | 0.5 | 0.5 | 0.4 | 0.5 | NA | NA | NA | NA | NA |
| CO, 0% O2 | 2177.8 | 226.5 | 617.6 | 57.9 | 95.9 | 52.5 | 36.7 | 69.4 | 3082.9 | 3124.9 | 1038.1 | 86.4 |

| | 26-Apr | 26-Apr | 26-Apr | 26-Apr | 26-Apr | 26-Apr | 26-Apr | 26-Apr | 26-Apr | 26-Apr | 26-Apr | 26-Apr |
|---|---|---|---|---|---|---|---|---|---|---|---|---|
| Time | 11:43 | 11:58 | 12:09 | 12:33 | 13:03 | 13:38 | 14:25 | 14:55 | 15:25 | 15:59 | 16:24 | 17:07 |
| Firing Side | R | L | L | R | L | R | R | L | R | L | R | L |
| Injection Location | Side | Side | Side | Side | Side | Side | Side | Side | Side | Side | Side | Side |
| Sample Location | Port 5 | Port 5 | Port 5 | Port 5 | Port 5 | Port 5 | Port 5 | Port 5 | Port 5 | Port 5 | Port 5 | Port 5 |
| O2, % | 0.11 | 1.21 | 0.2 | 1.96 | 1.2 | 2.15 | 2.8 | 2.2 | 2.69 | 1.79 | 2.82 | 2.24 |
| CO, ppm | 2900 | 243 | 3079 | 32 | 340 | 32 | 23 | 25 | 27 | 51 | 20 | 35 |
| CO2, % | 11.3 | 11.6 | 11 | 11.2 | 11.6 | 11 | 13.1 | 13.8 | 12.4 | 12.9 | 12 | 11.7 |
| NOx, ppm | 801 | 900 | 690 | 705 | 635 | 732 | 630 | 610 | 638 | 640 | 680 | 695 |
| Staging | no | no | no | yes | yes | yes | yes | yes | yes | yes | yes | yes |
| Staging O2 | 0 | 0 | 0 | 1650 | 1650 | 1650 | 1650 | 1650 | 1650 | 1650 | 1650 | 1650 |
| Staging Air | 0 | 0 | 0 | 7600 | 7600 | 7600 | 7600 | 7600 | 7600 | 7600 | 7600 | 7600 |
| PSR | 0 | 0 | 0 | 1.3 | 1.3 | 1.3 | 1.3 | 1.3 | 1.3 | 1.3 | 1.3 | 1.3 |
| OSR | 0 | 0 | 0 | 1.4 | 1.4 | 1.4 | 1.4 | 1.4 | 1.4 | 1.4 | 1.4 | 1.4 |
| NOx, 0% O2 | 805.2 | 955.0 | 696.6 | 777.6 | 673.5 | 815.5 | 726.9 | 681.4 | 731.7 | 699.6 | 785.5 | 778.0 |
| NOx, lb/ton | NA | NA | NA | 2.8 | 2.4 | 3.0 | 2.6 | 2.5 | 2.6 | 2.5 | 2.9 | 2.8 |
| CO, 0% O2 | 2915.3 | 257.9 | 3108.6 | 35.3 | 360.6 | 35.6 | 26.5 | 27.9 | 31.0 | 55.8 | 23.1 | 39.2 |

| | 26-Apr | 26-Apr | 26-Apr | 26-Apr | 26-Apr | 26-Apr | 26-Apr | 26-Apr | 26-Apr | 26-Apr | 26-Apr | 27-Apr |
|---|---|---|---|---|---|---|---|---|---|---|---|---|
| Time | 17:40 | 18:03 | 18:53 | 19:11 | 19:46 | 20:09 | 20:17 | 20:30 | 20:40 | 20:47 | 20:57 | 10:50 |
| Firing Side | R | L | R | L | R | L | L | L | R | R | R | L |
| Injection Location | Side | Side | Side | Side | Side | Side | Side | Side | Side | Side | Side | 1-Under |
| Sample Location | Port 5 | Port 5 | Port 5 | Port 5 | Stack | Stack | Stack | Stack | Stack | Stack | Stack | Port 5 |
| O2, % | 2.55 | 2.4 | 2.84 | 2.53 | 2.8 | 2.13 | 0.1 | 1.64 | 2.5 | 0.25 | 2.12 | 2.2 |
| CO, ppm | 22 | 42 | 23 | 37 | 26 | 55 | 3125 | 125 | 29 | 2834 | 32 | 80 |
| CO2, % | 11.1 | 11.1 | 11.4 | 11.3 | 11.3 | 12.3 | 11.5 | 11.9 | 11.7 | 12 | 11.7 | 11.7 |
| NOx, ppm | 685 | 703 | 730 | 750 | 755 | 600 | 640 | 750 | 685 | 780 | 920 | 1040 |
| Staging | yes | yes | yes | yes | yes | yes | yes | no | yes | no | no | no |
| Staging O2 | 1650 | 1650 | 1650 | 1650 | 1650 | 1650 | 1650 | 0 | 1650 | 0 | 0 | 0 |
| Staging Air | 7600 | 7600 | 7600 | 7600 | 7600 | 7600 | 7600 | 0 | 7600 | 0 | 0 | 0 |
| PSR | 1.3 | 1.3 | 1.3 | 1.3 | 1.3 | 1.3 | 1.3 | 1.3 | 1.3 | 1.3 | 1.3 | 1.3 |
| OSR | 1.4 | 1.4 | 1.4 | 1.4 | 1.4 | 1.4 | 1.4 | 1.3 | 1.4 | 1.3 | 1.3 | 1.3 |
| NOx, 0% O2 | 779.7 | 793.7 | 844.2 | 852.7 | 871.2 | 667.7 | 643.1 | 813.5 | 777.6 | 789.4 | 1023.3 | 1161.7 |
| NOx, lb/ton | 2.8 | 2.9 | 3.1 | 3.2 | 3.2 | 2.5 | 2.4 | 3.0 | 2.9 | 3.0 | 3.8 | 4.6 |
| CO, 0% O2 | 25.0 | 47.4 | 26.6 | 42.1 | 30.0 | 61.2 | 3140.0 | 135.6 | 32.9 | 2868.1 | 35.6 | 89.4 |

| | 27-Apr | 27-Apr | 27-Apr | 27-Apr | 27-Apr | 27-Apr | 27-Apr | 27-Apr | 27-Apr | 27-Apr | 27-Apr | 27-Apr |
|---|---|---|---|---|---|---|---|---|---|---|---|---|
| Time | 10:56 | 11:10 | 11:18 | 12:08 | 12:19 | 13:24 | 13:45 | 14:16 | 14:31 | 14:45 | 15:03 | 15:19 |
| Firing Side | L | R | R | R | L | R | L | R | R | L | L | R |
| Injection Location | 1-Under | 1-Under | 1-Under | 1-Under | 1-Under | 1-Under | 1-Under | 1-Under | 1-Under | 1-Under | 1-Under | 1-Under |
| Sample Location | Port 5 | Port 5 | Port 5 | Port 5 | Port 5 | Port 5 | Port 5 | Port 5 | Port 5 | Port 5 | Port 5 | Port 5 |
| O2, % | 0.13 | 2.17 | 0.25 | 0.8 | NA | 1.53 | 0.81 | 1.2 | 1.57 | 0.7 | 0.76 | 0.69 |
| CO, ppm | 3072 | 32 | 2500 | 700 | NA | 60 | 1055 | 400 | 70 | 2000 | 1800 | 1500 |
| CO2, % | 12.1 | 11.8 | 12 | 13.9 | NA | 12.6 | 12.7 | 12.2 | 12.2 | 12.8 | 12.5 | 12.1 |
| NOx, ppm | 870 | 1316 | 1088 | NA | NA | 1034 | 1024 | 1060 | 1070 | 880 | 980 | 1110 |
| Staging | no | no | no | yes | NA | yes | yes | yes | yes | yes | yes | yes |
| Staging O2 | 0 | 0 | 0 | 1650 | NA | 2500 | 1480 | 1950 | 2250 | 1950 | 3050 | 1950 |
| Staging Air | 0 | 0 | 0 | 7600 | NA | 9250 | 6200 | 9250 | 8350 | 5900 | 4250 | 7250 |
| PSR | 1.3 | 1.3 | 1.3 | 1.3 | 1.3 | 1.3 | 1.3 | 1.3 | 1.3 | 1.3 | 1.3 | 1.3 |
| OSR | 1.3 | 1.3 | 1.3 | 1.4 | 1.3 | 1.4 | 1.4 | 1.4 | 1.4 | 1.4 | 1.4 | 1.4 |
| NOx, 0% O2 | 875.4 | 1467.7 | 1101.1 | 0 | 0 | 1115.3 | 1065.1 | 1124.2 | 1156.5 | 910.3 | 1016.8 | 1147.7 |
| NOx, lb/ton | 3.5 | 5.8 | 4.3 | 0 | 0 | 4.3 | 4.2 | 4.4 | 4.5 | 3.6 | 3.9 | 4.5 |
| CO, 0% O2 | 3091.1 | 35.7 | 2530.1 | 727.7 | 0 | 64.7 | 1097.3 | 424.2 | 75.7 | 2069.0 | 1867.6 | 1551.0 |

| | 27-Apr | 27-Apr | 27-Apr | 27-Apr | 27-Apr | 27-Apr | 27-Apr | 27-Apr | 27-Apr | 27-Apr | 27-Apr | 27-Apr |
|---|---|---|---|---|---|---|---|---|---|---|---|---|
| Time | 15:30 | 15:52 | 16:03 | 16:21 | 16:57 | 17:25 | 17:37 | 17:54 | 18:01 | 18:06 | 18:20 | 18:35 |
| Firing Side | R | L | L | R | L | R | R | L | L | L | R | R |
| Injection Location | 1-Under | 1-Under | 1-Under | 1-Under | 1-Under | 1-Under | 1-Under | 1-Under | 1-Under | 1-Under | 1-Under | 1-Under |
| Sample Location | Port 5 | Port 5 | Port 5 | Port 5 | Port 5 | Port 5 | Port 5 | Port 5 | Port 5 | Port 5 | Port 5 | Port 5 |
| O2, % | 0.8 | 0.56 | 0.65 | 1.38 | 7.45 | 7.44 | 7.6 | 7.56 | 7.82 | 1.3 | 1.3 | 1 |
| CO, ppm | 639 | 2400 | 2500 | 150 | 8 | 9 | 8 | 40 | 8 | 350 | 180 | 170 |
| CO2, % | 12.2 | 12 | 11.9 | 12.1 | 8.4 | 8.4 | 8.3 | 8.6 | 8.6 | 11.8 | 12.2 | 12.1 |
| NOx, ppm | 1073 | 1060 | 1058 | 1200 | 833 | 876 | 810 | 800 | 820 | 1080 | 1180 | 1200 |
| Staging | yes | yes | yes | yes | no | no | no | no | yes | yes | yes | yes |
| Staging O2 | 1950 | 2450 | 2900 | 2500 | 0 | 0 | 0 | 0 | 2400 | 2400 | 2400 | 1200 |
| Staging Air | 6250 | 3400 | 2900 | 5800 | 0 | 0 | 0 | 0 | 0 | 0 | 0 | 0 |
| PSR | 1.3 | 1.3 | 1.3 | 1.3 | 1.3 | 1.3 | 1.3 | 1.3 | 1.3 | 1.3 | 1.3 | 1.3 |
| OSR | 1.4 | 1.4 | 1.4 | 1.4 | 1.3 | 1.3 | 1.3 | 1.3 | 1.4 | 1.4 | 1.4 | 1.3 |
| NOx, 0% O2 | 1115.5 | 1089.0 | 1091.8 | 1284.4 | 1291.0 | 1356.6 | 1269.4 | 1250.0 | 1306.5 | 1151.3 | 1257.9 | 1260.0 |
| NOx, lb/ton | 4.4 | 4.2 | 4.2 | 5.0 | 5.1 | 5.3 | 5.0 | 4.9 | 5.1 | 4.5 | 4.9 | 4.9 |
| CO, 0% O2 | 664.3 | 2465.8 | 2579.9 | 160.6 | 12.4 | 13.9 | 12.5 | 62.5 | 12.7 | 373.1 | 191.9 | 178.5 |

| | 29-Apr | 29-Apr | 29-Apr | 29-Apr | 29-Apr | 29-Apr | 29-Apr | 29-Apr | 29-Apr | 29-Apr | 29-Apr |
|---|---|---|---|---|---|---|---|---|---|---|---|
| Time | 9:24 | 9:37 | 9:54 | 10:09 | 10:33 | 11:08 | 11:28 | 11:45 | 11:58 | 12:12 | 12:31 |
| Firing Side | R | R | L | L | R | L | R | R | L | L | R |
| Injection Location | Crown | Crown | 2- Under | 2- Under | Crown | 2- Under | Crown | Crown | 2- Under | 2- Under | Crown |
| Sample Location | Port 5 | Port 5 | Port 5 | Port 5 | Port 5 | Port 5 | Port 5 | Port 5 | Port 5 | Port 5 | Port 5 |
| O2, % | 2.1 | 0.11 | 1.65 | 0.13 | 0.23 | 0.75 | 0.13 | 0.5 | 0.35 | 0.46 | 0.16 |
| CO, ppm | 34 | 3050 | 174 | 3063 | 2300 | 600 | 3000 | 1400 | 1260 | 750 | 3070 |
| CO2, % | 12 | 12.9 | 12.6 | 12.6 | 12.9 | 12.5 | 12.9 | 13 | 13.6 | 13.6 | 13.4 |
| NOx, ppm | 1283 | 980 | 1061 | 930 | 910 | 990 | 1000 | 930 | 1044 | 1000 | 940 |
| Staging | no | no | no | no | yes | yes | yes | yes | yes | yes | yes |
| Staging O2 | 0 | 0 | 0 | 0 | 0 | 1650 | 0 | 0 | 2150 | 2500 | 0 |
| Staging Air | 0 | 0 | 0 | 0 | 9400 | 7200 | 750 | 11250 | 6700 | 6350 | 6000 |
| PSR | 1.3 | 1.3 | 1.3 | 1.3 | 1.3 | 1.3 | 1.3 | 1.3 | 1.3 | 1.3 | 1.3 |
| OSR | 1.3 | 1.3 | 1.3 | 1.3 | 1.3 | 1.3 | 1.3 | 1.3 | 1.3 | 1.3 | 1.3 |
| NOx, 0% O2 | 1425.6 | 985.2 | 1151.3 | 935.8 | 920.1 | 1026.7 | 1006.2 | 952.7 | 1061.7 | 1022.4 | 947.2 |
| NOx, lb/ton | 5.6 | 3.9 | 4.5 | 3.7 | 3.6 | 4.0 | 4.0 | 3.8 | 4.1 | 4.0 | 3.7 |
| CO, 0% O2 | 37.8 | 3066.1 | 188.8 | 3082.1 | 2325.5 | 622.2 | 3018.7 | 1434.1 | 1281.4 | 766.8 | 3093.6 |

| | 29-Apr | 29-Apr | 29-Apr | 29-Apr | 29-Apr | 29-Apr | 29-Apr | 29-Apr | 29-Apr | 29-Apr | 29-Apr |
|---|---|---|---|---|---|---|---|---|---|---|---|
| Time | 12:43 | 13:00 | 13:15 | 13:30 | 13:44 | 14:03 | 14:04 | 14:33 | 14:45 | 15:02 | 15:20 |
| Firing Side | R | L | L | R | R | L | L | R | R | L | L |
| Injection Location | Crown | 2- Under | 2- Under | Crown | Crown | 2- Under | 2- Under | Crown | Crown | 2- Under | 2- Under |
| Sample Location | Port 5 | Port 5 | Port 5 | Port 5 | Port 5 | Port 5 | Port 5 | Port 5 | Port 5 | Port 5 | Port 5 |
| O2, % | 0.1 | 1.03 | 1.02 | 1 | 7.8 | 7.5 | 2.1 | 8.1 | 2.1 | 1.15 | 7.78 |
| CO, ppm | 3078 | 220 | 285 | 487 | 7 | 7 | 187 | 7 | 538 | 347 | 6 |
| CO2, % | 13.4 | 13.5 | 13.7 | 13.5 | 9.4 | 9.7 | 12 | 14 | 13.6 | 14.4 | 14.3 |
| NOx, ppm | 888 | 1030 | 1020 | 932 | 757 | 715 | 931 | 722 | 930 | 910 | 737 |
| Staging | yes | yes | yes | yes | yes | yes | yes | yes | yes | yes | yes |
| Staging O2 | 0 | 2250 | 2600 | 1950 | 1950 | 1650 | 1650 | 1950 | 1950 | 1650 | 1650 |
| Staging Air | 8000 | 4400 | 2700 | 9250 | 9250 | 6850 | 6850 | 9250 | 9250 | 6850 | 6850 |
| PSR | 1.3 | 1.3 | 1.3 | 1.3 | 1.3 | 1.3 | 1.3 | 1.3 | 1.3 | 1.3 | 1.3 |
| OSR | 1.3 | 1.3 | 1.4 | 1.4 | 1.4 | 1.4 | 1.3 | 1.4 | 1.4 | 1.4 | 1.4 |
| NOx, 0% O2 | 892.2 | 1083.1 | 1072.1 | 978.6 | 1204.3 | 1112.2 | 1034.4 | 1175.3 | 1033.3 | 962.7 | 1170.7 |
| NOx, lb/ton | 3.5 | 4.2 | 4.2 | 3.8 | 4.7 | 4.3 | 4.1 | 4.6 | 4.0 | 3.8 | 4.6 |
| CO, 0% O2 | 3092.7 | 231.3 | 299.5 | 511.4 | 11.1 | 10.9 | 207.8 | 11.4 | 597.8 | 367.1 | 9.5 |

| | 29-Apr | 29-Apr | 29-Apr | 29-Apr | 29-Apr | 29-Apr | 29-Apr | 29-Apr | 29-Apr | 29-Apr | 29-Apr |
|---|---|---|---|---|---|---|---|---|---|---|---|
| Time | 15:34 | 15:51 | 16:08 | 16:19 | 16:37 | 16:49 | 17:06 | 17:20 | 17:49 | 18:20 | 18:54 |
| Firing Side | R | R | L | L | R | R | L | L | R | L | R |
| Injection Location | Crown | Crown | 2- Under | 2- Under | Crown | Crown | 2- Under | 2- Under | Crown | 2- Under | Crown |
| Sample Location | Port 5 | Port 5 | Port 5 | Port 5 | Port 5 | Port 5 | Port 5 | Port 5 | Port 5 | Port 5 | Port 5 |
| O2, % | 8.17 | 1.68 | 1.25 | 7.8 | 1.55 | 7.82 | 7.85 | 1.6 | 7.53 | 7.65 | 7.48 |
| CO, ppm | 7 | 220 | 82 | 8 | 320 | 5 | 7 | 200 | 95 | 94 | 8 |
| CO2, % | 14.1 | 14 | 13.8 | 13.7 | 13.6 | 13.4 | 13.3 | 13.3 | 13.2 | 13.2 | 13.1 |
| NOx, ppm | 729 | 962 | 980 | 770 | 970 | 752 | 750 | 990 | 730 | 720 | 739 |
| Staging | yes | yes | yes | yes | yes | yes | yes | yes | no | no | no |
| Staging O2 | 1950 | 1950 | 1650 | 1650 | 1950 | 1950 | 1650 | 1650 | 0 | 0 | 0 |
| Staging Air | 9250 | 9250 | 6850 | 6850 | 9250 | 9250 | 6850 | 6850 | 0 | 0 | 0 |
| PSR | 1.3 | 1.4 | 1.3 | 1.3 | 1.3 | 1.3 | 1.3 | 1.3 | 1.3 | 1.3 | 1.3 |
| OSR | 1.4 | 1.4 | 1.4 | 1.4 | 1.4 | 1.4 | 1.4 | 1.4 | 1.3 | 1.3 | 1.3 |
| NOx, 0% O2 | 1193.2 | 1045.7 | 1042.0 | 1225.0 | 1047.3 | 1198.2 | 1197.7 | 1071.6 | 1138.1 | 1132.6 | 1147.9 |
| NOx, lb/ton | 4.6 | 4.0 | 4.0 | 4.7 | 4.0 | 4.6 | 4.6 | 4.1 | 4.4 | 4.4 | 4.4 |
| CO, 0% O2 | 11.5 | 239.1 | 87.2 | 12.7 | 345.5 | 8.0 | 11.2 | 216.5 | 148.1 | 147.9 | 12.4 |

| | 29-Apr | 23-Sep | 23-Sep | 23-Sep | 23-Sep | 23-Sep | 23-Sep | 23-Sep | 23-Sep | 23-Sep | 23-Sep |
|---|---|---|---|---|---|---|---|---|---|---|---|
| Time | 19:21 | 9:15 | 9:43 | 10:43 | 10:57 | 11:11 | 11:24 | 11:45 | 11:55 | 12:13 | 12:24 |
| Firing Side | L | R | L | L | L | R | R | L | L | R | R |
| Injection Location | 2- Under Full Furnace Testing | | | | | | | | | | |
| Sample Location | Port 5 | Stack | Stack | R1 | R2 | L1 | L2 | R3 | R4 | L3 | L4 |
| O2, % | 7.84 | 8.28 | 6.49 | 1.58 | 3.41 | 1.75 | 1.81 | 3.06 | 1.7 | 0.16 | 1.19 |
| CO, ppm | 8 | 9 | 3 | 24 | 13 | 19 | 21 | 16 | 84 | 1229 | 450 |
| CO2, % | NA | 10.3 | 10.1 | 14.6 | 13 | 14 | 13.5 | 12.8 | 13.3 | 14.4 | 14 |
| NOx, ppm | 825 | 431 | 465 | 524 | 577 | 574 | 582 | 710 | 660 | 510 | 458 |
| Staging | no | no | no | no | no | no | no | no | no | no | no |
| Staging O2 | 0 | 0 | 0 | 0 | 0 | 0 | 0 | 0 | 0 | 0 | 0 |
| Staging Air | 0 | 0 | 0 | 0 | 0 | 0 | 0 | 0 | 0 | 0 | 0 |
| PSR | 1.3 | 1.11 | 1.11 | 1.11 | 1.12 | 1.11 | 1.11 | 1.10 | 1.11 | 1.11 | 1.10 |
| OSR | 1.3 | 1.11 | 1.11 | 1.11 | 1.12 | 1.11 | 1.11 | 1.10 | 1.11 | 1.11 | 1.10 |
| NOx, 0% O2 | 1316.5 | 614.88 | 672.98 | 566.63 | 688.86 | 626.18 | 636.89 | 831.10 | 718.13 | 513.92 | 485.51 |
| NOx, lb/ton | 5.1 | 2.21 | 2.41 | 2.03 | 2.47 | 2.25 | 2.28 | 2.98 | 2.58 | 1.84 | 1.74 |
| CO, 0% O2 | 12.8 | 12.84 | 4.34 | 25.95 | 15.52 | 20.73 | 22.98 | 18.73 | 91.40 | 1238.44 | 477.03 |

| | 23-Sep | 23-Sep | 23-Sep | 23-Sep | 23-Sep | 23-Sep | 23-Sep | 23-Sep | 23-Sep | 23-Sep | 24-Sep |
|---|---|---|---|---|---|---|---|---|---|---|---|
| Time | 12:41 | 12:56 | 13:12 | 13:24 | 13:49 | 14:22 | 14:43 | 14:53 | 15:15 | 15:49 | 9:45 |
| Firing Side | L | L | R | R | L | R | L | L | R | L | L |
| Sample Location | R5 | R6 | L5 | L6 | Stack | Stack | Stack | Stack | Stack | Stack | Stack |
| O2, % | 0.32 | 0.55 | 2.75 | 0.36 | 5.5 | 5.38 | 5.3 | 5.56 | 5.95 | 6.2 | 6.35 |
| CO, ppm | 400 | 100 | 13 | 1221 | 300 | 876 | 1000 | 150 | 30 | 2 | 3 |
| CO2, % | 13.8 | 13.2 | NA | NA | NA | NA | NA | NA | NA | NA | |
| NOx, ppm | 472 | 420 | 494 | 440 | 311 | 311 | 285 | 355 | 400 | 436 | 436 |
| Staging | no | no | no | no | no | no | no | no | no | no | no |
| Staging O2 | 0 | 0 | 0 | 0 | 0 | 0 | 0 | 0 | 0 | 0 | 0 |
| Staging Air | 0 | 0 | 0 | 0 | 0 | 0 | 0 | 0 | 0 | 0 | 0 |
| PSR | 1.11 | 1.11 | 1.10 | 1.10 | 1.04 | 1.05 | 1.03 | 1.07 | 1.13 | 1.13 | 1.12 |
| OSR | 1.11 | 1.11 | 1.10 | 1.10 | 1.04 | 1.05 | 1.03 | 1.07 | 1.13 | 1.13 | 1.12 |
| NOx, 0% O2 | 479.30 | 431.30 | 568.44 | 447.67 | 421.35 | 418.12 | 381.21 | 482.84 | 558.14 | 618.65 | 624.98 |
| NOx, lb/ton | 1.72 | 1.55 | 2.04 | 1.61 | 1.51 | 1.50 | 1.37 | 1.73 | 2.00 | 2.22 | 2.22 |
| CO, 0% O2 | 406.19 | 102.69 | 14.96 | 1242.30 | 406.45 | 1177.72 | 1337.53 | 204.02 | 41.86 | 2.84 | 4.30 |

| | 24-Sep | 24-Sep | 24-Sep | 24-Sep | 24-Sep | 24-Sep | 24-Sep | 24-Sep | 24-Sep | 24-Sep | 24-Sep |
|---|---|---|---|---|---|---|---|---|---|---|---|
| Time | 10:18 | 10:33 | 10:39 | 10:42 | 10:49 | 10:53 | 10:58 | 11:07 | 11:10 | 11:14 | 11:18 |
| Firing Side | R | L | L | L | L | L | L | R | R | R | R |
| Sample Location | Stack | R1 | R2 | R3 | R4 | R5 | R6 | L1 | L2 | L3 | L4 |
| O2, % | 6.17 | 0.7 | 0.83 | 2.36 | 0.48 | 0.03 | 0 | 0.3 | 0.4 | 0.18 | 0.2 |
| CO, ppm | 43 | 120 | 60 | 15 | 982 | over | >1230 | >1230 | >1230 | >1230 | >1230 |
| CO2, % | 10.3 | 15 | 14.4 | 13.3 | 13.7 | 12.7 | 12.8 | 14.5 | 14 | 13.8 | 13.3 |
| NOx, ppm | 400 | 420 | 480 | 583 | 497 | 355.8 | 280 | 450 | 500 | 435 | 371 |
| Staging | no | no | no | no | no | no | no | no | no | no | no |
| Staging O2 | 0 | 0 | 0 | 0 | 0 | 0 | 0 | 0 | 0 | 0 | 0 |
| Staging Air | 0 | 0 | 0 | 0 | 0 | 0 | 0 | 0 | 0 | 0 | 0 |
| PSR | 1.12 | 1.04 | 1.05 | 1.04 | 1.04 | 1.04 | 1.04 | 1.04 | 1.04 | 1.04 | 1.04 |
| OSR | 1.12 | 1.04 | 1.05 | 1.04 | 1.04 | 1.04 | 1.04 | 1.04 | 1.04 | 1.04 | 1.04 |
| NOx, 0% O2 | 568.42 | 434.48 | 499.75 | 656.81 | 508.63 | 356.31 | 279.73 | 456.52 | 509.71 | 438.76 | 374.57 |
| NOx, lb/ton | 2.01 | 1.54 | 1.77 | 2.33 | 1.80 | 1.26 | 0.99 | 1.62 | 1.81 | 1.56 | 1.33 |
| CO, 0% O2 | 60.89 | 124.14 | 62.47 | 16.90 | 1004.97 | NA | NA | NA | NA | NA | NA |

| | 24-Sep | 24-Sep | 24-Sep | 24-Sep | 24-Sep | 24-Sep | 24-Sep | 24-Sep | 24-Sep | 24-Sep | 24-Sep |
|---|---|---|---|---|---|---|---|---|---|---|---|
| Time | 11:21 | 11:27 | 15:38 | 16:04 | 16:25 | 16:29 | 16:32 | 16:37 | 16:42 | 16:46 | 16:54 |
| Firing Side | R | R | L | R | L | L | L | L | L | L | R |
| Sample Location | L5 | L6 | Stack | Stack | R1 | R2 | R3 | R4 | R5 | R6 | L1 |
| O2, % | 1.1 | 0.21 | 6.35 | 5.96 | 2.02 | 3.1 | 3.06 | 1 | 0.29 | 0.2 | 1.58 |
| CO, ppm | 400 | >1230 | 80 | 187 | 17 | 14 | 13 | 300 | >1200 | >1200 | 21 |
| CO2, % | 13.3 | 12.2 | 10.8 | 10.9 | 14.6 | 13.6 | 13.2 | 14.6 | 14.5 | 14.8 | 15.2 |
| NOx, ppm | 411 | 307 | 320 | 304 | 413 | 458 | 536 | 480 | 365 | 345 | 421 |
| Staging | no | no | yes | yes | yes | yes | yes | yes | yes | yes | yes |
| Staging O2 | 0 | 0 | 4891 | 4891 | 4891 | 4891 | 4891 | 4891 | 4891 | 4891 | 4891 |
| Staging Air | 0 | 0 | 21118 | 21118 | 21118 | 21118 | 21118 | 21118 | 21118 | 21118 | 21118 |
| PSR | 1.04 | 1.04 | 1.02 | 1.02 | 1.02 | 1.02 | 1.02 | 1.02 | 1.02 | 1.02 | 1.02 |
| OSR | 1.04 | 1.04 | 1.12 | 1.12 | 1.12 | 1.12 | 1.12 | 1.12 | 1.12 | 1.12 | 1.13 |
| NOx, 0% O2 | 433.72 | 310.10 | 458.70 | 424.47 | 456.95 | 537.32 | 627.42 | 504.00 | 370.11 | 348.32 | 455.25 |
| NOx, lb/ton | 1.54 | 1.10 | 1.56 | 1.44 | 1.55 | 1.83 | 2.13 | 1.71 | 1.26 | 1.19 | 1.55 |
| CO, 0% O2 | 422.11 | NA | 114.68 | 261.10 | 18.81 | 16.42 | 15.22 | 315.00 | NA | NA | 22.71 |

| | 24-Sep | 24-Sep | 24-Sep | 24-Sep | 24-Sep | 24-Sep | 24-Sep | 25-Sep | 25-Sep | 25-Sep | 25-Sep |
|---|---|---|---|---|---|---|---|---|---|---|---|
| Time | 16:58 | 17:03 | 17:08 | 17:12 | 17:19 | 17:30 | 18:01 | 9:25 | 9:27 | 9:51 | 9:55 |
| Firing Side | R | R | R | R | R | L | R | R | L | R | R |
| Sample Location | L2 | L3 | L4 | L5 | L6 | Stack | Stack | Stack | Stack | L1 | L2 |
| O2, % | 1.13 | 0.21 | 0.45 | 2.4 | 0.42 | 6.19 | 6.1 | 6.89 | 6.84 | 2.44 | 1.74 |
| CO, ppm | 150 | >1205 | >1205 | 24 | >1205 | 22 | 32 | 3.68 | 3 | 14 | 18 |
| CO2, % | 14.6 | 15 | 14.4 | 13.2 | 13.5 | 10 | 10.1 | 9.81 | 10 | 14.1 | 13.9 |
| NOx, ppm | 495 | 411 | 404 | 411 | 335 | 444 | 397 | 400 | 491 | 465.1 | 485.3 |
| Staging | yes | yes | yes | yes | yes | no | no | no | no | yes | yes |
| Staging O2 | 4891 | 4891 | 4891 | 4891 | 4891 | 0 | 0 | 0 | 0 | 5602 | 5981 |
| Staging Air | 21118 | 21118 | 21118 | 21118 | 21118 | 0 | 0 | 0 | 0 | 22809 | 24351 |
| PSR | 1.02 | 1.02 | 1.02 | 1.02 | 1.02 | 1.13 | 1.13 | NA | 1.16 | 1.02 | 1.02 |
| OSR | 1.13 | 1.13 | 1.13 | 1.13 | 1.13 | 1.13 | 1.13 | NA | 1.16 | 1.14 | 1.14 |
| NOx, 0% O2 | 523.15 | 415.15 | 412.85 | 464.03 | 341.84 | 629.57 | 559.53 | 595.32 | 728.18 | 528.24 | 529.14 |
| NOx, lb/ton | 1.78 | 1.41 | 1.40 | 1.58 | 1.16 | 2.23 | 1.98 | NA | 2.49 | 1.76 | 1.76 |
| CO, 0% O2 | 158.53 | NA | NA | 27.10 | NA | 31.20 | 45.10 | 5.45 | 4.45 | 15.84 | 19.63 |

| | 25-Sep | 25-Sep | 25-Sep | 25-Sep | 25-Sep | 25-Sep | 25-Sep | 25-Sep | 25-Sep | 25-Sep | 25-Sep |
|---|---|---|---|---|---|---|---|---|---|---|---|
| Time | 9:59 | 10:03 | 10:07 | 10:11 | 10:22 | 10:25 | 10:30 | 10:35 | 10:38 | 10:43 | 10:55 |
| Firing Side | R | R | R | R | L | L | L | L | L | L | R |
| Sample Location | L3 | L4 | L5 | L6 | R1 | R2 | R3 | R4 | R5 | R6 | L1 |
| O2, % | 0.75 | 1.05 | 3 | 0.81 | 2.3 | 3.18 | 3.54 | 2 | 0.29 | 0.91 | 2.7 |
| CO, ppm | over | 538 | 18 | over | 11 | 11 | 11 | 81 | 968 | 61 | 13 |
| CO2, % | 14.9 | 14.1 | 12.8 | 13.6 | 13.9 | 12.8 | 13 | 13.2 | 14 | 13.4 | 13.9 |
| NOx, ppm | 452.4 | 450.2 | 401.3 | 359 | 421 | 5.11 | 609 | 580 | 485 | 460.3 | 470 |
| Staging | yes | yes | yes | yes | yes | yes | yes | yes | yes | yes | yes |
| Staging O2 | 5590 | 5898 | 5614 | 5697 | 5673 | 5721 | 5744 | 5803 | 5780 | 5602 | 5732 |
| Staging Air | 22761 | 24014 | 22857 | 23195 | 23098 | 23291 | 23388 | 23628 | 23532 | 22809 | 23339 |
| PSR | 1.02 | 1.02 | 1.02 | 1.02 | 1.02 | 1.02 | 1.02 | 1.02 | 1.02 | 1.02 | 1.02 |
| OSR | 1.14 | 1.14 | 1.14 | 1.14 | 1.14 | 1.14 | 1.14 | 1.14 | 1.14 | 1.14 | 1.14 |
| NOx, 0% O2 | 469.16 | 473.89 | 468.18 | 373.40 | 472.78 | 6.02 | 732.47 | 641.05 | 491.79 | 481.15 | 539.34 |
| NOx, lb/ton | 1.57 | 1.58 | 1.56 | 1.25 | 1.58 | 0.02 | 2.44 | 2.14 | 1.64 | 1.61 | 1.80 |
| CO, 0% O2 | NA | 584.21 | 21.00 | NA | 12.35 | 12.96 | 13.23 | 67.42 | 981.55 | 63.76 | 14.92 |
| Air, SCFH | 414500 | 414400 | 414400 | 414400 | 414100 | 414900 | 415900 | 415000 | 415500 | 415900 | 415500 |

| | 25-Sep | 25-Sep | 25-Sep | 25-Sep | 25-Sep | 25-Sep | 25-Sep | 25-Sep | 25-Sep | 25-Sep | 25-Sep | 25-Sep |
|---|---|---|---|---|---|---|---|---|---|---|---|---|
| Time | 11:02 | 11:09 | 11:21 | 11:29 | 11:38 | 11:53 | 12:23 | 12:24 | 12:31 | 12:35 | 12:40 | 12:43 |
| Firing Side | R | R | L | L | L | R | L | L | L | L | L | L |
| Sample Location | L1 | L1 | R1 | R1 | R1 | L1 | R1 | R2 | R3 | R4 | R5 | R6 |
| O2, % | 2.7 | 2.53 | 1.71 | 2.34 | 2.05 | 2.11 | 1.3 | 2.9 | 4.09 | 1.9 | 0.56 | 0.85 |
| CO, ppm | 13 | 14 | 45 | 13 | 13 | 14 | 30 | 8 | 8 | 15 | 275 | 38 |
| CO2, % | 13.6 | 13.9 | 13.5 | 13.4 | 13.5 | 13.1 | 13.6 | 12.5 | 11.9 | 12.5 | 13.4 | 13.2 |
| NOx, ppm | 448 | 454 | 408 | 440 | 405 | 475 | 387 | 500 | 580 | 552 | 462 | 481 |
| Staging | yes | yes | yes | yes | yes | no | no | yes | yes | yes | yes | yes |
| Staging O2 | 5744 | 5839 | 5496 | 5863 | 6099 | 0 | 0 | 6159 | 6064 | 5948 | 6135 | 6028 |
| Staging Air | 23388 | 23773 | 22375 | 23869 | 24833 | 0 | 0 | 25074 | 24689 | 24207 | 24978 | 24544 |
| PSR | 1.02 | 1.02 | 1.02 | 1.02 | 1.02 | 1.02 | 1.01 | 1.02 | 1.02 | 1.02 | 1.02 | 1.02 |
| OSR | 1.14 | 1.14 | 1.14 | 1.14 | 1.14 | 1.02 | 1.01 | 1.14 | 1.14 | 1.14 | 1.14 | 1.14 |
| NOx, 0% O2 | 514.10 | 518.19 | 444.17 | 495.18 | 448.31 | 528.06 | 412.54 | 580.11 | 720.28 | 606.91 | 474.66 | 501.29 |
| NOx, lb/ton | 1.72 | 1.72 | 1.49 | 1.65 | 1.49 | 1.85 | 1.45 | 1.93 | 2.40 | 2.02 | 1.58 | 1.67 |
| CO, 0% O2 | 14.92 | 15.92 | 48.99 | 14.63 | 14.41 | 15.58 | 31.98 | 9.28 | 9.93 | 16.49 | 282.53 | 39.60 |

| | 25-Sep | 25-Sep | 25-Sep | 25-Sep | 25-Sep | 25-Sep | 25-Sep | 25-Sep | 25-Sep | 25-Sep | 25-Sep | 25-Sep |
|---|---|---|---|---|---|---|---|---|---|---|---|---|
| Time | 12:50 | 12:54 | 13:00 | 13:04 | 13:08 | 13:12 | 13:23 | 13:31 | 13:40 | 13:50 | 14:06 | 14:56 |
| Firing Side | R | R | R | R | R | R | L | L | L | R | R | R |
| Sample Location | L1 | L2 | L3 | L4 | L5 | L6 | R2 | R2 | R2 | L2 | L5 | L5 |
| O2, % | 1.42 | 1.35 | 1 | 1.22 | 2.43 | 0.4 | 2.78 | 2.98 | 2.65 | 1.4 | 1.94 | 2.3 |
| CO, ppm | 20 | 27 | 77 | 167 | 21 | over | 8 | 10 | 12 | 98 | 33 | 18 |
| CO2, % | 13.6 | 13.4 | 13.6 | 13.4 | 12.5 | 12.8 | 12.5 | 12.6 | 12.5 | 13.3 | 11.9 | 14 |
| NOx, ppm | 445 | 487 | 475 | 429 | 438 | 380 | 478 | 508 | 510 | 498 | 448 | 436 |
| Staging | yes | yes | yes | yes | yes | yes | yes | yes | yes | yes | yes | yes |
| Staging O2 | 6099 | 6123 | 6088 | 6265 | 6313 | 6135 | 6076 | 5732 | 6135 | 6064 | 5803 | 5875 |
| Staging Air | 24833 | 24930 | 24785 | 25508 | 25701 | 24978 | 24737 | 23339 | 24978 | 24689 | 23628 | 23918 |
| PSR | 1.02 | 1.02 | 1.02 | 1.02 | 1.02 | 1.02 | 1.02 | 1.02 | 1.02 | 1.02 | 1.02 | 1.02 |
| OSR | 1.14 | 1.14 | 1.14 | 1.14 | 1.14 | 1.14 | 1.14 | 1.14 | 1.14 | 1.14 | 1.14 | 1.14 |
| NOx, 0% O2 | 477.27 | 520.46 | 498.75 | 455.48 | 495.32 | 387.38 | 550.93 | 592.01 | 583.65 | 533.57 | 493.60 | 489.63 |
| NOx, lb/ton | 1.59 | 1.73 | 1.56 | 1.51 | 1.54 | 1.29 | 1.83 | 1.98 | 1.94 | 1.78 | 1.65 | 1.63 |
| CO, 0% O2 | 21.45 | 28.85 | 80.85 | 177.30 | 23.75 | NA | 9.22 | 11.65 | 13.73 | 105.00 | 36.38 | 20.21 |

| | 25-Sep | 25-Sep | 25-Sep | 25-Sep | 25-Sep | 25-Sep | 25-Sep | 25-Sep | 25-Sep | 25-Sep | 25-Sep | 26-Sep |
|---|---|---|---|---|---|---|---|---|---|---|---|---|
| Time | 15:03 | 15:10 | 15:15 | 15:51 | 15:59 | 16:24 | 16:41 | 16:56 | 17:12 | 17:32 | 17:56 | 9:14 |
| Firing Side | R | R | R | R | R | L | L | R | R | L | R | R |
| Sample Location | L6 | L4 | L3 | Stack | Stack | Stack | Stack | Stack | Stack | Stack | Stack | Stack |
| O2, % | 0.49 | 1.1 | 1.2 | 6.29 | 6.34 | 6.61 | 6.71 | 6.31 | 5.7 | 6.82 | 6.68 | 6.5 |
| CO, ppm | over | 110 | 289 | 9 | 16 | 4 | 4 | 11 | 586 | 4 | 22 | 10 |
| CO2, % | 15 | 14.6 | 14.7 | 10.4 | 10.4 | 10.3 | 10.1 | 10.5 | 10.7 | 9.9 | 9.9 | 10 |
| NOx, ppm | 450 | 440 | 485 | 370 | 348 | 414 | 405 | 357 | 293 | 470 | 384 | 420 |
| Staging | yes | yes | yes | yes | yes | yes | yes | yes | no | no | no | no |
| Staging O2 | 5638 | 5685 | 5732 | 5626 | 5780 | 5046 | 5638 | 5614 | 0 | 0 | 0 | 0 |
| Staging Air | 22954 | 23147 | 23339 | 22906 | 23532 | 20544 | 22954 | 22857 | 0 | 0 | 0 | 0 |
| PSR | 1.02 | 1.02 | 1.02 | 1.02 | 1.02 | 1.02 | 1.02 | 1.02 | 1.03 | 1.13 | 1.13 | 1.16 |
| OSR | 1.14 | 1.14 | 1.14 | 1.14 | 1.14 | 1.14 | 1.14 | 1.14 | 1.03 | 1.13 | 1.13 | 1.16 |
| NOx, 0% O2 | 460.75 | 464.32 | 514.39 | 528.21 | 498.50 | 604.17 | 595.17 | 510.35 | 402.16 | 696.05 | 563.13 | 608.30 |
| NOx, lb/ton | 1.54 | 1.55 | 1.72 | 1.76 | 1.66 | 2.03 | 1.99 | 1.71 | 1.41 | 2.44 | 1.97 | 2.18 |
| CO, 0% O2 | NA! | 116.08 | 306.52 | 12.85 | 22.92 | 5.84 | 5.88 | 15.72 | 804.31 | 5.92 | 32.26 | 14.48 |

| | 26-Sep | 26-Sep | 26-Sep | 26-Sep | 26-Sep | 26-Sep | 26-Sep | 26-Sep | 26-Sep | 26-Sep | 26-Sep | 26-Sep |
|---|---|---|---|---|---|---|---|---|---|---|---|---|
| Time | 9:26 | 10:07 | 10:22 | 10:31 | 12:21 | 11:02 | 11:53 | 12:06 | 12:30 | 12:35 | 12:54 | 13:03 |
| Firing Side | L | R | L | L | L | R | R | R | L | L | R | R |
| Sample Location | Stack | Stack | Stack | Stack | Stack | Stack | Stack | Stack | Stack | Stack | Stack | Stack |
| O2, % | 6.47 | 6.16 | 6.4 | 6.34 | 6.43 | 6.16 | 6.31 | 6.2 | 6.7 | 6.69 | 6.32 | 6.29 |
| CO, ppm | 5 | 250 | 3 | 5 | 7 | 280 | 275 | 225 | 5 | 4 | 135 | 180 |
| CO2, % | 10 | 10.3 | 10.1 | 10 | 9.7 | 9.8 | 9.8 | 9.8 | 9.6 | 9.6 | 9.7 | 9.7 |
| NOx, ppm | 535 | 370 | 440 | 370 | 420 | 340 | 350 | 355 | 415 | 396 | 381 | 354 |
| Staging | no | yes | yes | yes | yes | yes | yes | yes | yes | yes | yes | yes |
| Staging O2 | 0 | 4934 | 5064 | 4922 | 5649 | 4934 | 5568 | 5459 | 5578 | 5720 | 5542 | 5684 |
| Staging Air | 0 | 20089 | 20620 | 20041 | 22998 | 20089 | 22661 | 22227 | 22709 | 23287 | 22564 | 23143 |
| PSR | 1.16 | 1.03 | 1.03 | 1.03 | 1.02 | 1.03 | 1.03 | 1.03 | 1.03 | 1.02 | 1.03 | 1.02 |
| OSR | 1.16 | 1.13 | 1.13 | 1.13 | 1.14 | 1.13 | 1.14 | 1.14 | 1.14 | 1.14 | 1.14 | 1.14 |
| NOx, 0% O2 | 773.23 | 523.58 | 632.88 | 530.01 | 605.35 | 481.13 | 500.34 | 503.72 | 609.44 | 581.13 | 545.03 | 505.37 |
| NOx, lb/ton | 2.77 | 1.80 | 2.18 | 1.83 | 2.07 | 1.56 | 1.71 | 1.73 | 2.09 | 1.99 | 1.87 | 1.73 |
| CO, 0% O2 | 7.23 | 353.77 | 4.32 | 7.16 | 10.09 | 396.23 | 393.12 | 319.26 | 7.34 | 5.87 | 193.12 | 256.97 |
| | | | | | | | | Note 1 | Note 2 | Note 3 | Note 4 | Note 5 |

| | 26-Sep | 26-Sep | 26-Sep | 26-Sep | 26-Sep | 26-Sep | 26-Sep | 26-Sep | 26-Sep | 26-Sep | 26-Sep | 26-Sep |
|---|---|---|---|---|---|---|---|---|---|---|---|---|
| Time | 13:12 | 13:21 | 13:33 | 13:50 | 13:59 | 14:04 | 14:09 | 14:32 | 14:53 | 15:00 | 15:04 | 15:30 |
| Firing Side | R | L | L | R | R | R | R | L | R | R | R | L |
| Sample Location | Stack | Stack | Stack | Stack | L5 | L6 | L4 | Stack | L5 | L5 | L6 | Stack |
| O2, % | 6.29 | 6.53 | 6.59 | 6.13 | 2.94 | 0.4 | 1.56 | 6.74 | 1.21 | 2.01 | 0.56 | 6.22 |
| CO, ppm | 280 | 5 | 5 | 166 | 18 | over | 180 | 3 | 250 | 45 | over | 5 |
| CO2, % | 9.6 | 9.6 | 9.6 | 9.7 | 11.8 | 13.1 | 13.3 | 9.7 | 12.7 | 12.3 | 11.8 | 9.7 |
| NOx, ppm | 336 | 423 | 412 | 364 | 420 | 410 | 412 | 395 | 397 | 395 | 320 | 358 |
| Staging | yes | yes | yes | yes | yes | yes | yes | yes | yes | yes | yes | yes |
| Staging O2 | 5649 | 5720 | 5743 | 5637 | 5672 | 5767 | 5576 | 8343 | 5353 | 5376 | 5294 | 5768 |
| Staging Air | 22998 | 23287 | 23384 | 22950 | 23095 | 23480 | 22709 | 12083 | 21793 | 21890 | 21552 | 8353 |
| PSR | 1.02 | 1.02 | 1.02 | 1.02 | 1.02 | 1.02 | 1.03 | 1.02 | 1.03 | 1.03 | 1.03 | 1.03 |
| OSR | 1.14 | 1.14 | 1.14 | 1.14 | 1.14 | 1.14 | 1.14 | 1.14 | 1.14 | 1.14 | 1.14 | 1.11 |
| NOx, 0% O2 | 479.67 | 613.89 | 600.42 | 514.06 | 488.37 | 417.96 | 445.06 | 581.70 | 421.27 | 436.81 | 328.77 | 508.66 |
| NOx, lb/ton | 1.64 | 2.10 | 2.05 | 1.76 | 1.67 | 1.43 | 1.53 | 1.95 | 1.45 | 1.50 | 1.13 | 1.74 |
| CO, 0% O2 | 399.73 | 7.26 | 7.29 | 234.43 | 20.93 | NA | 194.44 | 4.42 | 265.29 | 49.76 | NA | 7.10 |
| | Note 6 | Note 7 | Note 8 | Note 9 | Note 10 | Note 11 | Note 12 | Note 13 | Note 14 | Note 15 | Note 16 | Note 17 |

| | 26-Sep | 26-Sep | 26-Sep | 26-Sep | 26-Sep | 26-Sep | 26-Sep | 26-Sep | 26-Sep | 27-Sep | 27-Sep | 27-Sep |
|---|---|---|---|---|---|---|---|---|---|---|---|---|
| Time | 15:52 | 14:18 | 15:58 | 16:07 | 17:20 | 17:50 | 17:55 | 18:04 | 18:09 | 8:39 | 9:10 | 9:37 |
| Firing Side | R | L | R | R | L | R | R | R | R | L | R | L |
| Sample Location | L6 | Stack | L6 | L6 | Stack | L6 | L5 | L6 | Stack | Stack | Stack | Stack |
| O2, % | 0.54 | 6.54 | 0.74 | 0.78 | 6.4 | 0.93 | 4 | 2.36 | 6.68 | 6.55 | 6.64 | 6.68 |
| CO, ppm | over | 4 | over | over | 0 | over | 10 | | 1 | 2 | 45 | 3 |
| CO2, % | 12.1 | 9.7 | 12.6 | 13 | 9.3 | 12.5 | 11.2 | 12.3 | 9.3 | 10.2 | 10.1 | 10.3 |
| NOx, ppm | 380 | 407 | 430 | 510 | 420 | 410 | 400 | 380 | 350 | 538 | 400 | 459 |
| Staging | yes | yes | yes | yes | yes | yes | yes | yes | yes | no | no | yes |
| Staging O2 | 5234 | 7672 | 5282 | 5175 | 5270 | 5317 | 5436 | 5436 | 5471 | 0 | 0 | 6235 |
| Staging Air | 21311 | 15025 | 21504 | 21070 | 21456 | 21649 | 22131 | 22131 | 22275 | 0 | 0 | 25386 |
| PSR | 1.03 | 1.02 | 1.03 | 1.03 | 1.03 | 1.03 | 1.03 | 1.03 | 1.03 | 1.15 | 1.14 | 1.02 |
| OSR | 1.14 | 1.14 | 1.14 | 1.14 | 1.14 | 1.14 | 1.14 | 1.14 | 1.14 | 1.15 | 1.14 | 1.14 |
| NOx, 0% O2 | 369.50 | 591.08 | 445.71 | 529.67 | 604.11 | 429.00 | 494.12 | 428.1 | 513.3 | 781.9 | 585.0 | 673.1 |
| NOx, lb/ton | 1.27 | 1.99 | 1.53 | 1.82 | 2.08 | 1.47 | 1.70 | 1.5 | 1.8 | 2.8 | 2.1 | 2.3 |
| CO, 0% O2 | NA | 5.81 | NA | NA | 0 | NA | 12.35 | 0.0 | 1.5 | 2.9 | 65.8 | 4.4 |
| | Note 18 | | Note 19 | Note 20 | | | | Note 21 | Note 22 | | | |

| | 27-Sep | 27-Sep | 27-Sep | 27-Sep | 27-Sep | 27-Sep | 27-Sep | 27-Sep | 27-Sep | 27-Sep | 27-Sep | 27-Sep |
|---|---|---|---|---|---|---|---|---|---|---|---|---|
| Time | 9:45 | 10:05 | 10:20 | 10:43 | 11:13 | 11:24 | 11:43 | 11:52 | 12:05 | 12:08 | 12:11 | 12:14 |
| Firing Side | L | R | R | L | R | R | L | L | R | R | R | R |
| Sample Location | Stack | Stack | Stack | Stack | Stack | Stack | Stack | Stack | L6 | L5 | L4 | L3 |
| O2, % | 6.64 | 6.69 | 6.51 | 6.89 | 6.51 | 6.4 | 6.46 | 6.35 | 1.12 | 3.99 | 1.65 | 0.85 |
| CO, ppm | 3 | 3 | 3 | 4 | 10 | 33 | 3 | 3 | over | 15 | 80 | 600 |
| CO2, % | 10.2 | 10 | 10 | 9.6 | 9.7 | 9.6 | 9.6 | 9.7 | 12.4 | 11.3 | 12.3 | 13.3 |
| NOx, ppm | 445 | 350 | 340 | 437 | 341 | 335 | 429 | 410 | 275 | 346 | 387 | 442 |
| Staging | yes | yes | yes | yes | yes | yes | yes | yes | yes | yes | yes | yes |
| Staging O2 | 5645 | 5797 | 5597 | 4912 | 5114 | 4689 | 4701 | 4004 | 4685 | 4618 | 4819 | 4654 |
| Staging Air | 22982 | 23603 | 22790 | 20001 | 20820 | 19092 | 19140 | 16303 | 18995 | 18802 | 19622 | 18947 |
| PSR | 1.02 | 1.02 | 1.02 | 1.02 | 1.02 | 1.02 | 1.02 | 1.02 | 1.02 | 1.02 | 1.02 | 1.02 |
| OSR | 1.13 | 1.14 | 1.13 | 1.12 | 1.12 | 1.11 | 1.11 | 1.1 | 1.11 | 1.11 | 1.11 | 1.11 |
| NOx, 0% O2 | 850.8 | 513.6 | 492.8 | 650.4 | 494.2 | 481.8 | 619.6 | 587.7 | 290.5 | 427.2 | 420.0 | 460.6 |
| NOx, lb/ton | 2.2 | 1.7 | 1.7 | 2.2 | 1.7 | 1.6 | 2.1 | 2.0 | 1.0 | 1.5 | 1.4 | 1.6 |
| CO, 0% O2 | 4.4 | 4.4 | 4.3 | 6.0 | 14.5 | 47.5 | 4.3 | 4.3 | NA | 18.5 | 86.8 | 625.3 |

| | 27-Sep | 27-Sep | 27-Sep | 27-Sep | 27-Sep | 27-Sep | 27-Sep | 27-Sep | 27-Sep | 27-Sep | 27-Sep | 27-Sep |
|---|---|---|---|---|---|---|---|---|---|---|---|---|
| Time | 12:18 | 12:18 | 12:24 | 12:31 | 12:40 | 12:50 | 13:09 | 13:21 | 13:24 | 13:28 | 13:40 | 13:59 |
| Firing Side | R | R | R | R | L | L | R | R | R | R | L | L |
| Sample Location | L2 | L1 | L6 | L6 | Stack | Stack | L5 | L5 | L6 | Stack | Stack | Stack |
| O2, % | 1.8 | 1.8 | 1.62 | 1.2 | 6.25 | 6.25 | 2.75 | 3.55 | 1.37 | 6.11 | 6.01 | 5.95 |
| CO, ppm | 45 | 22 | over | over | 4 | 4 | 15 | 16 | 500 | 40 | 5 | 27 |
| CO2, % | 12.8 | 13.3 | 12.9 | 13.2 | 9.7 | 9.7 | 11.9 | 11.6 | 12.9 | 9.9 | 9.8 | 9.7 |
| NOx, ppm | 502 | 462 | 294 | 330 | 410 | 397 | 370 | 435 | 410 | 340 | 387 | 363 |
| Staging | yes | yes | yes | yes | yes | yes | yes | yes | yes | yes | yes | yes |
| Staging O2 | 4819 | 4689 | 4843 | 4689 | 5748 | 5942 | 4867 | 4926 | 4879 | 4890 | 4077 | 3202 |
| Staging Air | 19622 | 19092 | 19718 | 19092 | 11257 | 8605 | 19814 | 20055 | 19863 | 19911 | 16598 | 13038 |
| PSR | 1.02 | 1.02 | 1.02 | 1.02 | 1.02 | 1.02 | 1.02 | 1.02 | 1.02 | 1.02 | 1.02 | 1.02 |
| OSR | 1.11 | 1.11 | 1.11 | 1.11 | 1.1 | 1.1 | 1.11 | 1.11 | 1.11 | 1.11 | 1.09 | 1.08 |
| NOx, 0% O2 | 549.1 | 505.3 | 318.6 | 350.0 | 583.7 | 565.2 | 425.8 | 523.5 | 438.6 | 479.5 | 542.2 | 506.5 |
| NOx, lb/ton | 1.9 | 1.7 | 1.1 | 1.2 | 2.0 | 1.9 | 1.4 | 1.8 | 1.5 | 1.6 | 1.9 | 1.7 |
| CO, 0% O2 | 49.2 | 24.1 | NA | NA | 5.7 | 5.7 | 17.3 | 19.3 | 534.9 | 58.4 | 7.0 | 37.7 |
| | | | Note 23 | Note 24 | Note 25 | Note 26 | Note 27 | Note 28 | Note 29 | Note 30 | Note 31 | |

| | 27-Sep | 27-Sep | 27-Sep | 27-Sep | 27-Sep | 27-Sep | 27-Sep | 27-Sep | 27-Sep | 27-Sep | 27-Sep | 27-Sep |
|---|---|---|---|---|---|---|---|---|---|---|---|---|
| Time | 14:14 | 14:19 | 14:21 | 14:24 | 14:26 | 14:27 | 14:31 | 14:41 | 14:45 | 14:48 | 14:52 | 14:56 |
| Firing Side | R | R | R | R | R | R | R | L | L | L | L | L |
| Sample Location | Stack | L5 | L4 | L3 | L6 | L2 | L1 | R1 | R2 | R3 | R4 | R5 |
| O2, % | 5.91 | 3.1 | 1.36 | 0.41 | 1.54 | 1.12 | 1.3 | 1.35 | 1.4 | 2.7 | 2 | 0.5 |
| CO, ppm | 91 | 30 | 227 | over | 529 | over | 40 | 28 | 80 | 20 | 40 | 900 |
| CO2, % | 9.7 | 11.9 | 13.1 | 13.1 | 13.1 | 13.4 | 13.4 | 13.5 | 13.1 | 12.5 | 12.4 | 13.2 |
| NOx, ppm | 328 | 389 | 395 | 395 | 351 | 453 | 442 | 468 | 510 | 570 | 550 | 470 |
| Staging | yes | yes | yes | yes | yes | yes | yes | yes | yes | yes | yes | yes |
| Staging O2 | 4146 | 4642 | 4642 | 4642 | 4677 | 4583 | 4464 | 4087 | 4028 | 3980 | 4028 | 4158 |
| Staging Air | 16881 | 18899 | 18899 | 18899 | 19043 | 18658 | 18176 | 16640 | 16399 | 16206 | 16399 | 16929 |
| PSR | 1.02 | 1.02 | 1.02 | 1.02 | 1.02 | 1.02 | 1.02 | 1.02 | 1.02 | 1.02 | 1.02 | 1.02 |
| OSR | 1.1 | 1.11 | 1.11 | 1.11 | 1.11 | 1.11 | 1.11 | 1.1 | 1.1 | 1.1 | 1.1 | 1.1 |
| NOx, 0% O2 | 453.7 | 458.4 | 422.4 | 402.9 | 378.8 | 478.5 | 471.2 | 500.2 | 546.4 | 654.1 | 607.9 | 481.5 |
| NOx, lb/ton | 1.6 | 1.6 | 1.4 | 1.4 | 1.3 | 1.6 | 1.6 | 1.7 | 1.9 | 2.2 | 2.1 | 1.6 |
| CO, 0% O2 | 126.6 | 35.2 | 242.7 | NA | 570.9 | NA | 42.6 | 29.9 | 85.7 | 23.0 | 44.2 | 922.0 |

| | 27-Sep | 27-Sep | 27-Sep | 27-Sep | 27-Sep | 27-Sep | 27-Sep | 27-Sep | 27-Sep | 27-Sep | 27-Sep | 27-Sep |
|---|---|---|---|---|---|---|---|---|---|---|---|---|
| Time | 14:59 | 15:11 | 15:20 | 15:25 | 15:33 | 15:42 | 15:56 | 16:17 | 16:25 | 16:38 | 16:50 | 16:59 |
| Firing Side | L | R | R | R | R | L | L | R | R | R | L | L |
| Sample Location | R6 | L3 | L3 | Stack | Stack | Stack | Stack | Stack | Stack | Stack | Stack | Stack |
| O2, % | 1.4 | 6.5 | 0.55 | 5.6 | 6.02 | 5.67 | 6 | 6.25 | 6.2 | 6.25 | 5.76 | 6.26 |
| CO, ppm | 35 | 1000 | over | 30 | 8 | 9 | 5 | 170 | 209 | 141 | 5 | 8 |
| CO2, % | 12.6 | 13.1 | 13.4 | 9.6 | 9.6 | 9.8 | 9.6 | 9.6 | 9.5 | 9.5 | 9.6 | 9.6 |
| NOx, ppm | 420 | 430 | 431 | 320 | 323 | 384 | 380 | 320 | 317 | 323 | 374 | 372 |
| Staging | yes | yes | yes | yes | yes | yes | yes | yes | yes | yes | yes | yes |
| Staging O2 | 4063 | 4063 | 4393 | 4441 | 4334 | 3945 | 5898 | 5697 | 5685 | 6311 | 5367 | 7092 |
| Staging Air | 16544 | 16544 | 17887 | 18079 | 17646 | 16062 | 24014 | 23195 | 23146 | 25694 | 21852 | 13888 |
| FSR | 1.02 | 1.02 | 1.02 | 1.02 | 1.02 | 1.02 | 0.98 | 0.98 | 0.98 | 1.02 | 0.98 | 0.98 |
| OSR | 1.1 | 1.1 | 1.11 | 1.11 | 1.11 | 1.1 | 1.1 | 1.1 | 1.1 | 1.11 | 1.09 | 1.09 |
| NOx, 0% O2 | 450.0 | 622.8 | 442.8 | 436.4 | 452.8 | 528.0 | 532.0 | 455.6 | 449.8 | 459.9 | 515.4 | 530.0 |
| NOx, lb/ton | 1.5 | 2.1 | 1.5 | 1.5 | 1.5 | 1.8 | 1.8 | 1.5 | 1.5 | 1.5 | 1.7 | 1.8 |
| CO, 0% O2 | 37.5 | 1448.3 | NA | 40.9 | 11.2 | 12.3 | 7.0 | 242.0 | 296.6 | 200.7 | 6.9 | 8.5 |
| | | | Note 32 | Note 33 | Note 34 | Note 35 | Note 36 | Note 37 | Note 38 | Note 39 | | Note 40 |

| | 27-Sep | 28-Sep | 28-Sep | 28-Sep | 28-Sep | 28-Sep | 28-Sep | 28-Sep | 28-Sep | 28-Sep | 28-Sep | 28-Sep |
|---|---|---|---|---|---|---|---|---|---|---|---|---|
| Time | 17:07 | 8:41 | 9:11 | 9:46 | 10:16 | 10:37 | 11:03 | 11:08 | 11:11 | 11:14 | 11:17 | 11:20 |
| Firing Side | L | R | L | R | L | R | L | L | L | L | L | L |
| Sample Location | Stack | Stack | Stack | Stack | Stack | Stack | R1 | R2 | R3 | R4 | R5 | R6 |
| O2, % | 6.15 | 6.4 | 6.52 | 7.01 | 6.8 | 5.97 | 1.02 | 0.98 | 2.12 | 1.35 | 0.39 | 0.63 |
| CO, ppm | 6 | 176 | 3 | 4 | 4 | 73 | 22 | 162 | 18 | 88 | over | 135 |
| CO2, % | 9.6 | 10.4 | 10.3 | 9.9 | 10.2 | 10.2 | 13.8 | 13.8 | 13.3 | 13.4 | 13.7 | 13.4 |
| NOx, ppm | 350 | 398 | 548 | 389 | 410 | 306 | 506 | 540 | 602 | 579 | 457 | 442 |
| Staging | yes | no | no | yes | yes | yes | yes | yes | yes | yes | yes | yes |
| Staging O2 | 6242 | 0 | 0 | -1984 | 3970 | 3887 | 4112 | 3994 | 4195 | 4195 | 4219 | 4290 |
| Staging Air | 12223 | 0 | 0 | -8078 | 16164 | 15827 | 16743 | 16261 | 17080 | 17080 | 17177 | 17466 |
| FSR | 0.98 | 1.13 | 1.13 | 1.02 | 1.02 | 1.02 | 1.02 | 1.02 | 1.02 | 1.02 | 1.02 | 1.02 |
| OSR | 1.08 | 1.13 | 1.13 | 1.09 | 1.09 | 1.09 | 1.09 | 1.09 | 1.09 | 1.09 | 1.09 | 1.09 |
| NOx, 0% O2 | 494.9 | 572.5 | 794.8 | 583.9 | 606.3 | 427.5 | 531.8 | 568.4 | 669.6 | 618.8 | 465.6 | 455.7 |
| NOx, lb/ton | 1.7 | 2.0 | 2.8 | 2.1 | 2.1 | 1.5 | 1.8 | 1.9 | 2.3 | 2.1 | 1.6 | 1.6 |
| CO, 0% O2 | 8.5 | 253.2 | 4.4 | 6.0 | 5.9 | 102.0 | 23.1 | 169.9 | 20.0 | 94.0 | NA | 139.2 |
| | Note 41 | | | | | | | | | | | |

| | 28-Sep | 28-Sep | 28-Sep | 28-Sep | 28-Sep | 28-Sep | 28-Sep | 28-Sep | 28-Sep | 28-Sep | 28-Sep | 28-Sep |
|---|---|---|---|---|---|---|---|---|---|---|---|---|
| Time | 11:28 | 11:34 | 11:40 | 11:49 | 11:55 | 11:58 | 12:08 | 12:33 | 12:37 | 13:18 | 13:42 | 13:49 |
| Firing Side | L | R | R | R | R | R | L | L | R | L | R | R |
| Sample Location | R3 | L6 | L5 | L6 | Stack | Stack | Stack | Stack | Stack | Stack | Stack | Stack |
| O2, % | 1.71 | 0.77 | 2.73 | 0.86 | 5.96 | 5.84 | 5.93 | 5.95 | 5.8 | 5.75 | 5.84 | 5.79 |
| CO, ppm | 25 | over | 24 | over | 166 | 142 | 4 | 3 | 227 | 11 | 268 | 320 |
| CO2, % | 13.3 | 13 | 12.5 | 12.9 | 10 | 10 | 9.9 | 10 | 10.1 | 10.1 | 10.1 | 10.2 |
| NOx, ppm | 602 | 303 | 332 | 308 | 286 | 279 | 409 | 397 | 295 | 387 | 293 | 271 |
| Staging | yes | yes | yes | yes | yes | yes | yes | yes | yes | yes | yes | yes |
| Staging O2 | 4385 | 4148 | 4183 | 4266 | 4586 | 4183 | 4314 | 3982 | 4065 | 4160 | 4029 | 4124 |
| Staging Air | 17851 | 16887 | 17032 | 17369 | 18671 | 17032 | 17552 | 16213 | 16550 | 16936 | 16405 | 16791 |
| FSR | 1.02 | 1.02 | 1.02 | 1.02 | 1.02 | 1.02 | 1.02 | 1.02 | 1.02 | 1.02 | 1.02 | 1.02 |
| OSR | 1.09 | 1.09 | 1.09 | 1.09 | 1.09 | 1.09 | 1.09 | 1.09 | 1.09 | 1.09 | 1.09 | 1.09 |
| NOx, 0% O2 | 655.4 | 314.5 | 381.6 | 321.2 | 399.3 | 386.5 | 569.9 | 554.0 | 407.6 | 532.9 | 405.9 | 271.0 |
| NOx, lb/ton | 2.2 | 1.1 | 1.3 | 1.1 | 1.4 | 1.3 | 1.9 | 1.9 | 1.4 | 1.8 | 1.4 | 0.9 |
| CO, 0% O2 | 27.2 | NA | 27.6 | NA | 231.8 | 196.7 | 5.6 | 4.2 | 313.6 | 15.1 | 371.2 | 441.8 |
| | Note 42 | | | | Note 43 | Note 44 | Note 45 | Note 46 | | | | Note 47 |

| | 22-Oct | 22-Oct | 22-Oct | 22-Oct | 22-Oct | 22-Oct | 22-Oct | 22-Oct | 22-Oct | 22-Oct | 22-Oct | 22-Oct |
|---|---|---|---|---|---|---|---|---|---|---|---|---|
| Time | 9:16 | 9:46 | 10:28 | 10:48 | 11:12 | 11:27 | 11:43 | 11:54 | 12:02 | 12:21 | 12:55 | 13:03 |
| Firing Side | L | R | L | R | L | L | R | R | R | L | R | R |
| Sample Location | Stack | Stack | Stack | Stack | Stack | Stack | Stack | Stack | Stack | Stack | Stack | Stack |
| O2, % | 6.83 | 6.75 | 6.49 | 6.45 | 6.37 | 6.55 | 6.45 | 6.43 | 6.46 | 6.4 | 6.37 | 6.31 |
| CO, ppm | 3 | 3 | 2 | 100 | 3 | 3 | 21 | 79 | 101 | 3 | 56 | 76 |
| CO2, % | 9.9 | 9.8 | 9.9 | 10 | 10.1 | 9.9 | 10 | 9.9 | 10 | 10 | 9.8 | 9.9 |
| NOx, ppm | 560 | 503 | 446 | 402 | 436 | 415 | 420 | 411 | 393 | 423 | 420 | 397 |
| Staging | no | no | yes | yes | yes | yes | yes | yes | yes | yes | yes | yes |
| Staging O2 | 0 | 0 | 3887 | 3875 | 4100 | 4041 | 3816 | 4135 | 3982 | 4041 | 3733 | 4218 |
| Staging Air | 0 | 0 | 15825 | 15777 | 16693 | 16452 | 15536 | 16837 | 16211 | 16452 | 15198 | 17174 |
| FSR | 1.13 | 1.13 | 1.02 | 1.02 | 1.02 | 1.02 | 1.02 | 1.02 | 1.02 | 1.02 | 1.02 | 1.02 |
| OSR | 1.13 | 1.13 | 1.10 | 1.10 | 1.10 | 1.10 | 1.10 | 1.10 | 1.10 | 1.10 | 1.10 | 1.10 |
| NOx, 0% O2 | 829.92 | 741.26 | 645.49 | 580.21 | 625.84 | 603.11 | 606.19 | 592.38 | 567.61 | 608.42 | 602.87 | 567.53 |
| NOx, lb/ton | 3.07 | 2.73 | 2.31 | 2.07 | 2.23 | 2.15 | 2.17 | 2.11 | 2.03 | 2.17 | 2.16 | 2.02 |
| CO, 0% O2 | 4.45 | 4.42 | 2.89 | 144.33 | 4.31 | 4.36 | 30.31 | 113.86 | 145.87 | 4.32 | 80.38 | 108.65 |
| | | | | | | Note 48 | | Note 49 | Note 50 | | | Note 51 |

| | 22-Oct | 22-Oct | 22-Oct | 22-Oct | 22-Oct | 22-Oct | 22-Oct | 22-Oct | 22-Oct | 22-Oct | 22-Oct | 22-Oct |
|---|---|---|---|---|---|---|---|---|---|---|---|---|
| Time | 13:14 | 13:19 | 13:23 | 13:27 | 13:31 | 13:36 | 13:43 | 13:50 | 13:54 | 13:58 | 14:02 | 14:07 |
| Firing Side | L | L | L | L | L | L | R | R | R | R | R | R |
| Sample Location | R1 | R2 | R3 | R4 | R5 | R6 | L6 | L5 | L4 | L3 | L2 | L1 |
| O2, % | 1.89 | 2.89 | 2.01 | 1.36 | 0.24 | 1.06 | 0.76 | 1 | 0.53 | 0.11 | 0.75 | 3.14 |
| CO, ppm | 14 | 14 | 22 | 39 | 1000 | 44 | 27 | 200 | 653 | >1208 | 500 | 18 |
| CO2, % | 13.7 | 12.5 | 12.8 | 12.7 | 14 | 13.7 | 13.5 | 13.5 | 13.6 | 14.1 | 14.1 | 13.3 |
| NOx, ppm | 510 | 595 | 660 | 600 | 451 | 402 | 589 | 572 | 530 | 515 | 525 | 520 |
| Staging | yes | yes | yes | yes | yes | yes | yes | yes | yes | yes | yes | yes |
| Staging O2 | 4005 | 3958 | 4005 | 3887 | 4325 | 4230 | 4195 | 4112 | 4064 | 4064 | 4053 | 4206 |
| Staging Air | 16307 | 16114 | 16307 | 15825 | 17608 | 17223 | 17078 | 16741 | 16548 | 16548 | 16500 | 17126 |
| FSR | 1.02 | 1.02 | 1.02 | 1.02 | 1.02 | 1.02 | 1.02 | 1.02 | 1.02 | 1.02 | 1.02 | 1.02 |
| OSR | 1.10 | 1.10 | 1.10 | 1.10 | 1.10 | 1.10 | 1.1 | 1.1 | 1.1 | 1.1 | 1.1 | 1.1 |
| NOx, 0% O2 | 580.44 | 689.95 | 729.86 | 641.55 | 456.21 | 423.37 | 611.12 | 600.60 | 543.72 | 517.71 | 544.44 | 611.42 |
| NOx, lb/ton | 2.00 | 2.47 | 2.61 | 2.29 | 1.63 | 1.51 | 2.18 | 2.14 | 1.94 | 1.85 | 1.94 | 2.18 |
| CO, 0% O2 | 15.38 | 18.23 | 24.33 | 41.70 | 1011.56 | 46.34 | 28.01 | 210.00 | 669.91 | NA | 518.52 | 18.81 |

| | 22-Oct | 22-Oct | 22-Oct | 22-Oct | 22-Oct | 22-Oct | 22-Oct | 22-Oct | 23-Oct | 23-Oct | 23-Oct | 23-Oct |
|---|---|---|---|---|---|---|---|---|---|---|---|---|
| Time | 14:30 | 14:55 | 15:29 | 15:49 | 16:01 | 16:27 | 16:39 | 16:57 | 8:53 | 9:29 | 10:06 | 10:30 |
| Firing Side | L | R | L | R | R | L | L | R | L | R | L | R |
| Sample Location | Stack | Stack | Stack | Stack | Stack | Stack | Stack | Stack | Stack | Stack | Stack | Stack |
| O2, % | 6.23 | 6.08 | 6.08 | 6.03 | 5.98 | 6.13 | 6.23 | 5.96 | 6.84 | 6.58 | 6.6 | 6.35 |
| CO, ppm | 3 | 112 | 10 | 133 | 35 | 7 | 4 | 6 | 2 | 2 | 1 | 17 |
| CO2, % | 10 | 10 | 10.1 | 10 | 9.9 | 10 | 9.9 | 9.5 | 10.1 | 10.6 | 10.2 | 10.6 |
| NOx, ppm | 420 | 413 | 423 | 397 | 422 | 393 | 394 | 408 | 620 | 431 | 480 | 440 |
| Staging | yes | yes | yes | yes | yes | yes | yes | yes | no | yes | yes | yes |
| Staging O2 | 4041 | 4064 | 3982 | 3958 | 1898 | 5737 | 6275 | 0 | 0 | 3745 | 3792 | 3238 |
| Staging Air | 16452 | 16548 | 16211 | 16114 | 25050 | 8309 | 5149 | 35375 | 0 | 15247 | 15439 | 13185 |
| FSR | 1.02 | 1.02 | 1.02 | 1.02 | 1.02 | 1.02 | 1.02 | 1.02 | 1.15 | 1.02 | 1.02 | 1.02 |
| OSR | 1.1 | 1.1 | 1.1 | 1.1 | 1.1 | 1.1 | 1.1 | 1.1 | 1.15 | 1.10 | 1.10 | 1.09 |
| NOx, 0% O2 | 597.18 | 581.30 | 595.38 | 556.91 | 590.01 | 555.01 | 560.19 | 569.68 | 919.49 | 627.67 | 700.00 | 630.72 |
| NOx, lb/ton | 2.13 | 2.08 | 2.13 | 1.99 | 2.14 | 1.95 | 1.96 | 2.10 | 3.39 | 2.25 | 2.50 | 2.27 |
| CO, 0% O2 | 4.27 | 157.64 | 14.08 | 166.57 | 48.93 | 9.89 | 5.69 | 8.38 | 2.97 | 2.91 | 1.46 | 24.37 |
| | Note 52 | Note 53 | Note 54 | Note 55 | Note 56 | Note 57 | Note 58 | Note 59 | | | | |

| | 23-Oct | 23-Oct | 23-Oct | 23-Oct | 23-Oct | 23-Oct | 23-Oct | 23-Oct | 23-Oct | 23-Oct | 23-Oct | 23-Oct |
|---|---|---|---|---|---|---|---|---|---|---|---|---|
| Time | 10:42 | 11:00 | 11:11 | 11:30 | 11:45 | 12:03 | 12:12 | 12:27 | 12:45 | 13:01 | 13:14 | 13:33 |
| Firing Side | R | L | L | R | R | L | L | R | R | L | L | R |
| Sample Location | Stack | Stack | Stack | Stack | Stack | Stack | Stack | Stack | Stack | Stack | Stack | Stack |
| O2, % | 6.32 | 6.21 | 6.44 | 6.34 | 6.36 | 6.27 | 6.23 | 6.03 | 6.03 | 6.02 | 6.28 | 6.1 |
| CO, ppm | 60 | 30 | 1 | 0 | 13 | 3 | 18 | 150 | 113 | 23 | 3 | 80 |
| CO2, % | 10.4 | 10.5 | 10.4 | 10.2 | 10.2 | 10.4 | 10.4 | 10.4 | 10.2 | 10.9 | 10.8 | 10.8 |
| NOx, ppm | 400 | 466 | 488 | 419 | 401 | 436 | 425 | 409 | 385 | 426 | 415 | 395 |
| Staging | yes | yes | yes | yes | yes | yes | yes | yes | yes | yes | yes | yes |
| Staging O2 | 2720 | 2744 | 3839 | 2987 | 2545 | 2624 | 2165 | 2262 | 1193 | 1178 | 3191 | 1457 |
| Staging Air | 11074 | 11171 | 15632 | 20574 | 17529 | 18080 | 14912 | 15585 | 19976 | 19738 | 21981 | 24402 |
| PSR | 1.02 | 1.02 | 1.02 | 1.02 | 1.02 | 1.02 | 1.02 | 1.02 | 1.02 | 1.02 | 1.02 | 1.02 |
| OSR | 1.08 | 1.08 | 1.10 | 1.10 | 1.09 | 1.09 | 1.08 | 1.08 | 1.08 | 1.08 | 1.10 | 1.09 |
| NOx, 0% O2 | 572.21 | 661.66 | 675.00 | 600.20 | 575.20 | 621.59 | 604.27 | 573.75 | 540.08 | 597.20 | 592.05 | 556.7 |
| NOx, lb/ton | 2.06 | 2.39 | 2.41 | 2.16 | 2.08 | 2.24 | 2.19 | 2.08 | 1.97 | 2.18 | 2.13 | 2.03 |
| CO, 0% O2 | 85.83 | 42.60 | 1.44 | 0 | 18.65 | 11.41 | 25.59 | 210.42 | 158.52 | 32.24 | 4.28 | 112.75 |

| | 23-Oct | 23-Oct | 23-Oct | 23-Oct | 23-Oct | 23-Oct | 23-Oct | 23-Oct | 23-Oct | 23-Oct | 23-Oct | 23-Oct |
|---|---|---|---|---|---|---|---|---|---|---|---|---|
| Time | 13:49 | 14:04 | 14:12 | 14:38 | 14:48 | 15:06 | 15:16 | 16:07 | 16:19 | 16:36 | 16:48 | 17:15 |
| Firing Side | R | L | L | R | R | L | L | L | L | R | R | L |
| Sample Location | Stack | Stack | Stack | Stack | Stack | Stack | Stack | Stack | Stack | Stack | Stack | Stack |
| O2, % | 6.07 | 6.13 | 6.1 | 6 | 5.93 | 5.93 | 5.86 | 5.94 | 6.18 | 6.05 | 5.94 | 6.1 |
| CO, ppm | 12 | 2 | 3 | 80 | 190 | 83 | 96 | 20 | 3 | 5 | 120 | 4 |
| CO2, % | 10.7 | 10.8 | 10.9 | 10.6 | 10.7 | 10.8 | 10.9 | 10.7 | 10.5 | 10.4 | 10.5 | 10.6 |
| NOx, ppm | 402 | 410 | 406 | 403 | 380 | 402 | 398 | 412 | 427 | 426 | 398 | 430 |
| Staging | yes | yes | yes | yes | yes | yes | yes | yes | yes | yes | yes | yes |
| Staging O2 | 1650 | 1674 | 1481 | 0 | 0 | 0 | 0 | 0 | 0 | 0 | 0 | 1517 |
| Staging Air | 27638 | 28035 | 24799 | 36076 | 30591 | 30792 | 26408 | 35075 | 38658 | 38558 | 25407 | 25416 |
| PSR | 1.02 | 1.02 | 1.02 | 1.02 | 1.02 | 1.02 | 1.02 | 1.02 | 1.02 | 1.02 | 1.02 | 1.02 |
| OSR | 1.10 | 1.10 | 1.09 | 1.10 | 1.09 | 1.09 | 1.08 | 1.10 | 1.11 | 1.11 | 1.08 | 1.10 |
| NOx, 0% O2 | 565.44 | 579.02 | 572.21 | 584.20 | 529.53 | 560.19 | 552.05 | 574.50 | 605.06 | 598.39 | 554.98 | 606.04 |
| NOx, lb/ton | 2.06 | 2.11 | 2.09 | 2.08 | 1.95 | 2.07 | 2.04 | 2.12 | 2.23 | 2.21 | 2.05 | 2.21 |
| CO, 0% O2 | 16.88 | 2.82 | 4.23 | 112.00 | 264.78 | 115.86 | 133.16 | 27.89 | 4.25 | 7.02 | 167.33 | 5.64 |

| | 23-Oct | 23-Oct | 23-Oct | 23-Oct | 23-Oct | 23-Oct | 23-Oct | 24-Oct | 24-Oct | 24-Oct | 24-Oct | 24-Oct |
|---|---|---|---|---|---|---|---|---|---|---|---|---|
| Time | 17:42 | 18:12 | 18:49 | 20:11 | 22:04 | 20:44 | 22:42 | 0:14 | 0:41 | 2:16 | 2:48 | 4:25 |
| Firing Side | R | L | R | L | L | R | R | L | R | L | R | L |
| Sample Location | Stack | Stack | Stack | Stack | Stack | Stack | Stack | Stack | Stack | Stack | Stack | Stack |
| O2, % | 6.23 | 6.32 | 6.27 | 6.37 | 6.95 | 6.56 | 6.68 | 6.6 | 6.68 | 6.64 | 6.64 | 6.62 |
| CO, ppm | 16 | 3 | 10 | 4 | 4 | 7 | 5 | 4 | 3 | 2 | 3 | 2 |
| CO2, % | 10.7 | 10.8 | 10.7 | 10.5 | 10.2 | 10.6 | 10.5 | 10.6 | 10.7 | 10.5 | 10.4 | 10.7 |
| NOx, ppm | 420 | 438 | 445 | 458 | 506 | 450 | 473 | 497 | 458 | 505 | 472 | 508 |
| Staging | yes | yes | yes | yes | yes | yes | yes | yes | yes | yes | yes | yes |
| Staging O2 | 1555 | 2942 | 2729 | 2889 | 2827 | 2871 | 2827 | 2747 | 2782 | 2498 | 2702 | 2534 |
| Staging Air | 26051 | 20269 | 18800 | 19901 | 19473 | 19779 | 19473 | 18923 | 19167 | 17210 | 18617 | 17455 |
| PSR | 1.02 | 1.02 | 1.02 | 1.02 | 1.02 | 1.02 | 1.02 | 1.02 | 1.02 | 1.03 | 1.02 | 1.02 |
| OSR | 1.10 | 1.10 | 1.10 | 1.10 | 1.10 | 1.10 | 1.10 | 1.10 | 1.10 | 1.10 | 1.10 | 1.10 |
| NOx, 0% O2 | 597.16 | 626.57 | 634.42 | 654.55 | 756.30 | 654.43 | 693.65 | 724.79 | 671.65 | 738.51 | 690.25 | 741.86 |
| NOx, lb/ton | 2.18 | 2.26 | 2.29 | 2.36 | 2.73 | 2.36 | 2.50 | 2.62 | 2.42 | 2.67 | 2.49 | 2.68 |
| CO, 0% O2 | 22.75 | 4.29 | 14.28 | 5.74 | 5.98 | 10.18 | 7.33 | 5.83 | 4.40 | 2.92 | 4.39 | 2.92 |

| | 24-Oct | 24-Oct | 24-Oct | 24-Oct | 24-Oct | 24-Oct | 24-Oct | 24-Oct | 24-Oct | 24-Oct | 24-Oct | 24-Oct |
|---|---|---|---|---|---|---|---|---|---|---|---|---|
| Time | 4:56 | 9:29 | 10:06 | 10:26 | 10:39 | 10:59 | 11:44 | 12:07 | 15:16 | 15:44 | 16:11 | 16:43 |
| Firing Side | R | L | R | L | L | R | L | R | R | L | R | L |
| Sample Position | Stack | Stack | Stack | Stack | Stack | Stack | Stack | Stack | Stack | Stack | Stack | Stack |
| O2, % | 6.52 | 6.61 | 6.36 | 6.49 | 6.33 | 6.24 | 6.37 | 6.31 | 6.18 | 6.2 | 6.22 | 6.35 |
| CO, ppm | 3 | 1 | 15 | 0 | 2 | 120 | 3 | 5 | 4 | 8 | 3 | 21 |
| CO2, % | 10.7 | 10.7 | 10.6 | 10.6 | 10.7 | 10.7 | 10.5 | 10.5 | 10.9 | 11 | 11.1 | 10.9 |
| NOx, ppm | 459 | 520 | 445 | 495 | 465 | 417 | 453 | 435 | 455 | 488 | 431 | 490 |
| Staging | yes | yes | yes | yes | yes | yes | yes | yes | yes | yes | yes | yes |
| Staging O2 | 2889 | 2882 | 3049 | 3102 | 3299 | 3186 | 3839 | 3946 | 3750 | 3591 | 3653 | 2729 |
| Staging Air | 19901 | 19718 | 21003 | 21370 | 22728 | 21946 | 26447 | 27181 | 25837 | 24736 | 25164 | 18802 |
| PSR | 1.02 | 1.02 | 1.02 | 1.02 | 1.00 | 1.00 | 1.00 | 1.00 | 1 | 1 | 1 | 1.02 |
| OSR | 1.10 | 1.10 | 1.10 | 1.10 | 1.09 | 1.08 | 1.10 | 1.10 | 1.1 | 1.1 | 1.1 | 1.1 |
| NOx, 0% O2 | 665.58 | 758.86 | 638.32 | 716.40 | 665.64 | 593.29 | 650.24 | 621.85 | 644.74 | 692.43 | 612.38 | 702.39 |
| NOx, lb/ton | 2.40 | 2.74 | 2.30 | 2.58 | 2.39 | 2.13 | 2.33 | 2.22 | 2.36 | 2.54 | 2.24 | 2.59 |
| CO, 0% O2 | 4.35 | 1.46 | 21.52 | 0.00 | 2.86 | 170.73 | 4.31 | 7.15 | 5.87 | 11.35 | 4.26 | 30.10 |

| | 24-Oct | 24-Oct | 24-Oct | 24-Oct | 24-Oct | 24-Oct | 24-Oct | 25-Oct | 25-Oct | 25-Oct | 25-Oct | 25-Oct |
|---|---|---|---|---|---|---|---|---|---|---|---|---|
| Time | 17:15 | 18:53 | 19:17 | 20:45 | 21:17 | 22:47 | 23:19 | 0:52 | 1:15 | 4:47 | 5:16 | 8:42 |
| Firing Side | R | L | R | L | R | L | R | L | R | L | R | L |
| Sample Position | Stack | Stack | Stack | Stack | Stack | Stack | Stack | Stack | Stack | Stack | Stack | Stack |
| O2, % | 6.32 | 6.27 | 6.5 | 6.6 | 6.65 | 6.59 | 6.78 | 6.56 | 6.55 | 6.64 | 6.62 | 6.34 |
| CO, ppm | 40 | 6 | 5 | 3 | 4 | 4 | 2 | 4 | 2 | 13 | 12 | 3 |
| CO2, % | 11 | 10.7 | 10.8 | 10.7 | 10.8 | 10.9 | 10.9 | 10.5 | 10.6 | 10.8 | 10.8 | 10.9 |
| NOx, ppm | 430 | 470 | 457 | 518 | 460 | 510 | 447 | 509 | 454 | 503 | 472 | 471 |
| Staging | yes | yes | yes | yes | yes | yes | yes | yes | yes | yes | yes | yes |
| Staging O2 | 3031 | 2991 | 2911 | 2814 | 2840 | 2929 | 2609 | 2071.8 | 2142.8 | 2213.8 | 2080.6 | 2772.5 |
| Staging Air | 20882 | 20606 | 20055 | 19382 | 19566 | 20178 | 17976 | 14272.2 | 14761.5 | 15250.9 | 14333.4 | 19099.4 |
| PSR | 1.02 | 1.02 | 1.02 | 1.02 | 1.02 | 1.02 | 1.02 | 1 | 1 | 1 | 1 | 1 |
| OSR | 1.1 | 1.1 | 1.1 | 1.1 | 1.1 | 1.1 | 1.1 | 1.08 | 1.08 | 1.08 | 1.08 | 1.08 |
| NOx, 0% O2 | 615.12 | 670.06 | 661.86 | 755.42 | 673.17 | 743.23 | 660.13 | 740.24 | 659.79 | 735.58 | 689.29 | 674.69 |
| NOx, lb/ton | 2.26 | 2.44 | 2.41 | 2.76 | 2.45 | 2.71 | 2.41 | 2.71 | 2.42 | 2.59 | 2.53 | 2.41 |
| CO, 0% O2 | 57.22 | 8.55 | 7.24 | 4.38 | 5.85 | 5.83 | 2.95 | 5.82 | 2.91 | 19.01 | 17.52 | 4.30 |

| | 25-Oct | 25-Oct | 25-Oct | 25-Oct | 25-Oct | 25-Oct | 25-Oct | 25-Oct | 25-Oct | 25-Oct | 25-Oct | 12-Nov |
|---|---|---|---|---|---|---|---|---|---|---|---|---|
| Time | 9:19 | 10:47 | 11:13 | 11:48 | 12:14 | 14:19 | 14:45 | 15:15 | 15:42 | 16:19 | 16:43 | 14:30 |
| Firing Side | R | L | R | L | R | R | L | R | L | R | L | L |
| Sample Location | Stack | Stack | Stack | Stack | Stack | Stack | Stack | Stack | Stack | Stack | Stack | Stack |
| O2, % | 6.39 | 6.42 | 6.43 | 6.3 | 6.22 | 6.28 | 6.08 | 6.2 | 6.22 | 6.08 | 6.5 | 6.51 |
| CO, ppm | 4 | 3 | 3 | 3 | 3 | 15 | 8 | 3 | 3 | 3 | 3 | 175 |
| CO2, % | 11.2 | 11.5 | 11.3 | 11.1 | 11.1 | 11.1 | 11.1 | 11 | 11 | 11 | 11 | 10.1 |
| NOx, ppm | 420 | 450 | 405 | 450 | 385 | 390 | 455 | 390 | 470 | 403 | 490 | 518 |
| Staging | yes | yes | yes | yes | yes | yes | yes | yes | yes | yes | yes | no |
| Staging O2 | 2764 | 2941 | 2932 | 2923 | 3039 | 3030 | 3030 | 3083 | 3030 | 3057 | 2968 | 0 |
| Staging Air | 19038 | 20262 | 20200 | 20139 | 20935 | 20873 | 20873 | 21240 | 20873 | 21057 | 20445 | 0 |
| PSR | 1 | 1 | 1 | 1 | 1 | 1 | 1 | 1 | 1 | 1 | 1 | 1.13 |
| OSR | 1.08 | 1.08 | 1.08 | 1.08 | 1.08 | 1.08 | 1.08 | 1.08 | 1.08 | 1.08 | 1.08 | 1.13 |
| NOx, 0% O2 | 603.70 | 648.15 | 583.73 | 642.86 | 547.02 | 556.39 | 640.42 | 553.38 | 667.79 | 567.23 | 709.66 | 750.72 |
| NOx, lb/ton | 2.15 | 2.31 | 2.08 | 2.29 | 1.95 | 1.98 | 2.28 | 1.97 | 2.38 | 2.02 | 2.53 | 2.84 |
| CO, 0% O2 | 5.75 | 4.32 | 4.32 | 4.29 | 4.26 | 21.40 | 11.26 | 4.26 | 4.26 | 4.22 | 4.34 | 253.62 |

| | 12-Nov | 12-Nov | 12-Nov | 12-Nov | 13-Nov | 13-Nov | 13-Nov | 13-Nov | 13-Nov | 13-Nov | 13-Nov | 13-Nov |
|---|---|---|---|---|---|---|---|---|---|---|---|---|
| Time | 15:00 | 15:30 | 15:45 | 16:30 | 9:10 | 9:40 | 10:05 | 10:53 | 11:12 | 11:39 | 12:12 | 12:38 |
| Firing Side | R | L | R | L | R | L | R | L | R | L | R | L |
| Sample Location | Stack | Stack | Stack | Stack | Stack | Stack | Stack | Stack | Stack | Stack | Stack | Stack |
| O2, % | 6.7 | 6.05 | 6.12 | 5.89 | 6.58 | 6.23 | 6.43 | 6.36 | 6.35 | 6 | 6.04 | 6.04 |
| CO, ppm | 39 | 489 | 189 | 60 | 48 | 75 | 36 | 23 | 80 | 224 | 135 | 69 |
| CO2, % | 10.2 | 10.2 | 10.2 | 10.2 | 10.3 | 10.5 | 10.1 | 10 | 10 | 10.2 | 9.5 | 9.8 |
| NOx, ppm | 440 | 510 | 345 | 445 | 374 | 502 | 383 | 506 | 360 | 468 | 343 | 516 |
| Staging | no | no | yes | yes | yes | yes | yes | yes | yes | yes | yes | yes |
| Staging O2 | 0 | 0 | 3056 | 3056 | 3582 | 3689 | 3538 | 3458 | 3680 | 3795 | 3875 | 3076 |
| Staging Air | 0 | 0 | 21389 | 21389 | 24676 | 25410 | 24371 | 23820 | 25349 | 26144 | 26695 | 21190 |
| FSR | 1.14 | 1.12 | 1.02 | 1.02 | 1.02 | 1.02 | 1.02 | 1.02 | 1.02 | 1.02 | 1.02 | 1.02 |
| OSR | 1.14 | 1.12 | 1.10 | 1.10 | 1.1 | 1.1 | 1.1 | 1.1 | 1.1 | 1.1 | 1.1 | 1.1 |
| NOx, 0% O2 | 648.15 | 716.39 | 486.90 | 618.46 | 544.66 | 713.74 | 552.02 | 725.82 | 516.04 | 655.20 | 481.48 | 724.33 |
| NOx, lb/ton | 2.45 | 2.77 | 1.84 | 2.34 | 2.04 | 2.67 | 2.07 | 2.72 | 1.93 | 2.45 | 1.80 | 2.73 |
| CO, 0% O2 | 57.27 | 686.89 | 266.73 | 83.39 | 69.90 | 106.64 | 51.89 | 32.99 | 114.68 | 313.60 | 189.51 | 96.88 |

| | 13-Nov | 13-Nov | 13-Nov | 13-Nov | 13-Nov | 13-Nov | 14-Nov | 14-Nov | 14-Nov | 14-Nov | 14-Nov | 14-Nov |
|---|---|---|---|---|---|---|---|---|---|---|---|---|
| Time | 13:08 | 13:47 | 15:16 | 15:45 | 16:16 | 16:52 | 7:47 | 8:19 | 8:43 | 8:51 | 9:25 | 9:56 |
| Firing Side | R | L | R | L | R | L | R | L | R | R | L | R |
| Sample Location | Stack | Stack | Stack | Stack | Stack | Stack | Stack | Stack | Stack | Stack | Stack | Stack |
| O2, % | 6.25 | 6.04 | 6.68 | 6.41 | 6.8 | 6.42 | 7.34 | 7.07 | 7.16 | 7.18 | 7.16 | 6.95 |
| CO, ppm | 80 | 31 | 40 | 3 | 5 | 3 | 2 | 3 | 2 | 2 | 2 | 6 |
| CO2, % | | 9.4 | 10.3 | 10.6 | 10 | 10 | 9.9 | 10.2 | 9.9 | 9.9 | 9.8 | 9.6 |
| NOx, ppm | 380 | 463 | 418 | 547 | 441.6 | 532 | 425 | 482.5 | 431 | 411 | 490 | 410 |
| Staging | yes | yes | yes | yes | yes | yes | yes | yes | yes | yes | yes | yes |
| Staging O2 | 2801 | 2623 | 2534 | 2277 | 2277 | 3218 | 3817 | 3888 | 3640 | 3287 | 3260 | 3189 |
| Staging Air | 19293 | 18070 | 17458 | 15684 | 15684 | 22167 | 26298 | 26787 | 25075 | 22641 | 22457 | 21968 |
| FSR | 1.02 | 1.02 | 1.02 | 1.02 | 1.02 | 1.02 | 1.02 | 1.02 | 1.02 | 1.02 | 1.02 | 1.02 |
| OSR | 1.1 | 1.1 | 1.1 | 1.1 | 1.1 | 1.1 | 1.12 | 1.12 | 1.12 | 1.11 | 1.11 | 1.11 |
| NOx, 0% O2 | 541.02 | 649.93 | 612.99 | 787.32 | 653.07 | 766.26 | 653.37 | 727.39 | 653.97 | 624.53 | 743.50 | 612.81 |
| NOx, lb/ton | 2.04 | 2.45 | 2.32 | 2.98 | 2.47 | 2.82 | 2.34 | 2.60 | 2.34 | 2.24 | 2.67 | 2.18 |
| CO, 0% O2 | 113.90 | 43.52 | 58.66 | 4.32 | 7.39 | 4.32 | 3.07 | 4.52 | 3.03 | 3.04 | 3.03 | 8.97 |

| | 14-Nov | 14-Nov | 14-Nov | 14-Nov | 14-Nov | 14-Nov | 14-Nov | 14-Nov | 15-Nov | 15-Nov | 15-Nov | 15-Nov |
|---|---|---|---|---|---|---|---|---|---|---|---|---|
| Time | 10:29 | 10:54 | 11:37 | 12:00 | 12:30 | 13:01 | 13:29 | 14:01 | 9:41 | 9:57 | 10:30 | 11:00 |
| Firing Side | L | R | L | R | L | R | L | R | R | L | R | L |
| Sample Location | Stack | Stack | Stack | Stack | Stack | Stack | Stack | Stack | Stack | Stack | Stack | Stack |
| O2, % | 7.08 | 7.01 | 7.06 | 6.99 | 6.81 | 7.15 | 6.96 | 6.82 | 5.7 | 5.75 | 6.38 | 6.25 |
| CO, ppm | 2 | 3 | 2 | 3 | 2 | 6 | 2 | 3 | 503 | 662 | 142 | 37 |
| CO2, % | 9.6 | 9.5 | 10.2 | 10.1 | 10.3 | 10.2 | 10.5 | 10.5 | 10.4 | 10.9 | 10.5 | 10.6 |
| NOx, ppm | 486 | 403 | 505 | 406 | 475 | 403 | 468.5 | 392 | 320 | 440 | 371 | 450 |
| Staging | yes | yes | yes | yes | yes | yes | yes | yes | yes | yes | yes | yes |
| Staging O2 | 3073 | 3331 | 3331 | 3349 | 3420 | 3304 | 3358 | 3349 | 3050 | 3050 | 4200 | 4200 |
| Staging Air | 21173 | 22947 | 22947 | 23069 | 23558 | 22763 | 23130 | 23069 | 25000 | 25000 | 29500 | 29500 |
| FSR | 1.02 | 1.02 | 1.02 | 1.02 | 1.02 | 1.02 | 1.02 | 1.02 | 0.98 | 0.98 | 0.98 | 0.98 |
| OSR | 1.11 | 1.11 | 1.11 | 1.11 | 1.11 | 1.11 | 1.11 | 1.11 | 1.07 | 1.07 | 1.08 | 1.08 |
| NOx, 0% O2 | 733.19 | 604.93 | 760.76 | 608.57 | 702.96 | 611.05 | 700.75 | 580.54 | 439.22 | 605.90 | 532.90 | 640.68 |
| NOx, lb/ton | 2.61 | 2.15 | 2.70 | 2.16 | 2.49 | 2.17 | 2.49 | 2.06 | 1.67 | 2.30 | 2.01 | 2.41 |
| CO, 0% O2 | 3.02 | 4.50 | 3.01 | 4.50 | 2.96 | 9.10 | 2.99 | 4.44 | 690.39 | 911.81 | 203.97 | 52.68 |

| | 15-Nov | 15-Nov | 15-Nov | 15-Nov | 10-Dec | 10-Dec | 10-Dec | 10-Dec | 10-Dec | 10-Dec | 10-Dec | 10-Dec |
|---|---|---|---|---|---|---|---|---|---|---|---|---|
| Time | 11:34 | 12:00 | 12:12 | 12:28 | 10:05 | 10:25 | 10:37 | 10:52 | 11:29 | 13:31 | 13:40 | 13:58 |
| Firing Side | R | L | L | R | L | R | R | L | R | R | R | L |
| Sample Location | Stack | Stack | Stack | Stack | Stack | Stack | Stack | Stack | Stack | Stacx | Stack | Stack |
| O2, % | 6.27 | 6.33 | 6.33 | 6.69 | 7.45 | 7.64 | 6.73 | 6.91 | 6.72 | 5.53 | 6 | 6.5 |
| CO, ppm | 81 | 11 | 34 | 2 | 3 | 4 | 4 | 4 | 6.5 | over | over | 24 |
| CO2, % | 10.4 | 10.5 | 10.6 | 10.2 | 8 | 7.7 | 8.4 | 8.3 | 8.1 | 8.9 | 8.9 | 9.2 |
| NOx, ppm | 356 | 452 | 464 | 393 | 638 | 553 | 364 | 540 | 370 | 270 | 320 | 505 |
| Staging | yes | yes | yes | yes | no | no | OEAS | OEAS | OEAS | OEAS | OEAS | OEAS |
| Staging O2 | 4600 | 4600 | 5017 | 5017 | 0 | 0 | 2037 | 2037 | 2037 | 3056 | 3400 | 3400 |
| Staging Air | 32300 | 32300 | 35116 | 35116 | 0 | 0 | 14259 | 14259 | 14259 | 21389 | 23765 | 23765 |
| PSR | 0.98 | 0.98 | 0.98 | 0.98 | 1.18 | 1.18 | 1.03 | 1.02 | 1.02 | 1.04 | 1.05 | 1.04 |
| OSR | 1.09 | 1.09 | 1.10 | 1.10 | 1.18 | 1.18 | 1.10 | 1.09 | 1.09 | 1.12 | 1.13 | 1.13 |
| NOx, 0% O2 | 507.54 | 647.03 | 664.21 | 576.73 | 985.68 | 869.24 | 535.67 | 804.33 | 544.12 | 366.52 | 448.00 | 731.38 |
| NOx, lb/ton | 1.91 | 2.43 | 2.49 | 2.16 | 5.41 | 4.77 | 2.87 | 4.32 | 2.92 | 1.42 | 1.73 | 2.82 |
| CO, 0% O2 | 115.48 | 15.75 | 48.67 | 2.94 | 4.65 | 6.29 | 5.89 | 5.96 | 9.56 | NA | NA | 34.76 |

| | 10-Dec | 11-Dec | 11-Dec | 11-Dec | 11-Dec | 11-Dec | 11-Dec | 11-Dec | 11-Dec | 11-Dec | 11-Dec | 11-Dec |
|---|---|---|---|---|---|---|---|---|---|---|---|---|
| Time | 14:39 | 8:58 | 9:14 | 9:51 | 10:19 | 10:40 | 10:44 | 10:51 | 10:56 | 11:00 | 11:04 | 11:41 |
| Firing Side | R | R | L | R | L | R | R | R | R | R | R | R |
| Sample Location | Stack | Stack | Stack | Stack | Stack | L6 | L5 | L4 | L3 | L2 | L1 | L1 |
| O2, % | 6.07 | 6.07 | 6.12 | 6.47 | 6.08 | 0.77 | 0.3 | 0.25 | 0.4 | 1.75 | 1.58 | 1.85 |
| CO, ppm | 1156 | 337 | 400 | over | 600 | >1215 | >1215 | >1215 | >1215 | 280 | 35 | 19 |
| CO2, % | 8.8 | 9.7 | 9.8 | 9.8 | 9.9 | 12.5 | 12.8 | 12.3 | 13.4 | 12.8 | 13.8 | 13.4 |
| NOx, ppm | 319 | 390 | 513 | 245 | 410 | 440 | 420 | 320 | 340 | 414 | 370 | 423 |
| Staging | OEAS | no | no | OEAS | OEAS | OEAS | OEAS | OEAS | OEAS | OEAS | OEAS | OEAS |
| Staging O2 | 4070 | 0 | 0 | 3400 | 3400 | 3400 | 3400 | 3400 | 3400 | 3400 | 3400 | 3400 |
| Staging Air | 28482 | 0 | 0 | 23765 | 23765 | 23765 | 23765 | 23765 | 23765 | 23765 | 23765 | 23765 |
| PSR | 1.05 | 1.13 | 1.13 | 1.02 | 1.02 | 1.01 | 1.01 | 1.02 | 1.02 | 1.02 | 1.02 | 1.06 |
| OSR | 1.15 | 1.13 | 1.13 | 1.10 | 1.10 | 1.10 | 1.10 | 1.10 | 1.11 | 1.11 | 1.10 | 1.15 |
| NOx, 0% O2 | 448.69 | 548.56 | 723.99 | 354.09 | 577.08 | 456.75 | 428.09 | 323.86 | 346.60 | 451.84 | 400.10 | 463.86 |
| NOx, lb/ton | 1.72 | 2.12 | 2.86 | 1.36 | 2.22 | 1.76 | 1.54 | 1.25 | 1.34 | 1.74 | 1.54 | 1.79 |
| CO, 0% O2 | 1625.99 | 474.01 | 564.52 | NA | 844.50 | NA | NA | NA | NA | 305.45 | 37.85 | 20.84 |

| | 11-Dec | 11-Dec | 11-Dec | 11-Dec | 11-Dec | 11-Dec | 11-Dec | 11-Dec | 11-Dec | 11-Dec | 11-Dec | 11-Dec |
|---|---|---|---|---|---|---|---|---|---|---|---|---|
| Time | 11:45 | 11:50 | 11:55 | 12:02 | 12:06 | 12:13 | 12:17 | 12:21 | 12:27 | 12:32 | 12:37 | 12:54 |
| Firing Side | R | R | R | R | R | L | L | L | L | L | L | R |
| Sample Location | L2 | L3 | L4 | L5 | L6 | R6 | R5 | R4 | R3 | R2 | R1 | Stack |
| O2, % | 2.4 | 0.32 | 0.27 | 0.75 | 1.5 | 0.5 | 0.6 | 2.03 | 1.32 | 2.8 | 2.5 | 6.8 |
| CO, ppm | 25 | >1215 | >1215 | 900 | 180 | 900 | 1200 | 31 | 300 | 15 | 18 | 800 |
| CO2, % | 12.9 | 13.2 | 13 | 12.8 | 11.8 | 12.2 | 12.7 | 12.6 | 13.4 | 12.2 | 12.3 | 9.2 |
| NOx, ppm | 470 | 430 | 460 | 570 | 620 | 560 | 640 | 760 | 725 | 620 | 530 | 340 |
| Staging | OEAS | OEAS | OEAS | OEAS | OEAS | OEAS | OEAS | OEAS | OEAS | OEAS | OEAS | OEAS |
| Staging O2 | 3400 | 3400 | 3400 | 3400 | 3400 | 3400 | 3400 | 3400 | 3400 | 3400 | 3400 | 3400 |
| Staging Air | 23765 | 23765 | 23765 | 23765 | 23765 | 23765 | 23765 | 23765 | 23765 | 23765 | 23765 | 23765 |
| PSR | 1.06 | 1.06 | 1.06 | 1.06 | 1.06 | 1.06 | 1.06 | 1.06 | 1.06 | 1.06 | 1.06 | 1.07 |
| OSR | 1.15 | 1.15 | 1.14 | 1.14 | 1.15 | 1.15 | 1.14 | 1.14 | 1.15 | 1.15 | 1.14 | 1.15 |
| NOx, 0% O2 | 530.65 | 436.65 | 465.99 | 591.11 | 667.69 | 573.66 | 658.82 | 841.33 | 773.63 | 715.38 | 601.62 | 502.82 |
| NOx, lb/ton | 2.05 | 1.68 | 1.80 | 2.28 | 2.58 | 2.21 | 2.54 | 3.24 | 3.05 | 2.82 | 2.37 | 1.98 |
| CO, 0% O2 | 28.23 | NA | NA | 933.33 | 193.85 | 921.95 | 1235.29 | 34.32 | 320.12 | 17.31 | 20.43 | 1183.10 |

| | 11-Dec | 11-Dec | 11-Dec | 11-Dec | 11-Dec | 11-Dec | 11-Dec | 11-Dec | 11-Dec | 11-Dec | 11-Dec | 11-Dec |
|---|---|---|---|---|---|---|---|---|---|---|---|---|
| Time | 13:25 | 13:58 | 14:04 | 14:24 | 14:51 | 15:05 | 15:28 | 16:03 | 16:09 | 16:13 | 16:24 | 16:37 |
| Firing Side | L | R | R | L | R | R | L | R | R | R | L | L |
| Sample Position | Stack | Stack | Stack | Stack | Stack | Stack | Stack | Stack | Stack | Stack | Stack | Stack |
| O2, % | 6.28 | 6.55 | 6.71 | 6.42 | 6.45 | 6.8 | 6.7 | 0.8 | 0.5 | 0.53 | 6.5 | 6.67 |
| CO, ppm | 7 | 700 | 7.28 | 4 | 620 | 700 | 2 | 1200 | >1215 | >1215 | 143 | 4 |
| CO2, % | 9.5 | 9.3 | 9.2 | 9.3 | 9.3 | - | 9.1 | 12.9 | 12.7 | 11.9 | 9.7 | 9.4 |
| NOx, ppm | 506 | 330 | 336 | 530 | 342 | 360 | 520 | 580 | 480 | 338 | 470 | 485 |
| Staging | OEAS | OEAS | OEAS | OEAS | OEAS | OEAS | OEAS | OEAS | OEAS | OEAS | OEAS | OEAS |
| Staging O2 | 3400 | 3810 | 4275 | 4275 | 4275 | 4275 | 4275 | 4275 | 4275 | 4275 | 4275 | 4275 |
| Staging Air | 23765 | 26600 | 29890 | 29890 | 29890 | 35500 | 35500 | 35500 | 35500 | 35500 | 35500 | 35500 |
| PSR | 1.06 | 1.07 | 1.08 | 1.07 | 1.07 | 1.07 | 1.07 | 1.07 | 1.07 | 1.07 | 1.07 | 1.09 |
| OSR | 1.14 | 1.16 | 1.17 | 1.17 | 1.17 | 1.18 | 1.18 | 1.18 | 1.18 | 1.19 | 1.19 | 1.20 |
| NOx, 0% O2 | 721.38 | 479.58 | 493.77 | 763.37 | 493.61 | 532.39 | 763.84 | 602.97 | 491.71 | 346.75 | 680.69 | 710.75 |
| NOx, lb/ton | 2.84 | 1.89 | 1.93 | 3.06 | 1.98 | 2.13 | 3.06 | 2.46 | 2.01 | 1.42 | 2.78 | 2.91 |
| CO, 0% O2 | 9.99 | 1017.30 | 10.70 | 5.76 | 894.85 | 1035.21 | 2.94 | 1247.52 | NA | NA | 207.10 | 5.86 |

| | 11-Dec | 11-Dec | 11-Dec | 11-Dec | 11-Dec | 11-Dec | 11-Dec | 12-Dec | 12-Dec | 12-Dec | 12-Dec | 12-Dec |
|---|---|---|---|---|---|---|---|---|---|---|---|---|
| Time | 16:54 | 17:03 | 17:09 | 17:29 | 17:37 | 17:58 | 18:08 | 8:58 | 9:20 | 9:58 | 10:20 | 10:25 |
| Firing Side | R | R | R | L | L | R | R | L | R | L | R | R |
| Sample Position | Stack | Stack | Stack | Stack | Stack | Stack | Stack | Stack | Stack | Stack | Stack | Stack |
| O2, % | 6.6 | 6.51 | 6.34 | 6.37 | 6.55 | 6.62 | 6.48 | 5.3 | 6.4 | 6.5 | 6.79 | 6.29 |
| CO, ppm | >1214 | 898 | 800 | 256 | 25 | 704 | 523 | 2 | 254 | 2 | 460 | >1215 |
| CO2, % | 9.3 | 9.2 | 9.3 | 9.4 | 9.2 | 9 | 8.9 | 10.3 | 10 | 9.9 | 9.8 | 9.9 |
| NOx, ppm | 290 | 314 | 325 | 496 | 518 | 387 | 367 | 640 | 450 | 630 | 450 | 410 |
| Staging | OEAS | OEAS | OEAS | OEAS | OEAS | OEAS | OEAS | OEAS | OEAS | OEAS | OEAS | no |
| Staging O2 | 4275 | 5150 | 6500 | 3400 | 3400 | 3400 | 4275 | 4275 | 4275 | 4275 | 4275 | 0 |
| Staging Air | 35500 | 34000 | 33300 | 23765 | 23765 | 23765 | 29890 | 29890 | 29890 | 29890 | 33300 | 0 |
| PSR | 1.09 | 1.09 | 1.09 | 1.09 | 1.13 | 1.13 | 1.13 | 1.14 | 1.14 | 1.13 | 1.13 | 1.13 |
| OSR | 1.20 | 1.21 | 1.22 | 1.17 | 1.21 | 1.21 | 1.23 | 1.24 | 1.24 | 1.24 | 1.24 | 1.13 |
| NOx, 0% O2 | 422.92 | 455.07 | 465.55 | 711.96 | 752.80 | 535.95 | 530.79 | 856.05 | 647.26 | 912.41 | 665.02 | 585.32 |
| NOx, lb/ton | 1.73 | 1.85 | 1.88 | 2.93 | 3.10 | 2.21 | 2.17 | 3.43 | 2.60 | 3.66 | 2.67 | 2.41 |
| CO, 0% O2 | NA | 1301.45 | 1145.98 | 367.46 | 36.33 | 1028.09 | 756.40 | 2.68 | 365.34 | 2.90 | 679.80 | NA |

| | 12-Dec | 12-Dec | 12-Dec | 12-Dec | 12-Dec | 12-Dec | 12-Dec | 12-Dec | 12-Dec | 12-Dec | 12-Dec | 12-Dec |
|---|---|---|---|---|---|---|---|---|---|---|---|---|
| Time | 10:30 | 10:54 | 11:13 | 11:22 | 11:25 | 11:29 | 11:33 | 11:37 | 11:39 | 11:55 | 12:18 | 12:54 |
| Firing Side | R | L | R | R | R | R | R | R | R | L | R | L |
| Sample Position | Stack | Stack | Stack | L6 | L5 | L4 | L3 | L2 | L1 | Stack | Stack | Stack |
| O2, % | 6.42 | 6.3 | 6.26 | 0.54 | 0.5 | 0.5 | 0.75 | 1.75 | 2.5 | 6.06 | 6.3 | 6.84 |
| CO, ppm | 900 | 314 | 760 | >1218 | >1215 | >1215 | 900 | 32 | 33 | 160 | 1130 | 2 |
| CO2, % | 9.7 | 9.7 | 9.8 | 12.5 | 12.2 | 13.6 | 14.2 | 12.8 | 13.8 | 9.8 | 9.3 | 9.2 |
| NOx, ppm | 440 | 830 | 450 | 800 | 620 | 600 | 610 | 640 | 560 | 610 | 410 | 674 |
| Staging | no | no | no | no | no | no | no | no | no | no | no | OEAS |
| Staging O2 | 0 | 0 | 0 | 0 | 0 | 0 | 0 | 0 | 0 | 0 | 0 | 3400 |
| Staging Air | 0 | 0 | 0 | 0 | 0 | 0 | 0 | 0 | 0 | 0 | 0 | 23765 |
| PSR | 1.16 | 1.17 | 1.17 | 1.17 | 0.96 | 0.96 | 1.17 | 1.17 | 1.17 | 1.17 | 1.17 | 1.18 |
| OSR | 1.16 | 1.17 | 1.17 | 1.17 | 0.96 | 0.96 | 1.17 | 1.17 | 1.17 | 1.17 | 1.17 | 1.27 |
| NOx, 0% O2 | 633.74 | 900.00 | 641.11 | 821.11 | 635.12 | 614.63 | 632.59 | 598.18 | 635.68 | 857.43 | 585.71 | 999.58 |
| NOx, lb/ton | 2.61 | 3.71 | 2.64 | 3.38 | 2.62 | 2.53 | 2.61 | 2.88 | 2.62 | 3.53 | 2.41 | 4.03 |
| CO, 0% O2 | 1296.30 | 448.57 | 1082.77 | NA | NA | NA | 933.33 | 34.91 | 37.46 | 224.90 | 1614.29 | 2.97 |

| | 12-Dec | 12-Dec | 12-Dec | 12-Dec | 12-Dec | 12-Dec | 12-Dec | 12-Dec | 12-Dec | 12-Dec | 12-Dec | 12-Dec |
|---|---|---|---|---|---|---|---|---|---|---|---|---|
| Time | 13:24 | 13:53 | 14:21 | 14:30 | 14:58 | 15:06 | 15:28 | 15:34 | 16:00 | 16:28 | 16:35 | 17:04 |
| Firing Side | R | L | R | R | L | L | R | R | L | R | R | L |
| Sample Position | Stack | Stack | Stack | Stack | Stack | Stack | Stack | Stack | Stack | Stack | Stack | Stack |
| O2, % | 6.97 | 6.98 | 7 | 7.06 | 7.07 | 6.82 | 6.7 | 7.28 | 7.32 | 7.4 | 7.3 | 7.32 |
| CO, ppm | 42 | 3 | 21 | 110 | 3 | 3 | 550 | 400 | 2 | 33 | 140 | 3 |
| CO2, % | 9.2 | 9.3 | 9.2 | 9.2 | 9.1 | 9.1 | 9.1 | 8.8 | 9 | 8.8 | 8.9 | 8.8 |
| NOx, ppm | 470 | 663 | 480 | 452 | 674 | 622 | 410 | 420 | 670 | 450 | 440 | 680 |
| Staging | yes | OEAS | yes | yes | OEAS | OEAS | air | air | OEAS | OEAS | OEAS | OEAS |
| Staging O2 | 3400 | 3400 | 3400 | 4714 | 4714 | 0 | 0 | 0 | 2000 | 2000 | 2000 | 2000 |
| Staging Air | 23765 | 23765 | 23765 | 32950 | 32950 | 40000 | 35000 | 49000 | 39000 | 47000 | 38750 | 38750 |
| PSR | 1.18 | 1.18 | 1.20 | 1.18 | 1.18 | 1.17 | 1.18 | 1.18 | 1.18 | 1.18 | 1.18 | 1.18 |
| OSR | 1.26 | 1.26 | 1.29 | 1.29 | 1.29 | 1.26 | 1.25 | 1.29 | 1.28 | 1.30 | 1.28 | 1.28 |
| NOx, 0% O2 | 703.49 | 993.08 | 720.00 | 680.92 | 1016.08 | 921.16 | 602.10 | 642.86 | 1028.51 | 694.85 | 674.45 | 1043.86 |
| NOx, lb/ton | 2.84 | 4.01 | 2.85 | 2.57 | 3.98 | 3.72 | 2.43 | 2.60 | 4.10 | 2.71 | 2.63 | 4.07 |
| CO, 0% O2 | 62.87 | 4.49 | 31.50 | 165.71 | 4.52 | 4.44 | 807.69 | 612.24 | 3.07 | 50.96 | 214.60 | 4.61 |

| | 12-Dec | 13-Dec | 13-Dec | 13-Dec | 13-Dec | 13-Dec | 13-Dec | 13-Dec | 13-Dec | 13-Dec | 13-Dec | 13-Dec |
|---|---|---|---|---|---|---|---|---|---|---|---|---|
| Time | 17:27 | 8:54 | 9:17 | 9:17 | 10:06 | 10:20 | 10:45 | 10:55 | 11:50 | 11:52 | 12:31 | 12:48 |
| Firing Side | R | R | L | R | R | L | R | R | L | R | L | R |
| Sample Position | Stack | Stack | Stack | Stack | Stack | Stack | Stack | Stack | Stack | Stack | Stack | Stack |
| O2, % | 7.24 | 7.18 | 6.95 | 7.01 | 6.64 | 6.59 | 6.94 | 7.03 | 6.79 | 7.39 | 6.3 | 6.54 |
| CO, ppm | 129 | 40 | 2 | 296 | over | 2 | 223 | 60 | 2 | 6 | 180 | over |
| CO2, % | 8.7 | 8.9 | 8.9 | 8.6 | 8.9 | 8.9 | 8.7 | 8.5 | 8.5 | 8 | 8.8 | 9.3 |
| NOx, ppm | 426 | 390 | 565 | 367 | 320 | 619 | 425 | 450 | 630 | 510 | 520 | 283 |
| Staging | OEAS | yes | yes | yes | no | no | no | no | no | no | no | no |
| Staging O2 | 2000 | 2000 | 2000 | 0 | 0 | 0 | 0 | 0 | 0 | 0 | 0 | 0 |
| Staging Air | 48500 | 48500 | 48500 | 49000 | 0 | 0 | 0 | 0 | 0 | 0 | 0 | 0 |
| PSR | 1.18 | 1.14 | 1.14 | 1.13 | 1.13 | 1.18 | 1.18 | 1.21 | 1.21 | 1.25 | 1.13 | 1.13 |
| OSR | 1.31 | 1.27 | 1.27 | 1.24 | 1.13 | 1.18 | 1.18 | 1.21 | 1.21 | 1.25 | 1.13 | 1.13 |
| NOx, 0% O2 | 650.15 | 592.62 | 844.48 | 550.89 | 467.97 | 902.08 | 634.78 | 676.45 | 931.03 | 786.92 | 742.88 | 411.00 |
| NOx, lb/ton | 2.54 | 2.26 | 3.22 | 2.13 | 1.81 | 3.49 | 2.46 | 2.62 | 3.60 | 3.05 | 2.87 | 1.59 |
| CO, 0% O2 | 198.88 | 60.78 | 2.99 | 444.32 | NA | 2.91 | 333.07 | 90.19 | 2.96 | 9.28 | 257.14 | NA |

| | 13-Dec | 13-Dec | 13-Dec | 13-Dec | 13-Dec | 13-Dec | 13-Dec | 13-Dec | 13-Dec | 13-Dec | 13-Dec | 13-Dec |
|---|---|---|---|---|---|---|---|---|---|---|---|---|
| Time | 13:04 | 13:24 | 13:54 | 14:30 | 14:54 | 15:07 | 15:23 | 15:49 | 16:00 | 16:12 | 16:25 | 16:31 |
| Firing Side | R | L | R | L | R | R | L | R | R | R | L | L |
| Sample Position | Stack | Stack | Stack | Stack | Stack | Stack | Stack | Stack | Stack | Stack | Stack | Stack |
| O2, % | 6.85 | 6.83 | 7.23 | 6.65 | 7.39 | 7.8 | 7.57 | 7.61 | 7.55 | 7.53 | 7.46 | 7.45 |
| CO, ppm | 762 | 3 | 606 | 3 | 296 | 35 | 5 | 30 | 60 | 57 | 2 | 3 |
| CO2, % | 9.2 | 9.2 | 8.9 | 9.1 | 9 | 8.9 | 9 | 9.1 | 9.4 | 9.3 | 9.6 | 9.6 |
| NOx, ppm | 337 | 550 | 341 | 547 | 378.8 | 405 | 625 | 407 | 381 | 382 | 600 | 580 |
| Staging | yes | yes | yes | yes | yes | yes | yes | yes | yes | yes | yes | yes |
| Staging O2 | 3058 | 3050 | 3050 | 2050 | 2000 | 2000 | 2000 | 7000 | 10000 | 10000 | 10000 | 10000 |
| Staging Air | 28500 | 37000 | 47000 | 47000 | 47000 | 47000 | 47000 | 44000 | 42000 | 42000 | 33000 | 23000 |
| PSR | 1.13 | 1.12 | 1.13 | 1.13 | 1.15 | 1.19 | 1.19 | 1.14 | 1.11 | 1.10 | 1.10 | 1.10 |
| OSR | 1.22 | 1.24 | 1.27 | 1.25 | 1.27 | 1.31 | 1.31 | 1.30 | 1.29 | 1.29 | 1.27 | 1.24 |
| NOx, 0% O2 | 500.14 | 815.10 | 520.04 | 800.49 | 584.17 | 644.32 | 977.29 | 638.31 | 594.87 | 595.55 | 930.58 | 898.89 |
| NOx, lb/ton | 1.89 | 3.09 | 1.97 | 3.05 | 2.28 | 2.52 | 3.82 | 2.41 | 2.20 | 2.20 | 3.44 | 3.32 |
| CO, 0% O2 | 1130.88 | 4.45 | 924.18 | 4.39 | 456.72 | 55.68 | 7.82 | 47.05 | 93.68 | 88.86 | 3.10 | 4.65 |

| | 13-Dec | 13-Dec | 13-Dec | 13-Dec | 13-Dec | 14-Dec | 14-Dec | 18-Feb | 18-Feb | 18-Feb | 18-Feb | 18-Feb |
|---|---|---|---|---|---|---|---|---|---|---|---|---|
| Time | 18:39 | 16:59 | 17:06 | 17:20 | 12:58 | 8:49 | 9:18 | 10:53 | 11:27 | 12:00 | 12:30 | 14:31 |
| Firing Side | L | R | R | L | R | L | R | L | R | L | R | R |
| Sample Position | Stack | Stack | Stack | Stack | Stack | Stack | Stack | Stack | Stack | Stack | Stack | Stack |
| O2, % | 7.16 | 7.5 | 7.96 | 7.93 | 6.76 | 7.4 | 8.1 | 7.75 | 7.44 | 7.22 | 7.2 | 5.54 |
| CO, ppm | 3 | 15 | 3 | 3 | 684 | 3 | 3 | 5 | 5 | 5 | 5 | 930 |
| CO2, % | 9.8 | 9.2 | 8.5 | 8.8 | 9.3 | 8.9 | 8.8 | 9 | 9 | 9 | 8.9 | 10.4 |
| NOx, ppm | 560 | 420 | 486 | 725 | 329 | 760 | 571 | 686 | 679 | 730 | 663 | 329 |
| Staging | yes | yes | yes | yes | yes | yes | yes | no | no | no | no | yes |
| Staging O2 | 10000 | 10000 | 2000 | 2000 | 3056 | 2000 | 2000 | 0 | 0 | 0 | 0 | 4450 |
| Staging Air | 15000 | 42000 | 48000 | 47000 | 21389 | 38600 | 48260 | 0 | 0 | 0 | 0 | 29270 |
| PSR | 1.10 | 1.12 | 1.24 | 1.24 | 1.13 | 1.28 | 1.28 | 1.34 | 1.32 | 1.32 | 1.32 | 1.02 |
| OSR | 1.23 | 1.31 | 1.36 | 1.36 | 1.21 | 1.36 | 1.38 | 1.34 | 1.32 | 1.32 | 1.32 | 1.14 |
| NOx, 0% O2 | 849.71 | 653.33 | 782.87 | 1164.88 | 485.18 | 1173.53 | 929.53 | 1087.25 | 1051.55 | 1112.48 | 1008.91 | 446.90 |
| NOx, lb/ton | 3.13 | 2.47 | 3.12 | 4.65 | 1.84 | 4.73 | 3.75 | 4.22 | 4.08 | 4.32 | 3.87 | 1.62 |
| CO, 0% O2 | 4.55 | 23.33 | 4.83 | 4.82 | 1008.71 | 4.63 | 4.88 | 7.92 | 7.74 | 7.62 | 7.61 | 1263.26 |

| | 18-Feb | 18-Feb | 18-Feb | 18-Feb | 18-Feb | 18-Feb | 18-Feb | 18-Feb | 18-Feb | 18-Feb | 18-Feb | 18-Feb |
|---|---|---|---|---|---|---|---|---|---|---|---|---|
| Time | 14:31 | 14:42 | 14:52 | 14:58 | 15:07 | 15:30 | 15:37 | 15:55 | 16:04 | 16:18 | 16:25 | 16:37 |
| Firing Side | R | R | L | L | L | R | R | L | L | L | R | R |
| Sample Position | Stack | Stack | Stack | Stack | Stack | Stack | Stack | Stack | Stack | Stack | Stack | Stack |
| O2, % | 5.7 | 5.96 | 5.65 | 5.84 | 6.28 | 5.88 | 5.97 | 5.88 | 6.13 | 6.41 | 6.01 | 6.13 |
| CO, ppm | 693 | 242 | over | 351 | 19 | 219 | 13 | 437 | 105 | 7 | 92 | 5 |
| CO2, % | 10.3 | 10.4 | 10.1 | 10.1 | 10.1 | 909 | 9.8 | 9.7 | 9.6 | 9.3 | 9.7 | 9.5 |
| NOx, ppm | 358 | 328.6 | 307 | 392 | 431 | 410 | 440 | 391 | 442 | 470 | 428 | 484 |
| Staging | yes | yes | yes | yes | yes | yes | yes | yes | yes | yes | yes | yes |
| Staging O2 | 8310 | 12970 | 4290 | 8430 | 12699 | 4350 | 5130 | 4390 | 5000 | 3510 | 3510 | 4930 |
| Staging Air | 35340 | 35790 | 29860 | 33135 | 36410 | 30050 | 35350 | 30110 | 35500 | 25430 | 25370 | 32960 |
| PSR | 1.02 | 1.01 | 1.02 | 1.02 | 1.02 | 1.07 | 1.07 | 1.06 | 1.06 | 1.11 | 1.11 | 1.11 |
| OSR | 1.19 | 1.23 | 1.13 | 1.18 | 1.23 | 1.19 | 1.21 | 1.18 | 1.20 | 1.20 | 1.21 | 1.24 |
| NOx, 0% O2 | 488.63 | 458.82 | 420.00 | 543.01 | 614.88 | 569.44 | 614.77 | 543.06 | 624.21 | 676.49 | 599.60 | 683.52 |
| NOx, lb/ton | 1.72 | 1.56 | 1.53 | 1.91 | 2.10 | 2.07 | 2.22 | 1.97 | 2.26 | 2.48 | 2.19 | 2.48 |
| CO, 0% O2 | 951.18 | 337.90 | NA | 486.21 | 27.11 | 304.17 | 18.16 | 606.94 | 148.29 | 10.08 | 128.89 | 7.06 |

| | 18-Feb | 18-Feb | 18-Feb | 19-Feb | 19-Feb | 19-Feb | 19-Feb | 19-Feb | 19-Feb | 19-Feb | 19-Feb | 19-Feb |
|---|---|---|---|---|---|---|---|---|---|---|---|---|
| Time | 16:57 | 17:13 | 17:35 | 9:00 | 9:33 | 10:05 | 10:31 | 11:05 | 14:34 | 15:03 | 15:37 | 15:45 |
| Firing Side | L | L | R | R | L | R | L | R | L | R | L | L |
| Sample Position | Stack | Stack | Stack | Stack | Stack | Stack | Stack | Stack | Stack | Stack | Stack | Stack |
| O2, % | 6.51 | 7.41 | 7.29 | 7.85 | 7.99 | 7.4 | 7.45 | 7.1 | 6.49 | 6.15 | 6.52 | 6.81 |
| CO, ppm | 5 | 5 | 5 | 3 | 4 | 4 | 4 | 4 | 48 | 4 | 20 | 3 |
| CO2, % | 9.1 | 8.2 | 8.3 | 8.9 | 8 | NA | 8.8 | NA | 9 | 9 | 8.6 | 8.5 |
| NOx, ppm | 489 | 712 | 659 | 681 | 653 | 640 | 635 | 640 | 465 | 510 | 446 | 438 |
| Staging | yes | no | no | no | no | no | no | no | yes | yes | yes | yes |
| Staging O2 | 4490 | 0 | 0 | 0 | 0 | 0 | 0 | 0 | 2160 | 2190 | 2670 | 3740 |
| Staging Air | 33050 | 0 | 0 | 0 | 0 | 0 | 0 | 0 | 15380 | 17000 | 18270 | 28710 |
| PSR | 1.12 | 1.32 | 1.34 | 1.30 | 1.30 | 1.30 | 1.28 | 1.28 | 1.14 | 1.14 | 1.15 | 1.15 |
| OSR | 1.24 | 1.32 | 1.34 | 1.30 | 1.30 | 1.30 | 1.28 | 1.28 | 1.20 | 1.21 | 1.21 | 1.25 |
| NOx, 0% O2 | 708.70 | 1100.22 | 1009.41 | 1055.59 | 1054.04 | 988.24 | 984.13 | 966.91 | 672.98 | 721.21 | 646.82 | 648.20 |
| NOx, lb/ton | 2.58 | 4.13 | 3.79 | 4.01 | 4.00 | 3.75 | 3.74 | 3.67 | 2.52 | 2.70 | 2.41 | 2.40 |
| CO, 0% O2 | 7.25 | 7.73 | 7.66 | 4.79 | 6.46 | 6.18 | 6.20 | 6.04 | 69.47 | 5.68 | 29.01 | 4.44 |

| | 19-Feb | 19-Feb | 20-Feb | 20-Feb | 20-Feb | 20-Feb | 20-Feb | 20-Feb | 20-Feb | 20-Feb | 20-Feb | 20-Feb |
|---|---|---|---|---|---|---|---|---|---|---|---|---|
| Time | 16:13 | 16:42 | 9:00 | 9:29 | 9:59 | 10:10 | 10:45 | 10:57 | 11:07 | 11:16 | 11:27 | 11:34 |
| Firing Side | R | L | L | R | L | L | R | L | L | L | R | R |
| Sample Position | Stack | Stack | Stack | Stack | Stack | Stack | Stack | Stack | Stack | Stack | Stack | Stack |
| O2, % | 5.94 | 6.64 | 7.31 | 6.27 | 6.75 | 6.51 | 6.4 | 6.68 | 6.73 | 6.73 | 6.4 | 6.51 |
| CO, ppm | 3 | 3 | 1 | 2 | 2 | 18 | 1 | 54 | 15 | 4 | 2 | 2 |
| CO2, % | 8.9 | 8.7 | 9.7 | 10.1 | 9.7 | 9.6 | 9.7 | 9.5 | 9.6 | 9.2 | 9.8 | 9.7 |
| NOx, ppm | 442 | 409 | 450 | 480 | 400 | 390 | 517 | 390 | 426 | 390 | 501 | 524 |
| Staging | yes | yes | yes | yes | yes | yes | yes | yes | yes | yes | yes | yes |
| Staging O2 | 4320 | 7570 | 6800 | 4560 | 5740 | 4840 | 3420 | 6300 | 7900 | 2200 | 4560 | 8100 |
| Staging Air | 29100 | 40460 | 38000 | 2582 | 32000 | 26100 | 17900 | 17900 | 11600 | 38400 | 12940 | 12200 |
| PSR | 1.09 | 1.08 | 1.09 | 1.09 | 1.08 | 1.09 | 1.08 | 1.08 | 1.09 | 1.09 | 1.08 | 1.08 |
| OSR | 1.20 | 1.25 | 1.24 | 1.14 | 1.21 | 1.20 | 1.16 | 1.19 | 1.19 | 1.20 | 1.15 | 1.19 |
| NOx, 0% O2 | 616.33 | 598.12 | 690.28 | 684.32 | 589.47 | 565.22 | 743.63 | 571.93 | 626.91 | 573.93 | 720.62 | 759.42 |
| NOx, lb/ton | 2.27 | 2.15 | 2.50 | 2.51 | 2.15 | 2.07 | 2.75 | 2.07 | 2.24 | 2.15 | 2.64 | 2.71 |
| CO, 0% O2 | 4.18 | 4.39 | 1.53 | 2.85 | 2.95 | 26.09 | 1.44 | 79.19 | 22.07 | 5.89 | 2.88 | 2.90 |

| | 20-Feb | 20-Feb | 20-Feb | 20-Feb | 20-Feb | 20-Feb | 20-Feb | 20-Feb | 20-Feb | 20-Feb | 20-Feb | 20-Feb |
|---|---|---|---|---|---|---|---|---|---|---|---|---|
| Time | 11:40 | 11:56 | 12:00 | 12:05 | 12:09 | 12:15 | 12:18 | 12:27 | 12:33 | 12:37 | 12:41 | 12:46 |
| Firing Side | R | L | L | L | L | L | L | R | R | R | R | R |
| Sample Position | Stack | R6 | R5 | R4 | R3 | R2 | R1 | L6 | L5 | L4 | L3 | L2 |
| O2, % | 6.17 | 1.29 | 0.81 | 1.35 | 2.75 | 3.28 | 5.1 | 0.54 | 0.25 | 0.1 | 0.95 | 1.24 |
| CO, ppm | 2 | 1050 | >1226 | 800 | 25 | 16 | 11 | 500 | >1226 | >1226 | 170 | 27 |
| CO2, % | 9.5 | 12.7 | 13.8 | 13.4 | 13 | 11.8 | 11.5 | 12.7 | 13.3 | 13.6 | 13.8 | 13.9 |
| NOx, ppm | 453 | 470 | 415 | 523 | 529 | 520 | 493 | 527 | 529 | 573 | 694 | 636 |
| Staging | yes | yes | yes | yes | yes | yes | yes | yes | yes | yes | yes | yes |
| Staging O2 | 2500 | 5000 | 5000 | 4900 | 4900 | 4900 | 5200 | 5200 | 4900 | 5530 | 5100 | 5800 |
| Staging Air | 39100 | 26000 | 27800 | 27800 | 27000 | 27800 | 29700 | 28500 | 27400 | 31280 | 29200 | 32200 |
| PSR | 1.08 | 1.08 | 1.08 | 1.08 | 1.09 | 1.08 | 1.08 | 1.08 | 1.08 | 1.08 | 1.08 | 1.08 |
| OSR | 1.20 | 1.19 | 1.20 | 1.19 | 1.20 | 1.19 | 1.20 | 1.20 | 1.20 | 1.21 | 1.19 | 1.21 |
| NOx, 0% O2 | 641.47 | 500.78 | 431.85 | 558.93 | 608.71 | 816.25 | 651.13 | 540.91 | 535.37 | 575.74 | 728.88 | 875.91 |
| NOx, lb/ton | 2.39 | 1.83 | 1.58 | 2.05 | 2.23 | 2.26 | 2.38 | 1.98 | 1.96 | 2.10 | 2.66 | 2.46 |
| CO, 0% O2 | 2.83 | 1118.72 | NA | 854.98 | 28.77 | 13.96 | 14.53 | 513.20 | NA | NA | 178.05 | 28.69 |

| | 20-Feb | 20-Feb | 20-Feb | 20-Feb | 20-Feb | 20-Feb | 20-Feb | 20-Feb | 20-Feb | 20-Feb | 20-Feb | 20-Feb |
|---|---|---|---|---|---|---|---|---|---|---|---|---|
| Time | 12:52 | 13:06 | 13:13 | 13:33 | 13:45 | 14:06 | 14:23 | 14:36 | 14:44 | 15:07 | 15:22 | 15:37 |
| Firing Side | R | L | L | R | R | L | L | R | R | L | L | R |
| Sample Position | L1 | Stack | Stack | Stack | Stack | Stack | Stack | Stack | Stack | Stack | Stack | Stack |
| O2, % | 2.28 | 6.58 | 6.51 | 6.3 | 6.4 | 6.92 | 6.89 | 6.41 | 6.32 | 6.81 | 6.75 | 6.71 |
| CO, ppm | 18 | 90 | 9 | 2 | 2 | 2 | 2 | 1 | 2 | 2 | 4 | 2 |
| CO2, % | 13.1 | 8.8 | 8.8 | 9 | 8.9 | 8.6 | 8.7 | 9 | 9 | 8.9 | 8.7 | 8.8 |
| NOx, ppm | 538 | 430 | 427 | 520 | 521 | 446 | 444 | 546 | 528 | 460 | 482 | 512 |
| Staging | yes | yes | yes | yes | yes | yes | yes | yes | yes | yes | yes | yes |
| Staging O2 | 5300 | 3100 | 4000 | 3100 | 1290 | 5150 | 6510 | 3640 | 1950 | 8300 | 5530 | 4770 |
| Staging Air | 30000 | 16100 | 22000 | 17300 | 22190 | 28970 | 18940 | 19850 | 10610 | 12790 | 10460 | 28720 |
| PSR | 1.07 | 1.14 | 1.13 | 1.14 | 1.13 | 1.13 | 1.14 | 1.13 | 1.13 | 1.13 | 1.13 | 1.14 |
| OSR | 1.19 | 1.20 | 1.22 | 1.21 | 1.19 | 1.25 | 1.24 | 1.21 | 1.17 | 1.24 | 1.21 | 1.25 |
| NOx, 0% O2 | 603.53 | 626.21 | 618.84 | 742.86 | 749.38 | 665.20 | 660.81 | 785.88 | 755.31 | 680.76 | 710.32 | 752.41 |
| NOx, lb/ton | 2.20 | 2.33 | 2.28 | 2.76 | 2.82 | 2.44 | 2.40 | 2.91 | 2.83 | 2.44 | 2.59 | 2.76 |
| CO, 0% O2 | 20.19 | 131.07 | 13.04 | 2.86 | 2.88 | 2.98 | 2.98 | 1.44 | 2.86 | 2.96 | 5.89 | 2.94 |

| | 20-Feb | 20-Feb | 20-Feb | 20-Feb | 20-Feb | 20-Feb | 20-Feb | 20-Feb | 20-Feb | 20-Feb | 20-Feb | 20-Feb |
|---|---|---|---|---|---|---|---|---|---|---|---|---|
| Time | 16:00 | 16:04 | 16:07 | 16:12 | 16:16 | 16:20 | 16:31 | 16:35 | 16:40 | 16:44 | 16:50 | 16:56 |
| Firing Side | L | L | L | L | L | L | R | R | R | R | R | R |
| Sample Position | R1 | R2 | R3 | R4 | R5 | R6 | L1 | L2 | L3 | L4 | L5 | L6 |
| O2, % | 3.9 | 3 | 2.83 | 1.46 | 0.68 | 1.4 | 1.95 | 1.58 | 1.85 | 1.28 | 0.62 | 1.42 |
| CO, ppm | 9 | 15 | 20 | 340 | >1226 | 268 | 18 | 29 | 28 | 41 | 381 | 40 |
| CO2, % | 11.8 | 12.2 | 11.9 | 12.4 | 12.1 | 11.3 | 13 | 14.2 | 14.2 | 12.4 | 12.1 | 11.2 |
| NOx, ppm | 550 | 550 | 684 | 617 | 480 | 595 | 699 | 796 | 826 | 784 | 728 | 718 |
| Staging | yes | yes | yes | yes | yes | yes | yes | yes | yes | yes | yes | yes |
| Staging O2 | 2700 | 2700 | 2900 | 2500 | 2800 | 2800 | 2700 | 2600 | 2600 | 2700 | 2700 | 2700 |
| Staging Air | 15800 | 14600 | 15000 | 14800 | 16700 | 15800 | 15700 | 14900 | 15300 | 14200 | 15000 | 15000 |
| PSR | 1.13 | 1.13 | 1.13 | 1.13 | 1.12 | 1.13 | 1.13 | 1.13 | 1.13 | 1.13 | 1.14 | 1.13 |
| OSR | 1.19 | 1.19 | 1.19 | 1.19 | 1.19 | 1.20 | 1.19 | 1.19 | 1.19 | 1.19 | 1.20 | 1.20 |
| NOx, 0% O2 | 675.44 | 641.67 | 790.53 | 663.10 | 496.06 | 637.50 | 770.55 | 860.76 | 905.80 | 834.89 | 750.15 | 770.07 |
| NOx, lb/ton | 2.52 | 2.39 | 2.94 | 2.47 | 1.35 | 2.37 | 2.87 | 3.21 | 3.38 | 3.11 | 2.79 | 2.87 |
| CO, 0% O2 | 11.05 | 17.50 | 23.12 | 365.40 | NA | 287.14 | 19.84 | 31.36 | 30.70 | 43.66 | 392.59 | 42.90 |

| | 20-Feb | 20-Feb | 20-Feb | 20-Feb | 20-Feb | 21-Feb | 21-Feb | 21-Feb | 21-Feb | 21-Feb | 21-Feb | 21-Feb |
|---|---|---|---|---|---|---|---|---|---|---|---|---|
| Time | 17:08 | 17:16 | 17:23 | 17:37 | 17:45 | 9:40 | 10:06 | 10:18 | 10:33 | 10:48 | 11:07 | 11:19 |
| Firing Side | L | L | L | R | R | L | R | R | L | L | R | R |
| Sample Position | Stack | Stack | Stack | Stack | Stack | Stack | Stack | Stack | Stack | Stack | Stack | Stack |
| O2, % | 6.6 | 6.62 | 6.94 | 6.42 | 6.42 | 7.45 | 6.9 | 7.03 | 7.2 | 6.63 | 6.63 | 7.13 |
| CO, ppm | 60 | 5 | 2 | 2 | 2 | 2 | 2 | 2 | 3 | 2 | 2 | 1 |
| CO2, % | 8.3 | 8.1 | 8.2 | 8.4 | 8.5 | 10.1 | 9.9 | 9.6 | 9.3 | 9.5 | 9.5 | 9.5 |
| NOx, ppm | 453 | 472 | 452 | 507 | 545 | 442 | 520 | 538 | 460 | 486 | 537 | 537 |
| Staging | yes | yes | yes | yes | yes | yes | yes | yes | yes | yes | yes | yes |
| Staging O2 | 2600 | 3700 | 4700 | 4720 | 2530 | 5330 | 3650 | 4430 | 4470 | 3540 | 2200 | 5800 |
| Staging Air | 14200 | 19600 | 26000 | 26490 | 13280 | 28340 | 19800 | 24500 | 24820 | 19920 | 12880 | 32580 |
| PSR | 1.13 | 1.13 | 1.13 | 1.14 | 1.14 | 1.13 | 1.12 | 1.11 | 1.11 | 1.11 | 1.11 | 1.11 |
| OSR | 1.19 | 1.22 | 1.24 | 1.24 | 1.19 | 1.25 | 1.20 | 1.22 | 1.21 | 1.19 | 1.16 | 1.24 |
| NOx, 0% O2 | 660.63 | 689.29 | 675.11 | 730.25 | 784.98 | 685.02 | 774.47 | 808.73 | 700.00 | 710.23 | 828.60 | 813.05 |
| NOx, lb/ton | 2.46 | 2.55 | 2.48 | 2.68 | 2.93 | 2.51 | 2.86 | 2.97 | 2.57 | 2.63 | 3.10 | 2.96 |
| CO, 0% O2 | 87.50 | 7.30 | 2.99 | 2.88 | 2.88 | 3.10 | 2.98 | 3.01 | 4.57 | 2.92 | 2.92 | 1.51 |

| | 21-Feb | 21-Feb |
|---|---|---|
| Time | 11:39 | 11:49 |
| Firing Side | L | L |
| Sample Location | Stack | Stack |
| O2, % | 7.22 | 7.57 |
| CO, ppm | 400 | 3 |
| CO2, % | 9.7 | 9.5 |
| NOx, ppm | 457 | 463 |
| Staging | yes | yes |
| Staging O2 | 2390 | 6200 |
| Staging Air | 13720 | 34200 |
| PSR | 1.12 | 1.11 |
| OSR | 1.17 | 1.25 |
| NOx, 0% O2 | 696.44 | 723.98 |
| NOx, lb/ton | 2.60 | 2.63 |
| CO, 0% O2 | 609.58 | 4.69 |

# APPENDIX D
# BUSINESS PLAN

**OEAS**
**BUSINESS PLAN**
**(U.S. PATENT NO. 5,203,859)**

## TABLE OF CONTENTS


BACKGROUND ..... 1
- THE GLASS INDUSTRY ..... 1
- ENVIRONMENTAL REGULATIONS ..... 1
- THE OEAS TECHNOLOGY ..... 2

THE MARKET ..... 6
- GLASS PRODUCER REQUIREMENTS ..... 6
- OEAS SOLUTION ..... 6
- PRIMARY CUSTOMERS ..... 7
- COMPETITIVE SOLUTIONS & COSTS (CHART) ..... 7

100% Oxy-Fuel Fired Glass Furnaces ..... 8
Air Staging ..... 8
Fuel Staging or Cascade Heating For $NO_x$ Reduction ..... 8
Selective Catalytic (SCR) and Selective Non-Catalytic Reduction (SNCR) ..... 9
Pilkington 3R ..... 9

MARKET STRATEGY ..... 10
- SALES TACTICS ..... 11

General ..... 12
Oxygen Supply ..... 12
Compressed Air Supply ..... 12
RISKS & PROBLEMS ..... 13

OWNERSHIP and ROYALTIES ..... 13

# BACKGROUND

## THE GLASS INDUSTRY

The glass industry in the United States is reportedly the fourth largest industrial energy consumer. The majority of glass, representing container, flat, pressed, and blown, is produced in relatively large (100 to 1000 ton/day) regenerative glass tanks, which operate continuously for up to 10 years. The glass container segment alone, representing soda lime glasses in flint, amber, and green glass, accounts for about two-thirds of the total glass produced, and utilizes over 95 billion cuft of natural gas per year. Nearly all of the container and flat glass is produced in two types of regenerative furnaces - endport and sideport. Endport furnaces are smaller (100 to 400+ ton/day) with two ports located on one end of the glass tank. Sideport furnaces are larger (up to 1000 ton/day) with three to seven ports located on either side of the furnace. Container glass production is roughly split between the two furnace types, while nearly all of the flat glass is produced in sideport furnaces. A typical container glass furnace uses about $5 \times 10^6$ Btu's of energy per ton of glass produced, while a typical flat glass furnace uses about $7 \times 10^6$ Btu's. Overall, endport glass tanks consume 25 billion cubic feet of fuel to produce 5 million tons of glass, while sideport glass tanks consume 53 billion cubic feet of fuel to produce 9 million tons of glass. The bulk of the fuel represents natural gas, which is the fuel of choice, however, most of the glass furnaces utilize electric boosting, with the exception of flat glass furnaces, and a few use fuel oil. In this application, fuel oil produces somewhat lower $NO_x$ than natural gas.

## ENVIRONMENTAL REGULATIONS

The regenerative glass melters utilize extremely high combustion air preheat temperature (1800 to 2500 F) to improve production rate, product quality and furnace thermal efficiency. Furnace and flame temperatures and, consequently, $NO_x$ generation, are quite high. $NO_x$ emissions of over 3000 vppm are not uncommon[1,2] from natural gas-fired glass melters. The 1990 Clean Air Act establishes environmental objectives and directs the States to regulate emission sources to achieve these objectives. On a regional basis, these emissions are restricted in certain areas, the most stringent being in Southern California. The South Coast Air Quality Management District (Los Angeles area) currently restricts the $NO_x$ emissions from container glass melters to 4.0 lb/ton of glass produced. Even stricter regulations are now being considered for this region. The glass industry, in some cases, has been able to meet the current regulations through relatively simple combustion modification techniques, developed earlier [2,3] by IGT and Combustion Tec, Inc. (CTI) with funding support from GRI and SoCal Gas, and by increasing the electric boost as well as the percent of cullet in the feed. Some melters have been switched to fuel oil to control $NO_x$. Fuel oil does offer somewhat lower $NO_x$ emissions, but at the expense of additional $SO_x$ and particulate emissions, higher fuel system operating costs, and other operating problems. Further,

---

1 Barklage - Hilgefort, H., "Reduction of $NO_x$ Emission of Glass Melting Furnaces by Primary Measures."

2 Abbasi, H.A. and Fleming, D.K., "Development of $NO_x$ Control Methods for Glass Melting Furnaces." Final Report GRI-87/0202, Chicago, August 1987.

3 Abbasi, H.A., Khinkis, M.J. and Fleming, D.K., "Development of $NO_x$ Control Methods for Glass Melting Furnaces." Annual Report GRI-84/0053, Chicago, September 1983.

the presence of vanadium and sulfur, and the higher crown temperatures that result from oil firing somewhat reduce the furnace service life.[4] The high levels of electric boost currently utilized are also not desirable because of increased energy costs and reduced furnace service life.

## THE OEAS TECHNOLOGY

Oxygen enriched air staging (OEAS) is accomplished by reducing the combustion air flow (primary air) to the firing port and injecting oxygen enriched secondary air downstream. The bulk of the combustion is therefore relatively oxygen deficient (or fuel-rich) to inhibit $NO_x$ formation.

Splitting the combustion air in a regenerative glass tank is difficult because 1) it can require major modifications and 2) properly mixing the secondary air with the primary combustion gases requires higher secondary air pressures that are not desirable. A more attractive method is to operate the furnace with near-stoichiometric air and inject a small amount of high-velocity ambient secondary air near the exhaust port to burn out any residual CO and THC. This method of air staging was tested by IGT in its glass tank simulator using ambient secondary air and was found to be very effective in reducing $NO_x$ emissions.

Figure 1 shows that, in a furnace operating with a typical stoichiometric ratio of 1.15 (15 percent overall excess air), $NO_x$ reduction of 30 percent (from the current 4 lb/ton to 2.8 lb/ton) could be achieved by operating the port at a stoichiometric ratio of 1.04 to 1.06, which should not be very difficult. In the tests at IGT, there was a significant increase in heat transfer (Figure 2) at this level of primary air, even though the secondary air was ambient and was injected downstream of the exhaust port. The data also show that even greater $NO_x$ reductions could be achieved by further decreasing the primary stoichiometric ratio. The heat transfer would, however, somewhat decrease compared to the optimum at stoichiometric ratios of 1.04 to 1.06, but would be comparable to the levels achieved at 15 percent excess air.

In the marketed OEAS technique (Figure 3 and 4), secondary ambient air or oxygen enriched ambient air is injected into the melter upstream of the exhaust port. Through the use of a PLC system, the furnace operator is able to choose the second stage oxidant's flow rate and oxygen content. This will allow optimization of the staging system for operating costs, furnace effciency, and $NO_x$ control level. Using unenriched secondary ambient air may slightly adversly affect furnace efficiency, however it offers the lowest operating costs (i.e. no oxygen cost). Using oxygen enriched ambient air (up to 50% $O_2$ content) offers rapid CO and THC burnout within the melter, no adverse effects on furnace efficiency, and maximum $NO_x$ reduction; however its operating costs are relatively high compared to using unenriched air. Four (4) variations of air staging are being offered at this time and are listed below: The two OEAS systems offered are capable of air staging only with no oxygen enrichment.

1. Oxygen Enriched Air Staging (OEAS) using VSA oxygen and air blower.
2. Oxygen Enriched Air Staging (OEAS) using liquid oxygen and air blower.
3. Blower Air Staging (BAS)
4. Compressed Air Staging (CAS), offered on endport furnaces only at this time.

---

[4] Carvalho, M. and Lockwood, F.C., "Thermal Comparison of Glass Furnace Operation With Oil and Natural Gas," Glastech. Ber., 63, No., 9 (1990)

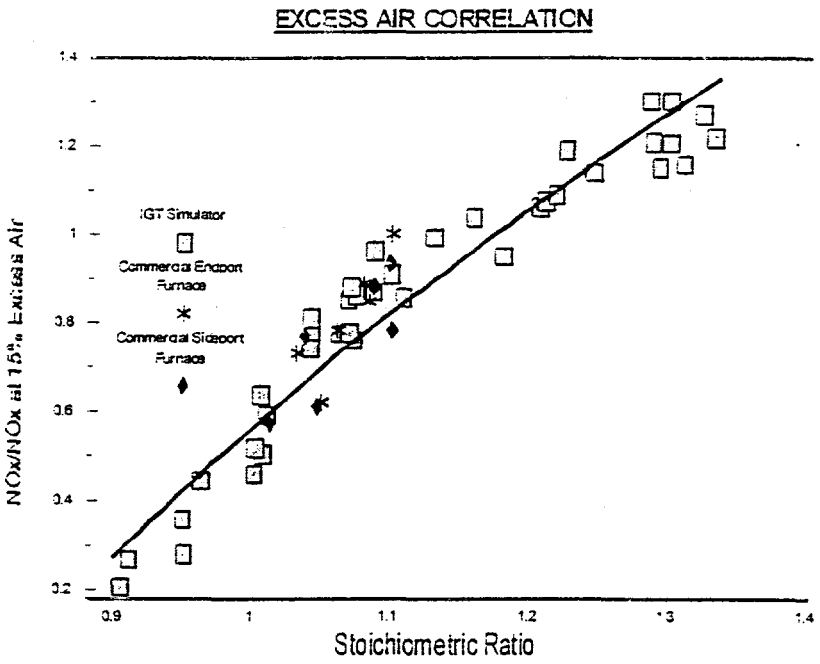


Figure 1. EFFECT OF FIRST-STAGE STOICHIOMETRIC RATIO ON NOx PRODUCTION
(IGT Simulator, 45÷Side-of-Port Burners, 23 m/s Fuel-Injection Velocity, 0.6 MWth Firing Rate, 1160 °C Combustion Air Temperature)

Curve Supplied by IGT

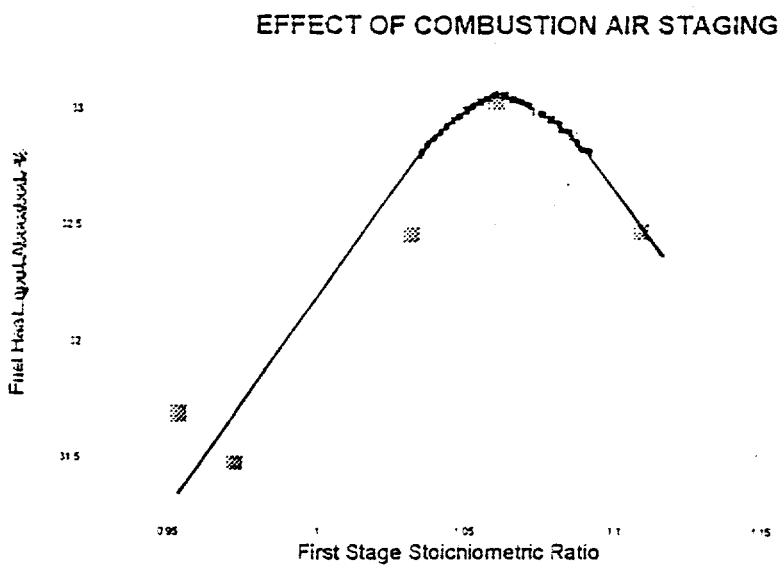


Figure 2. EFFECT OF FIRST-STAGE STOICHICMETRIC RATIO ON TOTAL HEAT ABSCRBED
(IGT Simulator, 45°Side-of-Port Burners, 23 m/s Fuel-Injection Velocity, 0.6 MWth Firing Rate, 1160°C Combustion Air Temperature)

Curve Supplied by IGT

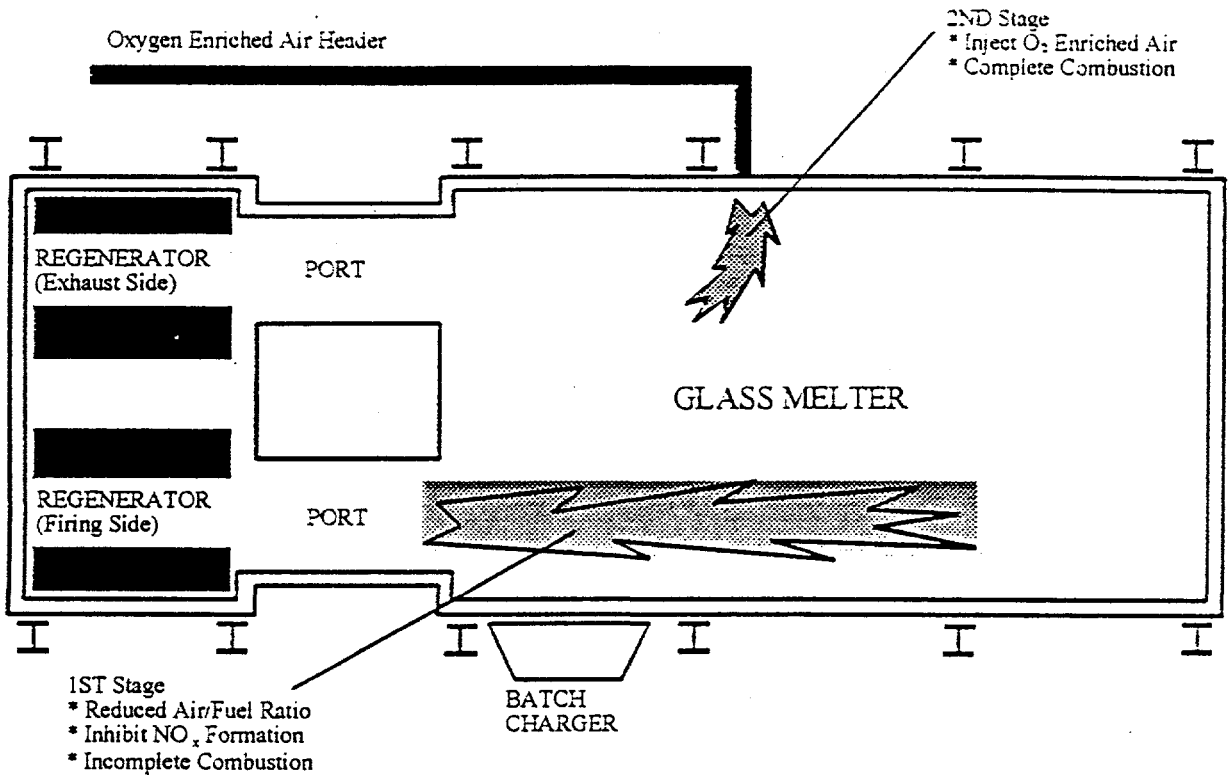


Figure 3. Oxygen Enriched Air Staging, Endport Furnace

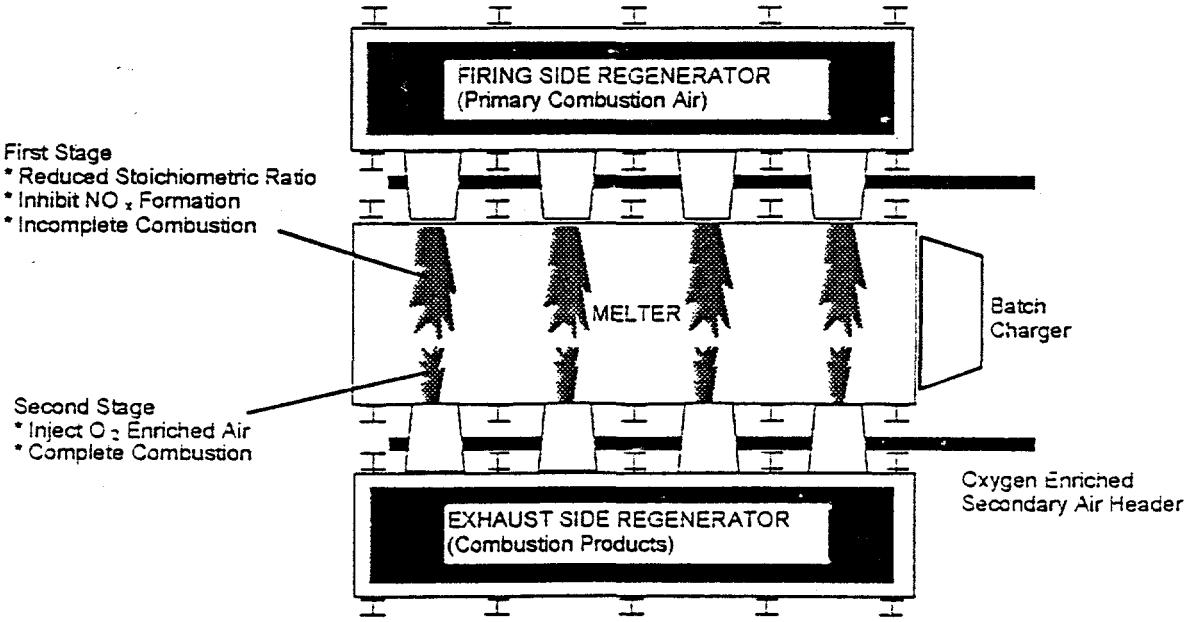


Figure 4. Oxygen Enriched Air Staging, Sideport Furnace

# THE MARKET

The OEAS Technology developed and described herein is applicable to staging on endport and sideport furnaces. In the U.S. market there are a total of approximately 500 major furnaces, consisting of sideports, endports, float glass furnaces (sideport furnaces), electric furnaces, direct fire furnaces, oxygen-fired furnaces, etc.

Considering the technology for endport and sideport furnaces which are the ones currently developed, we defer the fiberglass market since it is a direct-fired furnace.

Sales outside the U.S. are subject to non-infringement patent analysis to existing competing technologies, market demand with or without environmental regulation, and other matters and issues which will be evaluated later.

## GLASS PRODUCER REQUIREMENTS

The glass industry will operate their furnaces to meet the local regulation requirements. In some areas, these regulations are not well defined and do not give a restriction to the furnace operation. In other areas, such as the South Coast Air Quality Management District, very strict regulations are enforced. Part of Europe defines $NO_x$ reduction on a concentration basis, whereas the U.S. defines it on a mass basis. This does restrict the operational alternatives available to the manufacturer. Reduction in pull rate, use of increased electric boost, and post-combustion treatment, which are all expensive requirements to meet $NO_x$ regulations are a cost to the industry; therefore, if a low-cost method is available to meet the $NO_x$ requirements, this would be of significant interest to the glass industry. One option is oxy-fuel fired furnaces, however, there may be increased melting costs due to oxygen use. On the other hand, the oxy-gas technology produces very low $NO_x$ and usually offers lower capital rebuild costs. The use of the OEAS method would offer an economic alternative.

## OEAS SOLUTION

To assist the glass industry in meeting the current as well as anticipated future $NO_x$ regulations, SoCal Gas initiated a program with IGT, together with industrial partners, CTI and APCI, to develop cost effective low-$NO_x$ second generation combustion technology for near and mid-term needs (4 and 2 lb/ton, respectively) applicable to U.S. regenerative glass melters. Additional funding support was provided by GRI, DOE and several gas utilities, including Tokyo, Osaka, and Toho Gas, Korea Gas and Gaz de France.

This technology utilizes a unique method of combustion air staging to reduce the oxygen availability in the flame's high temperature zone and improve flame-temperature uniformity. This technique was tested on the IGT glass tank simulator during earlier work and showed potential for excellent $NO_x$ reduction. This OEAS system can give significant $NO_x$ reduction from 30% to 70% at an economic price. Second, it can be installed on the furnace without interrupting the operation. Third, it is transparent to the operation of the furnace regarding the operators and the quality of the product.

PRIMARY CUSTOMERS

The application of the OEAS system first applies to the U.S. regenerative glass furnace industry which includes container, TV, and float glass products. Of the different types of glass products, the container industry will be the primary market because container plants far out number any other type of glass furnace.

The U.S. glass container industry has approximately 150 furnaces and they are about equally divided between sideports and endports. Combustion Tec estimates that the maximum potential for conversion due to the application of environmental regulations not being in place or strict enough to encourage all the customers to make a conversion (assuming this is the primary available technology to them) would be about a 25% conversion rate over an eight year period or perhaps 19 endport furnaces and 15 sideport furnaces.

COMPETITIVE SOLUTIONS & COSTS (CHART)

Table 5 gives an approximate $NO_x$ reduction percentage potential, the productivity cost increase in dollars per ton of glass produced, and an abatement cost in dollars per ton of $NO_x$ reduction for varoius $NO_x$ control technologies.

Table 1
COMPARISON OF $NO_x$ REDUCTION TECHNOLOGIES
(For 250 TPD Furnace Operating at 10lb/ton $NO_x$)

| TECHNOLOGY | $NO_x$ REDUCTION (%) | COST INCREASE ($/Ton Glass) | ABATEMENT COST ($/Ton $NO_x$ Reduced) |
|---|---|---|---|
| Cullet Preheating* | 5 | 1.04 | 4160 |
| Electric Boost* | 15 | 6.08 | 8106 |
| SNCR* | 30 | 2.90 | 1933 |
| OEAS+ | 60 | 2.37 | 791 |
| SCR* | 75 | 9.11 | 2429 |
| Oxy-Fuel Firing+ | 85 | 6.78 | 1595 |

* ACS PAC RIM Meeting, Nov. 10, 1993, Honolulu, Hawaii
+ Combustion Tec, Inc. Internal Data
OEAS Cost Increase is Based on Oxygen Use @ 5% of S.R.
OEAS Oxygen @ $.24/CCF (LOX)
Oxy-Fuel Oxygen @ $.14/CCF (on site)

It is apparent that the technology to be chosen is in conformance with the requirements of the environmental regulations. In other words, if the requirement is a 90% $NO_x$ reduction, then the only technology available would be oxy/fuel firing. On the other hand, if there is a requirement for a reduction of up to 60% $NO_x$, then the OEAS technology is a stand-out selection. Bear in

mind the dollars per ton of glass at the 60% reduction for OEAS is an optimum selection and that there may be increases in dollars per ton at lower percentages $NO_x$ reduction since the optimum efficiency might not be achieved.

In any event, the chart shows clearly that OEAS technology is a preferred selection for reduction up to 60% and of all the technologies listed, has the lowest cost. This gives it a very good market potential.

Below find some additional discussion of the various $NO_x$ reduction technology options.

100% Oxy-Fuel Fired Glass Furnaces

It should be noted that in recent years there have been some significant installations for 100 percent oxygen/natural gas-fired combustion technologies for glass melters because of the significant $NO_x$ reduction when compared to current regenerative glass melters. Emission levels below 1 lb/ton $NO_x$ may be obtained, if high purity oxygen is employed. This, however, usually results in an increase in operating cost and product price. One solution is to use industrial oxygen (95-96 percent purity), which can be produced on-site and is less expensive. No long-term answer is yet available for the effect of oxygen use on furnace service life. It is still a question that existing regenerative glass tanks, which normally operate continuously for about 10 years between repair and modifications, would - before the end of this century - be economically converted to pure oxygen/natural gas firing without the environmental driving force of $NO_x$, particulate, etc. This approach, however, has significant potential to capture a large share of the market.

Air Staging

Körting Hanover AG of Germany has installed a patented system of air staging (not oxygen-enrichment) on an endport furnace, using air ejectors and ceramic lined piping around the furnace. Claims of upwards of 40% $NO_x$ reduction are made. To the best of our knowledge, only one (1) Körting system has been installed. We understand the price was about 1.5 million D marks, about $1 million U.S.

Fuel Staging or Cascade Heating For $NO_x$ Reduction

IGT and their program "Development of $NO_x$ Control Methods for Glass Melting Furnaces", funded by GRI and SoCal, performed fuel staging tests on their glass tank simulator model during the period 1982-83. Indications were that good $NO_x$ reduction could be accomplished with fuel staging, however, the work was not sufficient to establish that good flame characteristics could actually be obtained on a furnace in the field. Due to viable alternatives available by the Gas Firing Task Group of the glass industry, they deferred further follow-up of fuel staging at that time.

Sorg GmbH, a German glass furnace engineering company, is offering a competing system of fuel staging[5] called "cascading". They claim to have several installations in Europe mostly on oil fired furnaces. They currently are represented in the U.S. by Henry F. Teichmann, Inc., which is a glass engineering company located near Pittsburgh, Pennsylvania. Teichmann has been active in

marketing this Sorg cascading. As of yet, no U.S. systems have been installed. They claim similar $NO_x$ reductions of 40% to 50%. Teichmann gives capital costs of $156,000 for a 242 TPD endport furnace (container glass) or $250,000 for a 242 TPD sideport furnace, with operating cost of $1.19 per hour. This data is competitive with OEAS technology.

Sorg GmbH has just completed field tests on both end- and side-fired regenerative furnaces using this cascade heating (fuel staging) technology.[5] The $NO_x$ reduction on a limited basis was around 56% and 36% on end-fired and side-fired furnaces, respectively. To achieve this, the cascade heating system produced a secondary flame in the port neck by the introduction of additional gas. This secondary flame burns over the primary flame root, using a pre-determined fuel distribution; hence the primary flame is developed under sub-stoichiometric (rich) conditions. In this way, the availability of oxygen is reduced in the vicinity of the primary flame root. The $NO_x$ generation was reduced by operating the furnace under highly reducing conditions, at the same time the CO content was less than 100 $mg/Nm^3$. Sorg is currently evaluating this process on a complete furnace (using all ports) in the United States.

Detailed information for a complete sideport furnace on cascade heating, furnace operation, process economics, and engineering hardware to accomplish the above objectives are not available at this time.

Selective Catalytic (SCR) and Selective Non-Catalytic Reduction (SNCR)

The only currently available retrofit technologies for $NO_x$ reduction for glass tanks are SNCR and SCR, in increasing levels of $NO_x$ reduction (30 to 50% and 75 to 90% respectively) and costs. The lowest cost technology, SNCR, can reduce $NO_x$ by 30 to 50 percent at an estimated cost of $2000/ton of $NO_x$ removed, for a typical 250 ton/d glass tank. This represents $365,000 annually, or an increase in glass production fuel costs of 15 to 20 percent. Furthermore, SNCR suffers from a number of drawbacks including $NH_3$ slip, hazards of storing $NH_3$, and the potential for higher CO, $N_20$, and particulate emissions. There is, therefore, a need to develop advanced lower cost low-$NO_x$ technologies for retrofit to natural gas-fired regenerative glass melters. It should be noted these technologies can be used as post-combustion treatment for further reductions of $NO_x$ in the OEAS system.

Pilkington 3R

Outside the glass container industry, particularly in the float glass segment, Pilkington's 3R $NO_x$ control technology is CTI's main competitor. The 3R process involves injected fuel in the exhaust ports of a regenerative furnace, whereby this fuel mixes with $NO_x$ formed during the combustion process. The mixing continues throughout the regenerator and through chemical reactions $NO_x$ is reformed to nitrogen. At the bottom of the regenerators unburnt hydrocarbons and CO are oxidized by injecting air. Pilkington reported at the 57th Conference on Glass Problems (1996) the status of the 3R technology and gave the following cost figures for a 600 ton/day float furnace retrofited with the 3R technology. Capital costs of approximately $250,000 with operating costs of $36,000 per month. Pilkington states that greater than 75% $NO_x$

---

5 Metthias. Franke. "Cascade Heating System Reduces $NO_x$". Glass. pp. 141-142. April 1993.

reductions have been achieved yielding abatement cost at around $500/ton $NO_x$ reduced. No mention was made to system installation costs which factor into the cost of the technology.

## MARKET STRATEGY

PROCESSED FROM BEST AVAILABLE COPY

The overall strategy will be to bring this technology to the attention of the U.S. regenerative glass furnace industry for endport and sideport furnaces. The primary target market is the glass container segment because of the numerous container plants within the US. Reaching the glass container industry market will be done by several means:

1. Direct contact with the customer will be the principal means. This is by visit or by telephone.
2. Literature mailouts describing the technology.
3. Some limited advertising.
4. Technical trade show displays.
5. Technical articles to trade magazines for describing new products.
6. Technical papers at seminars and conferences.

Contact with the glass container industry in the U.S. can be accomplished for 90% of the furnaces through three (3) of the major companies, that being Owens-Brockway, Ball-Foster, and Anchor Glass. The balance of the furnaces are scattered among smaller companies. Each of these companies has a central engineering department where these decisions would originate from. This is not to state that visits to an individual plant would not be helpful since sometimes they push technology for their own local needs in contrast to the central engineering department priorities.

Contact with the prospective company will bring forth their needs as to the geographical area that is impacted by environmental regulation where they are having problems with compliance. These geographic areas include the south coast district in California, the northeast transport corridor, and varoius major metropolitan areas throughout the US.

The low cost OEAS technology with $NO_x$ reductions in the 30-60% range and continued environmental regulations makes this technology competitive and marketable in the glass industry.

### SALES TACTICS

Combustion Tec will give first priority to pursuing the markets in which patent protection is afforded and there is no risk of infringement on other patents. This is presumed to be the U.S. market on endport and sideport furnaces at this time. The second market to be considered by CTI will be outside the U.S. where patent protection is available, and where there is no infringement on other existing patents, and where environmental regulations will drive the use of this technology. The third market would be outside the U.S. where there is no patent protection and there are no infringement complications and technology is a driving force.

PROCESSED FROM BEST AVAILABLE COPY

## General

The first step in securing an OEAS sale, once customer contact has been made, is to gather pertanent furnace information and furnace drawings. This allows CTI to size an OEAS system, provide retrofit options, and initial economic analyses on the various options. CTI uses a one page questionnaire which the customer is asked to fill out and return. Once the different system options have been studied the customer would choose which route to pursue. At this point CTI can provide a quote for the basic system hardware.

The next step would be to conduct a retrofit survey of the plant. The survey is paid for by the customer and would be attended by a customer representative, a CTI engineer, and the customer's mechanical and electrical subcontractors. CTI would bring to the survey an initial process and instrumentation diagram (P&ID) and schetches of the proposed piping layout on the furnace. The survey would determine the feasability of the proposed retrofit, identify obstactles and work arounds, determine placement of flow control skids, PLC system, metering panel, and main header pipe routing. CTI would summarize the retrofit survey in a report. The subcontractors would provide the customer with estimates to install the system.
CTI can also provide assistance that the customer may need when dealing with local regulatory authorities. This may include technical merits of the staging technology, historical data, and economics.

## Oxygen Supply

The supply of oxygen for OEAS systems is in small ranges, from 1,000 to 18,000 SCFH. In this case the method of supply is probably liquid, hence the oxygen supplier would replenish on site storage by LOX (liquid oxygen)-truck service. Small oxygen generator units are also available which may provide a less expensive alternative to liquid oxygen. In the U.S.A., oxygen contracts are generally site specific, so if there is an existing agreement by an oxygen supplier at a plant site where OEAS equipment were to be installed, the existing supplier would probably be the OEAS supplier. If there is no oxygen supply at the plant, then this would, of course, be subject to bid by several suppliers. It could prove to be a competitive advantage having OEAS supply should a later conversion on the furnace be made to full 100% oxy-fuel firing for much higher oxygen consumption.

## Compressed Air Supply

For Compressed Air Staging (CAS) option, the compressed air supply (at 100 PSIG max.) would be utilized as the motive fluid for ejectors. A CAS system is strictly air staging with no oxygen enrichment capabilities. The compressed air flow requirements vary with furnace size and can be as much as 12,000SCFH for a large furnace. For plants without excess compressed air available a designated compressor would need to be installed. The choice for CAS would primarily be due to space contraint limitations and reduced piping installation costs.

Air cost will vary between 2¢/100 CF to 6¢/100 CF depending on amount of air and local electrical rates. Combustion Tec recommends the customer integrate this supply to his own available existing or new capacity, since the equipment can better be purchased by the customer. The CAS option may or may not be part of the OEAS technology, and this will be discussed between the parties.

## RISKS & PROBLEMS

The risks and problems as anticipated are outlined as follows:

1. $NO_x$ Reduction Warranty - Providing warranty performance for $NO_x$ reduction will have to be based on the customers' baseline data plus interpretation of all previous demonstration sites and commercial installations results.

2. Field Piping Cost - Quotations to the customer can be given in a general way, but they will have to be finalized by a visit to the field and perhaps, at least initially, actual bids for the field piping, which is a substantial portion of the cost and can have much variation due to the site conditions, the labor market, geographic location and customer's objectives.
3. Field Piping Life - Consideration will have to be given to the field piping with relationship to an 8-year furnace life. Many items are replaced at this point in time and the customer's input in this regard will influence pricing.

4. Installation - Care and attention will always have to be given to non-interference with the customer's furnace operation during the installation of this equipment. At the present state of knowledge, there should not be any problems to the customer's furnace while equipment is in use; in fact, this is a great advantage. At this point in time, we feel the equipment is invisible to the customer's furnace operation. Older furnaces, having more wear on them, would be subject to extra care in placing the holes in the furnace for the piping connections; hence, this risk would have to be evaluated and assumed by each customer.

5. Introduction of Oxygen - Introducing oxygen use into a plant where there is none becomes a new consideration. This is a new element for operating personnel and safety precautions will be emphasized.

## OWNERSHIP and ROYALTIES

This technology is under the ownership and licensing by the Institute of Gas Technology, US Patent #5,203,859 dated April 20, 1993. We are advised the patent has been filed in Denmark, France, Britain, Italy, Canada and Mexico. Data is not currently available on what other patents may exist that might present a conflict.

Under terms of the contract between IGT and Combustion Tec, Inc. licensing is to be provided by IGT to Combustion Tec, Inc.

Royalties will be paid in accordance with the licensing agreement.